

Copyright

By

Clifton Adam Boswell

2008

**Simple Design Details using Precast Concrete Panels at Skewed  
Expansion Joints**

by

**Clifton Adam Boswell, B.C.E.**

**Thesis**

Presented to the Faculty of the Graduate School of

The University of Texas at Austin

In Partial Fulfillment

Of the Requirements

For the Degree of

**Master of Science in Engineering**

**The University of Texas at Austin**

**May 2008**

**Simple Design Details using Precast Concrete Panels at Skewed  
Expansion Joints**

**Approved by  
Supervising Committee:**

---

**Sharon L. Wood, Supervisor**

---

**Oguzhan Bayrak**

## **Dedication**

To Jeri

To Dad, Mom, Erica, Sam, Spencer, Catherine, Alexandra, and  
my entire family

## **Acknowledgments**

I would like to first express my appreciation to the Texas Department of Transportation and the Center for Transportation Research for providing the opportunity and resources that made my graduate training possible.

Recognition should also be given to Blake Stasney and Dennis Phillip for their invaluable construction and logistical expertise during specimen fabrication and testing. Alan Kreisa, my research partner, deserves a special acknowledgment. His aptitude, dedication, and hard work account for a considerable portion of the success of this project.

Special thanks go to my beautiful bride, Jeri, and my family. They are the greatest cheering section a person could have.

Finally, particular recognition goes to Sharon Wood, James Jirsa, and Oguzhan Bayrak. Their extensive knowledge, passion for research, and dedication to teaching has provided the very backbone of this research endeavor.

May 4, 2008

## **Abstract**

# **Simple Design Details using Precast Concrete Panels at Skewed Expansion Joints**

Clifton Adam Boswell, M.S.E.

The University of Texas at Austin, 2007

Supervisor: Sharon L. Wood

The Texas Department of Transportation (TxDOT) has developed a new design detail that uses precast concrete panels as stay-in-place formwork adjacent to expansion joints in prestressed concrete bridges; however, skewed bridges present a unique challenge to the use of the precast panel system immediately adjacent to the expansion joint.

The objective of this research project was to investigate the response of trapezoidal precast panels used immediately adjacent to the expansion joint in skewed bridge decks. Five representative test specimens were constructed comprising two skew angles: 30° and 45°. Trapezoidal, precast panels for the 45° specimens were fabricated at Ferguson Structural Engineering Laboratory (FSEL) by project personnel. Trapezoidal, precast panels for the 30° specimens were manufactured by an independent precast

concrete supplier. Four of the specimens were subjected to statically applied loads on the ends of the skewed panels, and one of the panels was subjected to fatigue loading on the skewed end before being loaded monotonically to failure.

All test specimens containing the 45° precast panels fabricated at FSEL failed in diagonal shear at the short side of the trapezoidal panel when load was applied at midspan of the skewed end of the slab. All test specimens containing the 30° precast panels fabricated by an independent precast supplier failed by delamination due to horizontal shear between the panel and the cast-in-place topping slab when load was applied at midspan of the skewed end of the slab. Regardless of the failure mode for load applied at midspan of the skewed end of the specimen, all specimens failed in punching shear when load was applied at midspan of the square end of the trapezoidal panel.

Fatigue of the skewed panels did not limit the strength or stiffness of the panels along the skewed end. However, the maximum load carrying capacity along the skewed end may be limited if delamination occurs between the skewed panels and the topping slab. Current TxDOT specifications do not quantify levels of panel surface roughness for precast panels; therefore, additional testing is scheduled to take place in the summer of 2008 to further investigate the effect of panel surface roughness on the horizontal shear capacity between the trapezoidal panel and the cast-in-place topping slab.

The research team concluded that trapezoidal panels exhibit adequate strength and stiffness for current design loads if delamination is avoided.

## Table of Contents

Chapter 1 : Introduction.....	1
1.1    Background.....	1
1.2    Scope.....	4
1.3    Thesis Outline.....	4
Chapter 2 : Literature Review.....	5
2.1    Introduction.....	5
2.2    Prestressed Concrete Panels in Perpendicular Bridges.....	5
2.2.1    Coselli (2004).....	5
2.2.2    Agnew (2007).....	6
2.2.3    Dowell and Smith (2006).....	6
2.2.4    Merrill (2002).....	6
2.2.5    Abendroth (1994).....	7
2.2.6    Barker (1975).....	7
2.3    Prestressed Concrete Panels in Skewed Bridges.....	8
2.3.1    Merrill (2002).....	8
2.3.2    Abendroth (1994).....	8
2.3.3    Barker (1975).....	9
2.4    Research Significance.....	9
Chapter 3 : Test Specimens.....	11
3.1    Introduction.....	11
3.2    Preliminary Considerations.....	12
3.3    Material Properties.....	15
3.3.1    Concrete.....	15
3.3.2    Steel.....	16



3.3.3	Bedding Strip Material.....	17
3.4	Specimen Construction.....	19
3.4.1	Precast Panels Used in Test Specimens.....	20
3.4.1.1	45-Degree Panels.....	21
3.4.1.2	30-Degree Panels.....	24
3.4.1.3	Rectangular Panels.....	24
3.4.2	Longitudinal Beams.....	26
3.4.3	Cast-in-Place Topping Slab.....	26
3.5	Special Construction Considerations.....	30
3.5.1	Bedding Strip Compression.....	30
3.5.2	Concrete Consolidation in P45P2.....	31
Chapter 4 :	Loading and Instrumentation.....	33
4.1	Introduction.....	33
4.2	Specimen Loading.....	34
4.2.1	Static Loading.....	34
4.2.1.1	Loading Setup.....	34
4.2.1.2	Load Application.....	37
4.2.2	Fatigue Loading.....	40
4.2.2.1	Loading Setup.....	40
4.2.2.2	Load Application.....	40
4.3	Instrumentation.....	41
4.3.1	Specimen P45P1.....	43
4.3.1.1	Strain Gages.....	43
4.3.1.2	Linear Potentiometers.....	45

4.3.2	Specimen P45P2 .....	45
4.3.2.1	Strain Gages .....	45
4.3.2.2	Linear Potentiometers .....	48
4.3.3	Specimen P45P3 .....	49
4.3.3.1	Strain Gages .....	49
4.3.3.2	Linear Potentiometers .....	51
4.3.4	Specimens P30P1 and P30P2.....	52
4.3.4.1	Strain Gages .....	52
4.3.4.2	Linear Potentiometers .....	54
4.3.5	Data Collection .....	56
Chapter 5 : Measured Response of Test Specimens .....		57
5.1	Introduction.....	57
5.2	Load Tests.....	57
5.3	Measured Response of the 45-Degree Specimens .....	61
5.3.1	Response of Specimen P45P1.....	61
5.3.1.1	Load Applied at Midspan of Skewed End .....	62
5.3.2	Response of Specimen P45P2.....	69
5.3.2.1	Load Applied at Midspan of Skewed End .....	70
5.3.2.2	Load Applied at Midspan of Square End.....	79
5.3.3	Specimen P45P3 .....	88
5.3.3.1	Fatigue Load Applied at Midspan of Skewed End .....	88
5.3.3.2	Static Load to Failure Applied at Midspan of Skewed End.....	100
5.4	Measured Response of the 30-Degree Specimens .....	111
5.4.1	Specimen P30P1 .....	111

5.4.1.1	Load Applied at Midspan of Skewed End .....	111
5.4.1.2	Load Applied at the Square End .....	118
5.4.2	Specimen P30P2 .....	122
5.4.2.1	Load Applied at Skewed End.....	122
5.4.2.2	Load Applied at Midspan of Square End.....	130
5.5	Summary .....	134
Chapter 6	: Discussion of Results .....	137
6.1	Introduction.....	137
6.2	Summary .....	137
6.2.1	Load Applied Along Skewed End .....	138
6.2.2	Loads Applied Along Square End .....	146
6.3	Recommendations.....	147
Chapter 7	: Conclusions and Recommendations .....	149
7.1	Summary .....	149
7.2	Conclusions.....	149
7.3	Recommendations for Future Research .....	153
Appendix A	: Nondestructive Testing on Specimen P45P2 .....	154
A.1	Introduction.....	154
A.2	Impact-Echo Test .....	155
A.3	Ultrasonic Test .....	155
Appendix B	: Complete Set of Test Data.....	157
B.1	Specimen P45P1 .....	159
B.2	Specimen P45P2 .....	162
B.2.1	Load Applied at Midspan of Skewed End.....	162
B.2.2	Loads Applied at Midspan of Square End.....	167
B.3	Specimen P45P3 .....	171

B.3.1	Periodic Static Tests during Fatigue Loading.....	171
B.3.2	Static Load to Failure .....	188
B.4	Specimen P30P1 .....	192
B.4.1	Load Applied at Midspan of Skewed End.....	192
B.4.2	Load Applied at Midspan of Square End .....	195
B.5	Specimen P30P2 .....	196
B.5.1	Load Applied at Midspan of Skewed End.....	197
B.5.2	Load Applied at Midspan of Square End .....	200
References.....		201
Vita.....		202

## List of Tables

Table 3.1 – Characteristics of Skewed Test Specimens .....	12
Table 3.2 – Precast Panel Concrete Mix Design for Panels Fabricated at FSEL .....	16
Table 3.3 – Concrete Cylinder Strengths for Topping Slabs at 21-days .....	16
Table 3.4 – Support Beam and Topping Slab Concrete Mix Design.....	16
Table 3.5 – Panel Surface Roughness and Wetness before Topping Placement .....	28
Table 3.6 – Timeline of Specimen Construction and Testing .....	28
Table 3.7 – Average Overall Slab Depth at Midspan of Skewed End.....	30
Table 4.1 – Applied Loads to Test Specimens .....	33
Table 4.2 – Instrumentation Quantities for Each Specimen .....	42
Table 5.1 –Loads Corresponding to HL-93 Design Truck .....	60
Table 5.2 - Initial Stiffness and Inferred Cracking Load for Specimen P45P1 for Load Applied at Midspan of Skewed End .....	67
Table 5.3 – Initial Stiffness and Inferred Cracking Loads for Load Applied at Midspan of Skewed End of Specimen P45P2.....	76
Table 5.4 – Initial Stiffness and Inferred Cracking Load for Each Data Type for Specimen P45P2 for Load Applied at Midspan of Square End.....	84
Table 5.5 – Static Tests Conducted During Fatigue Test for Specimen P45P3 .....	89
Table 5.6 – Initial Stiffness and Inferred Cracking Loads for Specimen P45P3.....	97
Table 5.7 – Initial Stiffness and Estimated Cracking Loads for Specimen P30P1 for Load Applied at Midspan of Skewed End .....	116
Table 5.8 – Initial Stiffness and Inferred Cracking Loads for Specimen P30P2 for Load Applied at Midspan of Skewed End .....	127
Table 5.9 - Summary of Response of Test Specimens .....	136
Table 6.1 – Comparison of Precast Panel Detail to IBTS and UTSE Detail.....	142
Table A.1 – Impact-Echo Test Results for Specimen P45P2 .....	155
Table A.2 – Control Times for Ultrasonic Tests for Specimen P45P2 ( $\mu$ s).....	156
Table A.3 – Ultrasonic Travel Times for Specimen P45P2 ( $\mu$ s).....	156

Table B.1 – Adjusted Linear Potentiometer Data..... 158

## List of Figures

Figure 1.1 - Placement of Precast Panels in Bridge Deck Construction.....	2
Figure 1.2 – Comparison of Traditional IBTS Detail at Expansion Joint (top) and Precast Panels at Expansion Joint (bottom).....	3
Figure 1.3 – Trapezoidal Gap Adjacent to Skewed Expansion Joint .....	3
Figure 2.1 - Trapezoidal Panels for Composite Bridge Deck Systems (Abendroth, 1994)	9
Figure 3.1 – HL-93 Design Truck Loads on Bridge Deck .....	14
Figure 3.2 – Panel on Bedding Strip.....	18
Figure 3.3 – TxDOT Bedding Strip Dimensions (TxDOT, 2008).....	18
Figure 3.4 – General Specimen Construction .....	19
Figure 3.5 – Definitions of Boundaries in Trapezoidal Panels.....	21
Figure 3.6 - Skewed Panel Reinforcement for Specimen P45P1.....	22
Figure 3.7 – Skewed Panel Reinforcement for Specimen P45P2.....	23
Figure 3.8 – Skewed Panel Reinforcement for Specimen P45P3.....	23
Figure 3.9 – Skewed Panel Reinforcement for Specimens P30P1 and P30P2.....	24
Figure 3.10 – Alignment of Rectangular and Skewed Panels .....	25
Figure 3.11 – Backer Rod between Adjacent Panels.....	25
Figure 3.12 - Long Side Support Beam (left) and Short Side Support Beam (right) .....	26
Figure 3.13 – Formwork for Topping Slab in Position.....	27
Figure 3.14 – Cast-in-Place Topping Reinforcement .....	29
Figure 3.15 – Poor Consolidation at Expansion Joint of Specimen P45P2.....	31
Figure 3.16 – Extent of Poor Consolidation in Specimen P45P2.....	32
Figure 4.1 – Load Frame for Static Load Application.....	35
Figure 4.2 – Hydraulic Ram, Load Cell, and Load Plate for Specimen Loading.....	36
Figure 4.3 – Load Plate Positions on Test Specimens .....	38
Figure 4.4 – Load Plate Position over Square End of Skewed Precast Panel.....	39
Figure 4.5 – MTS Hydraulic Actuator.....	40
Figure 4.6 – Fatigue Loading Input and Feedback Signal .....	41

Figure 4.7 – Concrete Strain Gage Locations and Labels for Specimen P45P1.....	43
Figure 4.8 – SEJ Strain Gage Locations and Labels for Specimen P45P1 .....	44
Figure 4.9 – Linear Potentiometer and Dial Gage Locations and Labels for Specimen P45P1 .....	44
Figure 4.10 – Concrete Strain Gage Locations and Labels for Specimen P45P2 for Load Applied at Midspan of Skewed End .....	45
Figure 4.11 – Concrete Strain Gage Location and Labels for Specimen P45P2 for Load Applied at Midspan of Square End.....	46
Figure 4.12 – SEJ Strain Gage Locations and Labels for Specimen P45P2 for Load Applied at Midspan of Skewed End .....	46
Figure 4.13 – Rebar Strain Gage Locations and Labels for Specimen P45P2 for Load Applied at Midspan of Square End.....	47
Figure 4.14 – Strand Strain Gage Locations and Labels for Specimen P45P2 for Load Applied at Midspan of Skewed End .....	47
Figure 4.15 – Linear Potentiometer Locations and Labels for Specimen P45P2 for Load Applied at Midspan of Skewed End .....	48
Figure 4.16 – Linear Potentiometer Locations and Labels for Specimen P45P2 for Load Applied at Midspan of Square End.....	49
Figure 4.17 – Concrete Strain Gage Locations and Labels for Specimen P45P3 for Load Applied at Midspan of Skewed End .....	50
Figure 4.18 – SEJ Strain Gage Locations and Labels for Specimen P45P3 for Load Applied at Midspan of Skewed End .....	50
Figure 4.19 – Strand Strain Gage Locations and Labels for Specimen P45P3 for Load Applied at Midspan of Skewed End .....	51
Figure 4.20 – Linear Potentiometer Locations and Labels for Specimen P45P3 for Load Applied at Midspan of Skewed End .....	52
Figure 4.21 – Concrete Strain Gage Locations for Specimens P30P1 and P30P2 for Load Applied at Midspan of Skewed End .....	53



Figure 4.22 – Concrete Strain Gage Location for Specimens P30P1 and P30P2 for Load Applied at Midspan of Square End.....	53
Figure 4.23 – SEJ Strain Gage Locations for Specimens P30P1 and P30P2 for Load Applied at Midspan of Skewed End .....	54
Figure 4.24 – Linear Potentiometer Locations and Labels for Specimens P30P1 and P30P2 for Load Applied at Midspan of Skewed End.....	55
Figure 4.25 – Linear Potentiometer Locations and Labels for Specimens P30P1 and P30P2 for Load Applied at Midspan of Square End.....	55
Figure 4.26 – Data Collection System .....	56
Figure 5.1 – Rigid Body Movement of Loaded End of Skewed Specimen.....	58
Figure 5.2 – Presentation of Strain Gage Data .....	61
Figure 5.3 – Measured Displacement Response of Specimen P45P1 for Load Applied at Midspan of Skewed End .....	63
Figure 5.4 – Variation of Relative Displacements along Loaded End for Specimen P45P1 for Load Applied at Midspan of Skewed End .....	63
Figure 5.5 – Change in Tensile Strain on Bottom of Precast Panel for Specimen P45P1 for Load Applied at Midspan of Skewed End .....	64
Figure 5.6 – Distribution of Concrete Strain on the Bottom of the Panel along Skewed End of Specimen P45P1.....	65
Figure 5.7 – Measured Compressive Strain at Midspan of SEJ for Specimen P45P1 for Load Applied at Midspan of Skewed End .....	66
Figure 5.8 – Variation of Strain in SEJ along Skewed End of Specimen P45P1 .....	66
Figure 5.9 – Observed Crack Pattern at Conclusion of Static Test for Specimen P45P1.	68
Figure 5.10 – Photograph of Specimen P45P1 at Conclusion of Static Test.....	69
Figure 5.11 – Measured Displacement Response of Specimen P45P2 for Load Applied at Midspan of Skewed End .....	70
Figure 5.12 – Variation of Relative Displacements along Skewed End of Specimen P45P2 .....	71

Figure 5.13 - Tensile Strain on Bottom of Precast Trapezoidal Panel for Specimen P45P2 for Load Applied at Midspan of Skewed End .....	72
Figure 5.14 – Distribution of Concrete Strain on the Bottom of the Panel along Skewed End of Specimen P45P2.....	72
Figure 5.15 - Measured Compressive Strain at Midspan of SEJ for Specimen P45P2 for Load Applied at Midspan of Skewed End .....	73
Figure 5.16 - Variation of Strain in SEJ along Skewed End of Specimen P45P2.....	74
Figure 5.17 – Measured Change in Tensile Strain in Prestressing Strand in Specimen P45P2 for Load Applied at Midspan of Skewed End .....	74
Figure 5.18 – Variation of Maximum Strain in Prestressing Strands for Load Applied at Midspan of Skewed End for Specimen P45P2 .....	75
Figure 5.19 – Observed Crack Patterns at Conclusion of Static Test at Midspan of Skewed End for Specimen P45P2.....	77
Figure 5.20 – Photographs of Specimen P45P2 at Conclusion of Static Test at Midspan of Skewed End .....	78
Figure 5.21 - Measured Displacement Response for Specimen P45P2 for Load Applied at Midspan of Square End.....	80
Figure 5.22 – Variation of Displacements along Square End of Specimen P45P2 .....	81
Figure 5.23 – Measured Change in Tensile Strain on Bottom of Precast Panel for Specimen P45P2 for Load Applied at Midspan of Square End.....	82
Figure 5.24 – Distribution of Change in Concrete Strain on the Bottom of the Panel Along Square End of Specimen P45P2 .....	82
Figure 5.25 - – Measured Tensile Strains in Rebar for Specimen P45P2 for Load Applied at Midspan of Square End.....	83
Figure 5.26 – Distribution of Strain in Reinforcement Closest to Square End of Specimen P45P2 .....	84
Figure 5.27 - Measured Relative Displacement Response at Midspan of Trapezoidal and Rectangular Panels in Specimen P45P2 for Load Applied at Midspan of Square End .....	85

Figure 5.28 – Observed Crack Patterns at Conclusion of Static Test at Midspan of Square End for Specimen P45P2 .....	86
Figure 5.29 – Photographs of Specimen P45P2 at Conclusion of Static Test at Midspan of Square End.....	87
Figure 5.30 – Measured Displacement Response at Midspan of Skewed End for Specimen P45P3 during Periodic Static Tests before Overload Test.....	90
Figure 5.31 – Measured Displacement Response at Midspan of Skewed End for Specimen P45P3 during Periodic Static Tests after Overload Test.....	90
Figure 5.32 – Variation of Displacements along Skewed End of Specimen P45P3 during Static Overload Test.....	91
Figure 5.33 – Measured Change in Concrete Strain on the Bottom of Panel at Midspan of Skewed End for Specimen P45P3 during Periodic Static Tests before Overload Test .....	92
Figure 5.34 – Measured Change in Concrete Strain on the Bottom of Panel at Midspan of Skewed End for Specimen P45P3 during Periodic Static Tests after Overload Test	92
Figure 5.35 – Distribution of Change in Concrete Strain along Bottom of Panel for Specimen P45P3 during Static Overload Test .....	93
Figure 5.36 – Measured Strain at Midspan of SEJ for Specimen P45P3 for Periodic Static Loads Applied before Static Overload Test.....	94
Figure 5.37 – Measured Strain at Midspan of SEJ for Specimen P45P3 for Periodic Static Loads Applied after Static Overload Test.....	94
Figure 5.38 - Variation of Strain along SEJ for Specimen P45P3 during Static Overload Test.....	95
Figure 5.39 – Measured Change in Strain Response of Strand S12 during Periodic Static Tests before Overload for Specimen P45P3 for Loads Applied at Midspan of Skewed End .....	96
Figure 5.40 – Measured Change in Strain Response of Strand S12 during Periodic Static Tests after Overload for Specimen P45P3 for Loads Applied at Midspan of Skewed End .....	96

Figure 5.41 – Variation of Maximum Strain in Prestressing Strands for Load Applied at Midspan of Skewed End of Specimen P45P3 during Static Overload Test .....	97
Figure 5.42 – Observed Crack Pattern for Specimen P45P3 at Conclusion of Fatigue Test .....	99
Figure 5.43 – Measured Displacement Response of Specimen P45P3 for Load Applied at Midspan of Skewed End after Fatigue Test.....	100
Figure 5.44 – Variation of Displacements along Skewed End of Specimen P45P3 after Fatigue Test.....	101
Figure 5.45 – Change in Tensile Strain Data on Bottom of Precast Panel for Specimen P45P3 for Load Applied at Midspan of Skewed End after Fatigue Test.....	102
Figure 5.46 – Distribution of Change in Concrete Strain on the Bottom of the Panel along Skewed End of Specimen P45P3 after Fatigue Test.....	102
Figure 5.47 – Measured Compressive Strain at Midspan of SEJ for Specimen P45P3 after Fatigue Test.....	103
Figure 5.48 - Variation of Strain on SEJ along Skewed End of Specimen P45P3 after Fatigue Test.....	104
Figure 5.49 – Measured Change in Tensile Strain in Prestressing Strand in Specimen P45P3 for Load Applied at Midspan of Skewed End after Fatigue Test.....	105
Figure 5.50 – Variation of Maximum Strain in Prestressing Strands for Load Applied at Midspan of Skewed End for Specimen P45P3 after Fatigue Test .....	105
Figure 5.51 – Observed Crack Pattern for Specimen P45P3 for Static Test to Failure..	107
Figure 5.52 – Predominant Cracks at Southwest Corner of Specimen at Conclusion of Static Test to Failure of Specimen P45P3.....	108
Figure 5.53 – Predominant Cracks at Southeast Corner of Specimen P45P3 at Conclusion of Static Test to Failure.....	109
Figure 5.54 – Spalling on Bottom Surface of Specimen P45P3 at Conclusion of Static Test to Failure .....	110
Figure 5.55 – Measured Displacement Response of Specimen P30P1 for Load Applied at Midspan of Skewed End .....	112

Figure 5.56 - Variation of Displacement along Skewed End of Specimen P30P1 .....	112
Figure 5.57 – Change in Tensile Strain on Bottom of Panel at Midspan of Skewed End of Specimen P30P1 .....	113
Figure 5.58 – Distribution of Change in Concrete Strain on Bottom of Panel along Skewed End of Specimen P30P1 .....	114
Figure 5.59 – Compressive Strain at Midspan of SEJ in Specimen P30P1 .....	115
Figure 5.60 - Variation of Strain along SEJ of Specimen P30P1 .....	115
Figure 5.61 – Observed Cracks at Conclusion of Static Test of Specimen P30P1 for Load Applied at Midspan of Skewed End .....	117
Figure 5.62 – Photograph of Specimen P30P1 at Conclusion of Static Test for Load Applied at Midspan of Skewed End .....	118
Figure 5.63 – Measured Displacement Response at Midspan of Square End of Specimen P30P1 .....	120
Figure 5.64 – Observed Crack Pattern at Conclusion of Static Test for Specimen P30P1 for Load Applied at Midspan of Square End .....	120
Figure 5.65 – Photograph of Punching Shear Failure for Specimen P30P1 for Load Applied at Midspan of Square End.....	121
Figure 5.66 – Photograph of Trapezoidal Panel Displacement at Conclusion of Test of Specimen P30P1 for Load Applied at Midspan of Square End.....	122
Figure 5.67 - Measured Displacement Response at Midspan of Skewed End of Specimen P30P2 .....	123
Figure 5.68 - Variation of Displacements along Loaded End of Specimen P30P2 for Load Applied at Midspan of Skewed End .....	124
Figure 5.69 – Change in Tensile Strain on Bottom of Precast Panel at Midspan of Skewed End of Specimen P30P2.....	125
Figure 5.70 - Variation of Change in Strain on Bottom of Panel along Skewed End of Specimen P30P2 .....	125
Figure 5.71 – Compressive Strain at Midspan of SEJ in Specimen P30P2.....	126

Figure 5.72 - Variation of Strain in SEJ along Loaded End of Specimen P30P2 for Load Applied at Midspan of Skewed End .....	127
Figure 5.73 – Observed Crack Pattern for Specimen P30P2 for Load Applied at Midspan of Skewed End .....	129
Figure 5.74 – Photograph of Delamination of Trapezoidal Panel from Topping Slab for Specimen P30P2 for Load Applied at Midspan of Skewed End .....	130
Figure 5.75 – Measured Displacement Response at Midspan of Square End of Specimen P30P2 .....	131
Figure 5.76 – Observed Crack Pattern at Conclusion of Static Test for Specimen P30P2 for Load Applied at Midspan of Square End .....	132
Figure 5.77 – Photograph of Punching Shear Failure for Specimen P30P2 for Load Applied at Midspan of Square End.....	133
Figure 5.78 – Photograph of Shear Crack in Trapezoidal Panel at Short Side Support in Specimen P30P2 for Load Applied at Midspan of Square End.....	134
Figure 6.1 – Measured Displacement Response of 45° Specimens for Load Applied at Midspan of Skewed End .....	139
Figure 6.2 –Comparison of Measured Displacement Response of 0° and 45° Specimens .....	140
Figure 6.3 – Measured Compressive Strain at Midspan of SEJ for 0° and 45° Specimens .....	140
Figure 6.4 – Points of Load Application for Full-scale Test of IBTS and UTSE Details (Griffith, 2003).....	142
Figure 6.5 – Comparison of Displacement Response of Precast Panel Detail, UTSE Detail, and IBTS Detail.....	143
Figure 6.6 – Measured Displacement Response for 30° Specimens for Load Applied at Midspan of Skewed End .....	144
Figure 6.7 – Comparison of Measured Displacement Response of 30° and 45° Specimens .....	145

Figure 6.8 – Comparison of Measured Displacement Response of 30° and 0° Specimens .....	145
Figure 6.9 – Measured Compressive Strain at Midspan of SEJ for 0° and 30° Specimens .....	146
Figure 6.10 – Measured Displacement Response of Specimens P45P2, P30P1, and P30P2 for Load Applied at Midspan of Square End.....	147
Figure 7.1 – Recommended Trapezoidal Panel for Use at Expansion Joints in Skewed Bridge Decks.....	152
Figure A.1 – Grid Locations for Nondestructive Testing on Specimen P45P2.....	154
Figure B.1 – Measured Relative Displacements along Skewed End of Specimen P45P1 .....	159
Figure B.2 – Measured Support Displacements for Specimen P45P1 Loaded at Midspan of Skewed End .....	160
Figure B.3 – Measured Change in Tensile Strain on Bottom of Panel for Specimen P45P1 for Load Applied at Midspan of Skewed End .....	160
Figure B.4 – Measured Change in Tensile Strain on Bottom of Panel for Specimen P45P1 for Load Applied at Midspan of Skewed End .....	161
Figure B.5 – Measured Change in Tensile Strain on Bottom of Panel for Specimen P45P1 for Load Applied at Midspan of Skewed End .....	161
Figure B.6 – Measured Compressive Strain in SEJ for Specimen P45P1 for Load Applied at Midspan of Skewed End .....	162
Figure B.7 – Measured Relative Displacements for Specimen P45P2 for Load Applied at Midspan of Skewed End.....	163
Figure B.8 – Measured Support Displacements for Specimen P45P2 for Load Applied at Midspan of Skewed End.....	163
Figure B.9 – Measured Change in Tensile Strains on Bottom of Panel for Specimen P45P2 for Load Applied at Midspan of Skewed End.....	164
Figure B.10 – Measured Compressive Strain in SEJ for Specimen P45P2 for Load Applied at Midspan of Skewed End .....	164

Figure B.11 – Measured Change in Tensile Strain in Prestressing Strands S12, S13, and S14 for Specimen P45P2 for Load Applied at Midspan of Skewed End .....	165
Figure B.12 – Measured Change in Tensile Strains in Prestressing Strands S9, S10, and S11 for Specimen P45P2 for Load Applied at Midspan of Skewed End .....	165
Figure B.13 – Measured Change in Tensile Strain in Prestressing Strands S6, S7, and S8 for Specimen P45P2 for Load Applied at Midspan of Skewed End.....	166
Figure B.14 – Measured Change in Tensile Strain in Prestressing Strands S3 and S5 for Specimen P45P2 for Load Applied at Midspan of Skewed End .....	166
Figure B.15 – Measured Change in Tensile Strain in Prestressing Strands S1 and S2 for Specimen P45P2 for Load Applied at Midspan of Skewed End .....	167
Figure B.16 – Measured Relative Displacements for Specimen P45P2 for Load Applied at Midspan of Square End.....	167
Figure B.17 – Measured Support Displacements for Specimen P45P2 for Load Applied at Midspan of Square End.....	168
Figure B.18 – Measured Relative Midspan Displacement for Rectangular Panel for Specimen P45P2 for Load Applied at Midspan of Square End.....	168
Figure B.19 – Measured Support Displacements for Rectangular Panel for Specimen P45P2 for Load Applied at Midspan of Square End.....	169
Figure B.20 – Measured Change in Tensile Strain on Bottom of Panel for Specimen P45P2 for Load Applied at Midspan of Square End.....	169
Figure B.21 – Measured Tensile Strain in Rebar for Specimen P45P2 for Load Applied at Midspan of Square End.....	170
Figure B.22 – Measured Tensile Strain in Rebar for Specimen P45P2 for Load Applied at Midspan of Square End.....	170
Figure B.23 – Measured Tensile Strain in Rebar for Specimen P45P2 for Load Applied at Midspan of Square End.....	171
Figure B.24 – Measured Relative Displacements at L2 for Periodic Static Tests during Fatigue Loading of Specimen P45P3 before Overload.....	172



Figure B.25 – Measured Relative Displacements at L3 for Periodic Static Tests during Fatigue Loading of Specimen P45P3 before Overload.....	172
Figure B.26 – Measured Relative Displacements at L4 for Periodic Static Tests during Fatigue Loading of Specimen P45P3 before Overload.....	173
Figure B.27 – Measured Relative Displacements for Static Overload of Specimen P45P3 during Fatigue Loading.....	173
Figure B.28 – Measured Relative Displacements at L2 for Periodic Static Tests during Fatigue Loading of Specimen P45P3 after Overload .....	174
Figure B.29 – Measured Relative Displacements at L3 for Periodic Static Tests during Fatigue Loading of Specimen P45P3 after Overload .....	174
Figure B.30 – Measured Relative Displacements at L4 for Periodic Static Tests during Fatigue Loading of Specimen P45P3 after Overload .....	175
Figure B.31 – Measured Change in Tensile Strain on Bottom of Panel at Location C1 during Fatigue Loading of Specimen P45P3 before Overload.....	175
Figure B.32 – Measured Change in Tensile Strain on Bottom of Panel at Location C1 during Fatigue Loading of Specimen P45P3 after Overload.....	176
Figure B.33 – Measured Change in Tensile Strain on Bottom of Panel at Location SS1 during Fatigue Loading Specimen P45P3 before and after Overload .....	176
Figure B.34 – Measured Change in Tensile Strain on Bottom of Panel for Periodic Static Tests during Fatigue Loading of Specimen P45P3 before and after Overload.....	177
Figure B.35 – Measured Compressive Strain on Top Surface of SEJ at SEJ2 for Periodic Static Tests during Fatigue Loading for Specimen P45P3 before Overload .....	177
Figure B.36 - Measured Compressive Strains on Top Surface of SEJ at SEJ2 for Periodic Tests during Fatigue Loading for Specimen P45P3 after Overload .....	178
Figure B.37 – Measured Compressive Strains on Top Surface of SEJ at SEJ1 for Periodic Static Tests during Fatigue Loading of Specimen P45P3 before and after Overload .....	178

Figure B.38 – Measured Compressive Strain on Top Surface of SEJ at SEJ3 for Periodic Static Tests during Fatigue Loading of Specimen P45P3 before and after Overload .....	179
Figure B.39 – Measured Change in Tensile Strain in Strand S12 for Periodic Static Tests during Fatigue Loading of Specimen P45P3 before Overload .....	179
Figure B.40 – Measured Change in Tensile Strain in Strand S12 for Periodic Static Tests during Fatigue Loading of Specimen P45P3 after Overload .....	180
Figure B.41 – Measured Change in Tensile Strain in Strand S11 for Periodic Static Tests during Fatigue Loading of Specimen P45P3 before Overload .....	180
Figure B.42 – Measured Change in Tensile Strain in Strand S11 for Periodic Static Tests during Fatigue Loading of Specimen P45P3 after Overload .....	181
Figure B.43 – Measured Change in Tensile Strain in Strand S10 for Periodic Static Tests during Fatigue Loading of Specimen P45P3 before Overload .....	181
Figure B.44 – Measured Change in Tensile Strain in Strand S10 for Periodic Static Tests during Fatigue Loading of Specimen P45P3 after Overload .....	182
Figure B.45 – Measured Change in Tensile Strains in Strand S9 for Periodic Static Tests during Fatigue Loading of Specimen P45P3 before Overload .....	182
Figure B.46 – Measured Change in Tensile Strain in Strand S9 for Periodic Static Tests during Fatigue Loading of Specimen P45P3 after Overload .....	183
Figure B.47 – Measured Change in Tensile Strain in Strand S8 for Periodic Static Tests during Fatigue Loading of Specimen P45P3 before Overload .....	183
Figure B.48 – Measured Change in Tensile Strain in Strand S8 for Periodic Static Tests during Fatigue Loading of Specimen P45P3 after Overload .....	184
Figure B.49 – Measured Change in Tensile Strain in Strand S7 for Periodic Static Test during Fatigue Loading of Specimen P45P3 before and after Overload .....	184
Figure B.50 – Measured Change in Tensile Strain in Strand S6 for Periodic Static Tests during Fatigue Loading of Specimen P45P3 before and after Overload .....	185
Figure B.51 – Measured Change in Tensile Strain in Strand S5 for Periodic Static Tests during Fatigue Loading of Specimen P45P3 before and after Overload .....	185

Figure B.52 – Measured Change in Tensile Strain in Strand S4 for Periodic Static Tests during Fatigue Loading of Specimen P45P3 before and after Overload .....	186
Figure B.53 – Measured Change in Tensile Strain in Strand S3 for Periodic Static Tests during Fatigue Loading of Specimen P45P3 before and after Overload .....	186
Figure B.54 – Measured Change in Tensile Strain in Strand S2 for Periodic Static Tests during Fatigue Loading of Specimen P45P3 before and after Overload .....	187
Figure B.55 – Measured Change in Tensile Strain in Strand S1 for Periodic Static Tests during Fatigue Loading of Specimen P45P3 before and after Overload .....	187
Figure B.56 – Measured Displacements for Specimen P45P3 for Static Test to Failure for Load Applied at Midspan of Skewed End .....	188
Figure B.57 – Measured Support Displacements for Specimen P45P3 for Static Test to Failure for Load Applied at Midspan of Skewed End .....	188
Figure B.58 – Measured Change in Tensile Strain on Bottom of Panel for Specimen P45P3 for Static Overload for Load Applied at Midspan of Skewed End .....	189
Figure B.59 – Measured Compressive Strain in SEJ for Specimen P45P3 for Static Overload for Load Applied at Midspan of Skewed End.....	189
Figure B.60 – Measured Change in Tensile Strain in Strands S10, S11, and S12 in Specimen P45P3 for Static Overload Test for Load Applied at Midspan of Skewed End .....	190
Figure B.61 – Measured Change in Tensile Strain in Strands S7, S8, and S9 in Specimen P45P3 for Static Overload Test for Load Applied at Midspan of Skewed End .....	190
Figure B.62 – Measured Change in Tensile Strain in Strands S4, S5, and S6 for Specimen P45P3 for Static Overload Test for Load Applied at Midspan of Skewed End .....	191
Figure B.63 – Measured Change in Tensile Strain in Strands S1, S2, and S3 for Specimen P45P3 for Static Overload Test for Load Applied at Midspan of Skewed End .....	191
Figure B.64 – Measured Relative Displacements for Specimen P30P1 for Load Applied at Midspan of Skewed End .....	192
Figure B.65 – Measured Support Displacements for Specimen P30P1 for Load Applied at Midspan of Skewed End .....	193

Figure B.66 – Measured Change in Tensile Strain on Bottom of Panel for Specimen P30P1 for Load Applied at Midspan of Skewed End.....	193
Figure B.67 – Measured Change in Tensile Strain on Bottom of Panel for Specimen P30P1 for Load Applied at Midspan of Skewed End.....	194
Figure B.68 – Measured Change in Tensile Strain on Bottom of Panel for Specimen P30P1 for Load Applied at Midspan of Skewed End.....	194
Figure B.69 – Measured Compressive Strain in SEJ for Specimen P30P1 for Load Applied at Midspan of Skewed End .....	195
Figure B.70 – Measured Relative Displacement at Midspan of Square End of Specimen P30P1 for Load Applied at Midspan of Square End.....	195
Figure B.71 – Measured Support Displacements for Specimen P30P1 for Load Applied at Midspan of Square End.....	196
Figure B.72 – Measured Relative Displacements for Specimen P30P2 for Load Applied at Midspan of Skewed End .....	197
Figure B.73 – Measured Support Displacements for Specimen P30P2 for Load Applied at Midspan of Skewed End.....	197
Figure B.74 – Measured Change in Tensile Strain on Bottom of Panel for Specimen P30P2 for Load Applied at Midspan of Skewed End.....	198
Figure B.75 – Measured Change in Tensile Strain on Bottom of Panel for Specimen P30P2 for Load Applied at Midspan of Skewed End.....	198
Figure B.76 – Measured Change in Tensile Strain on Bottom of Panel for Specimen P30P2 for Load Applied at Midspan of Skewed End.....	199
Figure B.77 – Measured Compressive Strain on Top Surface of SEJ for Specimen P30P2 for Load Applied at Midspan of Skewed End .....	199
Figure B.78 – Measured Relative Displacement at Midspan of Square End for Load Applied at Midspan of Square End.....	200
Figure B.79 – Measured Support Displacements for Specimen P30P2 for Load Applied at Midspan of Square End.....	200

## Chapter 1: Introduction

Essential information needed to understand the objective and scope of this investigation is provided in this chapter. A brief background on the use of precast panels in bridge decks is provided in Section 1.1. The scope of the research is given in Section 1.2, and an outline for this thesis provided in Section 1.3.

### 1.1 BACKGROUND

The Texas Department of Transportation (TxDOT) has, in recent decades, dedicated considerable resources to improving bridge construction methods. Evolving from this effort is the current practice of using prestressed concrete panels in bridge decks. The use of these panels eliminates the majority of formwork for concrete bridge decks, decreases construction time, and reduces construction costs.

Prestressed concrete panels in bridges span from girder to girder and run the length of the bridge, as shown in Figure 1.1. Precast panels are 4 in. thick and are topped with a 4-in. cast-in-place slab. The entire 8-in. deep composite section comprises the bridge deck. In the past, precast concrete panels have been placed at 4 ft. away from the expansion joint in the bridge deck and traditional forming techniques have been used to cast a 10-in. I-beam thickened slab (IBTS) adjacent to the expansion joint. However, TxDOT has sponsored two recent research projects to develop new design details for the end of the slab adjacent to the expansion joint. In TxDOT project 0-4418, researchers constructed a full-scale bridge deck with  $0^\circ$  skew and concluded that the precast panel system provided adequate strength and reduced construction costs compared with the traditional cast-in-place details at the expansion joint. Cross sections of precast panels used at expansion joints are provided in Figure 1.2. The first phase of the investigation in TxDOT Project 0-5367 evaluated the fatigue response of precast panels at the expansion joint in  $0^\circ$  skew bridges. The second phase of this investigation evaluates the use of trapezoidal precast panels at the expansion joint in skewed bridge decks.

Skewed expansion joints in bridge decks present a unique challenge for precast panel bridge deck systems. Precast panels are generally rectangular in shape and, as shown in Figure 1.3, leave trapezoid-shaped gaps at the end of the deck adjacent to the expansion joint. Current bridge construction practices call for the use of stay-in-place sheet metal forms or timber forming methods to construct the IBTS detail at the end of the bridge deck.

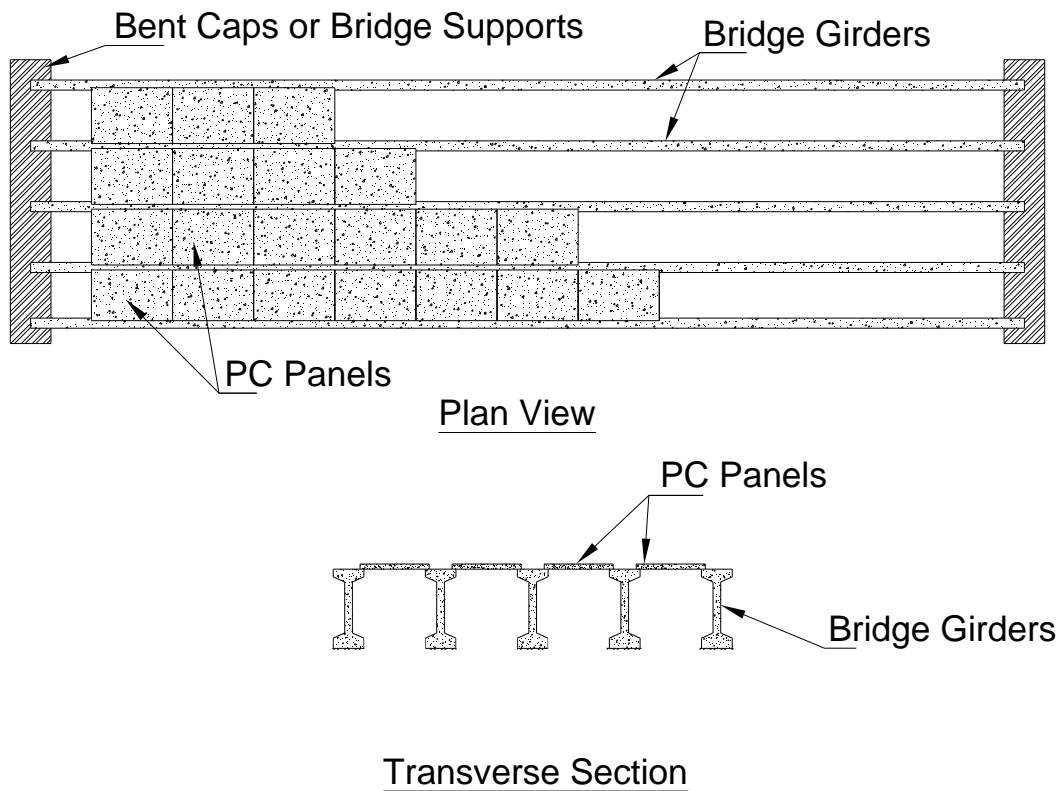


*Figure 1.1 - Placement of Precast Panels in Bridge Deck Construction (Agnew 2007)*

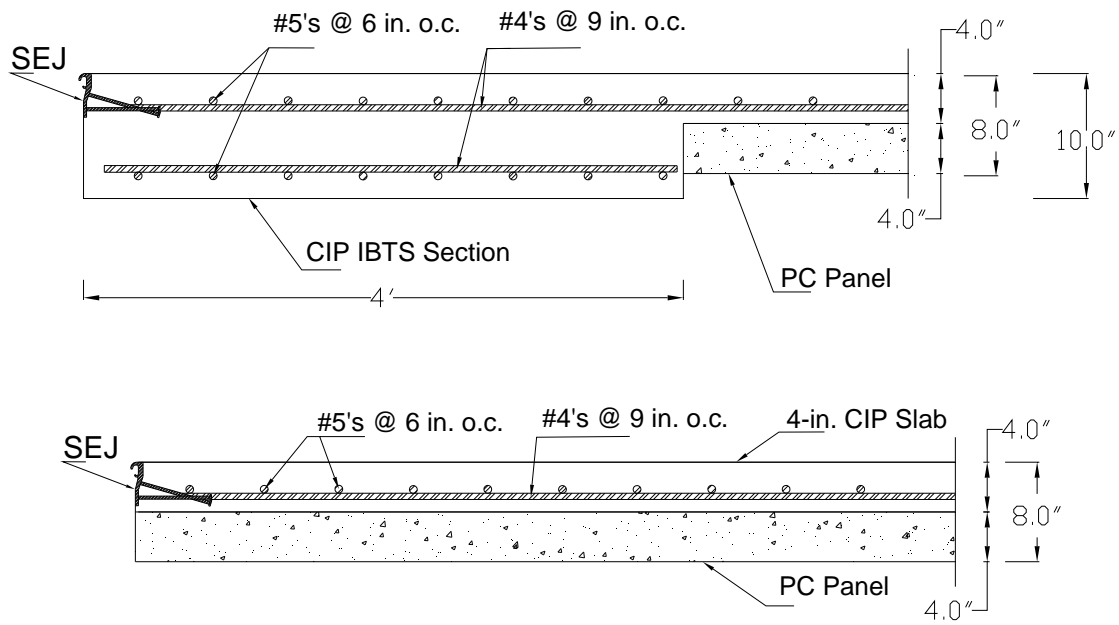


**Figure 1.2 – Comparison of Traditional IBTS Detail at Expansion Joint (top) and Precast Panels at Expansion Joint (bottom)**

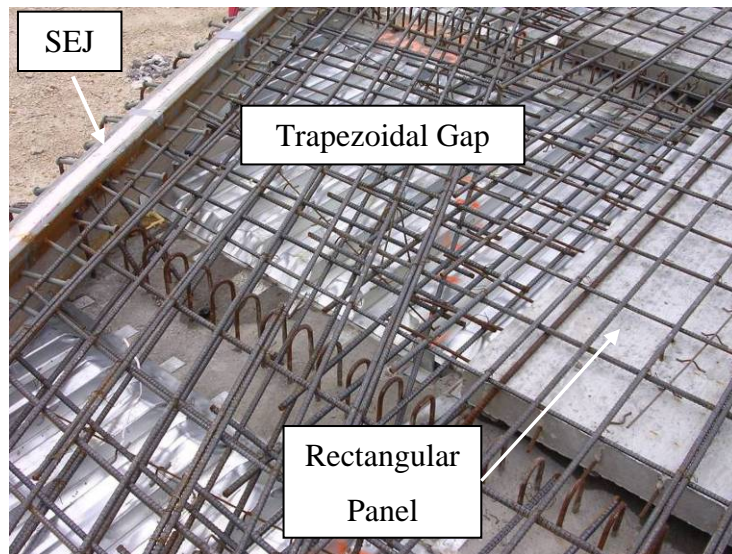


**Figure 1.3 – Trapezoidal Gap Adjacent to Skewed Expansion Joint**

## **1.2 SCOPE**

The primary objective of this investigation is to provide design details for the use of precast concrete panels immediately adjacent to skewed expansion joints. One part of this phase of the research project was to investigate the constructability issues surrounding the use of trapezoidal, precast concrete panels at expansion joints in skewed bridge decks. Trapezoidal panels with two different strand patterns were fabricated. Panels with a 45° skew were fabricated by project personnel, and panels with a 30° skew were fabricated by an independent precast concrete supplier. Documentation of the fabrication of trapezoidal panels and other constructed related topics are addressed in a separate thesis by Kreisa (2008). This thesis documents the response of trapezoidal panels used adjacent to skewed expansion joints in bridge decks subjected to point loads, which represent critical pattern loads in the bridge deck.

Five test specimens were constructed using full-scale precast panels and sealed expansion joints. Two skew angles were tested: 30° and 45°. Four of the test specimens were subjected to statically applied loads only, and one specimen was subjected to fatigue loads along the skewed end. The results of the tests are presented in this thesis, as well as recommendations for the use of trapezoidal panels in bridge deck construction.

## **1.3 THESIS OUTLINE**

This thesis is divided into seven chapters. A review of the literature related to the use of precast panels in bridge decks is provided in Chapter 2. A description of the test specimens is given in Chapter 3, and information regarding the test loads and instrumentation is given in Chapter 4. The results of the research are presented in Chapter 5, and a discussion of the results is provided in Chapter 6. Finally conclusions drawn from this research are given in Chapter 7.



## **Chapter 2: Literature Review**

### **2.1 INTRODUCTION**

Prestressed concrete panels are simple and inexpensive to fabricate, so their use in bridge deck construction continues to grow. This chapter provides a discussion of previous research related to the use of prestressed concrete panels in bridge decks. The discussion begins with rectangular panels and then moves to precast panels with skewed ends. Particular emphasis is given to precast panel systems that include a structural cast-in-place topping. Finally the significance of the previous research is discussed.

### **2.2 PRESTRESSED CONCRETE PANELS IN PERPENDICULAR BRIDGES**

The results of six investigations are summarized in this section. Two of the six studies were sponsored by the TxDOT, and one was produced by TxDOT. The other three investigations were performed outside of Texas.

#### **2.2.1 Coselli (2004)**

Traditionally, TxDOT used a thickened cast-in-place detail at expansion joints in prestressed concrete bridges. This is known as the “IBTS” detail. Coselli (2004) studied an alternative detail where precast panels were extended to the expansion joint. Because rectangular precast panels were used routinely in bridge decks in Texas, continuing the panels to the expansion joint was studied as a cost-saving alternative to the IBTS detail.

Full-scale bridge decks with  $0^\circ$  skew were constructed using both the IBTS detail and the precast panels. The precast panel end detail used 4-in. thick prestressed panels with a 4-in. cast-in-place topping. Coselli determined that behavior under service level loads for both end details was comparable and that the reserve capacity of the precast panel end detail was more than sufficient for bridge deck design.

### **2.2.2 Agnew (2007)**

Agnew (2007) expanded the work done by Coselli (2004) by studying the fatigue behavior of prestressed precast panels at expansion joints under positive and negative moment. Specimens with  $0^\circ$  skew were constructed using 4-in. precast panels and a 4-in. cast-in-place topping. Agnew concluded that the precast panel end detail at the expansion joint provided sufficient fatigue strength for routine use in bridge deck design. Agnew also observed that no delamination between the precast panels and the topping slab occurred under fatigue loading. Finally, Agnew noted that the measured response of the precast panel slab end detail did not deteriorate with increased cyclic loading.

### **2.2.3 Dowell and Smith (2006)**

Dowell and Smith (2006) studied the relationship between panel surface roughness and horizontal shear transfer between the topping slab and the prestressed panel. The researchers tested 3½-in. precast panels with a 3½-in. topping. Specimens were simply-supported beams loaded with a single point load at midspan. Panel surface finishes were labeled “coarse broom,” “medium broom,” and “carpet drag” finishes. Dowell and Smith (2006) concluded that all the finishes provided sufficient horizontal shear strength to prevent slip between the panel and topping slab interface, and that if sufficient surface roughness is provided on the top of the panel, the system will perform as a fully-composite cross section.

### **2.2.4 Merrill (2002)**

Merrill (2002) reviewed the use of precast concrete stay-in-place forms in Texas bridge decks. He discussed the benefits and shortcomings of the system. Among the benefits included speed, cost savings, construction safety, and serviceability. The potential problems were longitudinal cracking, transverse cracking, and unique construction considerations. Merrill also addressed specific construction aspects of the system. These aspects involved both panel fabrication and deck construction issues. In particular, Merrill called attention to the consolidation of the concrete under the end of

the panel and the moisture content of the panel before topping placement. If the top surface of the panels is not saturated, surface dry at the time the deck concrete is placed, the panels may pull moisture from the fresh concrete. Overall, Merrill concluded that weaknesses in the system could be minimized by attention to construction details and that rectangular prestressed concrete panels provided very efficient bridge deck systems.

### **2.2.5 Abendroth (1994)**

Abendroth (1994) tested composite bridge deck systems using 2½-in. prestressed panels with 5½-in. cast-in-place toppings. The systems modeled sections adjacent to and away from the abutment. Sections away from the abutment were supported only along the ends of the panels, but sections adjacent to the abutment were supported on three sides – on the ends of the panel (over the beam) and along one end (supported by the abutment). The tops of the panels were roughened with a rake finish. Abendroth studied these systems by monitoring strand slip in the panels, degradation of bond between the panel and topping interface, and distribution of bending strains along the specimen length under HS-20 wheel loads. Abendroth concluded that first strand slip, first interface slip, and first topping slip all occurred at loads greater than twice the design wheel load amplified for impact (20.8 kip). He also noted that the specimens had a significant amount of reserve strength after the initial slip was recorded.

### **2.2.6 Barker (1975)**

Barker (1975) compiled information on three different bridge forming techniques - precast prestressed panels, steel stay-in-place forms, and wood forms. In the study, precast panel systems with the full-depth bridge deck systems were compared. Some panels had raked surface finishes and others had shear reinforcing bars extending above the top of the panel. Barker reported from various tests that no shear reinforcement was needed between the panel and the topping slab for sufficient interface shear capacity. He also reported that the joints between panels did not affect the performance of the system. Overall, Barker reported that precast panel bridge decks provided a very efficient bridge

deck system, streamlining the construction process while maintaining complete structural integrity.

### **2.3 PRESTRESSED CONCRETE PANELS IN SKEWED BRIDGES**

To date, only three researchers have studied the use of precast panels in skewed bridges.

#### **2.3.1 Merrill (2002)**

Merrill (2002) presented the use of prestressed concrete panels as stay-in-place forms in Texas bridge decks, as has already been discussed. However, Merrill also concluded that skewed bridges introduced a level of complexity that required special forming around the expansion joint.

#### **2.3.2 Abendroth (1994)**

Besides the 0° skew tests, Abendroth (1994) also tested precast panels in skewed bridge decks. Trapezoidal panels were fabricated with 15°, 30°, and 40° skew angles. The trapezoidal panels, shown in Figure 2.1, were 2½-in. thick topped with a 5½-in. cast-in-place topping. Prestressing strands were parallel to the perpendicular end of the trapezoidal panel. The edges of the panel were supported by the girders, and the skewed end was supported on the abutment or diaphragm. Abendroth reported that the trapezoidal panels performed satisfactorily under service level loads and that the panels exhibited significant reserve strength beyond the service level design loads. Abendroth noted that the acute corner of the trapezoidal panel was subject to uplift loads due to the shape of the panel and the presence of the diaphragm support under the skewed end.

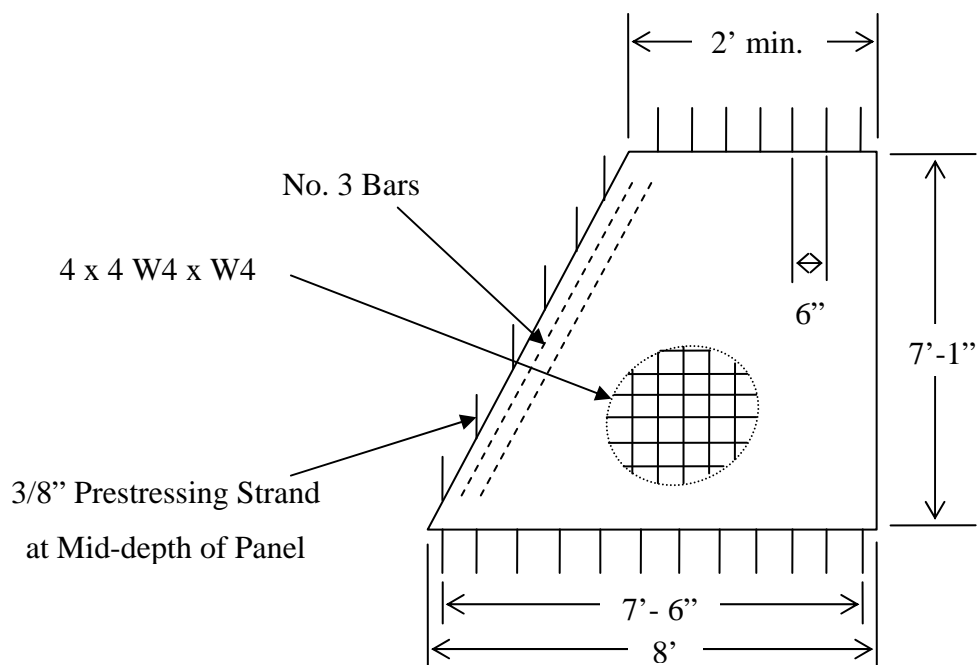


**Figure 2.1 - Trapezoidal Panels for Composite Bridge Deck Systems (Abendroth, 1994)**

### 2.3.3 Barker (1975)

As discussed earlier, Barker (1975) summarized several studies involving the use of precast panels in bridge deck construction. Barker noted that skewed ends could be handled by simply saw cutting one end of a rectangular panel to match the skew of the bridge. The skewed ends of saw cut panels in Barker's report were supported on diaphragms.

## 2.4 RESEARCH SIGNIFICANCE

The use of precast panels as efficient stay-in-place formwork for bridge decks has been successfully applied for several decades. Rectangular panels are inexpensive to fabricate, so their popularity for use in bridge decks continues to grow. The current literature, however, contains little information about the use of skewed panels at expansion joints. Because diaphragms were typically used at span ends in bridge deck

construction and the diaphragm supports the skewed end of the panel, the performance of skewed precast panels along an unsupported expansion joint has not been studied experimentally. Recently, Texas has sponsored research studies on the behavior of unsupported slab ends where precast panels are used in  $0^\circ$  skew situations, but there is little documentation devoted to the behavior of unsupported, skewed precast panel ends at slab ends. The purpose of this research is to study the behavior of unsupported skewed ends of precast panels used immediately adjacent to the expansion joint at ends of bridge decks.

## Chapter 3: Test Specimens

### 3.1 INTRODUCTION

Five test specimens were constructed at Ferguson Structural Engineering Laboratory to study the behavior of skewed prestressed concrete panels under static and fatigue loading when used adjacent to the expansion joint. The test subjects were single-span specimens, consisting of precast panels spanning transversely between longitudinal support beams topped with a cast-in-place slab. This chapter summarizes the preliminary design considerations, material properties, specimen construction, and procedures used to construct the test specimens.

The five specimens were identified using the notation developed by Agnew (2007):

ABCD

where

A is either “P” or “N”. “P” is used when the specimen is subjected to positive moment. “N” is used when the specimen is subjected negative moment. All specimens tested in this phase of the investigation were subjected to positive moment.

B is the angle of the skew. Agnew (2007) tested four specimens with 0° skew. In this phase of the investigation, skew angles of 30° and 45° were considered.

C is “P” for all specimens and refers to the precast deck system.

D refers to the number of the test.

The characteristics of the five specimens tested in this phase of the investigation are summarized in Table 3.1. All skewed specimens were subjected to positive moment.

**Table 3.1 – Characteristics of Skewed Test Specimens**

	Specimen				
	P45P1	P45P2	P45P3	P30P1	P30P2
Skew Angle	45°	45°	45°	30°	30°
No. of Panels	1	2	2	2	2
Skewed Panel Strand Pattern	Fanned	Parallel to Skew	Parallel to Skew	Parallel to Skew	Parallel to Skew
Skewed Panel Fabrication Site	FSEL	FSEL	FSEL	Off-site	Off-site
Long Beam Length	14'-6"	18'-6"	17'-3"	13'-3"	13'-3"
Long Beam Cross Section	12" x 12"	12" x 12"	12" x 12"	16" x 12"	12" x 12"
Short Beam Length	5'	9'-0"	7'-9"	7'-9"	7'-9"
Short Beam Cross Section	12" x 12"	12" x 12"	12" x 12"	16" x 12"	12" x 12"
Beam Clear Spacing	9'-0"	9'-0"	9'-0"	9'-0"	9'-0"
Bedding Strip Type	Foamular Rigid Foam Insulation	Dow Styrofoam Highload 40	Dow Styrofoam Highload 40	Dow Styrofoam Highload 40	Dow Styrofoam Highload 40
Bedding Strip Strength	25 psi	40 psi	40 psi	40 psi	40 psi

### 3.2 PRELIMINARY CONSIDERATIONS

The test specimens were designed to be representative of prestressed concrete bridges in Texas. In all cases, the transverse, centerline spacing between girders was assumed to be 10 ft. The prestressed concrete panel thickness was assumed to be 4 in., and the cast-in-place topping slab thickness was assumed to be 4 in.

Early in the research project, a decision was made to impose loads representative of the HL-93 Design Truck on the test specimens, rather than the HL-93 Design Tandem, which was used in TxDOT Project 0-4418 (Agnew, 2007). Agnew determined analytically that the HL-93 Design Truck induced greater tensile stresses in the bridge deck than the HL-93 Design Tandem for a skew angle of zero. Those results were



extrapolated to skewed bridges, and the research team decided to use the HL-93 Design Truck to test the skewed specimens.

Figure 3.1 shows the HL-93 Design Truck axle arrangement and three possible ways that the axle loads could be applied to the bridge deck. The HL-93 Design Truck axles are far enough apart that deck behavior is only influenced by the axle directly over it. Axle position A induces the largest positive moment in the bridge deck, while axle position C induces the largest negative moment. Agnew (2007) used both configurations for the non-skewed specimens; however, the skewed specimens were subjected to positive moment only.

Agnew (2007) developed finite element models of a full bridge deck and an idealized test specimen that comprised one precast panel, two side beams, and a topping slab. The results indicated that the moments induced in the test specimen for a point load applied at midspan of the end along the sealed expansion joint exceeded those induced in the non-skewed bridge deck under representative loading conditions (Figure 3.1). Therefore, the skewed test specimens were also loaded using a single wheel load at midspan of the end of the sealed expansion joint.

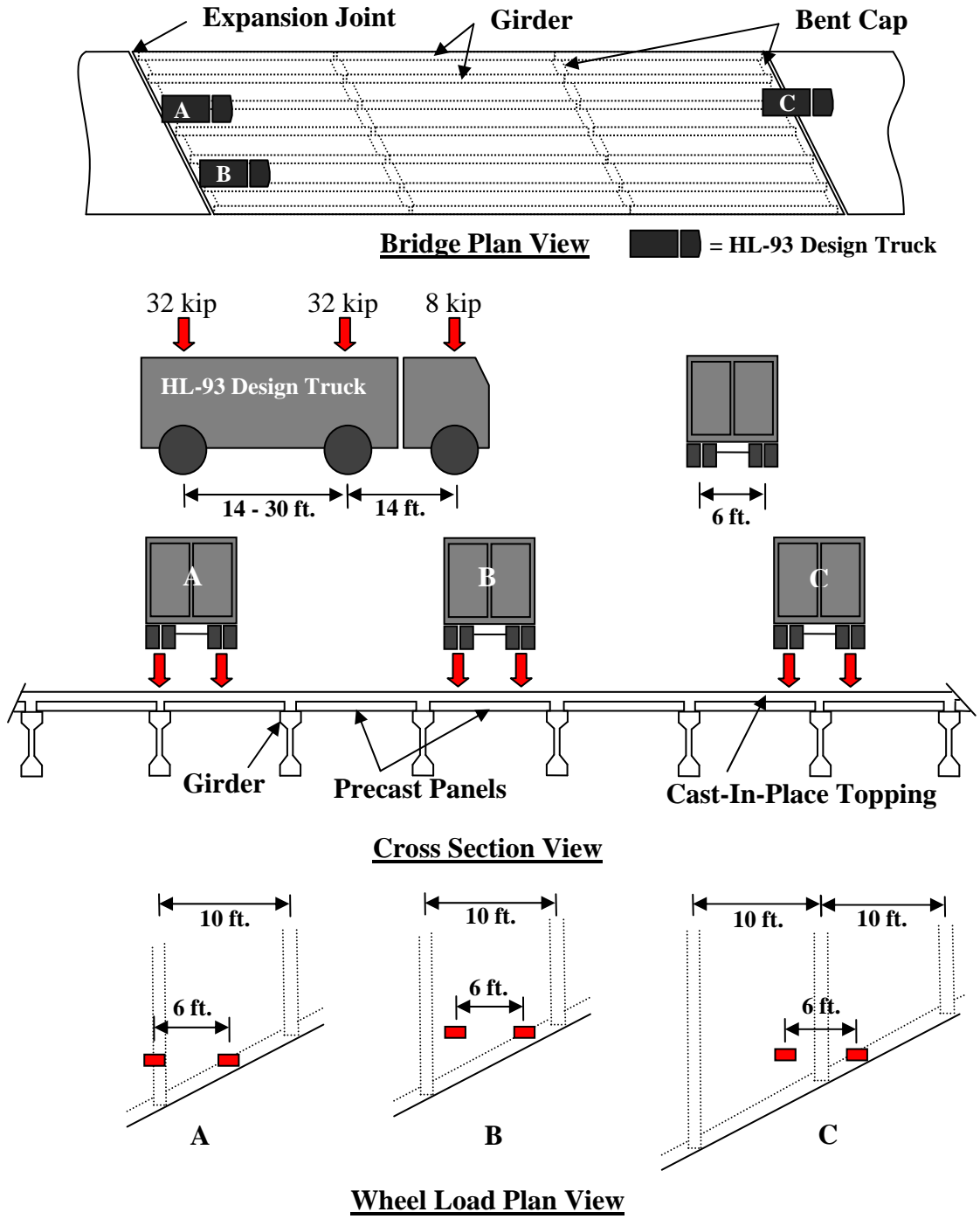


Figure 3.1 – HL-93 Design Truck Loads on Bridge Deck

### **3.3 MATERIAL PROPERTIES**

The characteristics of the concrete, reinforcement, prestressing strand, sealed expansion joint, and bedding strips are summarized in this section.

#### **3.3.1 Concrete**

The concrete used to construct the support beams, precast panels, and topping slab for each specimen was placed at different times. In addition, the mixture design was different for the precast panels than the support beams and topping slabs.

The precast panels were constructed using Type III cement, which is typical of construction practices in commercial precast yards. Because it was not possible to order concrete mixtures with Type III cement directly from local ready-mix suppliers, the aggregate was provided by a ready-mix supplier and the Type III cement and water were added to the mixture at FSEL. The three panels with 45° skew were cast at FSEL using the mixture proportions given in Table 3.2. The mixture design corresponds to a specified 28-day strength of 5000 psi; however, cylinders tested at 28 days were approximately 8000 psi. The 30° panels were cast at a precast yard, and no data are available about the mixture design or the strength of the concrete. A more detailed description of the panel construction is covered by Kreisa (2008).

The support beams and topping slab were cast using TxDOT specifications for Class “S” Structural Concrete. The specified strength is 4000 psi, and the measured 21-day strength was approximately 7000 psi. Current TxDOT specifications require that cast-in-place bridge deck slabs be free of load for 21 days following concrete placement. Therefore, available data for the strength of the concrete in the topping slab at the time of the test for each specimen is provided in Table 3.3. Concrete for the topping slab was provided by a local ready-mix plant. Concrete mixture proportions are reported in Table 3.4.

**Table 3.2 – Precast Panel Concrete Mix Design for Panels Fabricated at FSEL**

Cement	SSD Fine Aggregate	SSD Coarse Aggregate	Water
lb/yd <sup>3</sup>	lb/yd <sup>3</sup>	lb/yd <sup>3</sup>	lb/yd <sup>3</sup>
658	1276	1776	251

**Table 3.3 – Concrete Cylinder Strengths for Topping Slabs at 21-days**

	Specimen				
	P45P1	P45P2	P45P3	P30P1	P30P2
Topping Slab 21-day Strength (psi)	5088	7236	NA	7316	7316

\* Topping slabs for Specimens P30P1 and P30P2 were placed at the same time

**Table 3.4 – Support Beam and Topping Slab Concrete Mix Design**

Cement	SSD Fine Aggregate	SSD Coarse Aggregate	Water	Fly Ash
lb/yd <sup>3</sup>	lb/yd <sup>3</sup>	lb/yd <sup>3</sup>	lb/yd <sup>3</sup>	lb/yd <sup>3</sup>
479	1350	1857	250	85

### 3.3.2 Steel

Grade 60 reinforcement was used to construct the support beams, precast panels, and topping slab. The precast panels were constructed using 3/8-in diameter, grade 270, seven-wire strand.

The sealed expansion joint (SEJ) was fabricated from A36 steel plate. Mill reports indicate a yield strength of 48 ksi. The SEJ-A section was selected, which is 3.5 in. deep with 6 in. studs spaced at 6 in. on center.

### 3.3.3 Bedding Strip Material

The bedding strips are continuous strips of foam that are placed on the top of the beam to support the panels until the topping concrete is placed. The panels extend beyond the bedding strips to allow the topping concrete to flow under the sides of the panel, providing a uniform bearing surface (Figure 3.2). In the field, the bedding strips vary in height along the length of the beam to account for the camber of the prestressed girder, but continuous 2" x 2" strips were used in the test specimens. Bedding strip dimensions are set by TxDOT, as shown in Figure 3.3; the minimum 1-1/2" overhang was used in all test specimens.

Two different materials were used for the bedding strips. Specimen P45P1 was constructed using Foamular Rigid Foam Insulation. The Foamular foam board has a relatively low compressive strength (approximately 25 psi). Although the insulation is not a structural building material, it was used by Agnew (2007) for all test specimens. For specimen P45P1, three, 3/4" x 2" strips of foam were laminated together to make a 2-1/4" tall strip. This proved to be unsatisfactory because the foam compressed excessively after the skewed panel was placed on it.

All other skewed specimens were constructed using Dow Styrofoam Highload 40, which has a compressive strength of approximately 40 psi. This material is commonly used for bridge construction in Texas; however, it also experienced significant distortion when the precast panels were placed on it.

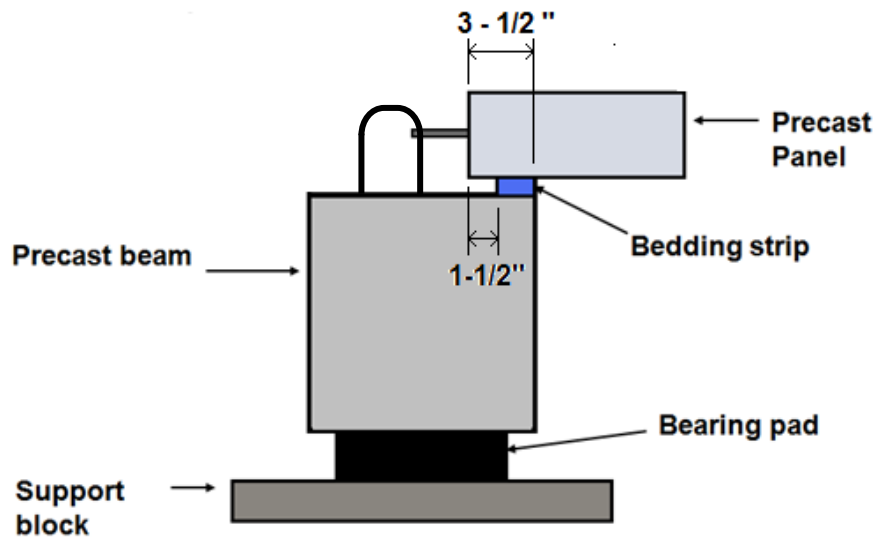
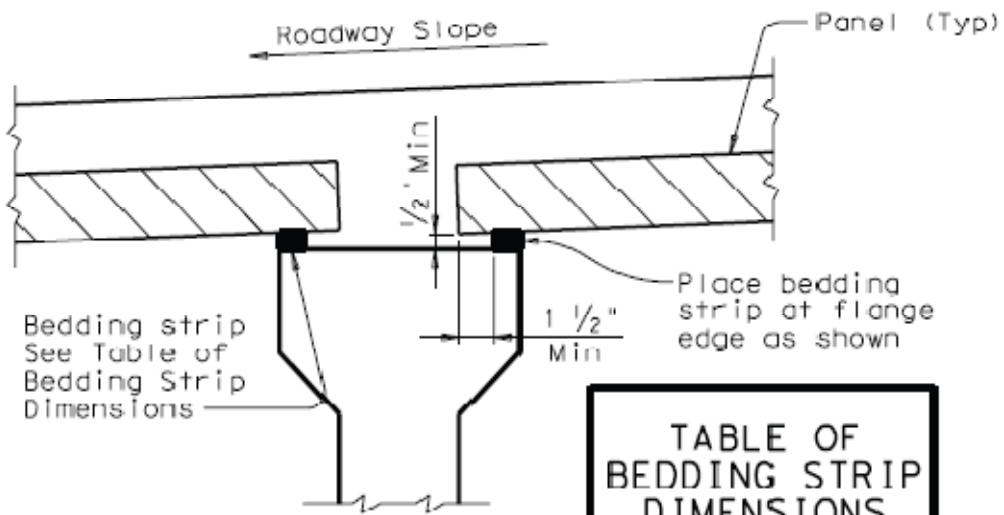


Figure 3.2 – Panel on Bedding Strip



WIDTH	HEIGHT (2)	
	Min	Max
1" (Min)	1/2"	2"
1 1/4"	1/2"	2 1/2"
1 1/2"	1/2"	3"
1 3/4"	1/2"	3 1/2"
2" (Max)	1/2"	4"

Figure 3.3 – TxDOT Bedding Strip Dimensions (TxDOT, 2008)

### 3.4 SPECIMEN CONSTRUCTION

All five test specimens were built following the sequence shown in Figure 3.4. All specimens consisted of the same key elements. TxDOT currently limits the transverse centerline spacing of precast girders to 10'-0"; however, a spacing of 8'-0" is more common. With the introduction of the new cross-sectional shapes for prestressed I-beams in Texas, the centerline spacing of the girders will increase, but the clear spacing between the top flanges will remain constant at 9'-0". Therefore, the longitudinal beams were placed with a clear spacing of 9'-0". Prestressed concrete panels, 4 in. thick, spanned between longitudinal beams, and then a 4-in, cast-in-place topping slab was used to connect the longitudinal components. A summary of the elements in each specimen is provided in Table 3.1.

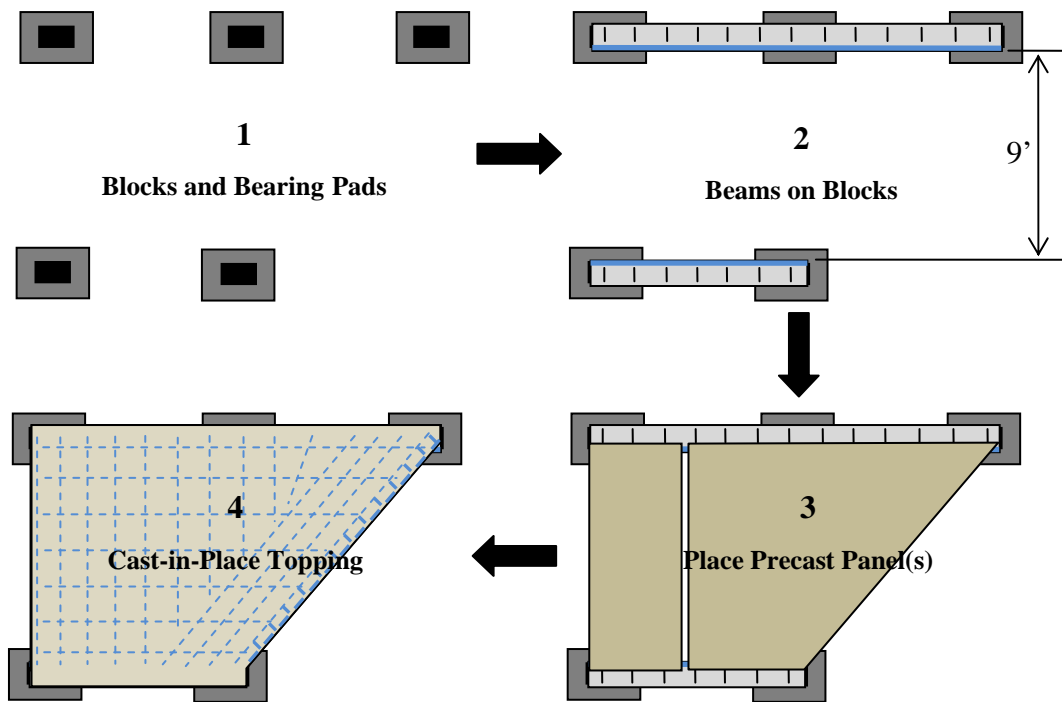


Figure 3.4 – General Specimen Construction

### 3.4.1 Precast Panels Used in Test Specimens

Because the purpose of the tests was to study the behavior of skewed, prestressed panels adjacent to an expansion joint, different configurations of precast panels were tested. All skewed panels were trapezoidal in shape. The skewed end of the panel was precast to be the same angle as the skew of the test specimen and in the field would be the same as the skew angle of the bridge. In this study, two different angles were tested: 30 and 45 degrees. The 45-degree skew was the largest tested because 92% percent of all skewed bridges in Texas have a skew of 45° or less (Van Landuyt, 2006).

While Specimen P45P1 was constructed using a single, skewed panel, the other four test specimens were constructed using two panels: a skewed panel and a rectangular panel. The rectangular panel was used when the strands in the skewed panel were parallel to the skewed end. The reasons for including the rectangular panel are discussed later in this section.

All three 45° panels were fabricated at Ferguson Laboratory by project personnel. The two 30° panels and the four rectangular were purchased from a precast concrete supplier. The configuration of each precast panel is summarized below, but additional information is provided in Kreisa (2008). All precast panels were 4 in. deep with prestressing strands aligned at mid-depth of the panel.

Frequent references will be made to the boundaries of the trapezoidal panels. To reduce confusion, the boundaries of the panel that are supported directly by the beams will be called the “sides” of the panel. Due to the trapezoidal shape of the panels one side is longer than the other. The boundaries of the panel that are not supported by the beams will be called the “ends” of the panel, as shown in Figure 3.5. The skewed end corresponds to the location of the sealed expansion joint. The square end is adjacent to the rectangular panel.



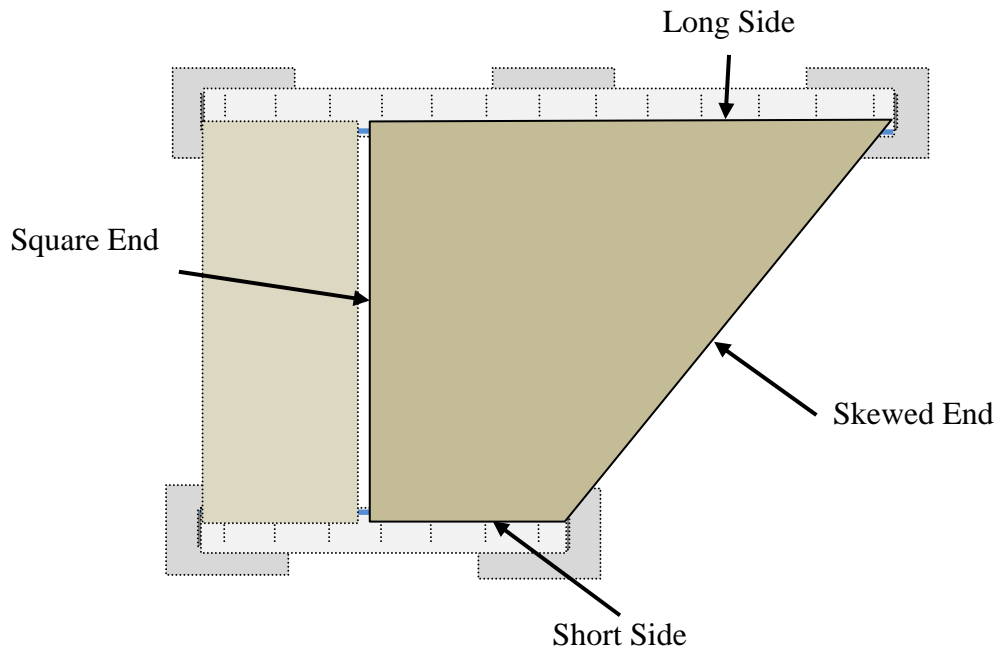


*Figure 3.5 – Definitions of Boundaries in Trapezoidal Panels*

#### **3.4.1.1 45-Degree Panels**

All 45° panels were fabricated at Ferguson Lab. The top surface of the panels was finished with a broom after placement of the concrete. After the initial set, the panels were covered with plastic to promote curing. The skewed, prestressed panel in specimen P45P1 had prestressing strands in a fanned arrangement to provide a distributed prestress force throughout the panel, as shown in Figure 3.6. The 45° panels in Specimens P45P2 and P45P3 have parallel strands spaced at 6 in. on center running in the direction of the skew angle (Figure 3.7 and Figure 3.8). This arrangement leaves a corner in the panel void of prestressing strands because the length of these strands would be insufficient to develop the prestressing force. These corners were reinforced only with mild reinforcement.

While the fanned strand pattern provides a more uniform distribution of prestress forces in the panel, the panels with parallel strands are easier to fabricate, as discussed by Kreisa (2008).

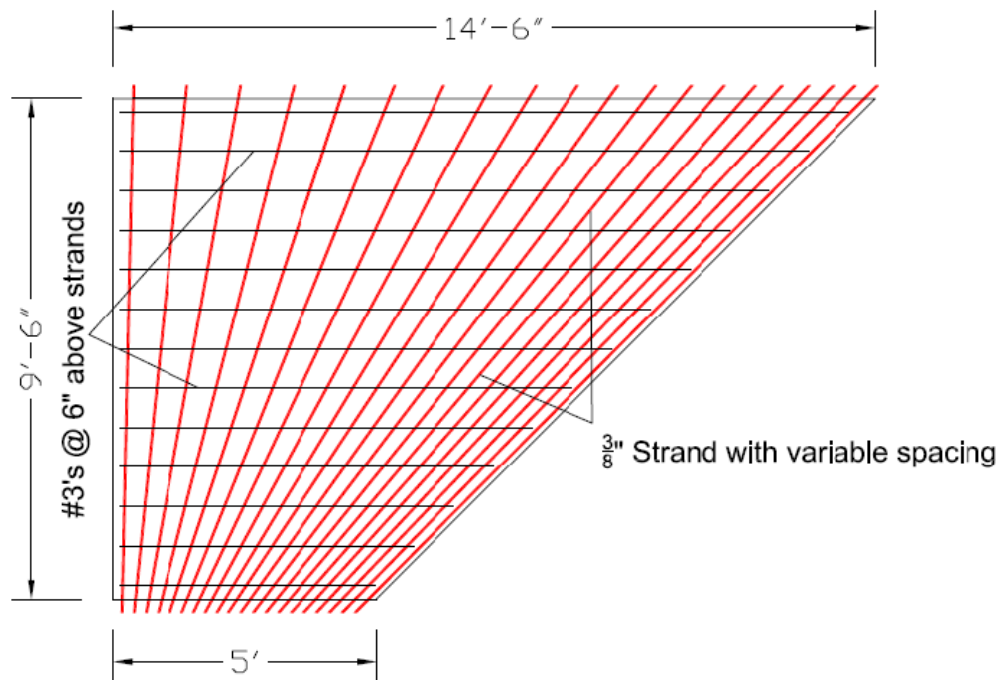


**Figure 3.6 - Skewed Panel Reinforcement for Specimen P45P1**

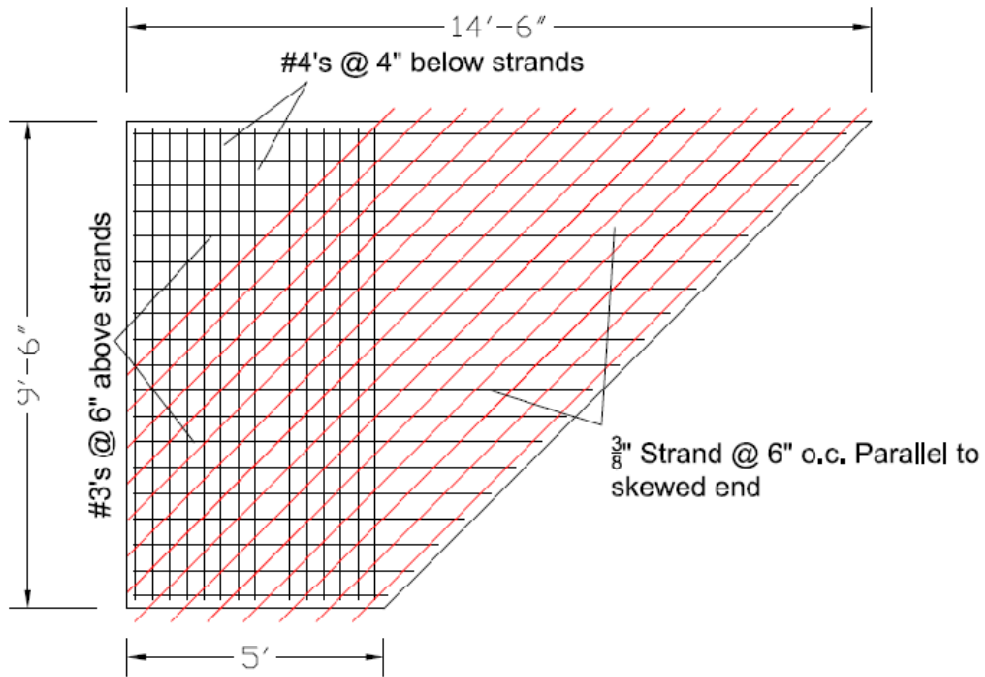


**Figure 3.7 – Skewed Panel Reinforcement for Specimen P45P2**

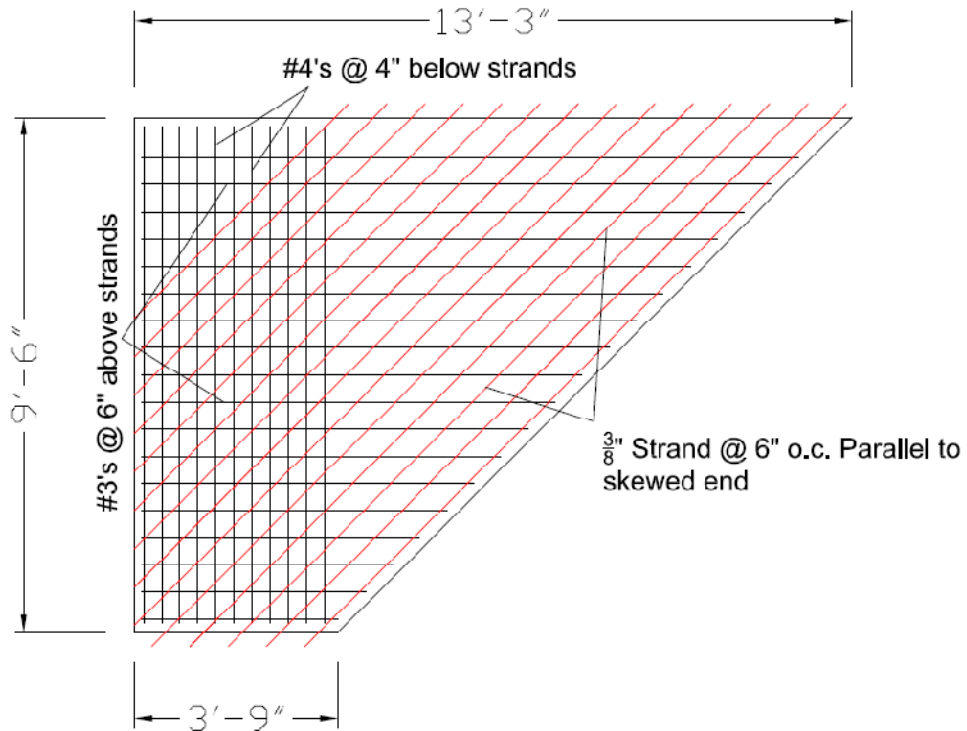


**Figure 3.8 – Skewed Panel Reinforcement for Specimen P45P3**

### 3.4.1.2 30-Degree Panels

Both 30° panels were fabricated by a commercial supplier. The top surface of the panels was finished with a broom after placement of the concrete, and then the panels were flooded to promote curing. Prestressing strands in these panels are equally spaced at 6 in. on center with the strands running in the direction of the skew angle. As with the panels in Specimens P45P2 and P45P3, mild reinforcement was provided in these panels in the corner where no prestressing strands were present (Figure 3.9).

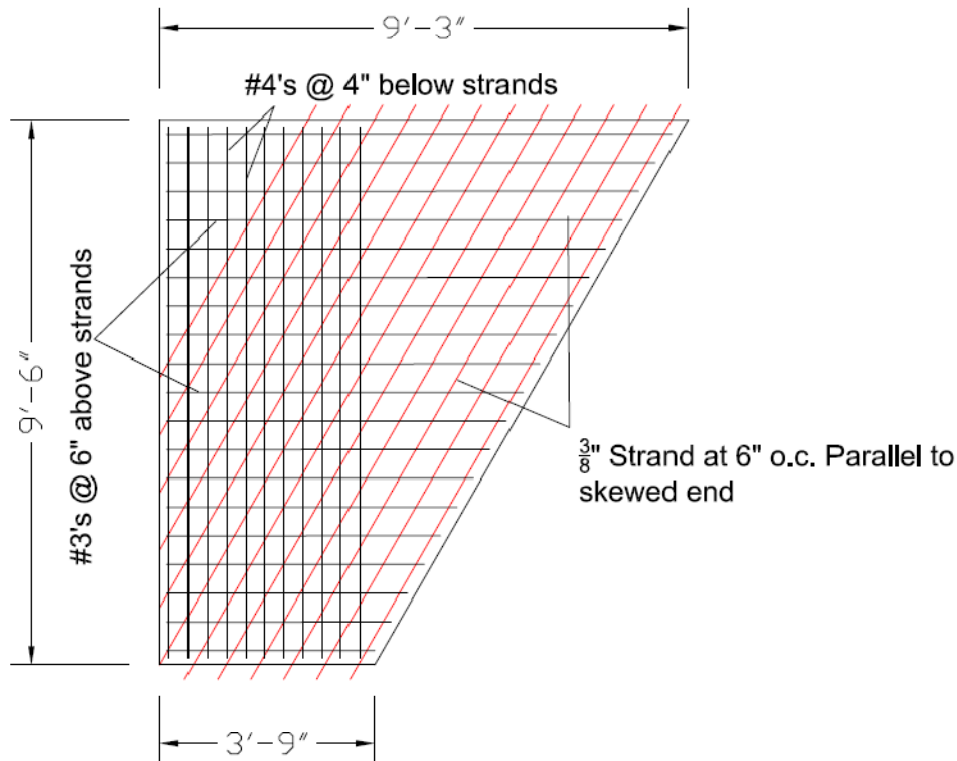


**Figure 3.9 – Skewed Panel Reinforcement for Specimens P30P1 and P30P2**

### 3.4.1.3 Rectangular Panels

For Specimens P45P2, P45P3, P30P1, and P30P2 there was concern about the strength of the panels in the corner bounded by the long side and the square end because no prestressing strands were present. These specimens included a 4-ft, rectangular panel adjacent to the skewed panel. The rectangular and trapezoidal panels were placed next to each other, as shown in Figure 3.10, with a 3/4" gap between them. Then the gap was

filled with a foam backer rod (Figure 3.11). These gaps between panels leave contractors some placement tolerance.

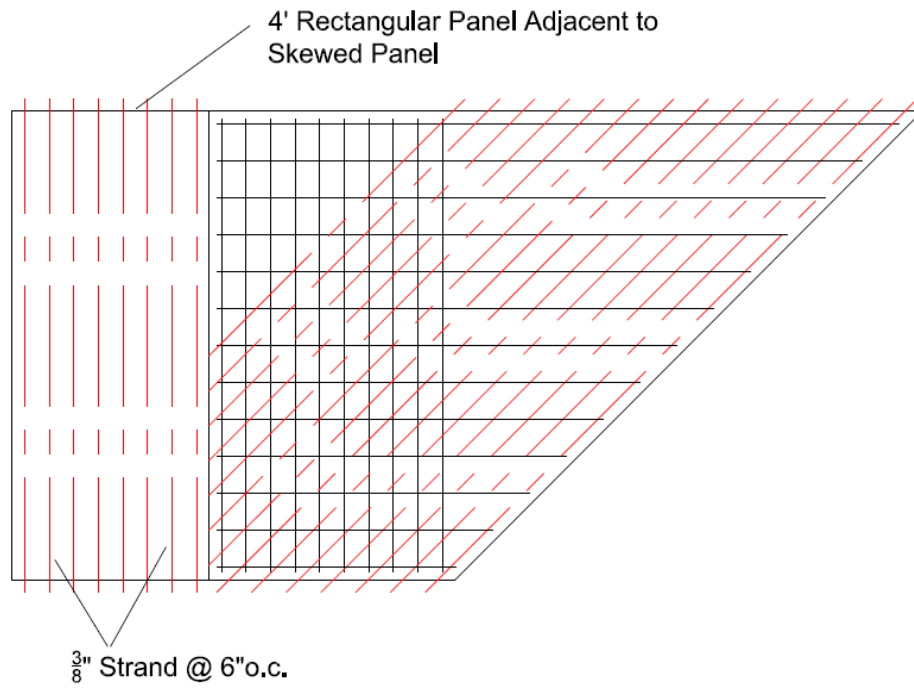


***Figure 3.10 – Alignment of Rectangular and Skewed Panels***

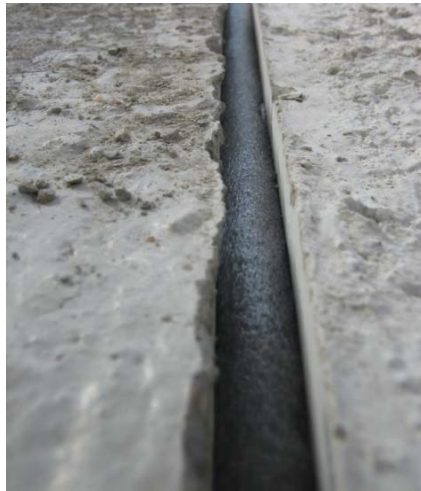


***Figure 3.11 – Backer Rod between Adjacent Panels***

### 3.4.2 Longitudinal Beams

The precast panels described in Section 3.4.1 were supported by reinforced concrete beams with rectangular cross sections. Two beams were used for each specimen – one to support the long side and one to support the short side of the precast panel. The



*Figure 3.12 - Long Side Support Beam (left) and Short Side Support Beam (right)*

long side beam was supported at the ends and in the middle by elastomeric bearing pads resting on concrete blocks. These elastomeric bearing pads measure 9" x 13" x 2-1/2" and model the bearing pads that are used to support prestressed concrete girders in TxDOT bridges. The short side beam was only supported at its ends. Figure 3.12 illustrates the beam configuration. The transverse reinforcement in the beams extended into the cast-in-place topping slab to resist horizontal shear. In the early specimens, these U-bars were oriented square to the longitudinal axis of the beams (Figure 3.2) to simulate the orientation of shear reinforcement in prestressed girders. However, in later specimens, U-bars were rotated 90° (Figure 3.12) to facilitate construction.

### 3.4.3 Cast-in-Place Topping Slab

A 4-in. cast-in-place topping slab was placed on top of the panels and longitudinal beams. Formwork was erected around the beams and panels so that the topping slab would be 4" over the panels and 10" over the beams, as shown in Figure 3.13. Reinforcement was provided in the topping slab to represent standard TxDOT details (Figure 3.14). The vertical leg of the sealed expansion joint rail was fastened to the

inside of the formwork along the skewed end. The top of the SEJ was flush with the top of the finished slab. In some cases, the top of the panels was moistened before the placement of the cast-in-place topping to keep the dry panels from drawing moisture from the freshly placed concrete. Vibrators were used to consolidate the concrete over the longitudinal beams and to help the topping flow under the sides of the panels. The vibrators were also used on the deck portion of the topping slab.

Panel surface roughness also contributes to the interaction between the cast-in-place topping and the panels. However, current panel specifications in Texas do not quantify the level of required surface roughness. The top surface of the panels was brushed with a broom after initial set of the concrete. As will be shown in Chapter 5, the two 30° specimens, which were tested before the last two 45° specimens (Table 3.6), failed by delamination of the panels from the topping slab. The research team concluded that the likely cause of the delamination was the relatively smooth top surfaces of the 30° panels. Consequently, close attention was paid to the surface roughness of the trapezoidal panels for Specimen P45P2 and Specimen P45P3. A summary of the panel surface roughness and moisture level before placement of the topping for each specimen is provided in Table 3.5.

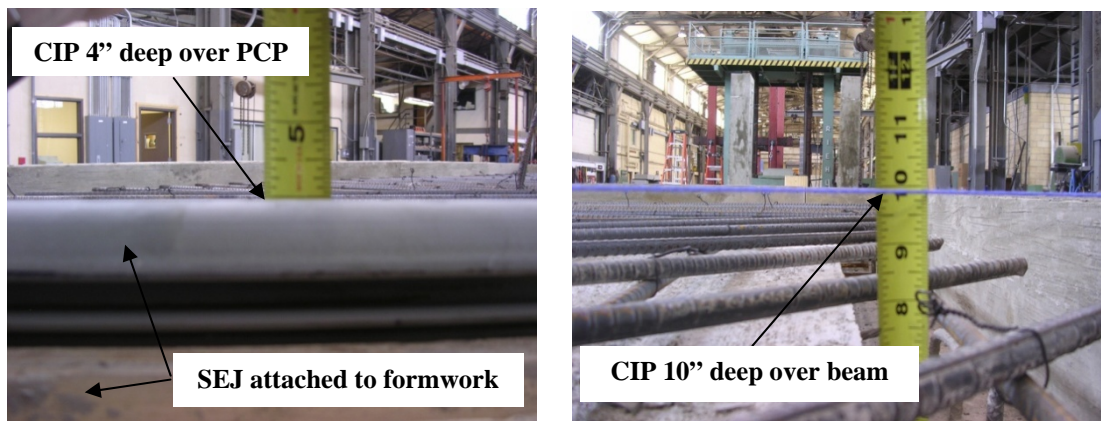


*Figure 3.13 – Formwork for Topping Slab in Position*

Current TxDOT specifications require that cast-in-place bridge deck slabs be free of load for 21 days after concrete placement. Therefore, testing of each specimen began only after a 21-day waiting period following the topping placement. A timeline for the construction and testing of each specimen is provided in Table 3.6. In this investigation, test specimens were covered with a heavy sheet of plastic for 7 days after placement of the concrete to facilitate curing.

**Table 3.5 – Panel Surface Roughness and Wetness before Topping Placement**

	Specimen				
	P45P1	P45P2	P45P3	P30P1	P30P2
Relative Panel Surface Roughness	Rough	Rough	Rough	Smooth	Smooth
Panel Surface Moisture Content	Dry	Wet	Wet	Dry	Dry

**Table 3.6 – Timeline of Specimen Construction and Testing**

	Specimen				
	P45P1	P45P2	P45P3	P30P1	P30P2
Date Panel Cast	9/7/2007	1/10/2007	1/31/2007	11/6/2007	11/6/2007
Date Deck Cast	9/20/2007	1/29/2007	2/20/2007	11/27/2007	11/27/2007
Date of First Test	10/12/2007	2/26/2008	3/19/2008	12/18/2007	12/19/2007
Date of Second Test	-	2/26/2008	4/17/2008	12/18/2007	12/19/2007



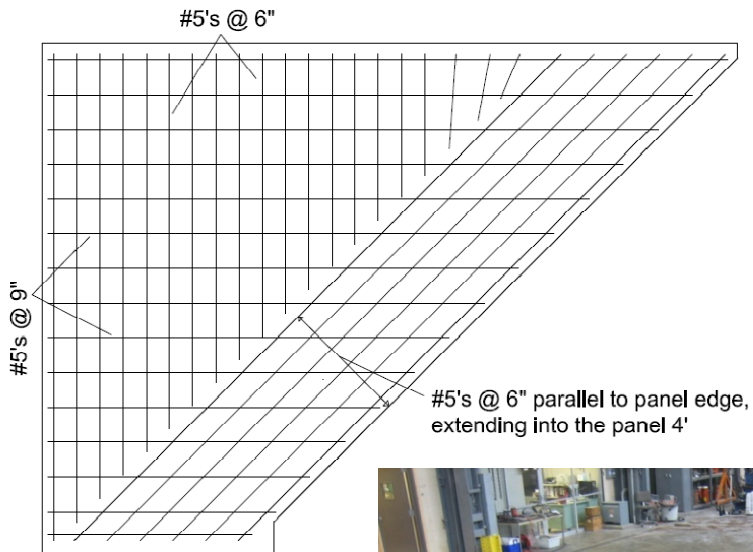


**Figure 3.14 – Cast-in-Place Topping Reinforcement**

### 3.5 SPECIAL CONSTRUCTION CONSIDERATIONS

During construction of the test specimens a few construction issues arose related to excessive compression of the bedding strips under the weight of the trapezoidal panels and the consolidation of the concrete around the studs in the SEJ. They are addressed in this section.

#### 3.5.1 Bedding Strip Compression

Due to the trapezoidal shape of the skewed panels, the stress under the short side is higher than the stress under the long side. As described in Section 3.3.3, two types of bedding strip materials were used. Specimen P45P1 was constructed using laminated strips of foam insulating board. This material crushed under the dead load of the trapezoidal panel along the short side support. In order to get the correct topping slab thickness, the panel in Specimen P45P1 was supported at the correct height using floor jacks. Despite the jacks, the panel shifted slightly during placement of the topping slab resulting in an average overall composite slab depth of 8-3/4".

Higher strength bedding strips were used to construct the other four specimens. However compression of the bedding strips along the short side still occurred, though it was less severe in the 30-degree panels. The compression of the bedding strips resulted in larger slab depths, but the research team determined that the increase in slab depth was acceptable and no attempt was made to modify the slab depth when the 40-psi bedding strips were used. Still, the topic of bedding strip compression may require more study. A summary of the overall slab depths at midspan of the skewed end of each specimen is provided in Table 3.7. More information about the bedding strip compression at the short side support is presented by Kreisa (2008).

**Table 3.7 – Average Overall Slab Depth at Midspan of Skewed End**

	Specimen				
	P45P1	P45P2	P45P3	P30P1	P30P2
Overall Depth at Load Point	8-3/4"	8-3/4"	8-1/2"	8-1/4"	8-1/8"

### 3.5.2 Concrete Consolidation in P45P2

Vibrators were used to consolidate the concrete over the beams and to help the concrete flow under the sides of the panel for each specimen. The vibrators were also used to consolidate the concrete in the deck portion of the topping slab. But despite the use of vibrators, evidence of poor consolidation was visible below the SEJ on P45P2 (Figure 3.15) when the formwork was removed. Since no determination as to the extent of the poor consolidation was possible visually, nondestructive testing techniques,

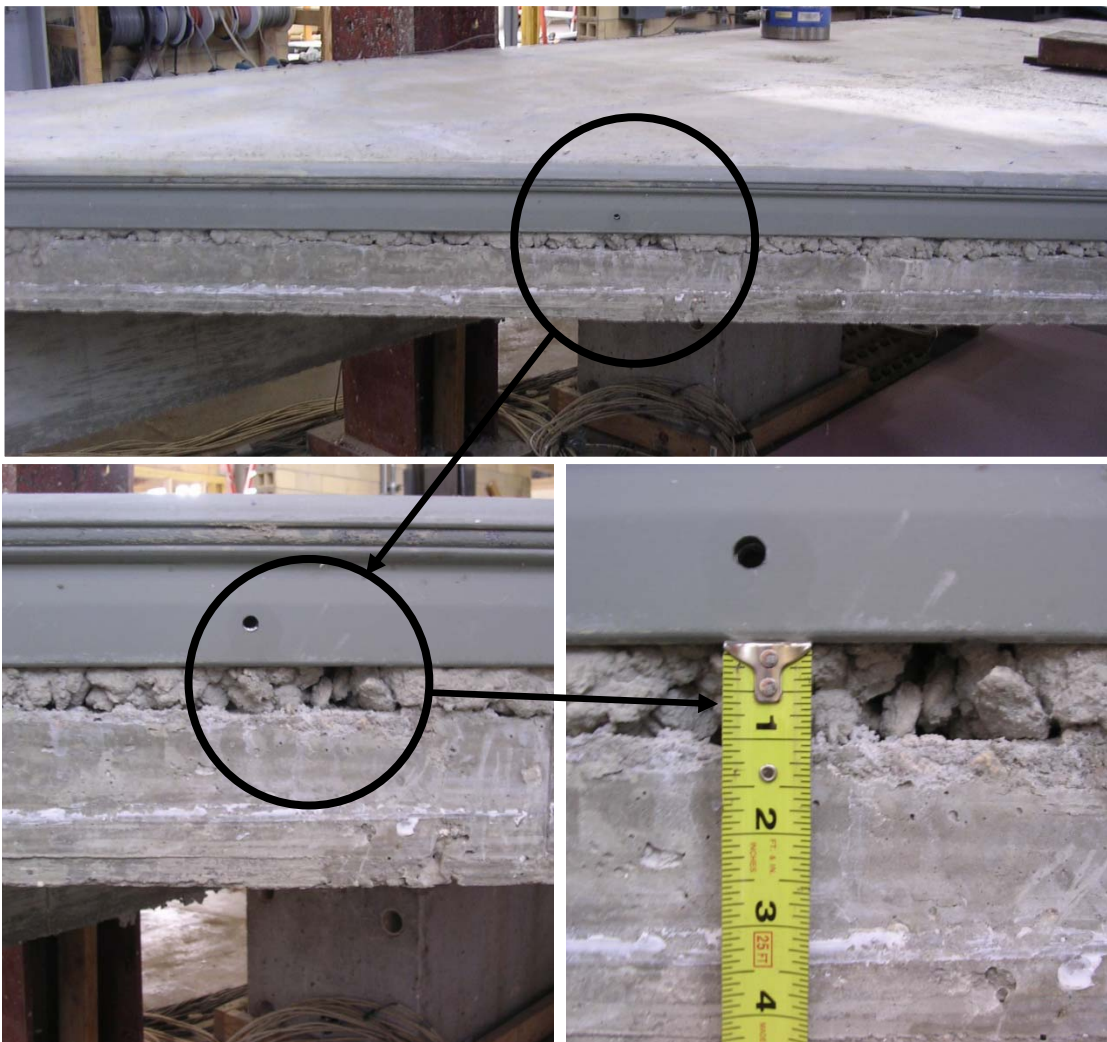


*Figure 3.15 – Poor Consolidation at Expansion Joint of Specimen P45P2*

including both impact-echo testing and ultrasonic testing, were used to determine the extent of the problem.

The results of the nondestructive tests are provided in Appendix A. In summary, it was determined that the extent of the poorly consolidated concrete did not extend into the panel past the studs in the SEJ (Figure 3.16). The specimen was tested without any attempt to repair the area, and the test results, presented in Chapter 5, indicate that the lack of consolidation did not influence the static strength of the specimen.

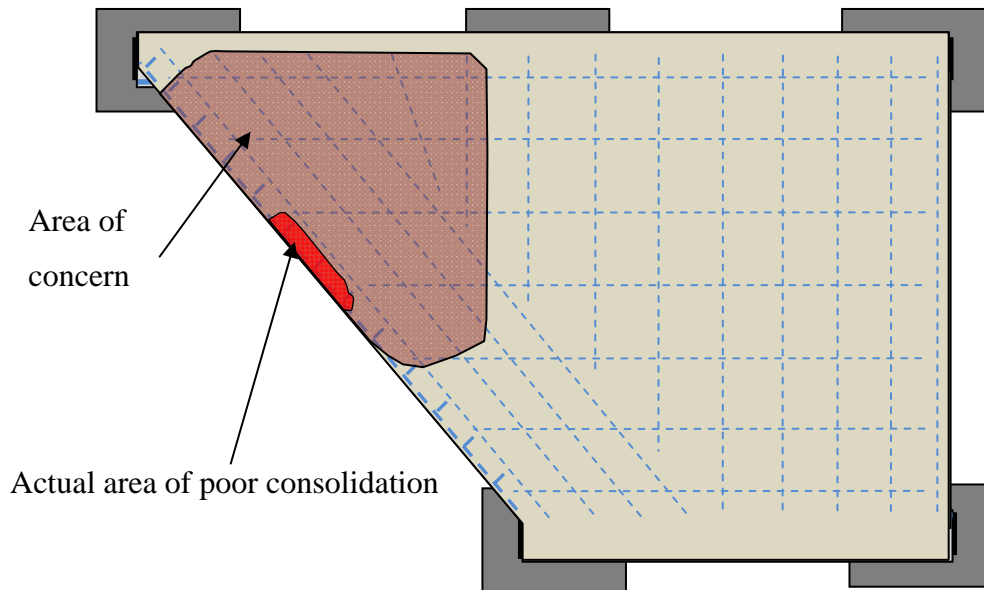


*Figure 3.16 – Extent of Poor Consolidation in Specimen P45P2*

## Chapter 4: Loading and Instrumentation

### 4.1 INTRODUCTION

Two types of loading were used to study the behavior of trapezoidal prestressed panels adjacent to the expansion joint in bridge decks. All specimens were tested statically, and one specimen was tested in fatigue. A summary of the tests performed on each specimen is provided in Table 4.1. This chapter addresses specific issues relating to the loading such as load plate locations and the fatigue load program. The instrumentation used to measure the behavior of these specimens under the applied loading is also presented.

The purpose of the tests was to study the behavior of *skewed* panels adjacent to expansion joints in bridge deck systems. Therefore, the loads were applied to the cast-in-place deck above the skewed prestressed panel. The “ends” used to define the location of the applied load refer to the skewed and square ends of the skewed panel, even when the test specimens included a rectangular panel.

**Table 4.1 – Applied Loads to Test Specimens**

	Specimen				
	P45P1	P45P2	P45P3	P30P1	P30P2
No. of Tests	1	2	2	2	2
Test 1 Location	Skewed End	Skewed End	Skewed End	Skewed End	Skewed End
Test 1 Type	Static	Static	Fatigue	Static	Static
Test 2 Location	NA	Non-skewed End	Skewed End	Non-skewed End	Non-skewed End
Test 2 Type	NA	Static	Static	Static	Static
Date of Test 1	10/12/2007	2/26/2008	3/19/2008	12/18/2007	12/19/2007
Date of Test 2	NA	2/26/2008	4/17/2008	12/18/2007	12/19/2007

## **4.2 SPECIMEN LOADING**

The two types of load, static and fatigue, used to study the behavior of the trapezoidal panels are discussed in this section. Because all specimens were tested under monotonically increasing static loads, the static tests are discussed first. Specimen P45P3 was also subjected to fatigue loading, which is discussed in Section 4.2.2.

### **4.2.1 Static Loading**

#### ***4.2.1.1 Loading Setup***

A simple portal frame was used to apply the vertical loads to the test specimens (Figure 4.1). The columns were tied to the strong floor using four, 3/4-in. threaded rods, and the cross beams comprised two, W-sections bolted to the flanges of the columns.

A 150-ton hydraulic ram was secured to the bottom flanges of the cross beam and a 100-kip load cell was used to measure the applied load. A steel plate (10 in. wide by 20 in. long by 2.5 in. thick) was positioned on top of an elastomeric bearing pad (Figure 4.2) to simulate the bearing area of a wheel from the HL-93 Design Truck.

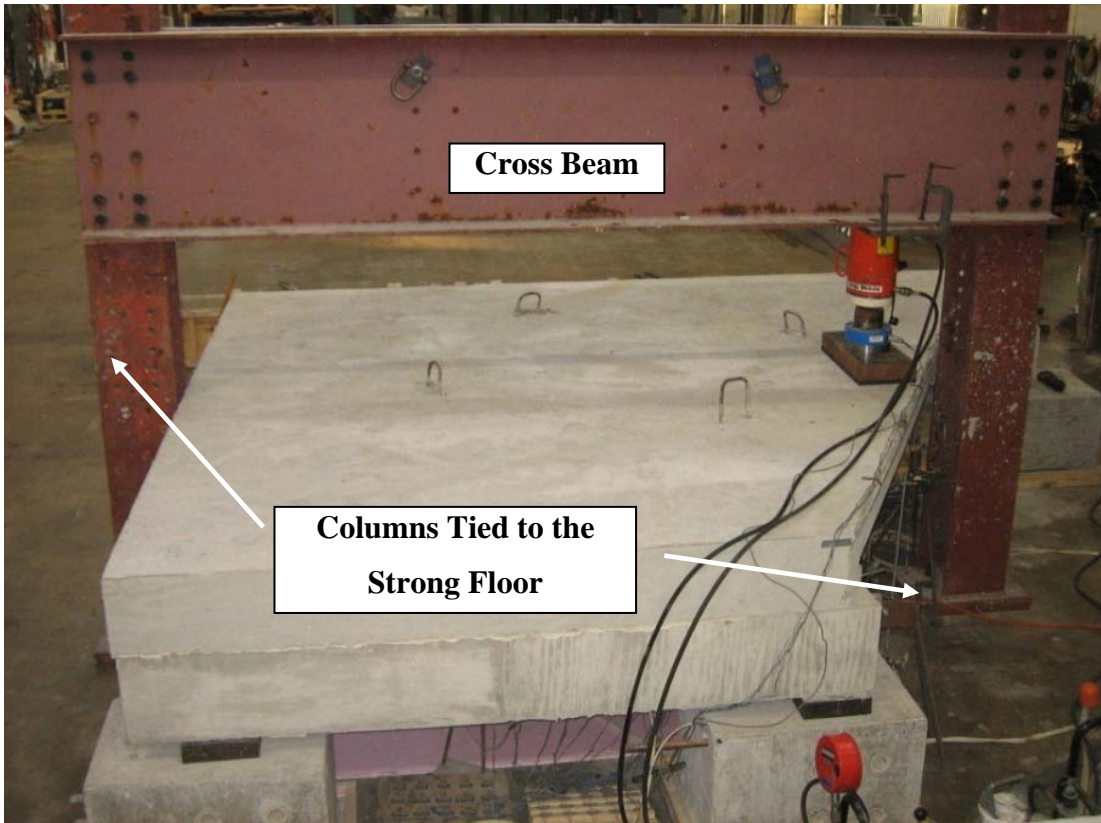


*Figure 4.1 – Load Frame for Static Load Application*



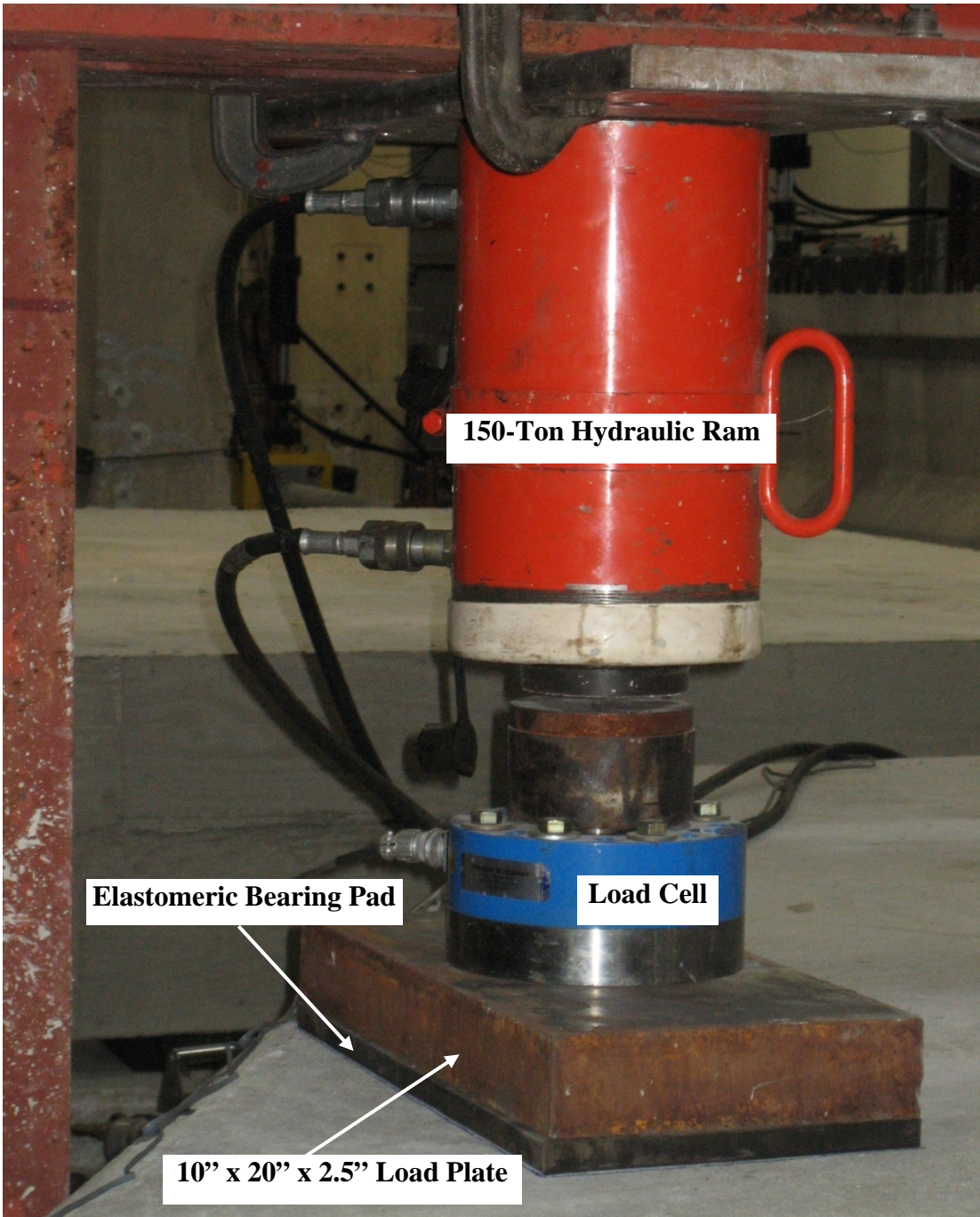


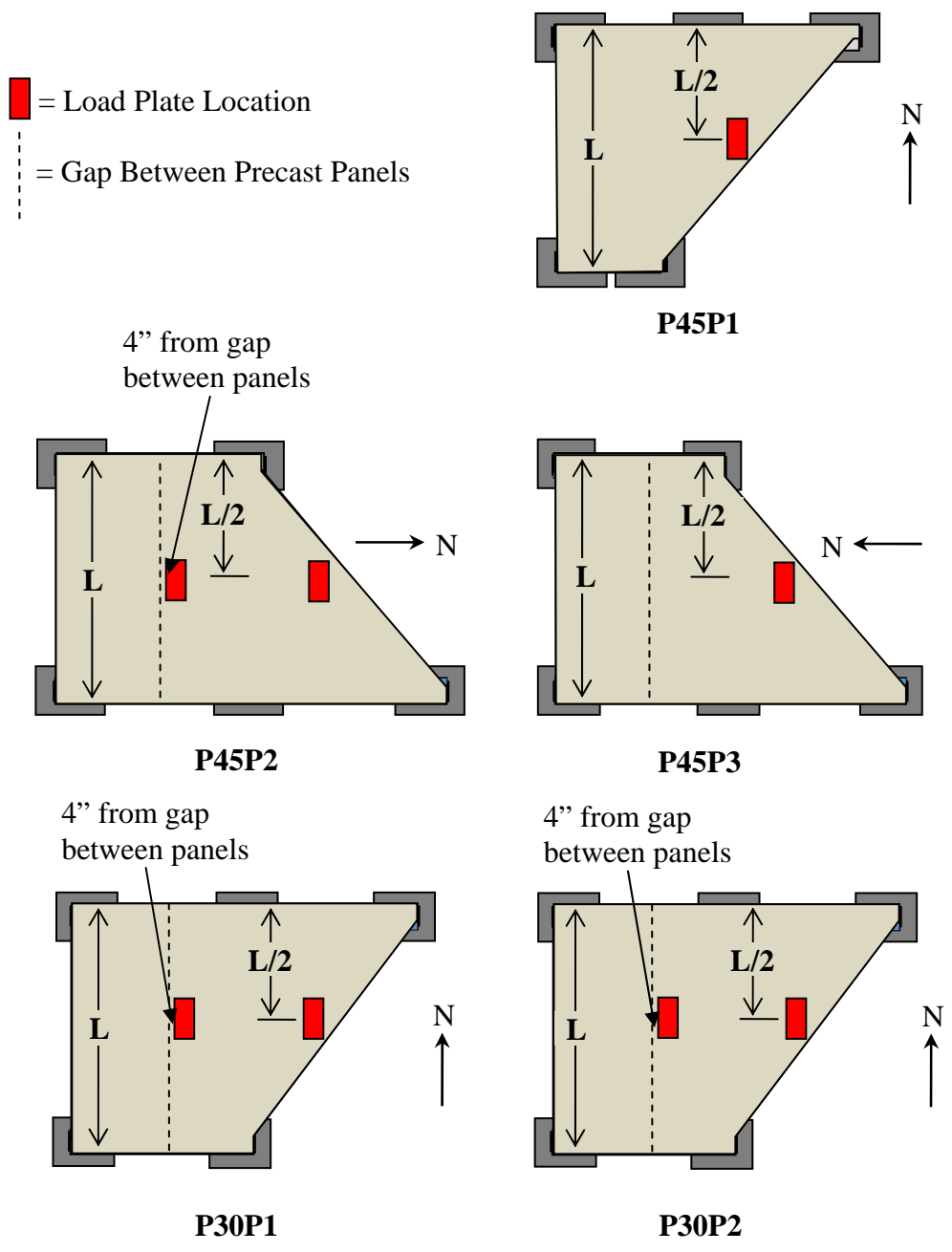
*Figure 4.2 – Hydraulic Ram, Load Cell, and Load Plate for Specimen Loading*



#### ***4.2.1.2 Load Application***

Static loads were applied in small increments (between 5 and 8 kip) at the locations shown in Figure 4.3. P45P1 and P45P3 were loaded only at midspan of the skewed end. P30P1 was the first specimen to be loaded at both the skewed and square end of the skewed precast panel. The specimen was loaded to failure along the skewed end first, and then was loaded to failure along the square end. Originally, the research team planned to test specimen P30P2 using the opposite sequence: test the square end first and then the skewed end. However, Specimen P30P1 failed by delamination, which was unexpected. Therefore, specimen P30P2 was tested using the same loading sequence to verify the results from Specimen P30P1.

When loads were applied to the skewed end of the specimens, the load plate was positioned so that the entire area of the plate was on the concrete. The load plate did not overlap the SEJ. For loads applied over the square end of the trapezoidal panels, the load plate was positioned 4 in. from the gap between the adjacent precast panels. This position was selected to apply the entire load to the non-prestressed corner of the trapezoidal precast panel. The research team estimated that the effective width of the load would increase linearly with depth below the load plate. Since the topping slab was nominally 4 in. thick, the load plate was positioned 4 in. away from the gap between the panels (Figure 4.4).



**Load Plan View**

*Figure 4.3 – Load Plate Positions on Test Specimens*

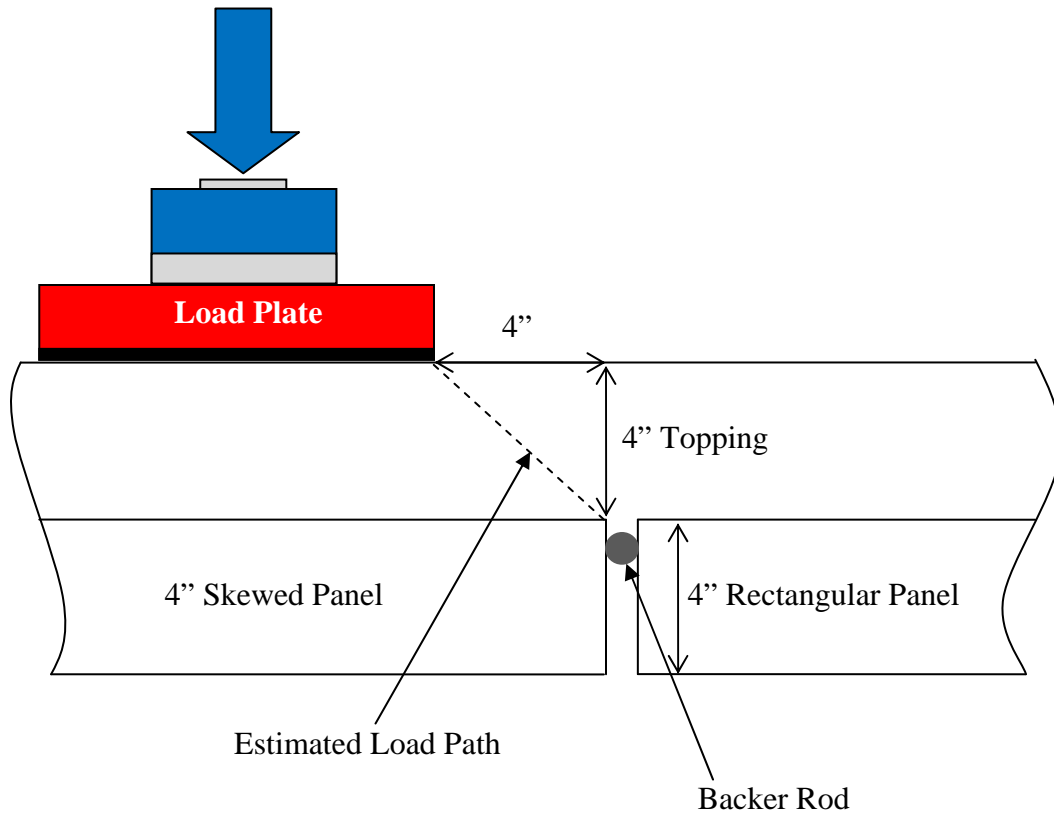


**Figure 4.4 – Load Plate Position over Square End of Skewed Precast Panel**

## 4.2.2 Fatigue Loading

### 4.2.2.1 Loading Setup

The same loading frame used for the static tests was used for the fatigue test of Specimen P45P3. A 50-kip, MTS hydraulic actuator was used to apply the cyclic loading (Figure 4.5). The actuator had a 10-in. stroke and an internal load cell.



*Figure 4.5 – MTS Hydraulic Actuator*

### 4.2.2.2 Load Application

The fatigue loads were applied at midspan of the skewed end of Specimen P45P3. The procedures used by Agnew (2007) were used for this test, except the frequency of the applied load was slightly lower. The fatigue load is characterized by the set point, the span, and the frequency. The set point defines the mean load. The span represents the maximum deviation from the set point, and the frequency is the number of complete loading cycles in one second. In the case of P45P3, the set point and span were set to match the wheel load from the HL-93 Design Truck – 16 kip. That is, the set point was 9 kip, and the span was +/- 8 kip so that the applied load cycled between 1 and 17 kip. The loading frequency was 2.5 Hz. Load limits were set to keep the specimen from being

overloaded. The upper and lower load limits were 17.8 and 0.2 kip, respectively. A summary of these parameters with a plot of the input and feedback signals is provided in Figure 4.6.

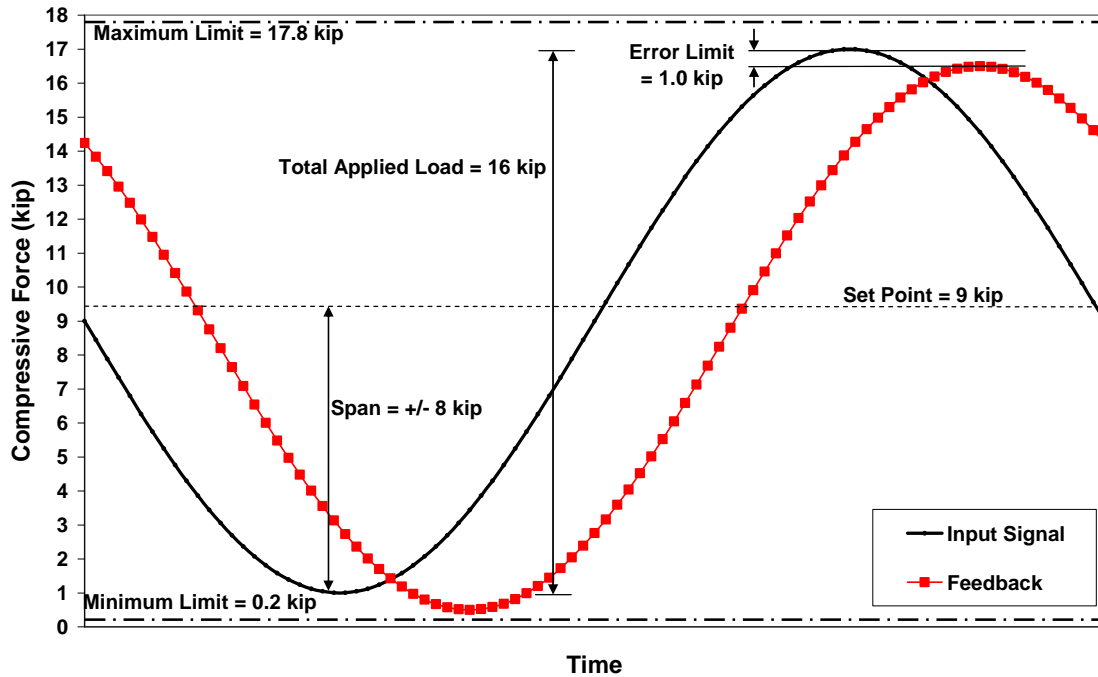


**Figure 4.6 – Fatigue Loading Input and Feedback Signal**

Throughout the fatigue loading, static tests to 16 kip were used to monitor any change of stiffness of the specimen. In order to determine the initial stiffness of the system, P45P3 was tested statically to 16 kip. P45P3 was then subjected to 2 million fatigue cycles, with the stiffness monitored every 250,000 cycles. After 2 million cycles, the specimen was loaded statically to 42 kip to simulate cracking from an overload event. The specimen was then subjected to another 2 million fatigue cycles, before loaded monotonically to failure.

### 4.3 INSTRUMENTATION

Several types of instruments were used to measure the response of the test specimens under the applied loads. Strain gages were used to measure the changes in strain on the bottom surface of the concrete panels, in the SEJ, in the strand in the panels,

and in the rebar in the panels. The concrete strain gages were 60-mm long, while all the strain gages used on steel (rebar, strand and SEJ) were 5-mm long. Linear potentiometers and dial gages were used to measure vertical deflections. A summary of the number of each type of instrument for each specimen is provided in Table 4.2. This section is divided by specimen to present the instrumentation used in each test.

**Table 4.2 – Instrumentation Quantities for Each Specimen**

	Specimen				
	P45P1	P45P2	P45P3	P30P1	P30P2
Concrete Strain Gages	9	6	6	19	19
Rebar Strain Gages	0	6	6	0	0
Strand Strain Gages	0	14	12	0	0
SEJ Strain Gages	3	3	3	3	3
Linear Potentiometers	3	8	5	5	5
Dial Gages	2	0	0	0	0

### 4.3.1 Specimen P45P1

#### 4.3.1.1 Strain Gages

Strain gages were used to measure strain on the bottom of the precast panel and strain on the top surface of the SEJ. The concrete strain gages are labeled in Figure 4.7, and the SEJ gages are shown in Figure 4.8. All the strain gages were spaced 24" on center starting from the skewed end. Strain gages were attached to the strands in the panel when the panel was fabricated, but they were damaged during panel fabrication. Therefore, no data were collected during the static test.

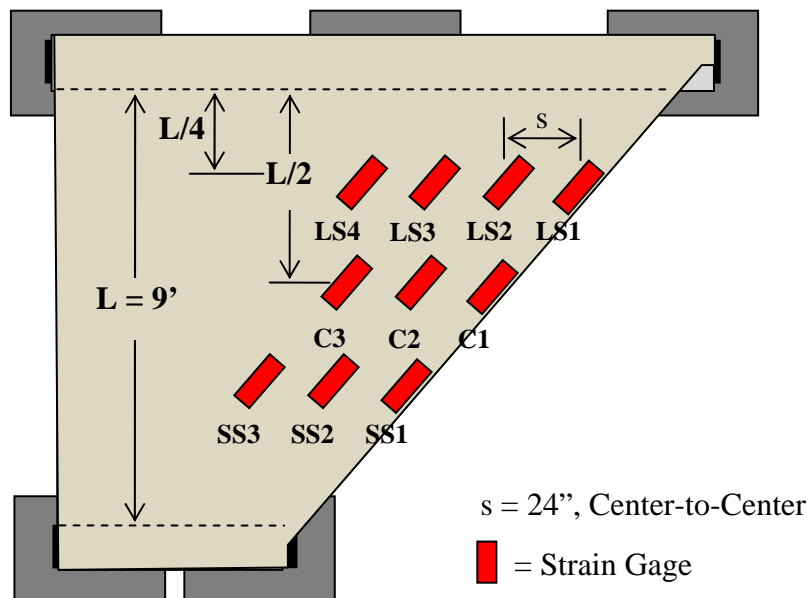


*Figure 4.7 – Concrete Strain Gage Locations and Labels for Specimen P45P1*

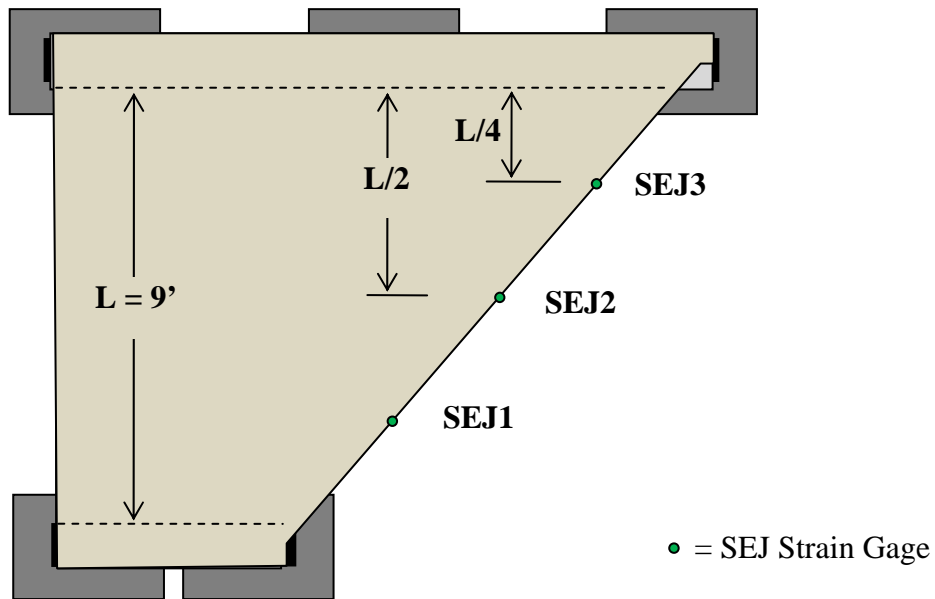


*Figure 4.8 – SEJ Strain Gage Locations and Labels for Specimen P45P1*

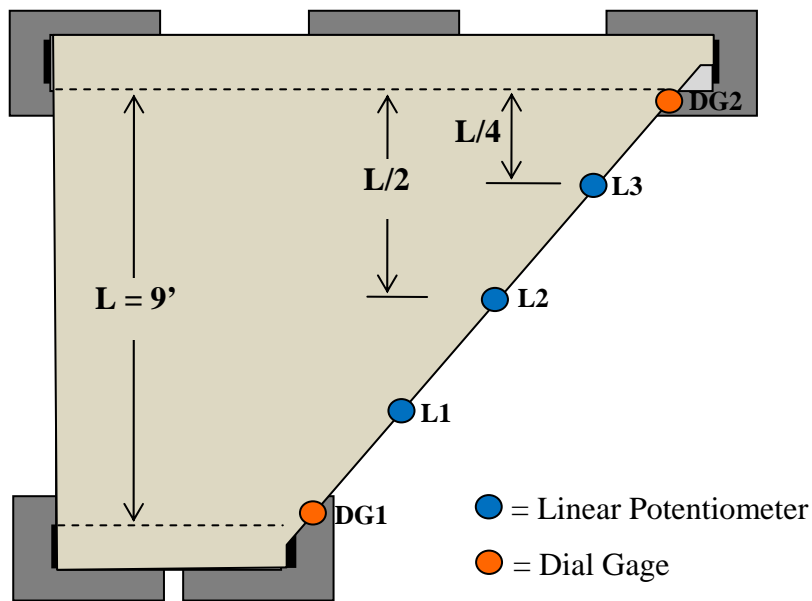


*Figure 4.9 – Linear Potentiometer and Dial Gage Locations and Labels for Specimen P45P1*



#### 4.3.1.2 Linear Potentiometers

Vertical deflections were measured using 2-in. linear potentiometers at the locations shown in Figure 4.9. For Specimen P45P1, dial gages were used to track the deflection of the panels at the supports. Measurements were taken at 5-kip intervals.

### 4.3.2 Specimen P45P2

#### 4.3.2.1 Strain Gages

Fewer concrete strain gages were used to measure the response of Specimen P45P2 than P45P1, but the specimen had strain gages on the strands. Also the two rebar in the trapezoidal panel closest to the square end were also instrumented with strain gages. The prestressing strands were instrumented in the center of the strand. The locations and labels of the strain gages for P45P2 are provided in Figure 4.10 through Figure 4.14.

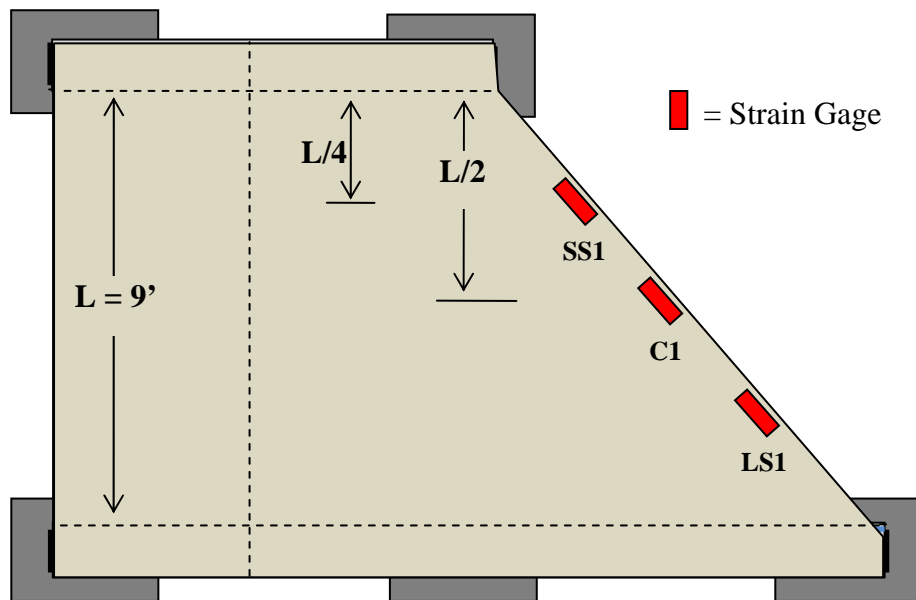


**Figure 4.10 – Concrete Strain Gage Locations and Labels for Specimen P45P2 for Load Applied at Midspan of Skewed End**

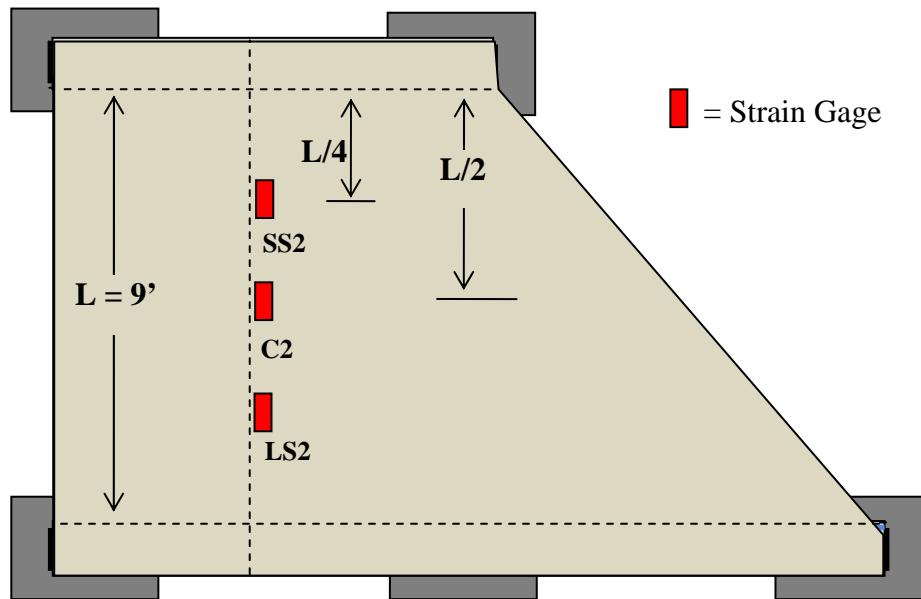


*Figure 4.11 – Concrete Strain Gage Location and Labels for Specimen P45P2 for Load Applied at Midspan of Square End*

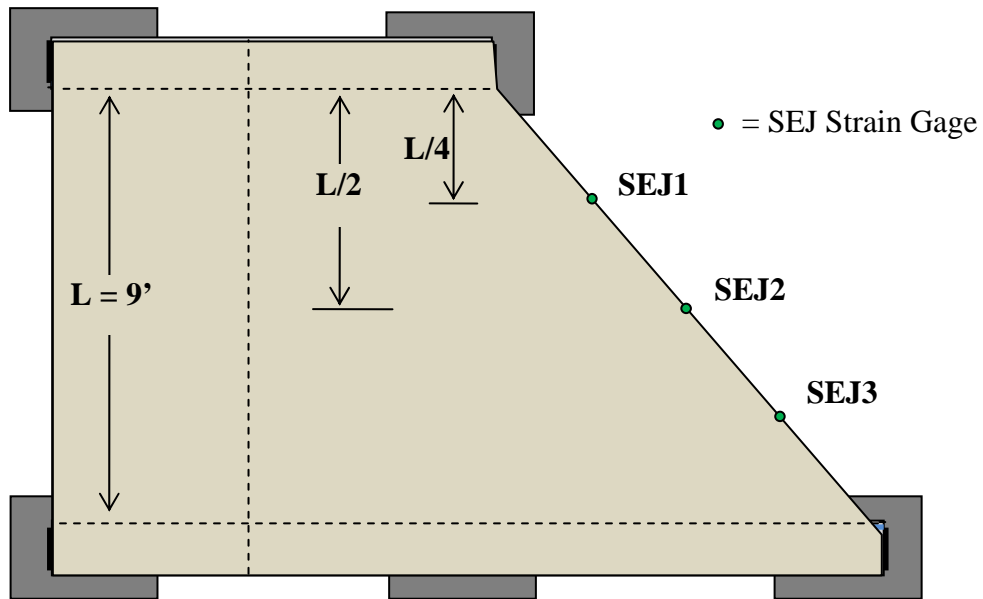
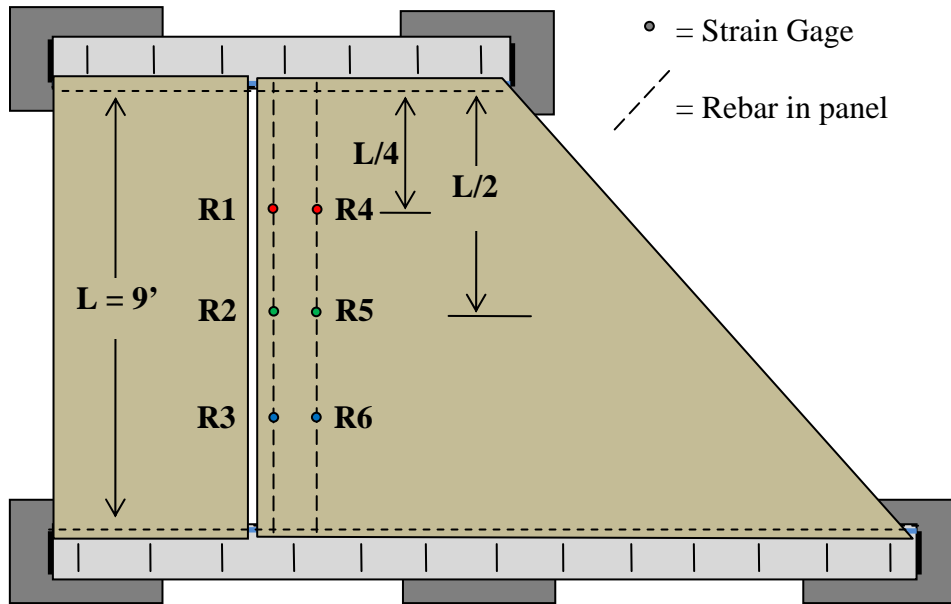
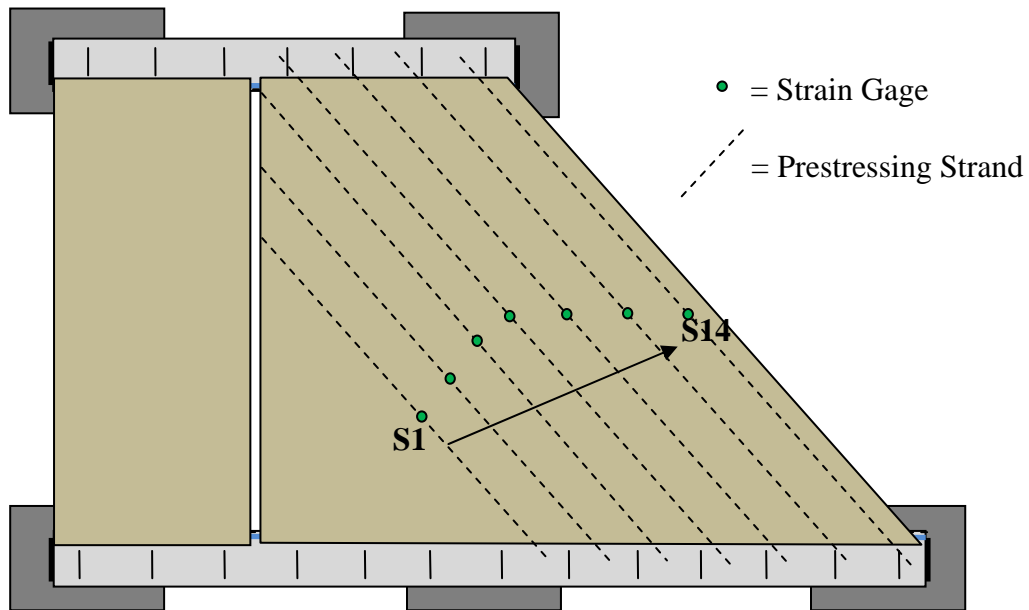


*Figure 4.12 – SEJ Strain Gage Locations and Labels for Specimen P45P2 for Load Applied at Midspan of Skewed End*



\* Not all panel reinforcement shown for clarity

**Figure 4.13 – Rebar Strain Gage Locations and Labels for Specimen P45P2 for Load Applied at Midspan of Square End**



\* P45P2 Contained 14 Strands. Not all panel reinforcement is shown for clarity

**Figure 4.14 – Strand Strain Gage Locations and Labels for Specimen P45P2 for Load Applied at Midspan of Skewed End**

#### 4.3.2.2 Linear Potentiometers

Five linear potentiometers were used to measure the deflection response of Specimen P45P2 when loaded at midspan of the skewed end. Eight linear potentiometers were used when the specimen was loaded at midspan of the square end. The locations and labels of the linear potentiometers are provided in Figure 4.15.

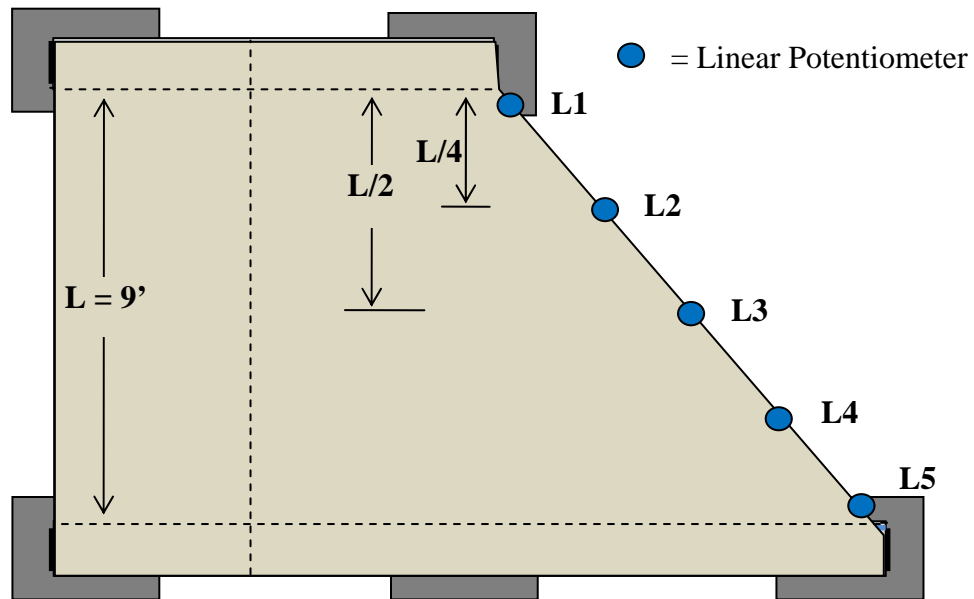


*Figure 4.15 – Linear Potentiometer Locations and Labels for Specimen P45P2 for Load Applied at Midspan of Skewed End*

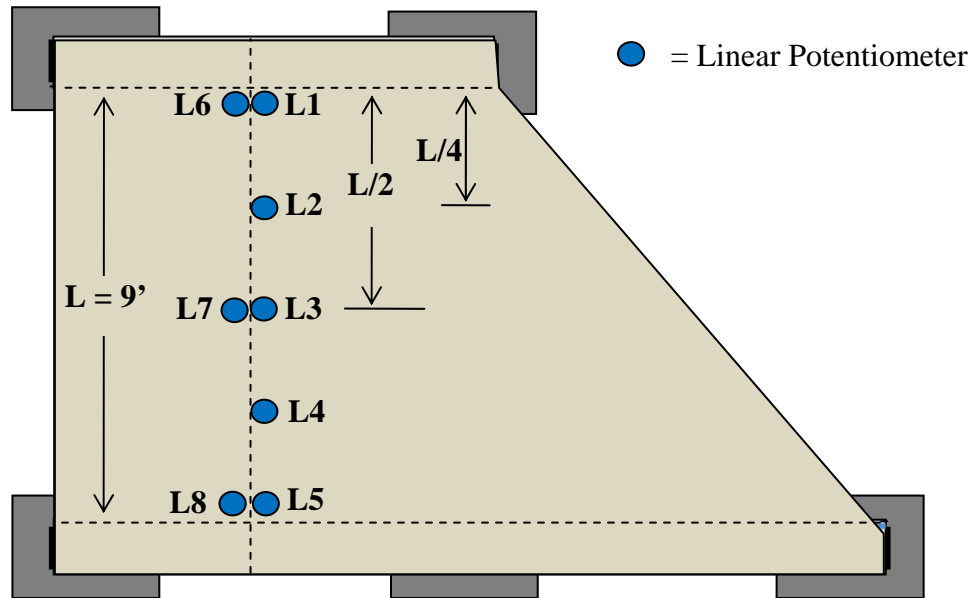


*Figure 4.16 – Linear Potentiometer Locations and Labels for Specimen P45P2 for Load Applied at Midspan of Square End*

### 4.3.3 Specimen P45P3

#### 4.3.3.1 Strain Gages

The instrumentation for Specimen P45P3 was very similar to Specimen P45P2. The trapezoidal panel in Specimen P45P3 was shorter and, therefore, contained two fewer prestressing strands. So the strand gage numbering only went through S12. Other than this difference, the instrumentation was the same. Locations and labels for the strain gages in Specimen P45P3 are presented in Figure 4.17 through Figure 4.19.

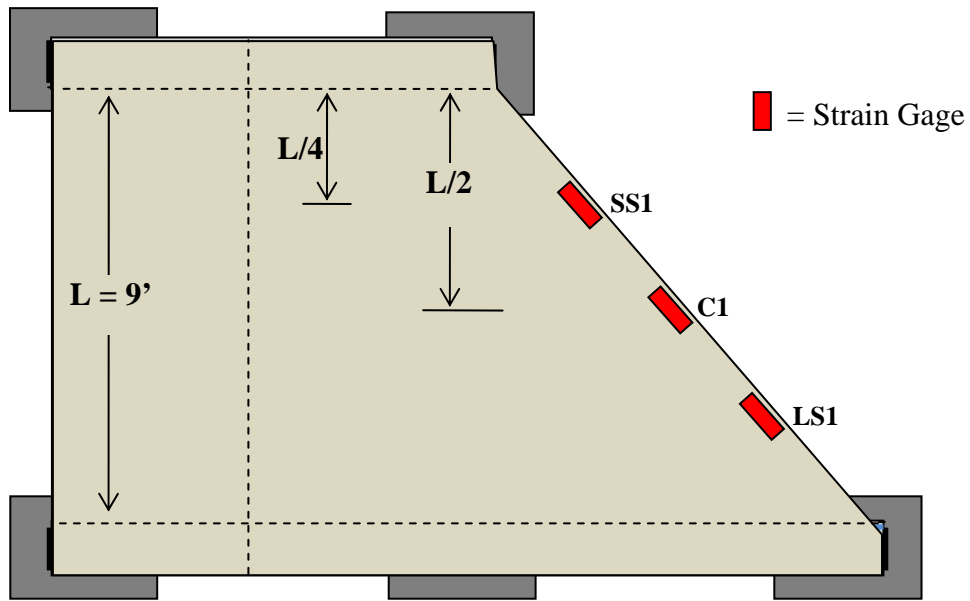


*Figure 4.17 – Concrete Strain Gage Locations and Labels for Specimen P45P3 for Load Applied at Midspan of Skewed End*

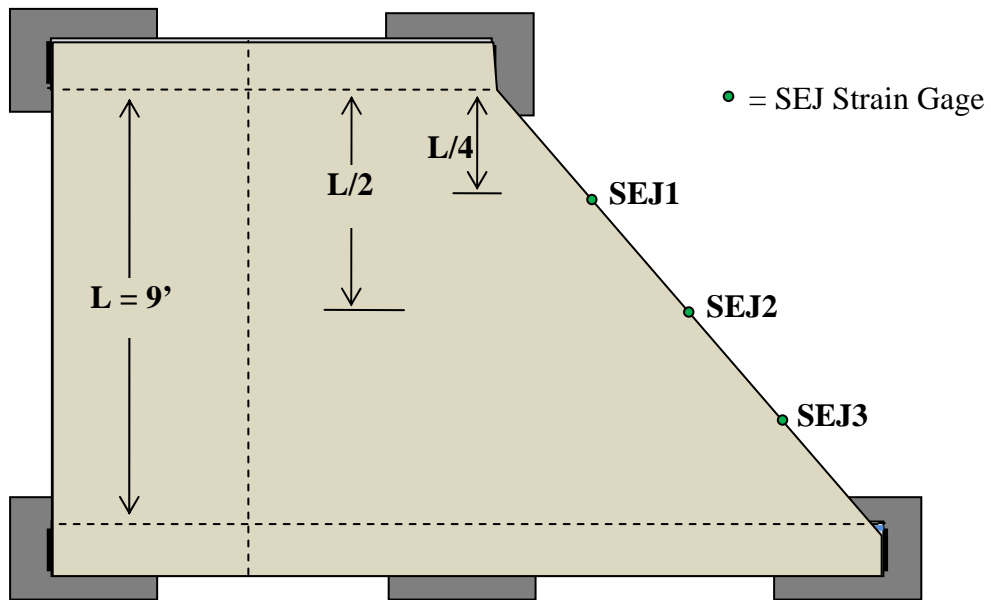
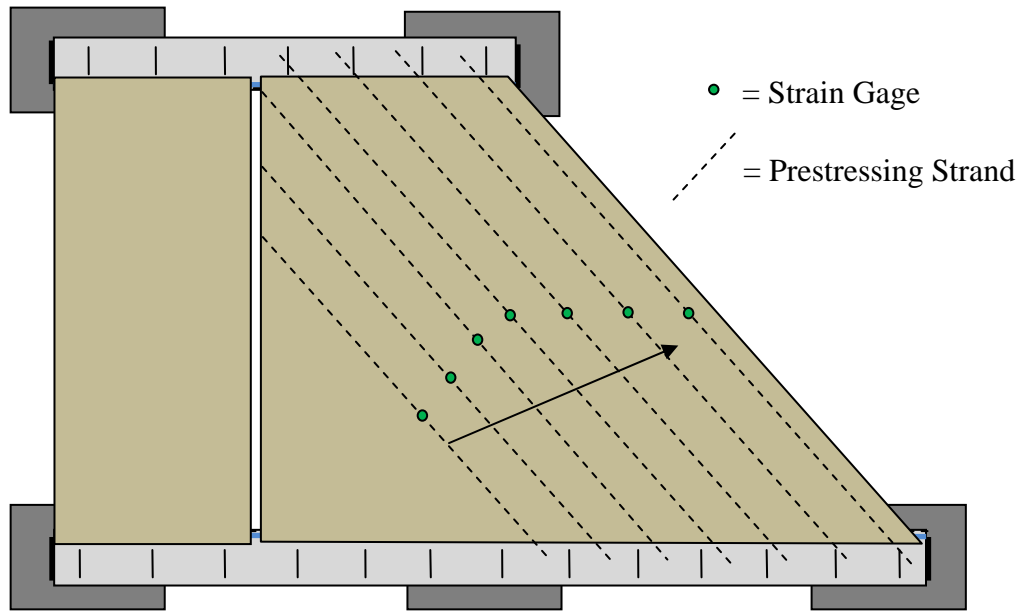


*Figure 4.18 – SEJ Strain Gage Locations and Labels for Specimen P45P3 for Load Applied at Midspan of Skewed End*



*\* P45P3 Contained 12 Strands. Not all panel reinforcement is shown for clarity*

**Figure 4.19 – Strand Strain Gage Locations and Labels for Specimen P45P3 for Load Applied at Midspan of Skewed End**

#### **4.3.3.2 Linear Potentiometers**

Five linear potentiometers were used to measure the deflection response of Specimen P45P3. The locations and labels for the linear potentiometers are provided in Figure 4.20.

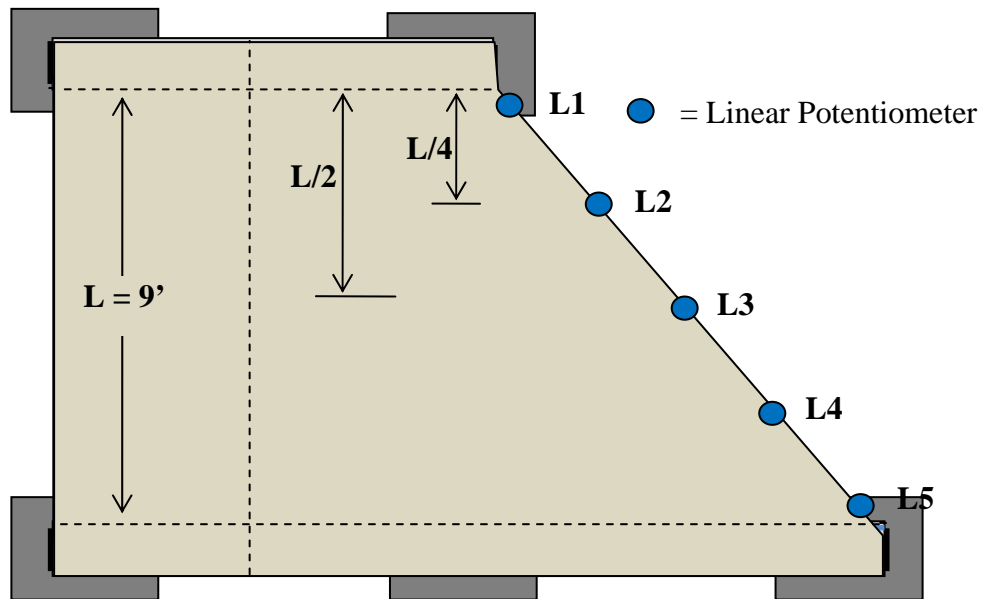


**Figure 4.20 – Linear Potentiometer Locations and Labels for Specimen P45P3 for Load Applied at Midspan of Skewed End**

#### **4.3.4 Specimens P30P1 and P30P2**

Specimens P30P1 and P30P2 were built identically. The following instrumentation information applies to both.

##### **4.3.4.1 Strain Gages**

The 30-degree trapezoidal panels were fabricated by an independent supplier. Therefore, no strain gages were installed on the prestressing strands or rebar in the panels. However the bottom side of the panel was instrumented with 19, 60-mm strain gages spaced at 12” on center. The SEJ was also instrumented with three strain gages. The locations and labels for the strain gages on the 30-degree specimens are shown in Figure 4.21 through Figure 4.23.



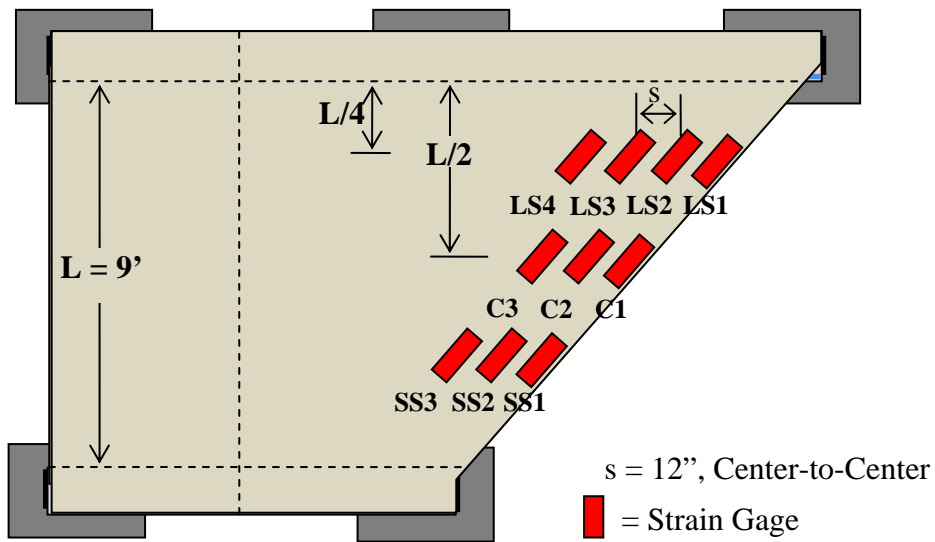


**Figure 4.21 – Concrete Strain Gage Locations for Specimens P30P1 and P30P2 for Load Applied at Midspan of Skewed End**

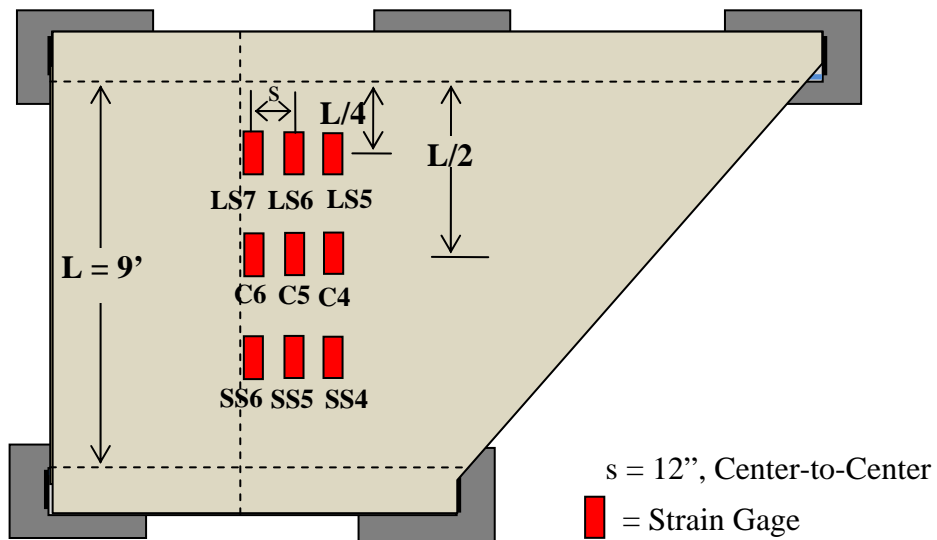


**Figure 4.22 – Concrete Strain Gage Location for Specimens P30P1 and P30P2 for Load Applied at Midspan of Square End**

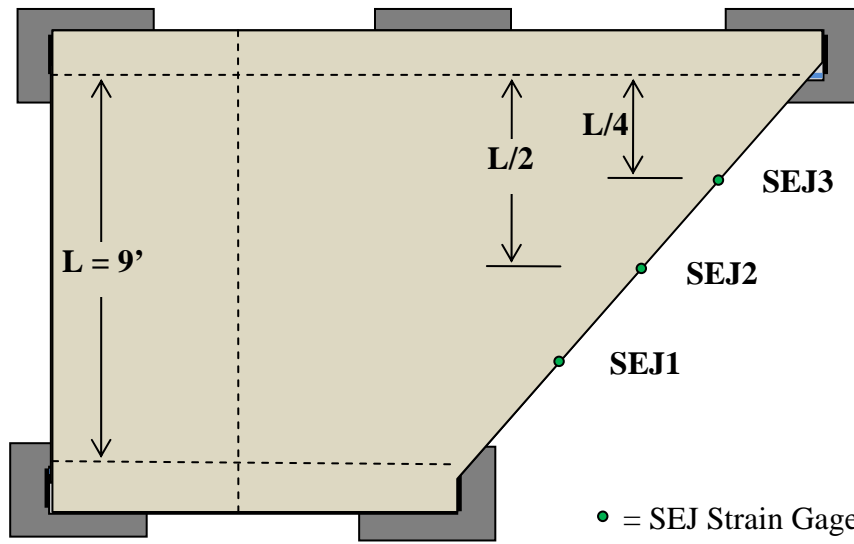


**Figure 4.23 – SEJ Strain Gage Locations for Specimens P30P1 and P30P2 for Load Applied at Midspan of Skewed End**

#### 4.3.4.2 Linear Potentiometers

Five linear potentiometers were used to measure the deflection response of Specimens P30P1 and P30P2 for load applied at midspan of the skewed end. Three linear potentiometers were used to measure the deflection response of Specimens P30P1 and P30P2 for load applied at midspan of the square end. The location and labels of the linear potentiometers are shown in Figure 4.24 and Figure 4.25.

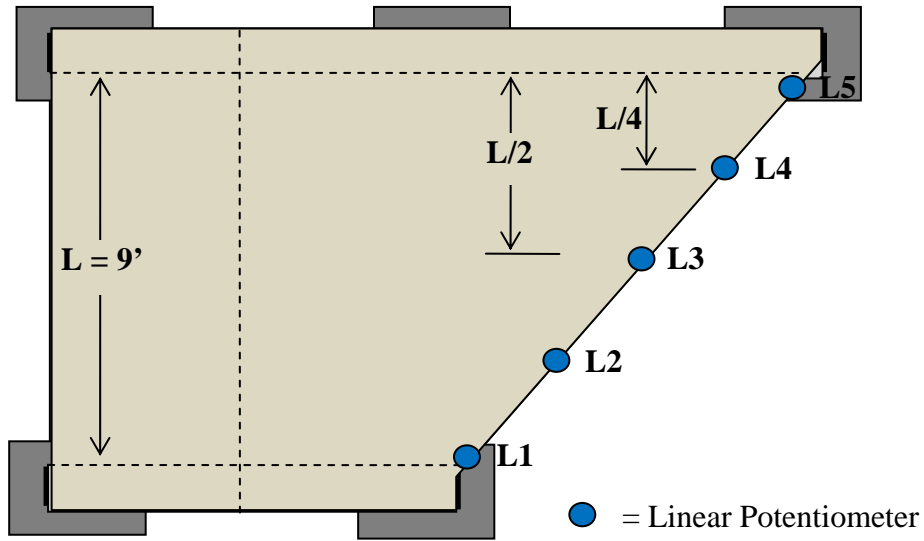


**Figure 4.24 – Linear Potentiometer Locations and Labels for Specimens P30P1 and P30P2 for Load Applied at Midspan of Skewed End**

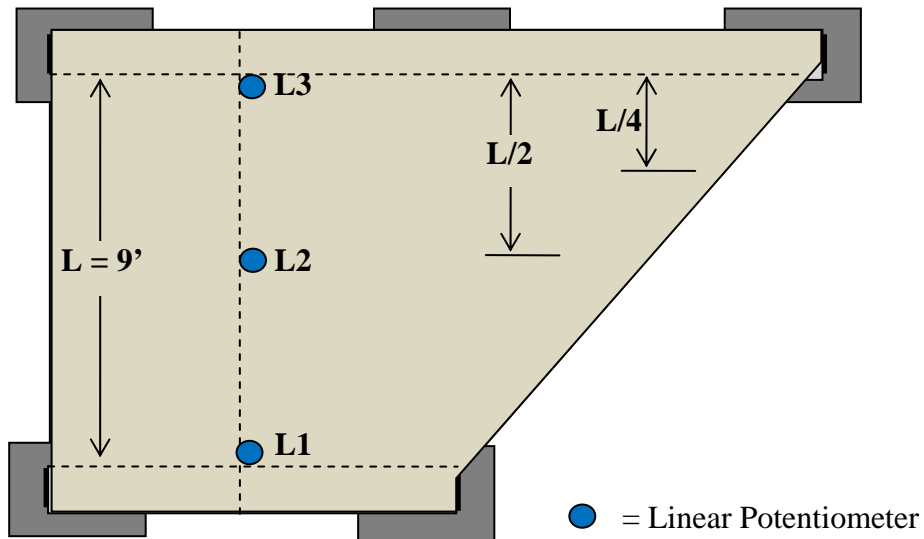


**Figure 4.25 – Linear Potentiometer Locations and Labels for Specimens P30P1 and P30P2 for Load Applied at Midspan of Square End**

### 4.3.5 Data Collection

Deflection, strain, and load data were collected using a digital data collection system shown in Figure 4.26. Signals from the load cell, strain gages, and linear potentiometers were collected through a combination of “full” and “half” bridges and relayed to a computer. National Instrument’s LabView 7.1 software was used as the user interface for the data collection process.

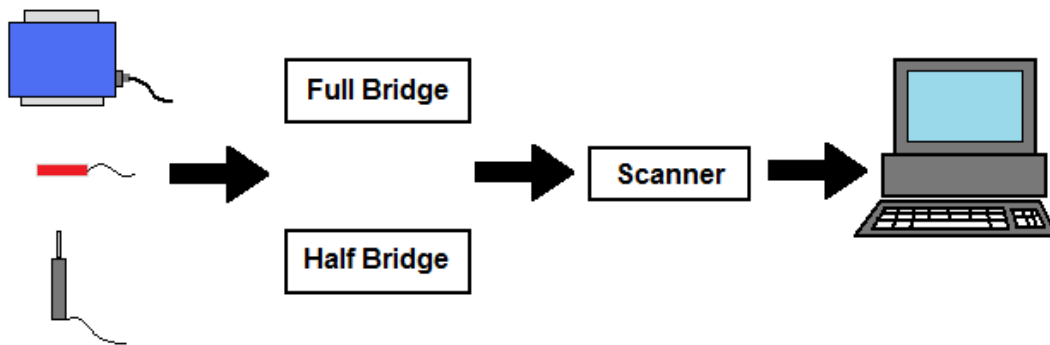


*Figure 4.26 – Data Collection System*

## Chapter 5: Measured Response of Test Specimens

### 5.1 INTRODUCTION

The behavior of skewed prestressed concrete panels used adjacent to expansion joints was studied using the procedures presented in the previous chapters. Five test specimens were constructed and tested. The response of these specimens is presented in this chapter. Section 5.2 presents the specific issues needed to understand the presentation of the data. Section 5.3 presents the response of the 45-degree specimens, and the response of the two 30-degree specimens is presented in Section 5.4.

### 5.2 LOAD TESTS

As discussed in Chapter 4, eight static and one fatigue tests were conducted. In all cases, the vertical loads were applied at midspan of the ends of the skewed precast panel. The response of the specimens to the applied loads is evaluated in this chapter using the measured strains and deflections. Key data needed to understand the response of the test specimens are presented in this chapter. All of the measured data are provided in Appendix B. Deflections were measured along the end where the load was applied. Therefore, all deflection measurements correspond to the loaded end. The deflections have been adjusted to reflect the relative displacement of the slab due to the compression of the bearing pads. Figure 5.1 shows the idealized rigid body movement of the loaded end of the slab. A linear relationship (Equation 5.1 and Equation 5.2) was developed to calculate the deflection at any location  $x$ ,  $\delta_x$ , from the displacements at the supports,  $\delta_L$  and  $\delta_S$ . The displacements due to rigid-body movement were calculated at the locations of the linear potentiometers, and these rigid-body displacements were subtracted from the measured displacements to determine the relative displacement response of the specimens.

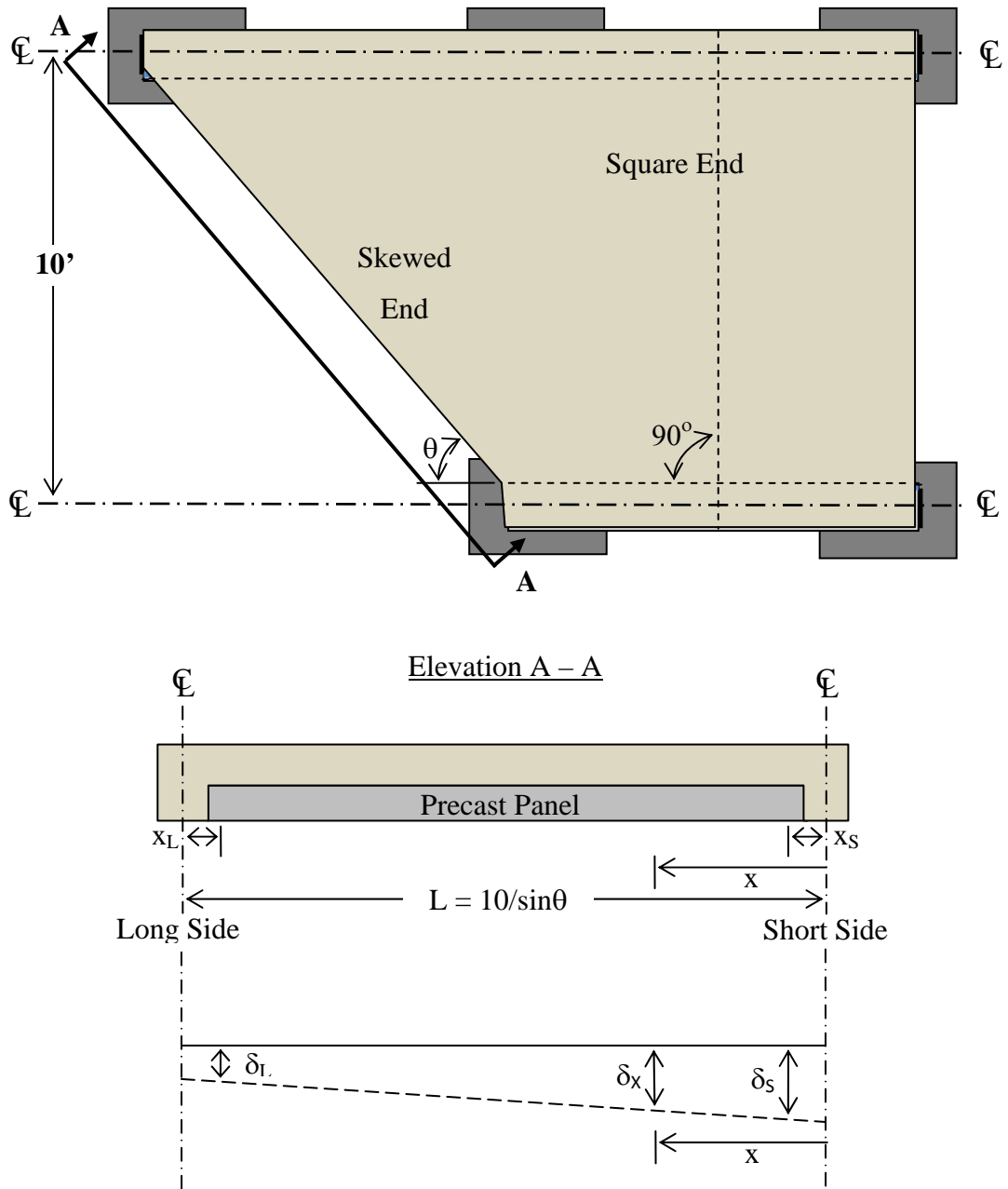


**Figure 5.1 – Rigid Body Movement of Loaded End of Skewed Specimen**

$$\Delta(x) = \Delta_m(x) - \delta_x \quad (\text{Equation 5.1})$$

$$\delta_x = \left( \frac{\delta_L - \delta_S}{L - (x_L + x_S)} \right) x + \delta_S \quad (\text{Equation 5.2})$$

$\Delta(x)$  = Relative displacement at location  $x$

$\Delta_m(x)$  = Measured displacement at location  $x$

$\delta_x$  = Rigid-body Movement at location  $x$

$\delta_L$  = Measured displacement near long support (L5 or DG2)

$\delta_S$  = Measured displacement near short support (L1 or DG1)

$L$  = Length along displaced end from centerline to centerline of supports

$x_L$  = Distance from centerline of long side support to L5 or DG2

$x_S$  = Distance from centerline of short side support to L1 or DG1

$x$  = Distance from centerline of short side support to location  $x$

The test specimens included prestressed and non-prestressed concrete elements. No data are available for changes in strand strain due to creep and shrinkage between release of the strands in the precast panels and testing of the specimens. Also, the complex geometry of the trapezoidal panels prevents precise calculation of the precompression in the concrete due to prestressing. Therefore, reported strain values on the bottom of the panels and in the prestressing strands provided in this chapter are live load induced strains due to the applied load on the specimen. Strain levels in the prestressing strands at release ( $\epsilon_{pi}$ ) are provided in the appropriate figures for reference. The primary purpose of the instrumentation is to indicate a change of stiffness in the system as a result of the applied load.

In discussing the response of the test specimens, several loads are used for comparison. With respect to the HL-93 Design Truck, three loads are considered, as defined in Table 5.1. The Service Wheel Load,  $P_w$ , refers to one half of the rear axle load for the HL-93 Design Truck. The Design Wheel Load corresponds to the Service

Wheel Load amplified for impact, where  $I = 0.33$ . The Factored Wheel Load is the product of the live load factor the Design Wheel Load.

In addition, the response of the specimen changed at several loads. The term “apparent cracking load” refers to the load at which visible cracks formed on the surface of the specimen. The term “cracking load” refers to the load at which the system stiffness, measured by the instrumentation, changed appreciably. And the term “maximum applied load” corresponds to the failure load.

***Table 5.1 –Loads Corresponding to HL-93 Design Truck***

Load	Designation	Expression	Numerical Value
Service Wheel Load	$P_w$	$P_w$	16 kip
Design Wheel Load	$P_L$	$(1+I) P_w$	21.3 kip
Factored Wheel Load	$P_U$	$1.75 P_L$	37.3 kip

In some cases, strain gages were damaged during the test due to events such as formation of a crack at the location of a strain gage on the surface of the concrete or debonding of the gage from the reinforcement. When this occurs, the data for that strain gage are unreliable beyond that point. An “X” was used to identify the load at which the damage occurred. Figure 5.2 provides an example using concrete strain gages to show how the data are displayed when the strain gage was damaged during loading.



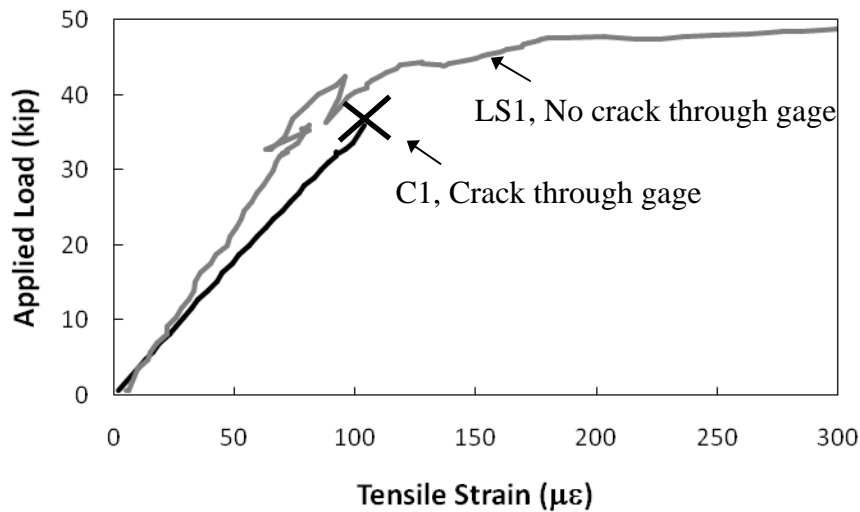
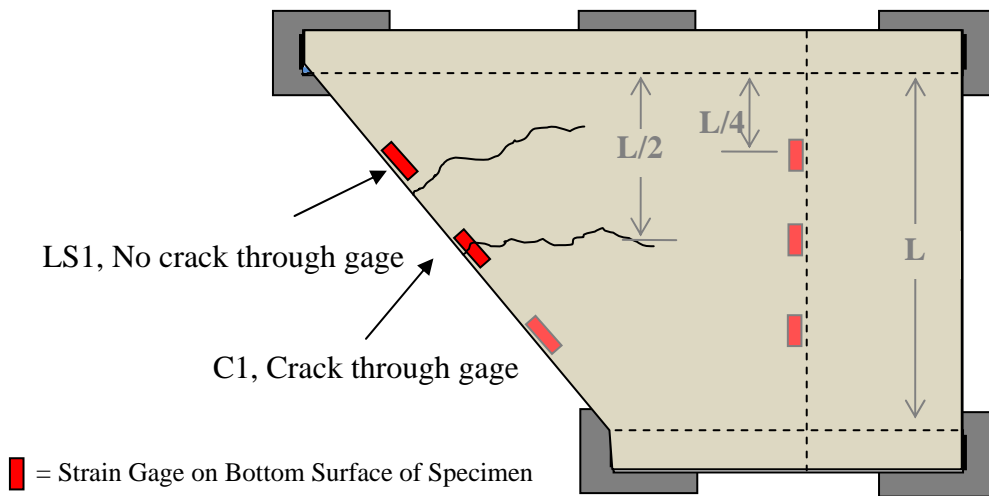


*Figure 5.2 – Presentation of Strain Gage Data*

### 5.3 MEASURED RESPONSE OF THE 45-DEGREE SPECIMENS

Measured data from the three specimens with 45-degree skews are summarized in this section.

#### 5.3.1 Response of Specimen P45P1

Specimen P45P1 was tested only at midspan of the skewed end. The load was applied monotonically to failure. Key data from this test include relative displacements

of the loaded end, strain on the bottom surface of the panel, and strain in the SEJ. Each is discussed below.

#### ***5.3.1.1 Load Applied at Midspan of Skewed End***

The relative displacement at midspan of the skewed end under the applied load is shown in Figure 5.3. Specimen P45P1 used dial gages to measure the displacement at the supports due to the compression of the bearing pads. Displacement measurements from the dial gages were recorded at 5-kip intervals. At the L1, L2, and L3 locations along the skewed end, displacements were measured continuously using linear potentiometers. Continuous support movement, to be used with the linear potentiometer data, was estimated using straight-line interpolation between recorded dial gage measurements. The load-displacement plot in Figure 5.3 shows a cracking load of approximately 31 kip. The apparent cracking load of the specimen was 35 kip. The variation of recorded displacements along the skewed end for service and factored wheel loads is presented in Figure 5.4. Relative displacements were highest at midspan under the load point, and the lowest displacement was at the quarter-span location close to the long side.

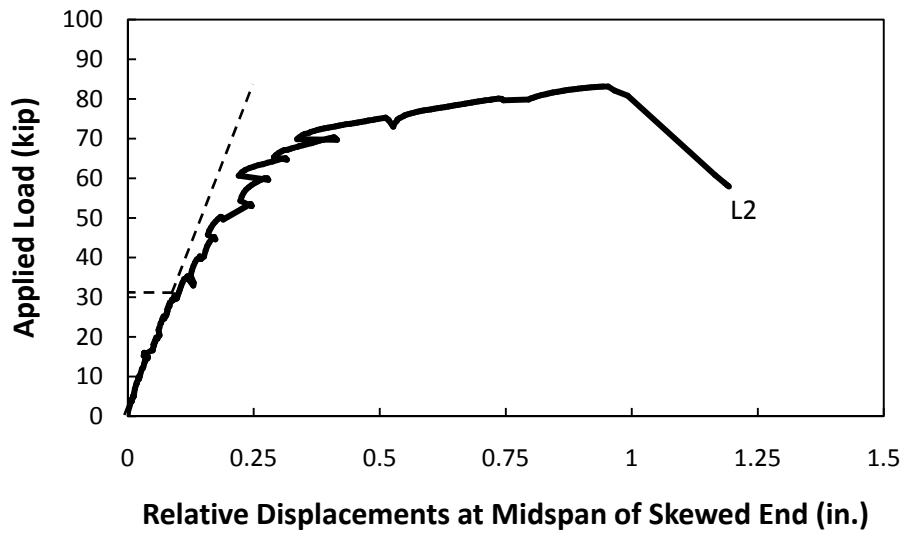


*Figure 5.3 – Measured Displacement Response of Specimen P45P1 for Load Applied at Midspan of Skewed End*

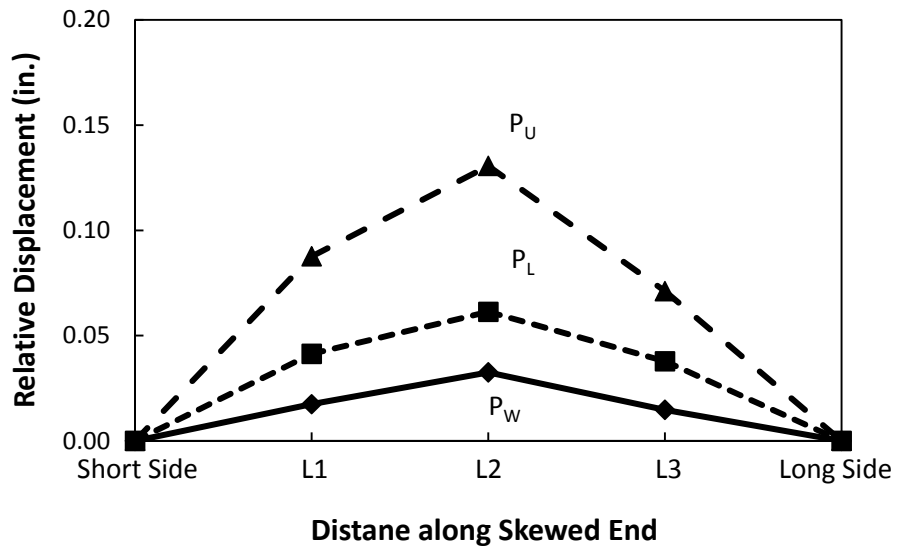


*Figure 5.4 – Variation of Relative Displacements along Loaded End for Specimen P45P1 for Load Applied at Midspan of Skewed End*

The change in strain at midspan of the loaded end is shown in Figure 5.5. Strain data from the bottom of the panel show a cracking load of approximately 33 kip. The strain variation along the loaded end is presented in Figure 5.6. At each of the characteristic load levels ( $P_W$ ,  $P_L$ , and  $P_U$ ), strains were highest at midspan under the load point, and the lowest strain was recorded at the quarter-span location near the long side.

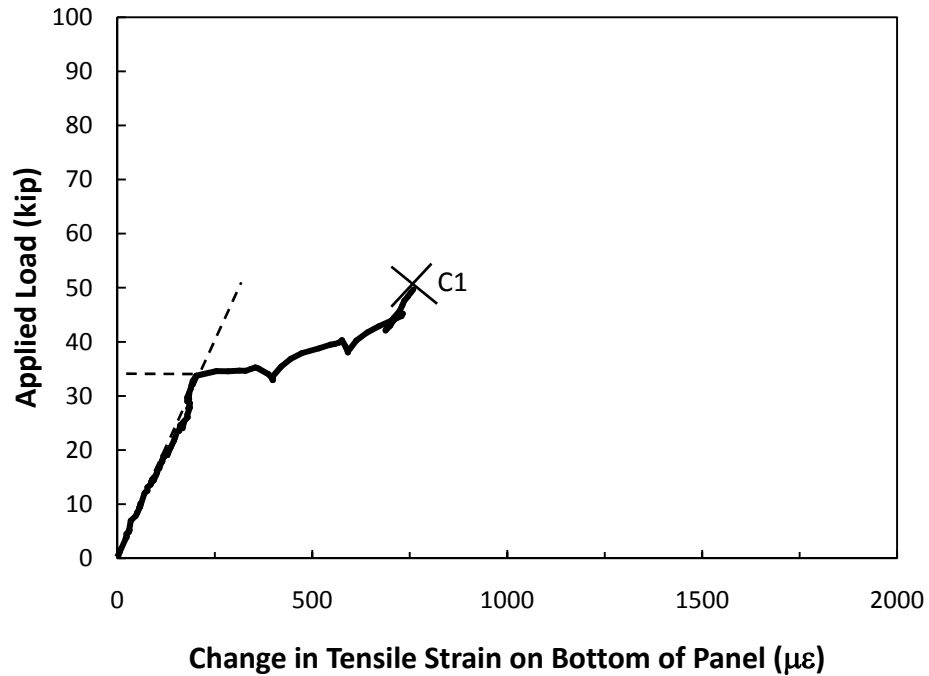


*Figure 5.5 – Change in Tensile Strain on Bottom of Precast Panel for Specimen P45P1 for Load Applied at Midspan of Skewed End*

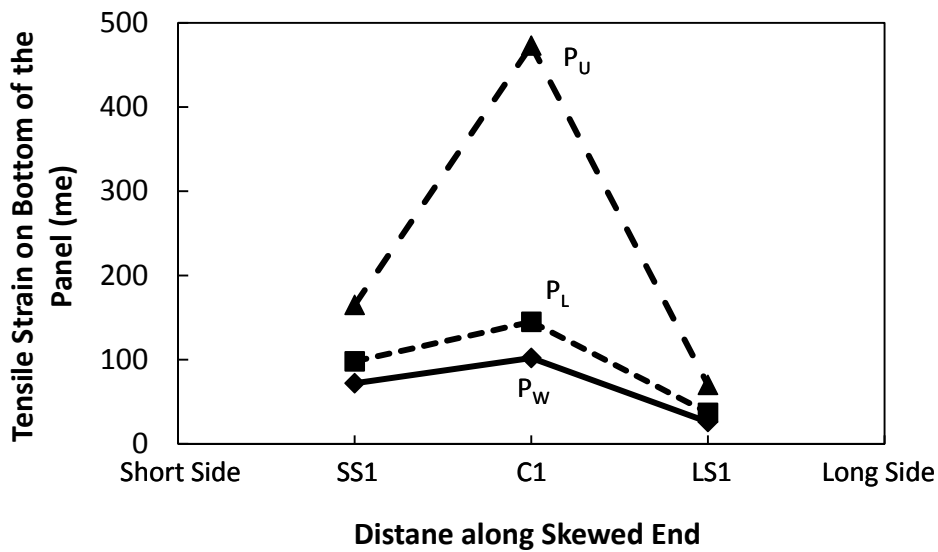


**Figure 5.6 – Distribution of Concrete Strain on the Bottom of the Panel along Skewed End of Specimen P45P1**

Compressive strain data at midspan of the SEJ is shown in Figure 5.7. The SEJ shows a cracking load of approximately 33 kip. The strain variation along the SEJ is shown in Figure 5.8. Again, the strain is highest at midspan, followed by lower strains at the quarter-span location near the short side and the lowest strains near the long side.

The cracking loads for Specimen P45P1 are summarized in Table 5.2. The average cracking load for load applied at midspan of the skewed end is 33 kip.

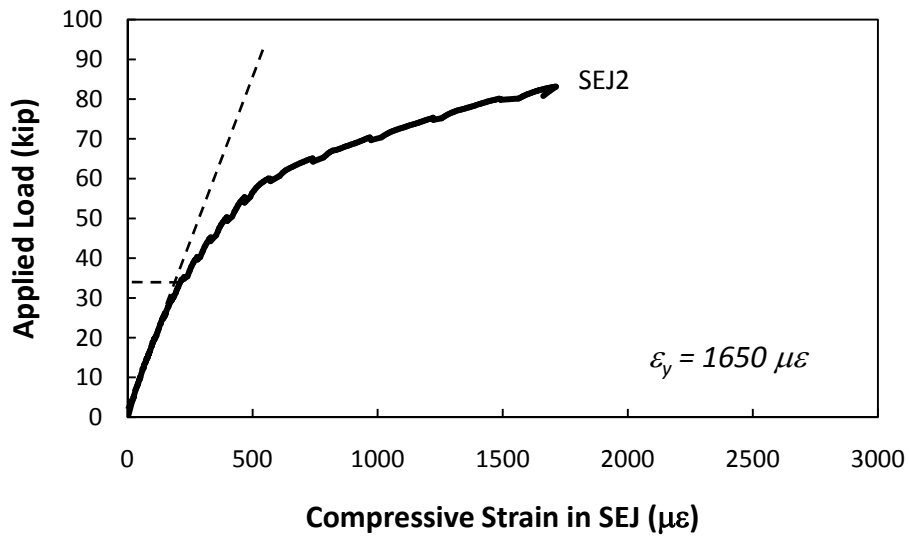


*Figure 5.7 – Measured Compressive Strain at Midspan of SEJ for Specimen P45P1 for Load Applied at Midspan of Skewed End*

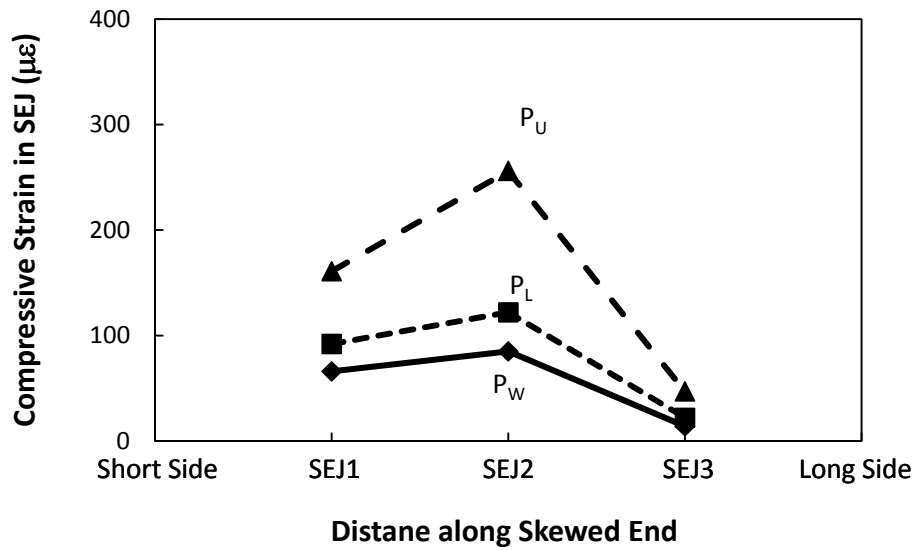
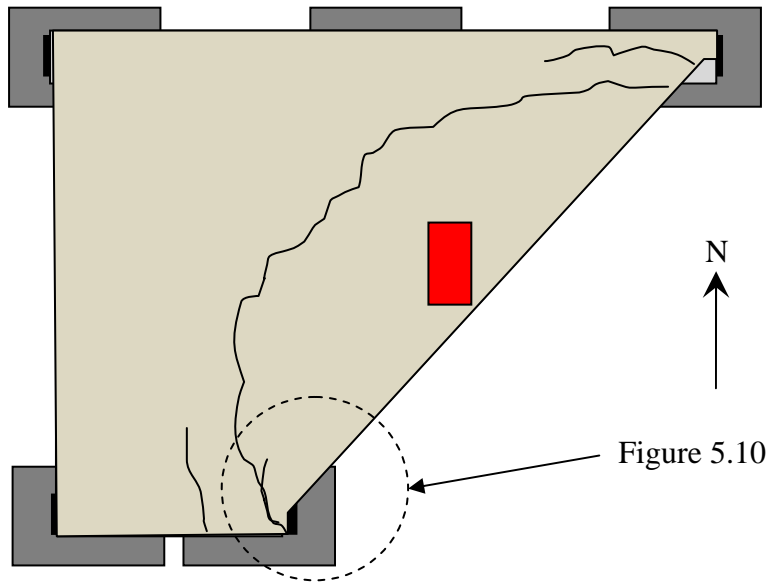


*Figure 5.8 – Variation of Strain in SEJ along Skewed End of Specimen P45P1*

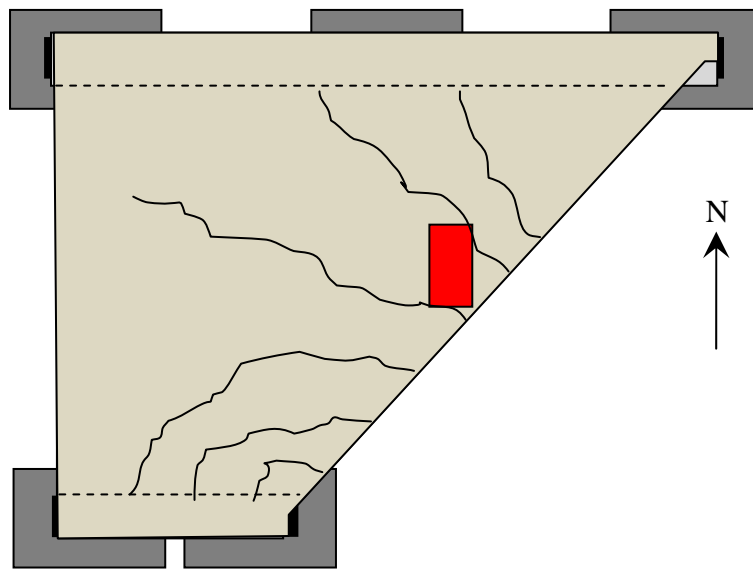
**Table 5.2 - Initial Stiffness and Inferred Cracking Load for Specimen P45P1 for Load Applied at Midspan of Skewed End**

	Initial Stiffness (k/in, k/ $\mu\epsilon$ )	Inferred Cracking Load (kip)
Displacement	307.4	31
Concrete Strain on Bottom of Panel	0.167	33
SEJ Strain	0.163	33
Apparent Cracks	-	35

Observed cracks at the conclusion of the static test are shown in Figure 5.9. The specimen failed in shear at the short side support. The precast trapezoidal panel pulled away from the topping slab at failure (Figure 5.10).



Predominant Cracks on Top Surface of Specimen



Predominant Cracks on Bottom Surface of Specimen

*Figure 5.9 – Observed Crack Pattern at Conclusion of Static Test for Specimen*

*P45P1*



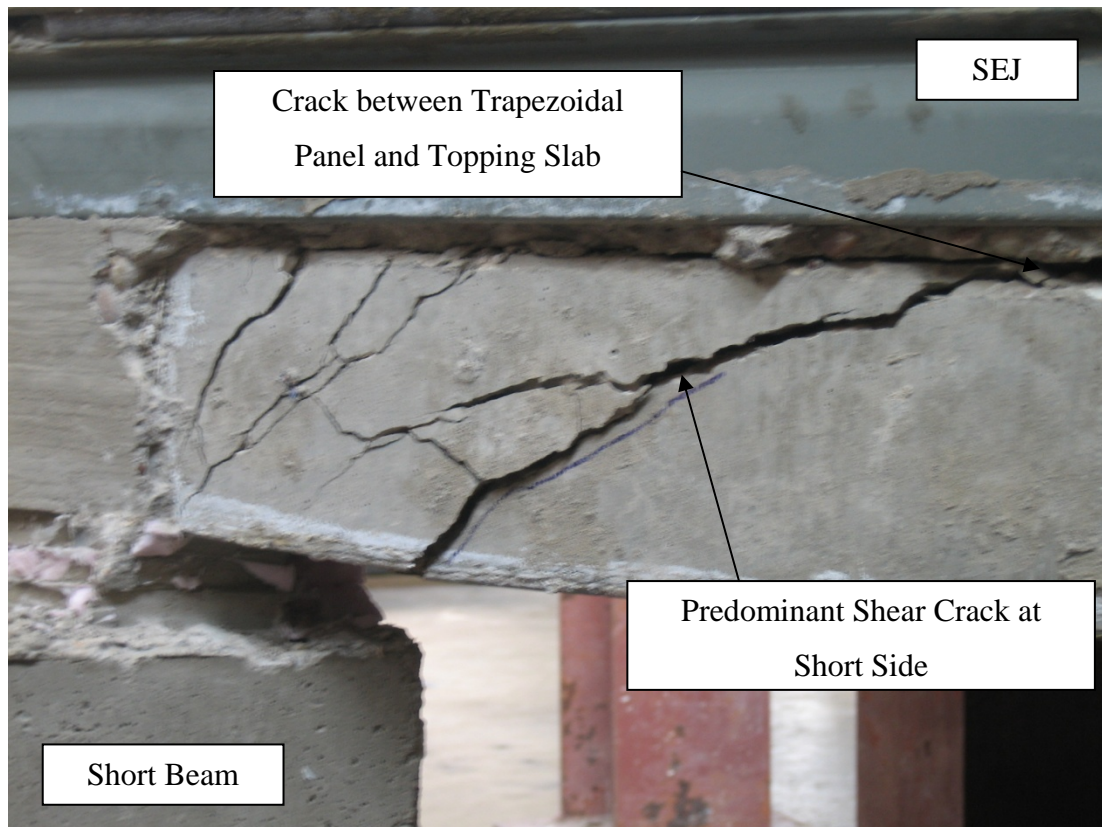


*Figure 5.10 – Photograph of Specimen P45P1 at Conclusion of Static Test*

### **5.3.2 Response of Specimen P45P2**

Specimen P45P2 was tested monotonically to failure two times. During the first test, the load was applied near midspan of the SEJ along the skewed end of the trapezoidal panel. For the second test, load was applied near midspan of the perpendicular end of the trapezoidal panel. Key data from the test include relative displacements, concrete tensile strain, compressive strain in the SEJ, and tensile strain in the prestressing strands.

### 5.3.2.1 Load Applied at Midspan of Skewed End

The relative displacement at midspan of the skewed end under the applied load is shown in Figure 5.11. According to the load-displacement data, the specimen cracked at approximately 31 kip, but cracks did not begin to appear on the surface of the specimen until the applied load reached 37 kip. Displacements are largest under the load point, with displacements at the quarter point near the short side exceeding those at the quarter point near the long side (Figure 5.12). The unsymmetrical distribution of displacements about midspan of the skewed end resulted from the unsymmetrical load path created by the trapezoidal panel.

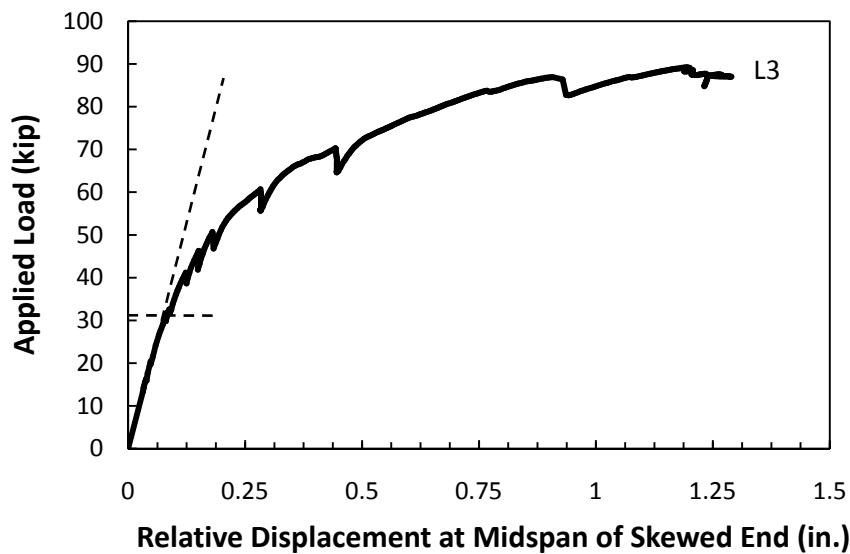


*Figure 5.11 – Measured Displacement Response of Specimen P45P2 for Load Applied at Midspan of Skewed End*

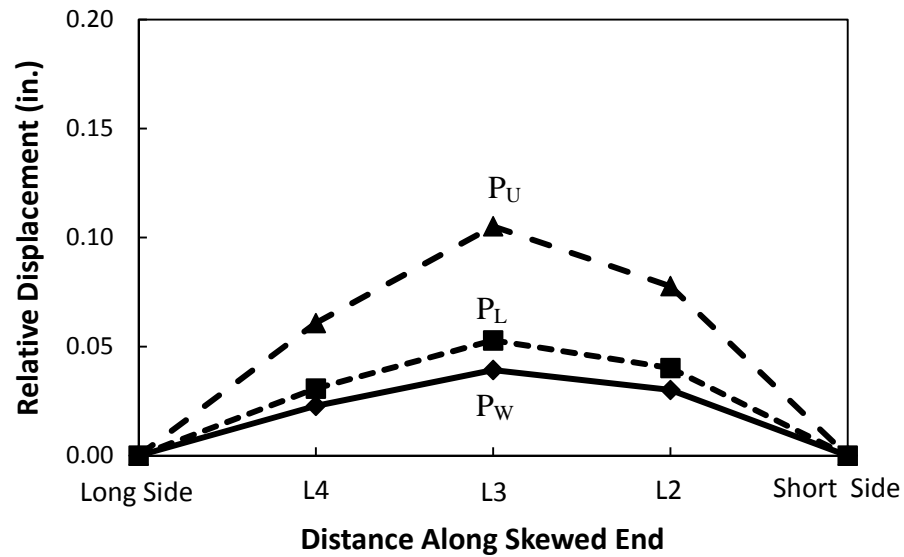


*Figure 5.12 – Variation of Relative Displacements along Skewed End of Specimen P45P2*

Tensile strain data from the concrete show that the strain gage was damaged at approximately 28 kip (shown in Figure 5.13); therefore, the change in stiffness corresponding to the cracking load can not be approximated from this data. Figure 5.14 shows the strain variation on the bottom of the panel along the loaded end. The most strain occurs at midspan and the quarter-span location closest to the short side support experienced higher strains than the quarter-span location near the long side.

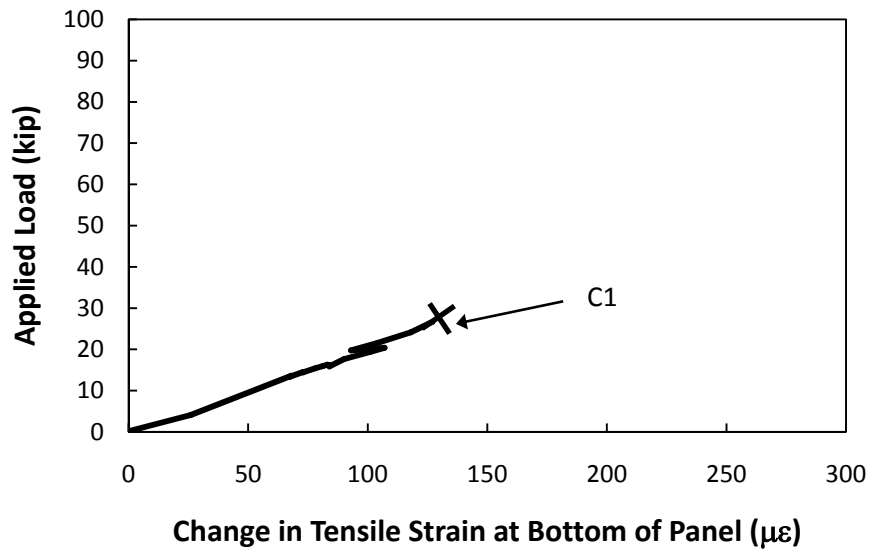


**Figure 5.13 - Tensile Strain on Bottom of Precast Trapezoidal Panel for Specimen P45P2 for Load Applied at Midspan of Skewed End**

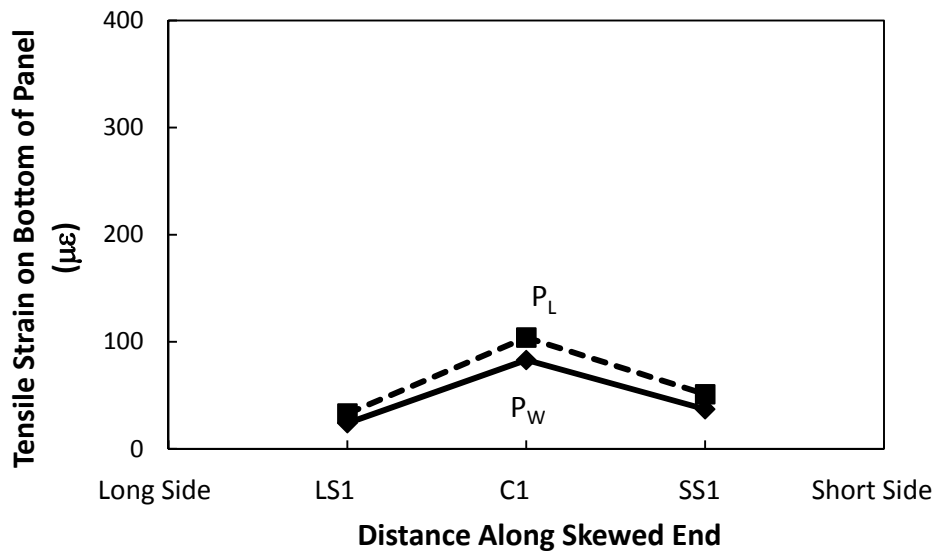


**Figure 5.14 - Distribution of Concrete Strain on the Bottom of the Panel along Skewed End of Specimen P45P2**

Compressive strain gage data for the SEJ show that expansion joint did not yield under the applied load. It also shows that the specimen cracked around 30 kip (Figure 5.15). Figure 5.16 shows the variation in SEJ strain along the loaded end. The same trend is seen here as in the displacement and concrete strain data. The highest strain was measured at midspan, followed by the quarter-span location near the short side, and the lowest strain was recorded at the quarter-span location near the long side.

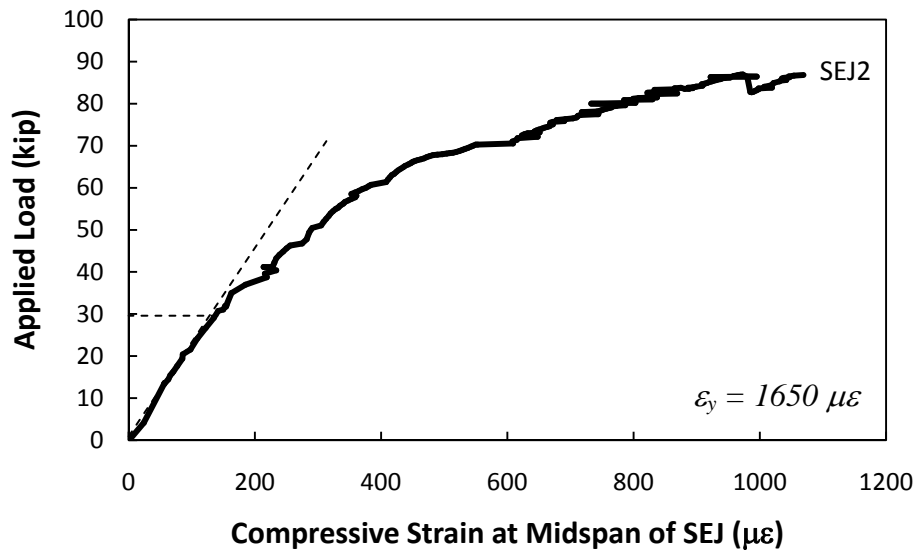


**Figure 5.15 - Measured Compressive Strain at Midspan of SEJ for Specimen P45P2 for Load Applied at Midspan of Skewed End**

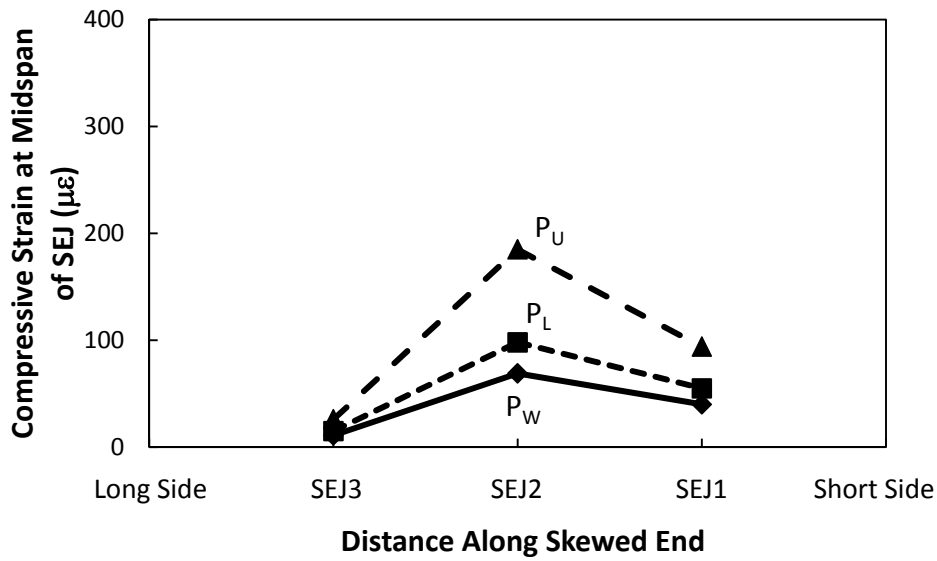


*Figure 5.16 - Variation of Strain in SEJ along Skewed End of Specimen P45P2*

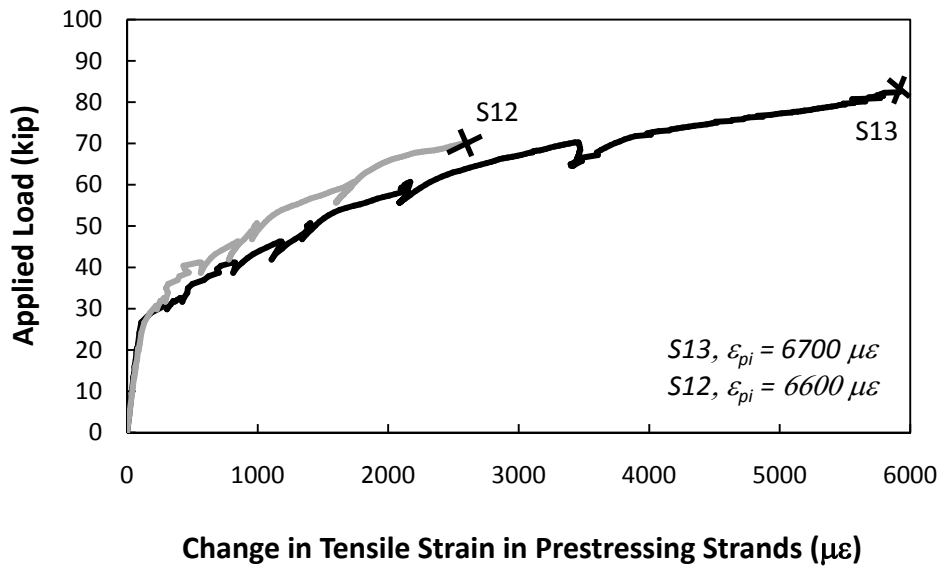


*Figure 5.17 – Measured Change in Tensile Strain in Prestressing Strand in Specimen P45P2 for Load Applied at Midspan of Skewed End*

The strain gage data on the prestressing strands indicate that the cracking load for the skewed end was approximately 28 kip as shown in Figure 5.17. Variation of the change in prestressing strand strain is shown in Figure 5.18. It can be seen that changes

in strains in the strands are highest under the load point and decrease sharply as distance from the loaded end increases.

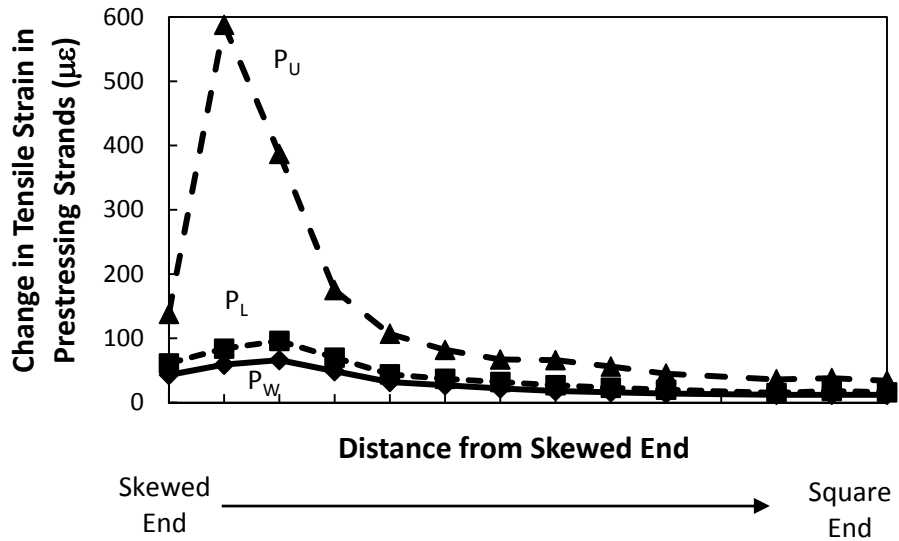


**Figure 5.18 – Variation of Maximum Strain in Prestressing Strands for Load Applied at Midspan of Skewed End for Specimen P45P2**

The cracking loads inferred from the measured response are summarized in Table 5.3. The inferred cracking loads from the instrumentation and the apparent cracking load varied from 28 to 37 kip, with an average of 32 kip.

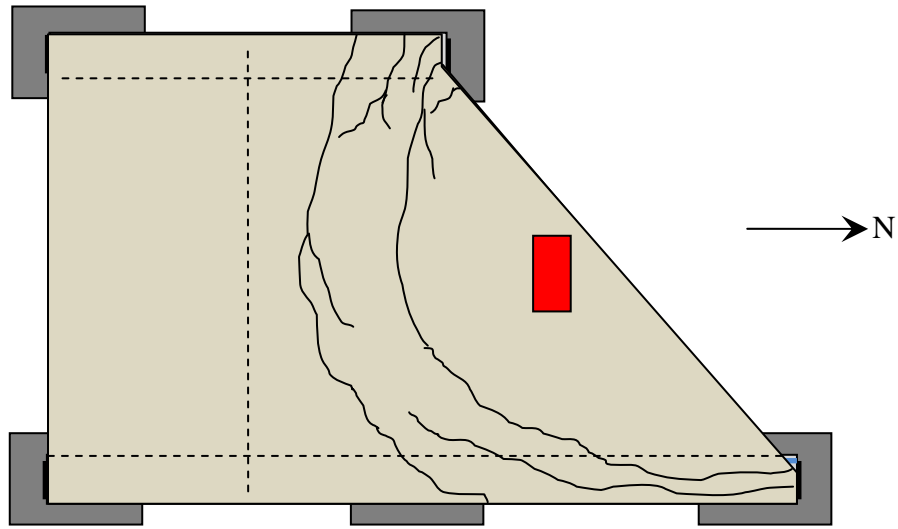
**Table 5.3 – Initial Stiffness and Inferred Cracking Loads for Load Applied at Midspan of Skewed End of Specimen P45P2**

	Initial Stiffness (k/in, k/ $\mu\epsilon$ )	Inferred Cracking Load (kip)
Displacement	390	31
Concrete Strain on Bottom of Panel	0.210	-
SEJ Strain	0.216	30
Strain in Prestressing Strand*	0.245	28
Apparent Cracking	-	37

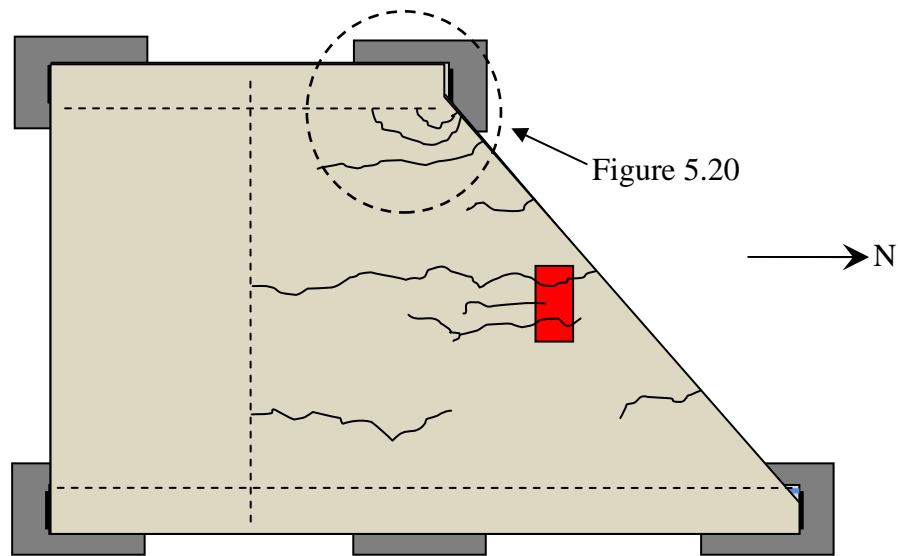
\* Data from gage S12 and S13

Observed cracks at the conclusion of the static test at midspan of the skewed end are shown in Figure 5.19. It should be noted that these figures represent the crack patterns corresponding to the major cracks and not a complete crack map of every crack formed. Photographs of the failure are shown in Figure 5.20. A diagonal shear crack formed (Figure 5.20 (a)) at the support on the short side of the trapezoidal panel and propagated to the top surface of the specimen. Severe cracking also occurred on the bottom surface of the specimen near the support on the short side (Figure 5.20 (b)).



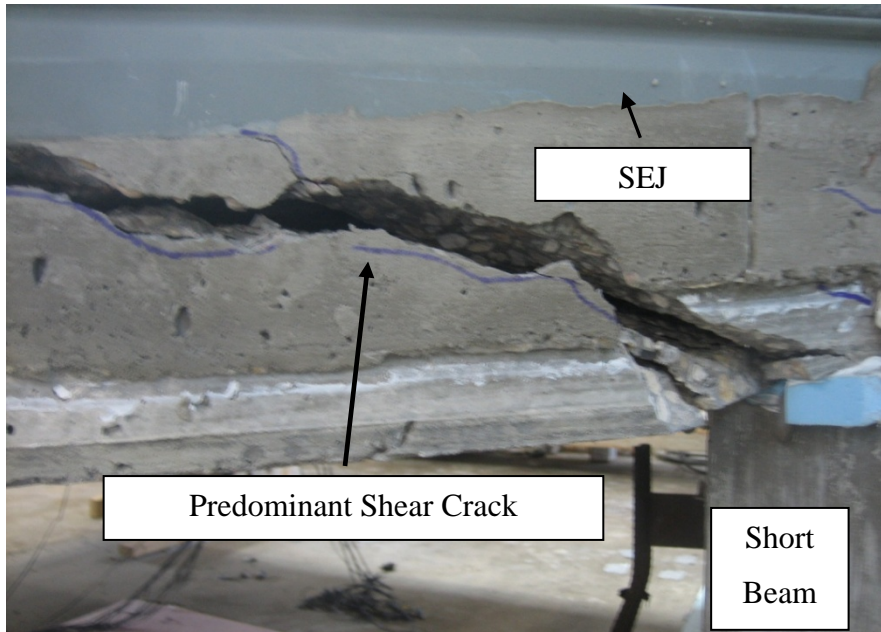


Predominant Cracks on Top Surface of Specimen

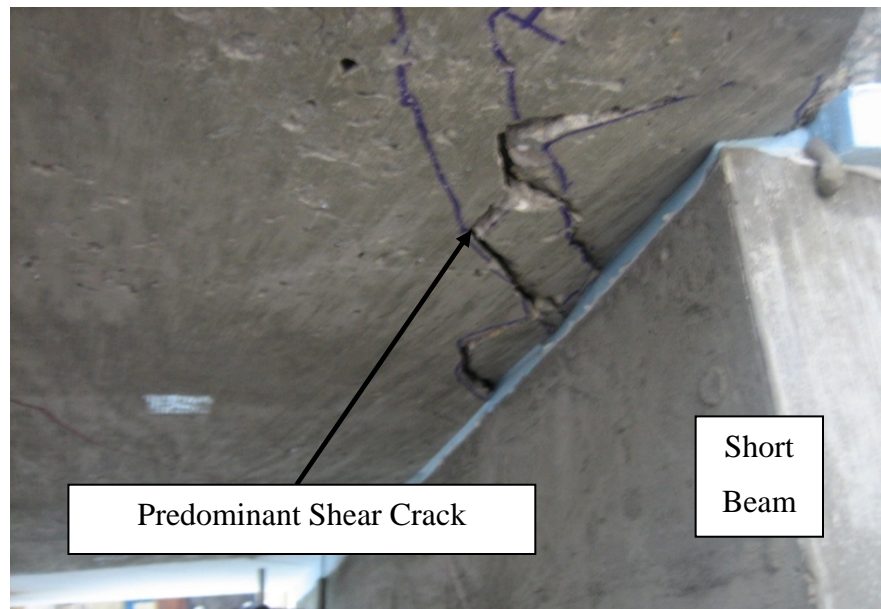


Predominant Cracks on Bottom Surface of Specimen

***Figure 5.19 – Observed Crack Patterns at Conclusion of Static Test at Midspan of Skewed End for Specimen P45P2***



(a) Northwest Corner of Specimen Viewed from Side



(b) Northwest Corner of Specimen Viewed from Below

**Figure 5.20 – Photographs of Specimen P45P2 at Conclusion of Static Test at Midspan of Skewed End**

### ***5.3.2.2 Load Applied at Midspan of Square End***

Following the completion of the first static test, load was applied at midspan of the square end of the trapezoidal panel. In this test, the capacity of the specimen exceeded 100 kip, which was the capacity of the load cell. Therefore, the specimen had to be unloaded and reloaded using a 200-kip load cell. Thus, there are two curves in the load-displacement plot in Figure 5.21. The unloading curve was not recorded when the load cell was changed. In order to approximate the unloading curve, a straight line with the same slope as the initial stiffness of the system was plotted (the dotted line). The second curve was then shifted by the same amount as the offset from the unloading plot. Because the specimen experienced cracks during the previous test, it was not possible to identify the load at which new cracks appeared. However, Figure 5.21 indicates a change in stiffness near 40 kip for the first loading. Figure 5.22 shows the displacement variation along the loaded end; it shows that the displacement distribution was more uniform on the square end of the specimen than along the skewed end of the specimen (Figure 5.12). Figure 5.22 also shows that displacements under the applied load were significantly smaller along the square end compared with the skewed end. In this case, displacements near the long side were slightly larger than those closer to the short side. This is likely due to the reduced panel stiffness in the corner of the panel without prestressing strands.

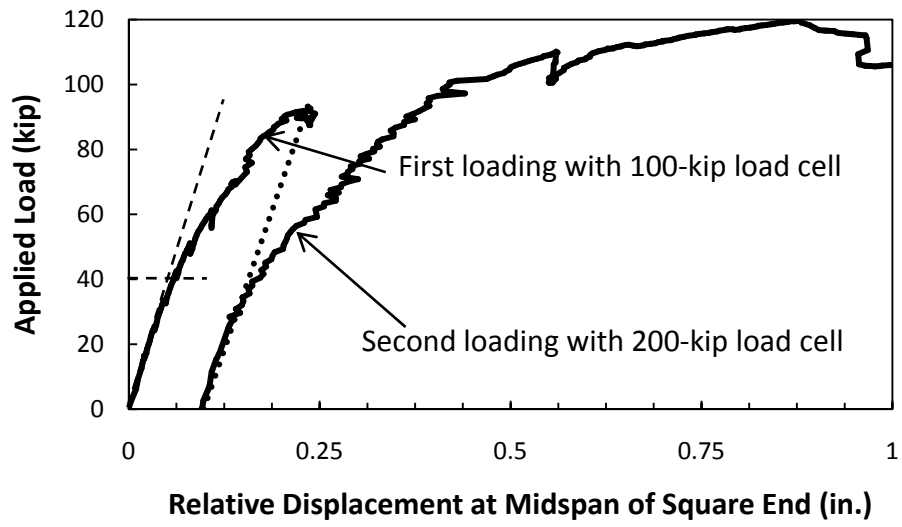


*Figure 5.21 - Measured Displacement Response for Specimen P45P2 for Load Applied at Midspan of Square End*

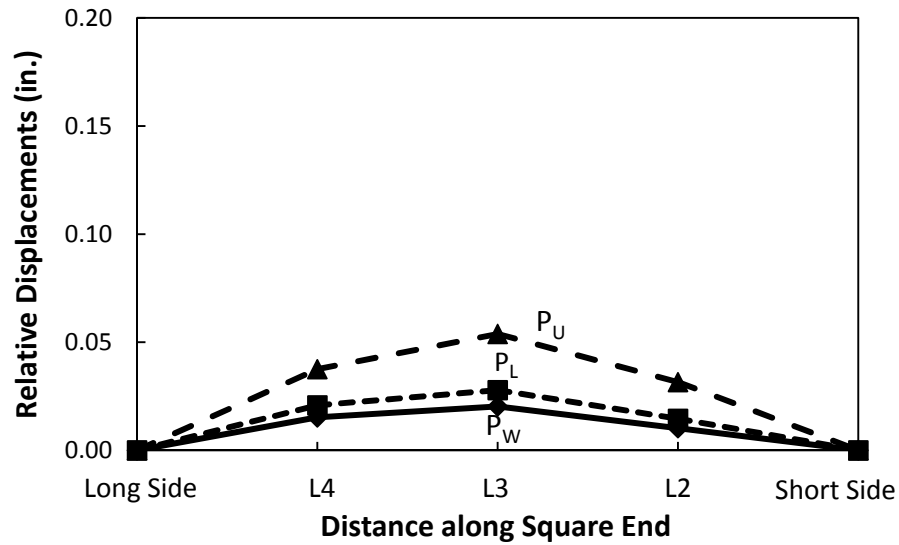


*Figure 5.22 – Variation of Displacements along Square End of Specimen P45P2*

Strain data from the bottom side of the panel along the loaded end also indicated a cracking load of approximately 40 kip (Figure 5.23). The distribution of strain along the bottom of the panel at the loaded end (Figure 5.24) shows larger strains at the quarter-span locations than at midspan of the square end. This trend is not consistent with those in other data sets and suggests that cracks near the supports from the previous loading contributed to a reduced stiffness and higher strains near the supports than would be expected for an undamaged specimen.

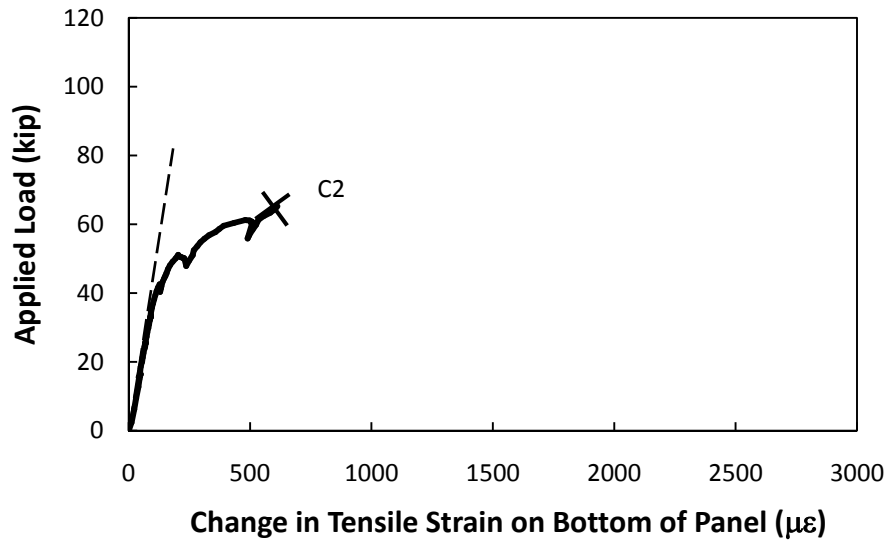


*Figure 5.23 – Measured Change in Tensile Strain on Bottom of Precast Panel for Specimen P45P2 for Load Applied at Midspan of Square End*

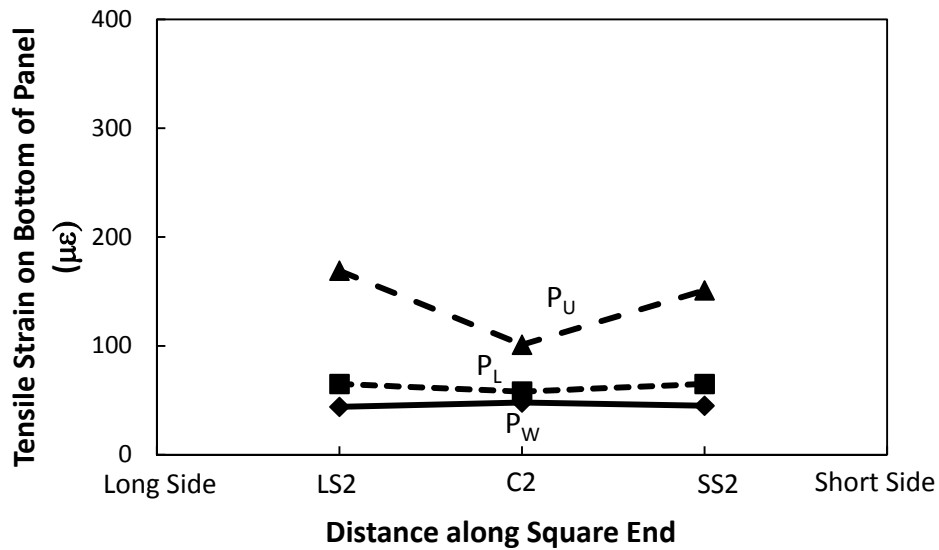


*Figure 5.24 – Distribution of Change in Concrete Strain on the Bottom of the Panel Along Square End of Specimen P45P2*

Strain data from the rebar in the panel along the square end again show a cracking load of approximately 40 kip (Figure 5.25). The difference in the departure from the

initial tangent for each rebar shows that the crack propagated from R2 to R5. The variation of strain in the rebar along the loaded end, Figure 5.26, shows strains highest at midspan and lower at the quarter-span locations. Also, when compared to the strain variation in the SEJ along the skewed end (Figure 5.15), strain in the rebar is more symmetric with respect to midspan on the square end.

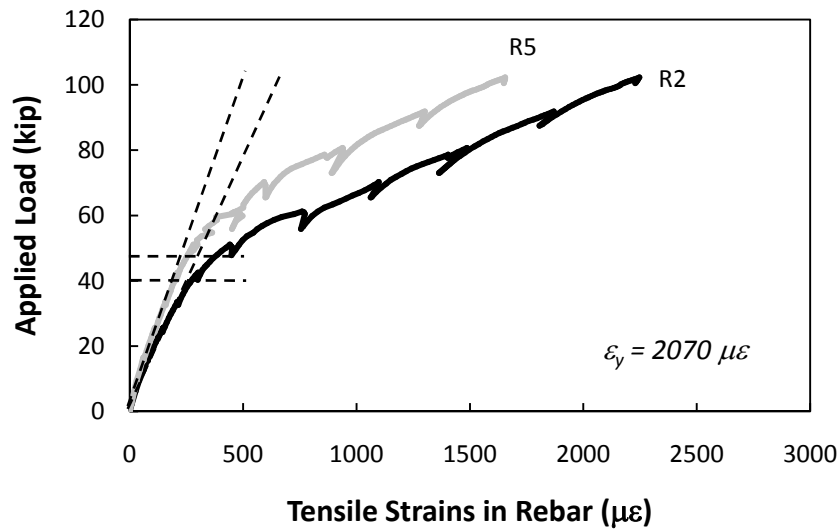


*Figure 5.25 - - Measured Tensile Strains in Rebar for Specimen P45P2 for Load Applied at Midspan of Square End*

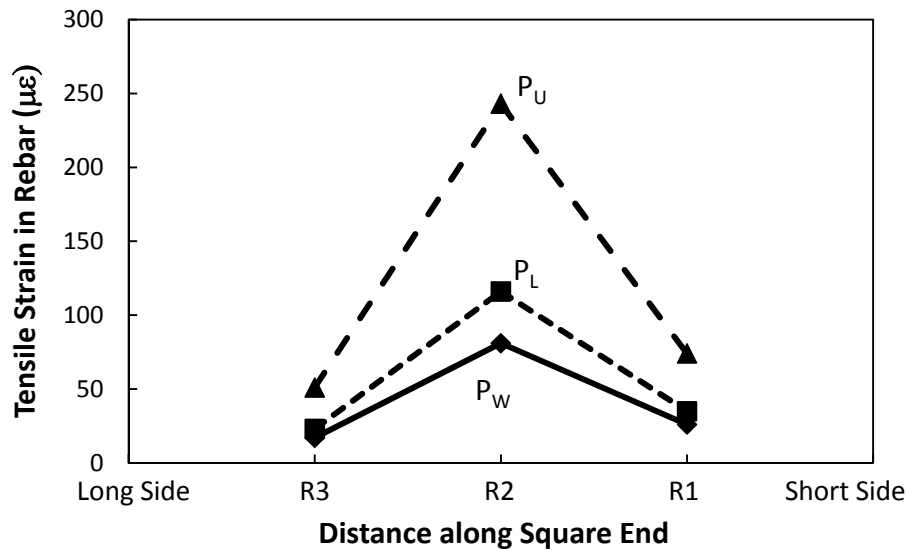


**Figure 5.26 – Distribution of Strain in Reinforcement Closest to Square End of Specimen P45P2**

Load-displacement data, concrete strain data on the bottom of the panel, and rebar strain data indicate a cracking load of approximately 40 kip on the square end (Table 5.4). This load is higher than the cracking load on the skewed end of the specimen.

**Table 5.4 – Initial Stiffness and Inferred Cracking Load for Each Data Type for Specimen P45P2 for Load Applied at Midspan of Square End**

	Initial Stiffness (k/in, k/με)	Inferred Cracking Load (kip)
Displacement	685	40
Concrete Strain on Bottom of Panel	0.352	40
Strain in Rebar	0.146	40

Also, an observation was made about the interaction of the two adjacent panels in the specimen. Even though an attempt was made to isolate the trapezoidal panel by positioning the load plate 4 in. back from the square end of the panel, significant load was



shared between the two panels. This is seen in Figure 5.27 where it was observed that the trapezoidal and rectangular panels displace similarly under the applied load on the square end of the trapezoidal panel.

Ultimately, the specimen failed in punching shear at a load of 120 kip. Concrete on the bottom of the panel spalled off, exposing the bottom layer of reinforcement. The crack pattern at the conclusion of the static test is shown in Figure 5.28. Photographs of the failure in Figure 5.29 show the punching shear crack around the load plate on the top side of the specimen and the spalled concrete and prominent punching shear cracks on the bottom side.

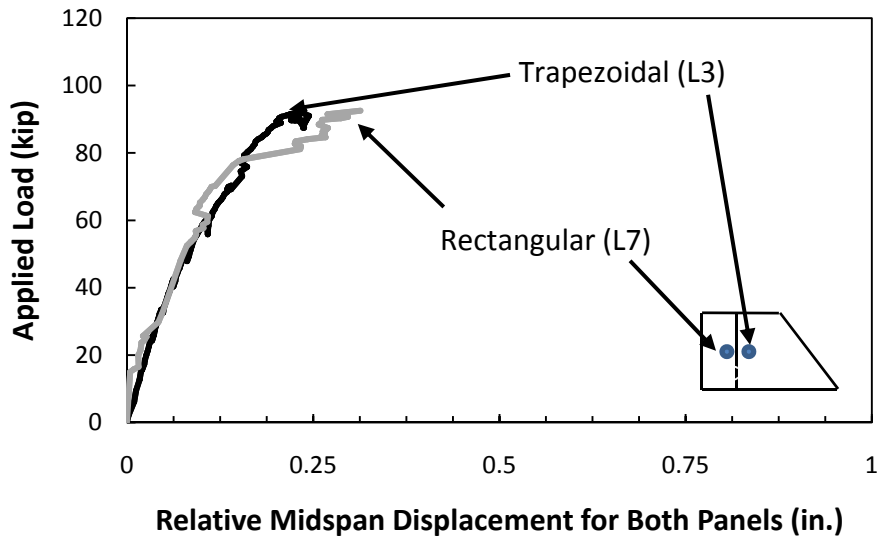
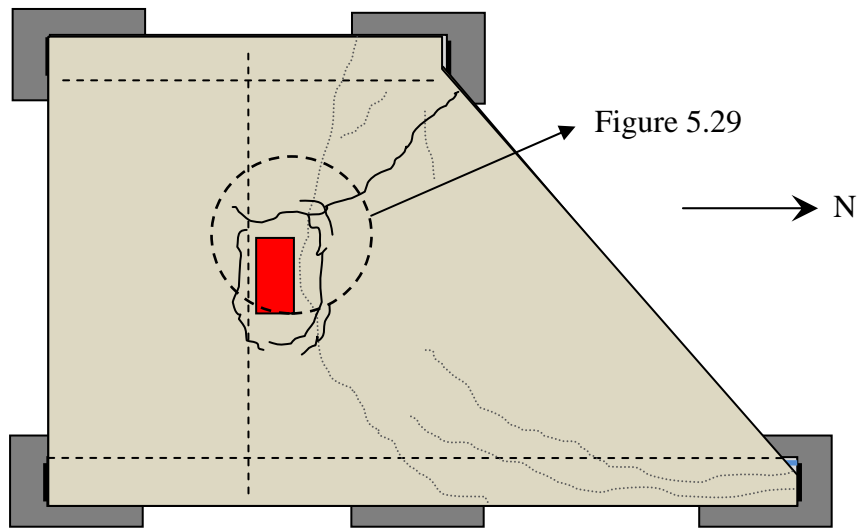
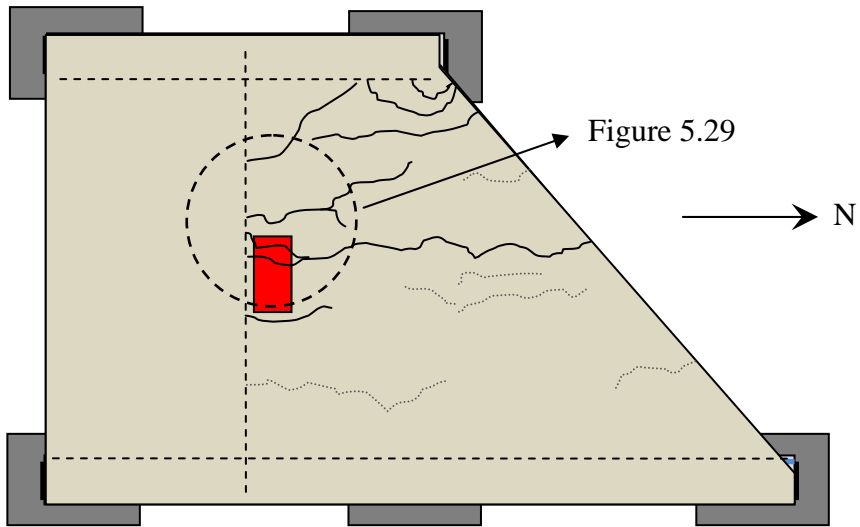


**Figure 5.27 - Measured Relative Displacement Response at Midspan of Trapezoidal and Rectangular Panels in Specimen P45P2 for Load Applied at Midspan of Square End**

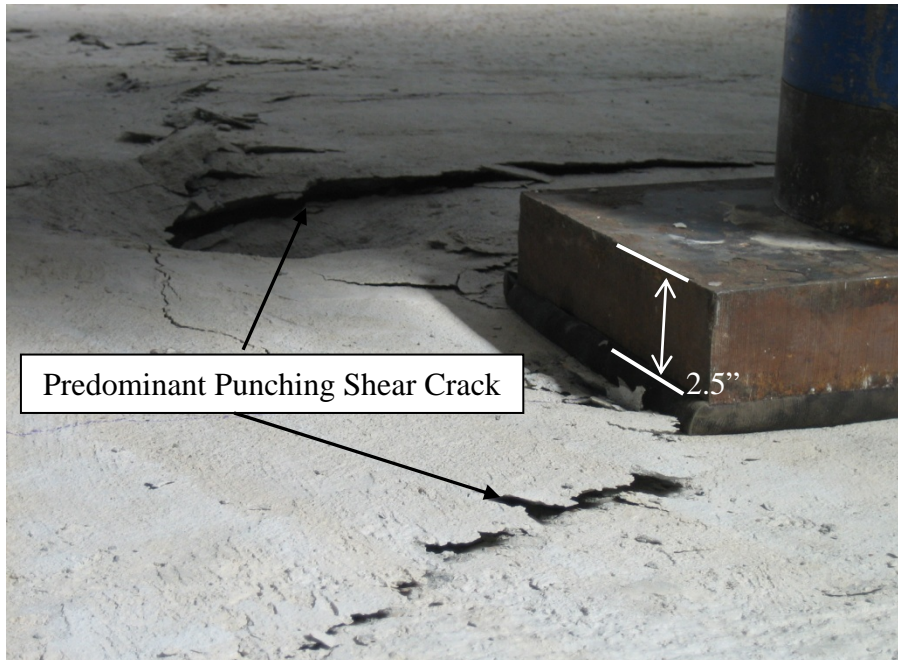


Predominant Cracks on Top Surface of Specimen

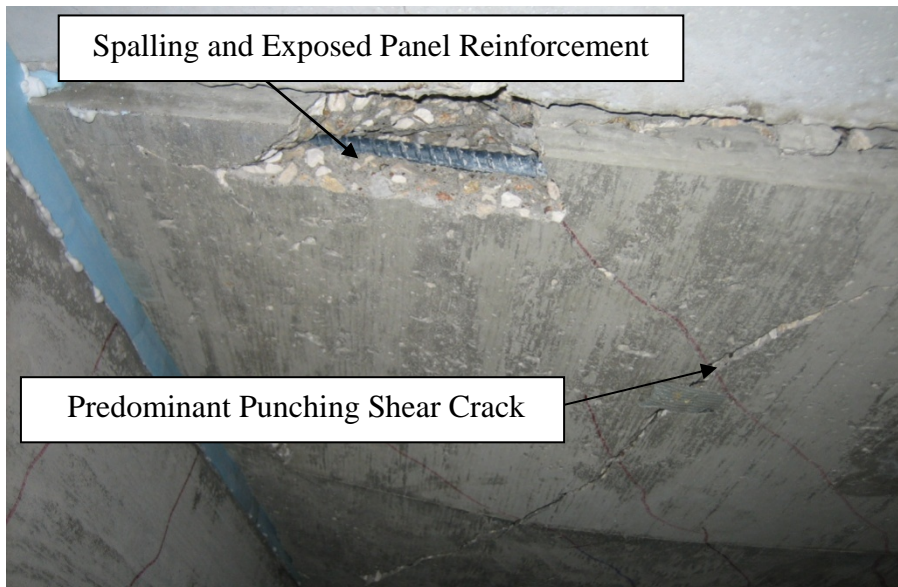


Predominant Cracks on Bottom Surface of Specimen

*Figure 5.28 – Observed Crack Patterns at Conclusion of Static Test at Midspan of Square End for Specimen P45P2*



(a) Top of Specimen at Midspan of Square End



(b) Southwest Corner of Specimen Viewed from Below

***Figure 5.29 – Photographs of Specimen P45P2 at Conclusion of Static Test at Midspan of Square End***

### 5.3.3 Specimen P45P3

Specimen P45P3 was subjected to two types of loading. In the first test, fatigue loads were applied near midspan of the SEJ along the skewed end of the trapezoidal panel. The specimen was subjected to four million loading cycles during the fatigue test. In the second test, the specimen was loaded monotonically to failure near midspan of the SEJ along the skewed end of the trapezoidal panel.

#### 5.3.3.1 *Fatigue Load Applied at Midspan of Skewed End*

During the fatigue test, the peak-to-peak amplitude of the applied load was 16 kip. In the first phase of the test, the specimen was subjected to two million loading cycles. The fatigue tested was stopped periodically – approximately every 250,000 cycles – to measure the static response of the specimen. No cracks were observed during the first phase of the fatigue test. After two million fatigue cycles, the specimen was loaded until flexural cracks formed. The maximum applied load was 43 kip and was considered to be representative of an overload. After cracking, the specimen was subjected to two million additional fatigue cycles. Periodic static tests were again conducted to detect changes in specimen stiffness. The complete load history for Specimen P45P3 is summarized in Table 5.5. For convenience in presenting the data, only representative periodic tests, marked with an asterisk in the table, are presented.

The measured displacement response of Specimen P45P3 during representative periodic tests before the static overload test is presented in Figure 5.30, and data recorded after the overload are presented in Figure 5.31. The static overload plot indicates that cracking occurred load at approximately 32 kip, and the apparent cracking load of the specimen was 34 kip. The overall stiffness of the test specimen did not change appreciably during the fatigue test. However, the displacement data recorded after 1,100,000 fatigue cycles were stiffer than expected. The linear potentiometers were repositioned before each periodic static test. Therefore, it is likely that the data reflect an error in positioning the transducers, rather than a change in the response of the test specimen.

Variation of the displacement along the loaded end for the specimen during the static overload test is provided in Figure 5.32. The largest displacements were recorded at midspan, and displacements were marginally higher at the quarter-span location near the short side support than near the long side support.

**Table 5.5 – Static Tests Conducted During Fatigue Test for Specimen P45P3**

Type of Static Test	Accumulated Fatigue Cycles	Maximum Applied Load (kip)	Condition at Conclusion of Test
Initial *	0	16	Uncracked
Periodic	250,000	16	
Periodic	500,000	16	
Periodic	850,000	16	
Periodic *	1,100,000	16	
Periodic	1,400,000	16	
Periodic	1,700,000	16	
Periodic *	2,000,000	16	
Overload *	2,000,000	43	
Periodic *	2,000,000	16	
Periodic	2,225,000	16	
Periodic	2,500,000	16	
Periodic	2,850,000	16	
Periodic *	3,100,000	16	
Periodic	3,300,000	16	
Periodic	3,500,000	16	
Periodic	3,850,000	16	
Periodic *	4,000,000	16	

\* Static Tests Used in Data Presentation

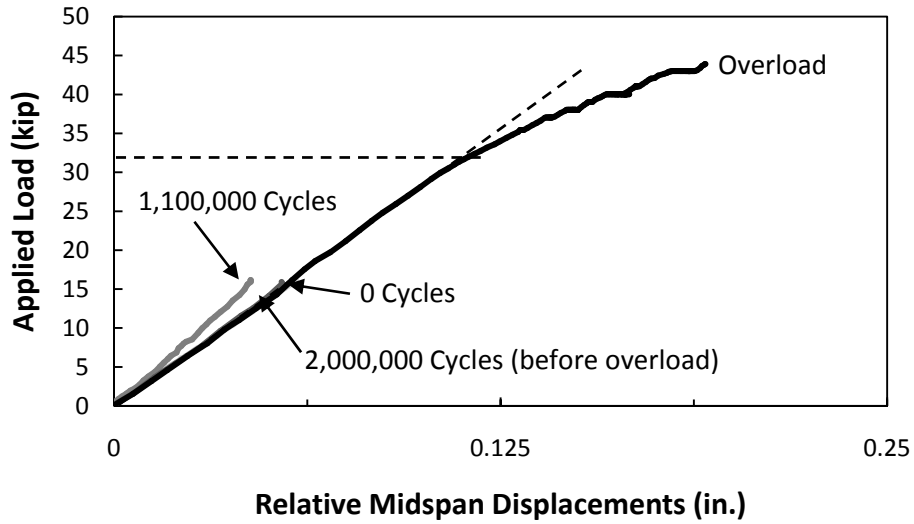


*Figure 5.30 – Measured Displacement Response at Midspan of Skewed End for Specimen P45P3 during Periodic Static Tests before Overload Test*

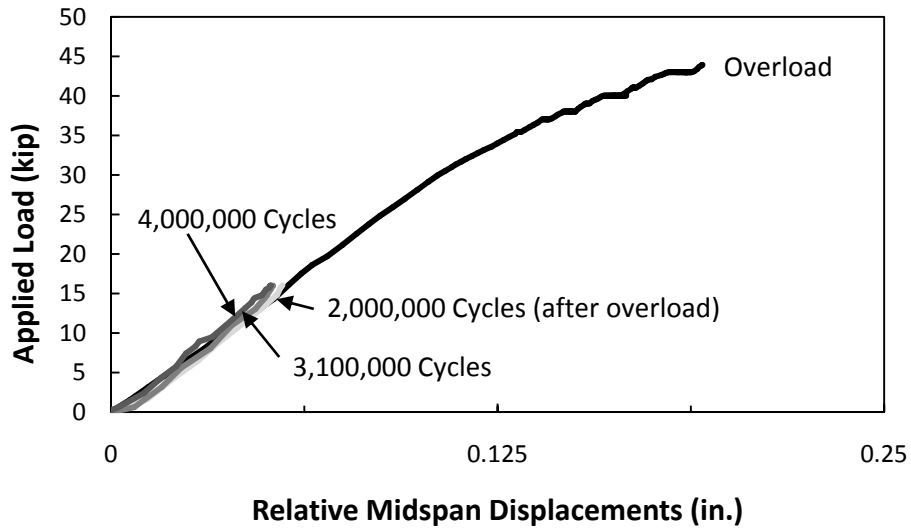


*Figure 5.31 – Measured Displacement Response at Midspan of Skewed End for Specimen P45P3 during Periodic Static Tests after Overload Test*

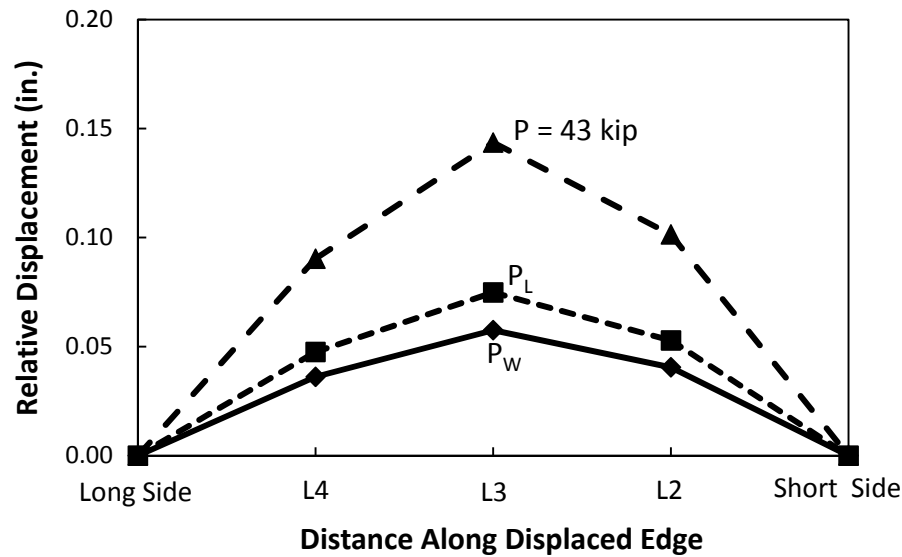


**Figure 5.32 – Variation of Displacements along Skewed End of Specimen P45P3 during Static Overload Test**

Live load induced tensile strain data along the bottom of the panel at the skewed end are presented for static tests before the static overload test in Figure 5.33, and live load induced strains for periodic static tests after the overload are provided in Figure 5.34. The figure shows that a crack passed through the strain gage on the concrete at an applied load of approximately 29 kip. Because no change in stiffness occurred before the gage was destroyed, no cracking load can be inferred from live load induced strain data during the static over load test. No significant change in stiffness along the loaded end occurred during the fatigue loading. Periodic tests after the overload show a nonlinear strain response that is likely due to opening of cracks during the overload test. Variation in strain along the bottom end of the panel for the static overload test is provided in Figure 5.35.

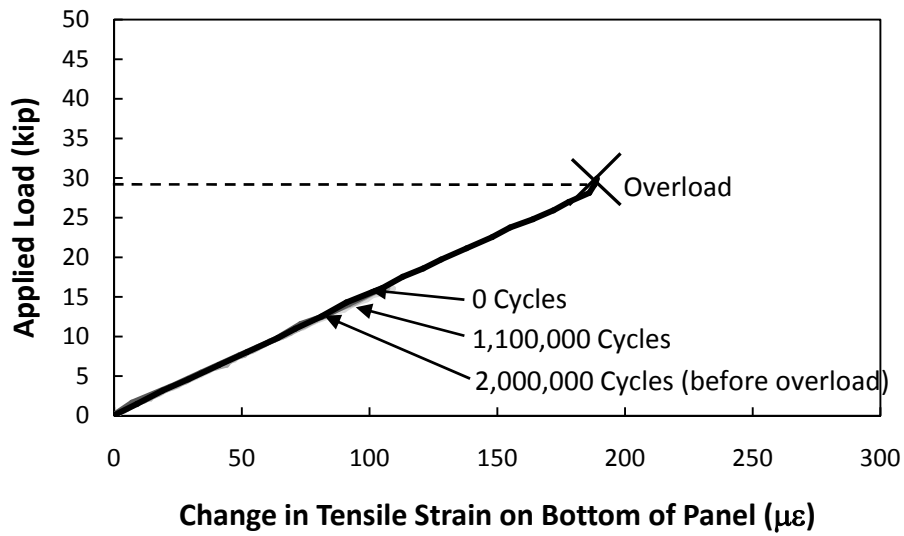


*Figure 5.33 – Measured Change in Concrete Strain on the Bottom of Panel at Midspan of Skewed End for Specimen P45P3 during Periodic Static Tests before Overload Test*

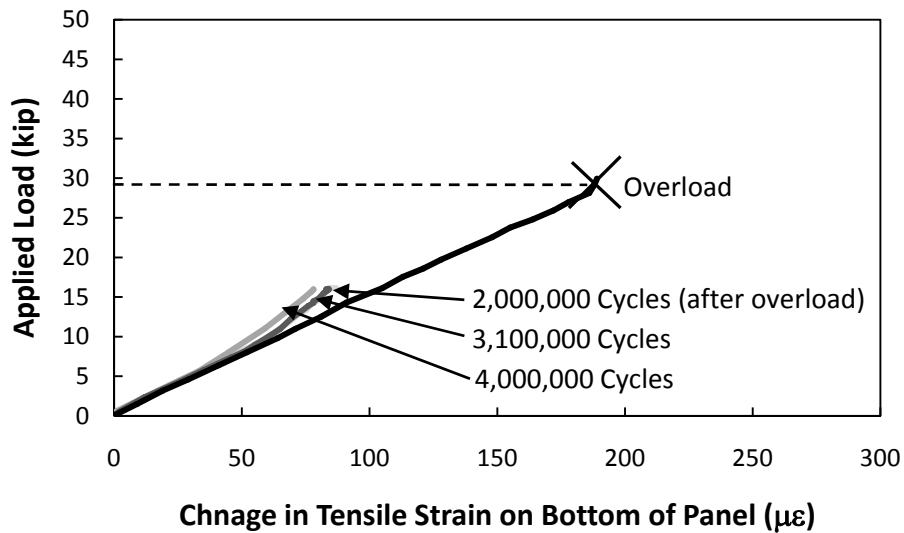


*Figure 5.34 – Measured Change in Concrete Strain on the Bottom of Panel at Midspan of Skewed End for Specimen P45P3 during Periodic Static Tests after Overload Test*



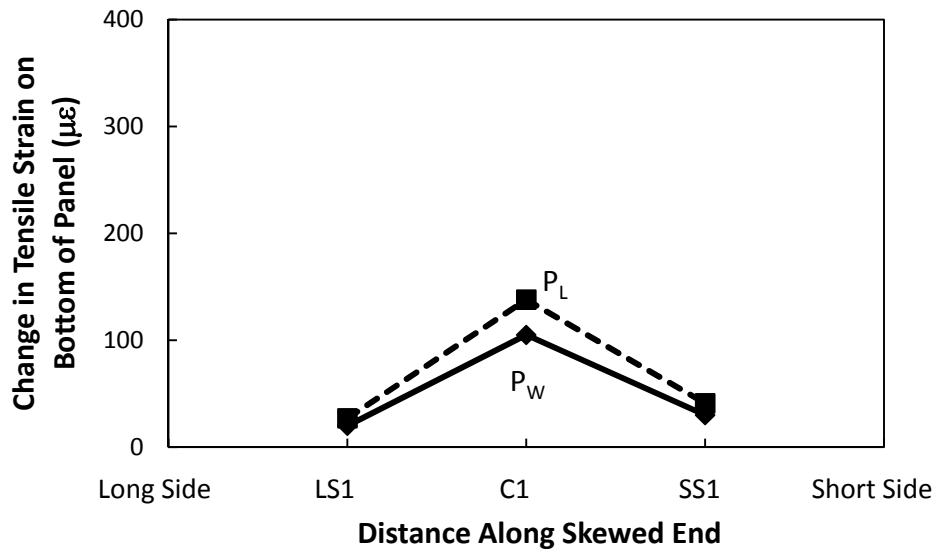


**Figure 5.35 – Distribution of Change in Concrete Strain along Bottom of Panel for Specimen P45P3 during Static Overload Test**

Compressive strain data from midspan of the SEJ (Figure 5.36) indicate a cracking load of approximately 32 kip. Periodic static tests before and after the overload are shown in Figure 5.36 and Figure 5.37 respectively. The SEJ data also indicate no significant change in stiffness during the fatigue process. Variation of SEJ strain along the loaded end, Figure 5.38, again shows highest strains at midspan and lowest strains at the quarter-span location near the long side.

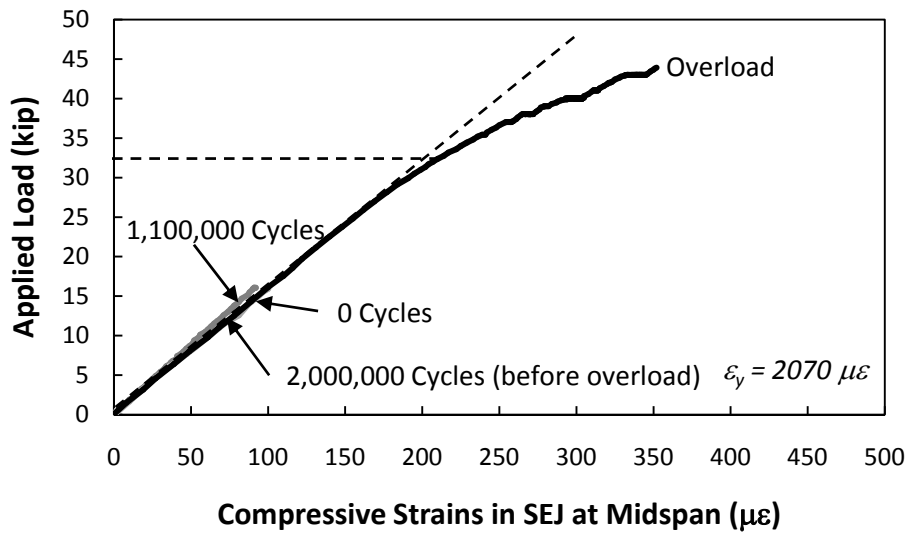


*Figure 5.36 – Measured Strain at Midspan of SEJ for Specimen P45P3 for Periodic Static Loads Applied before Static Overload Test*

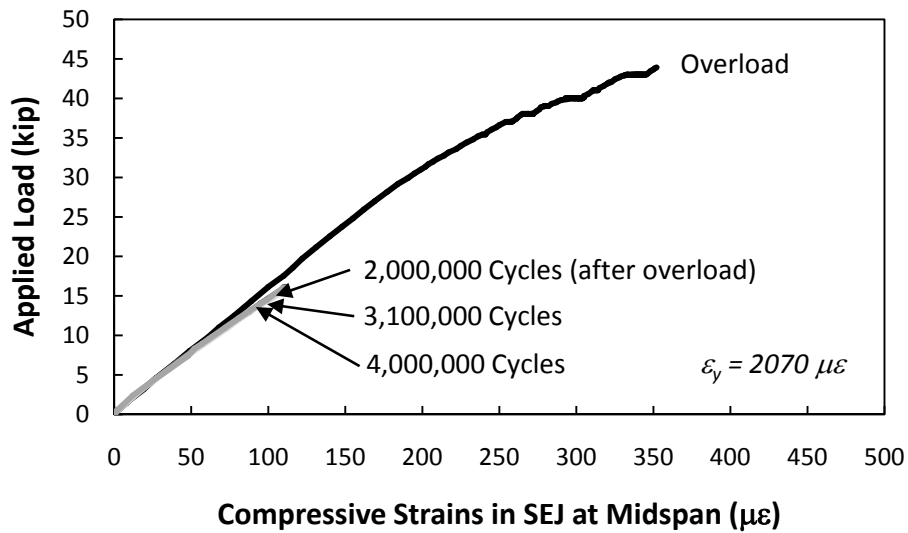


*Figure 5.37 – Measured Strain at Midspan of SEJ for Specimen P45P3 for Periodic Static Loads Applied after Static Overload Test*

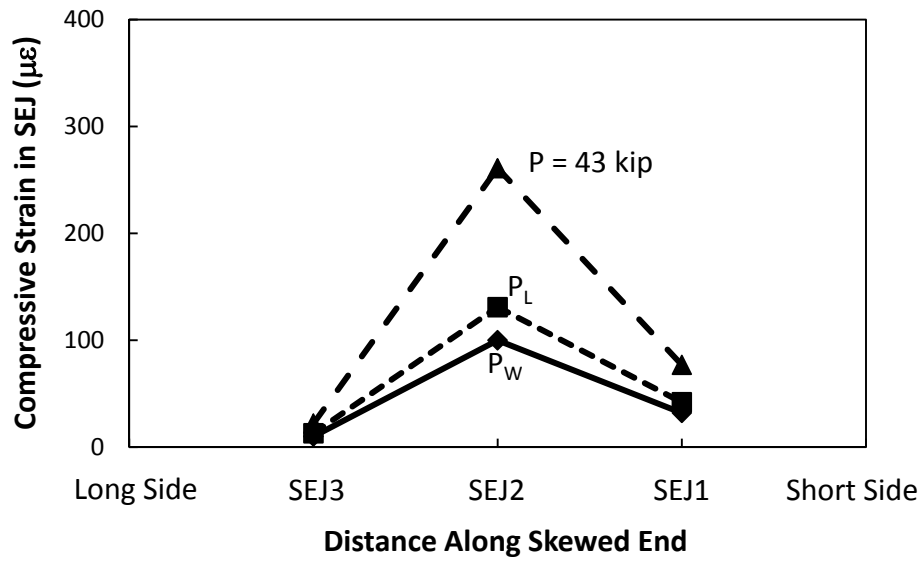


**Figure 5.38 - Variation of Strain along SEJ for Specimen P45P3 during Static Overload Test**

Live load induced tensile strain data for strand S12 are presented for periodic tests conducted before the static overload test in Figure 5.39 and after the static overload test in Figure 5.40. Again no significant changes in stiffness were observed with the fatigue loading. Variation of strain in the prestressing strands during the overload test from the loaded end towards the interior of the panel is shown in Figure 5.41. The largest changes in strain were observed directly beneath the load point, at the skewed end and then quickly drop off as distance from the loaded end increases.

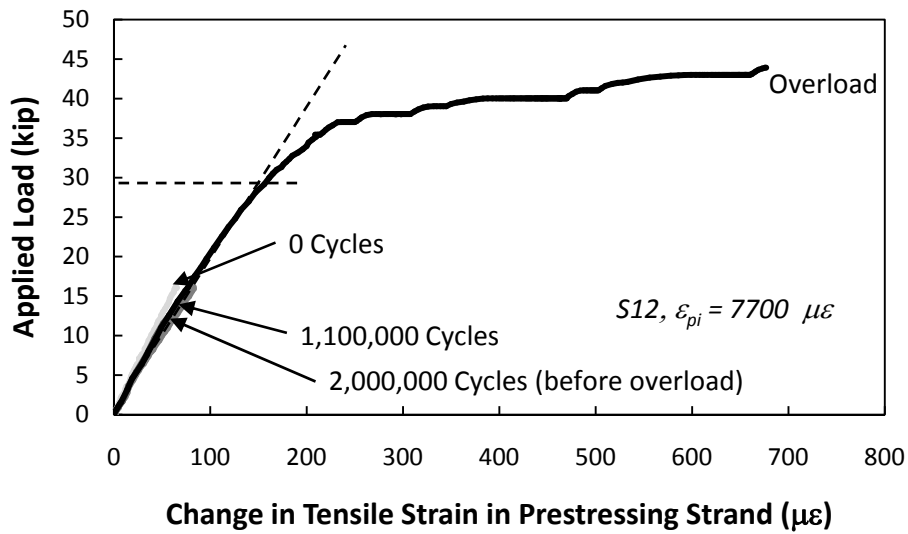


*Figure 5.39 – Measured Change in Strain Response of Strand S12 during Periodic Static Tests before Overload for Specimen P45P3 for Loads Applied at Midspan of Skewed End*

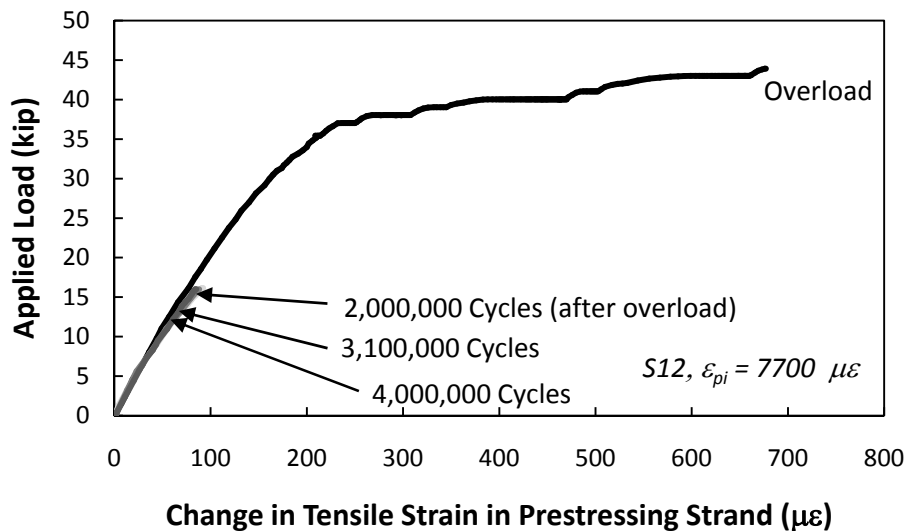


*Figure 5.40 – Measured Change in Strain Response of Strand S12 during Periodic Static Tests after Overload for Specimen P45P3 for Loads Applied at Midspan of Skewed End*

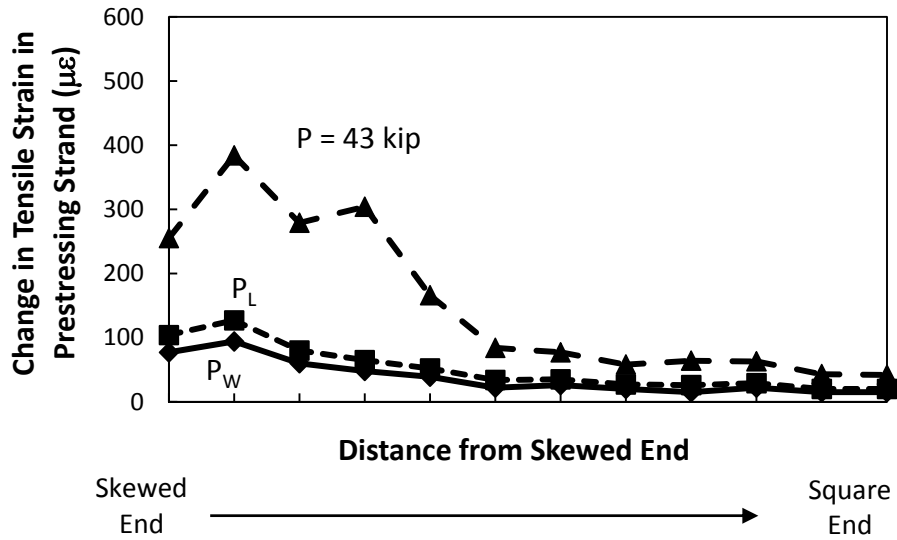


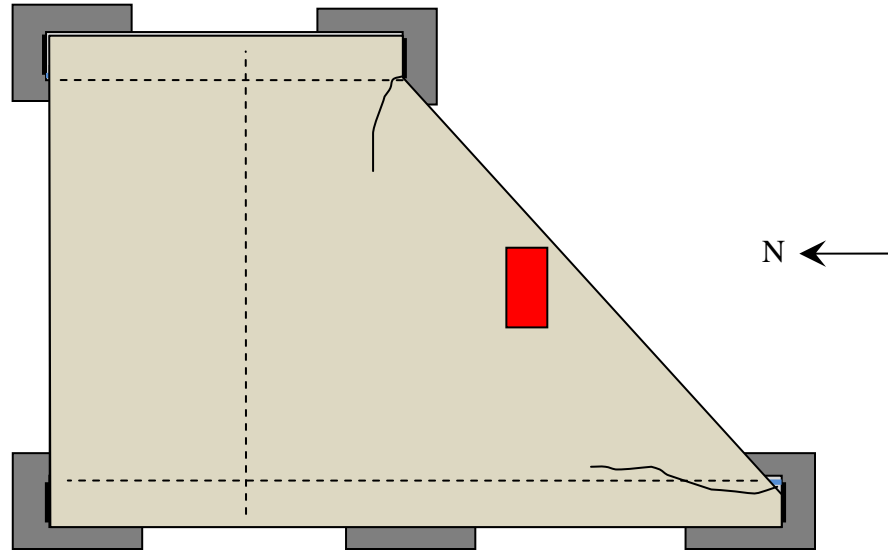
**Figure 5.41 – Variation of Maximum Strain in Prestressing Strands for Load Applied at Midspan of Skewed End of Specimen P45P3 during Static Overload Test**

A summary of the initial stiffness and estimated cracking load for each data set collected during the static overload test is provided in Table 5.6. The inferred cracking load from the instrument and the apparent cracking load ranged from 30 to 34 kip, with an average cracking load of 32 kip.

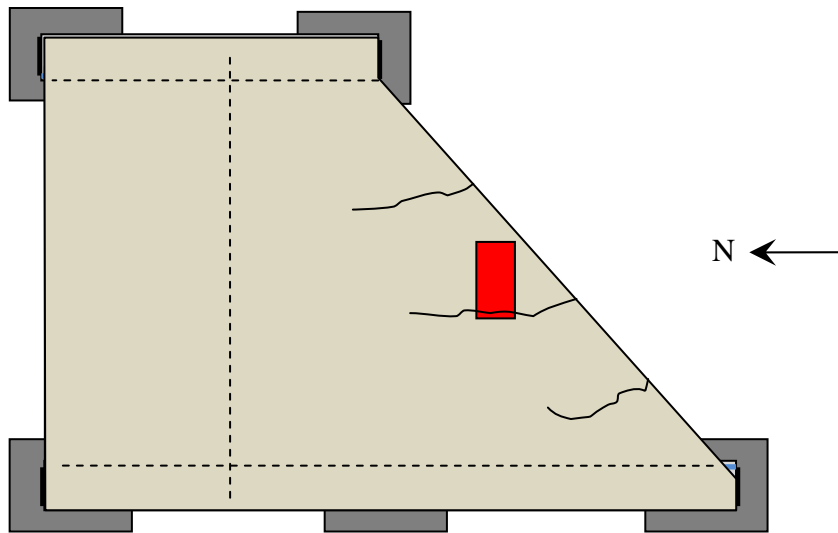
**Table 5.6 – Initial Stiffness and Inferred Cracking Loads for Specimen P45P3**

	Initial Stiffness (k/in, k/µε)	Inferred Cracking Load (kip)
Displacement	278	32
Concrete Strain on Bottom of Panel	0.158	-
SEJ Strain	0.154	32
Strain in Prestressing Strand	0.185	30
Apparent Cracking	-	34

Observed cracks for Specimen P45P3 are shown in Figure 5.42. At the conclusion of the fatigue test, cracks that formed during the static overload test had not propagated any further, and no delamination was observed between the precast panels and the topping slab.



Predominant Cracks on Top Surface of Specimen



Predominant Cracks on Bottom Surface of Specimen

*Figure 5.42 – Observed Crack Pattern for Specimen P45P3 at Conclusion of Fatigue Test*

### 5.3.3.2 Static Load to Failure Applied at Midspan of Skewed End

At the conclusion of the fatigue test, Specimen P45P3 was loaded statically to failure. Key data for the test are presented in this section.

Relative displacements at midspan of the skewed end of Specimen P45P3 are plotted against the applied load in Figure 5.43. The specimen was already cracked, but the plot in Figure 5.43 exhibits a change in stiffness at approximately 40 kip. The variation of displacements along the loaded end is presented in Figure 5.44. For levels of applied load less than the Design Wheel Load, the displacements are nearly symmetric about midspan. However, at the Factored Design Load, the highest displacements occurred at midspan and larger displacements were recorded at the quarter-span location near the short side than the quarter-span location near the long side.

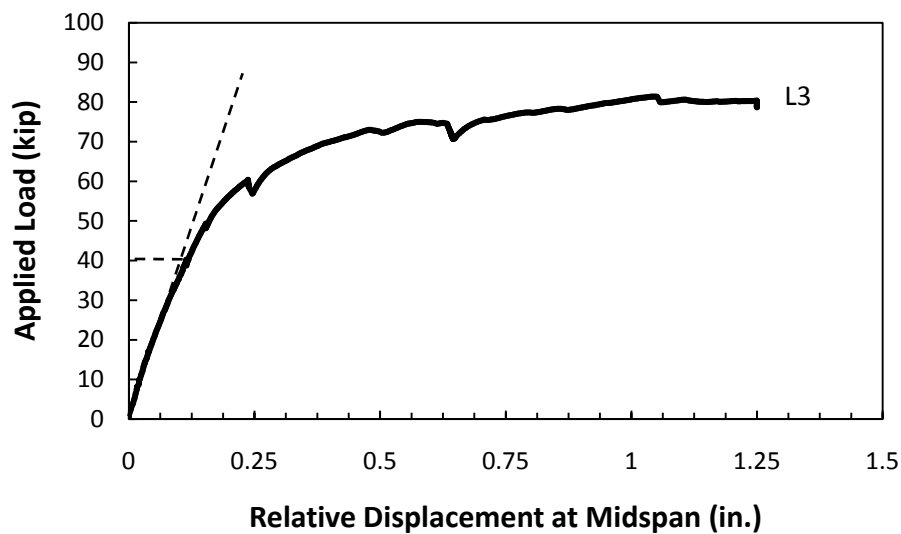


*Figure 5.43 – Measured Displacement Response of Specimen P45P3 for Load Applied at Midspan of Skewed End after Fatigue Test*



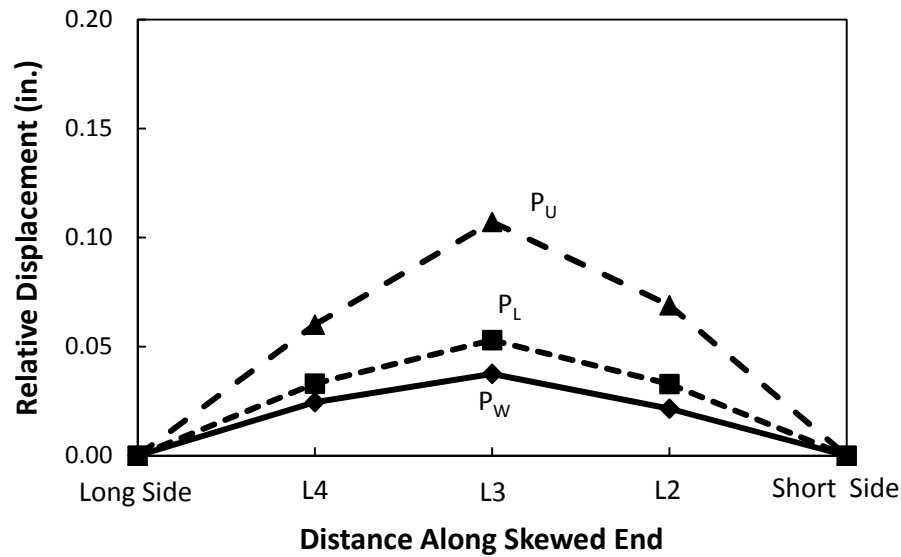


**Figure 5.44 – Variation of Displacements along Skewed End of Specimen P45P3 after Fatigue Test**

Cracks from the fatigue test influenced the strain gage data on the bottom side of the panel in the static test to failure. Data from midspan of the skewed end are plotted in Figure 5.45. The strain data exhibit a low initial stiffness, and then the stiffness increases before the data become unreliable. Because the change in stiffness begins at low load levels (less than 20 kip), the change in stiffness along the plot may have resulted from the propagation of cracks under the applied load that originally formed during the fatigue test. Strain variation along the loaded end is presented in Figure 5.46. Strains are only slightly higher on the short side than on the long side.

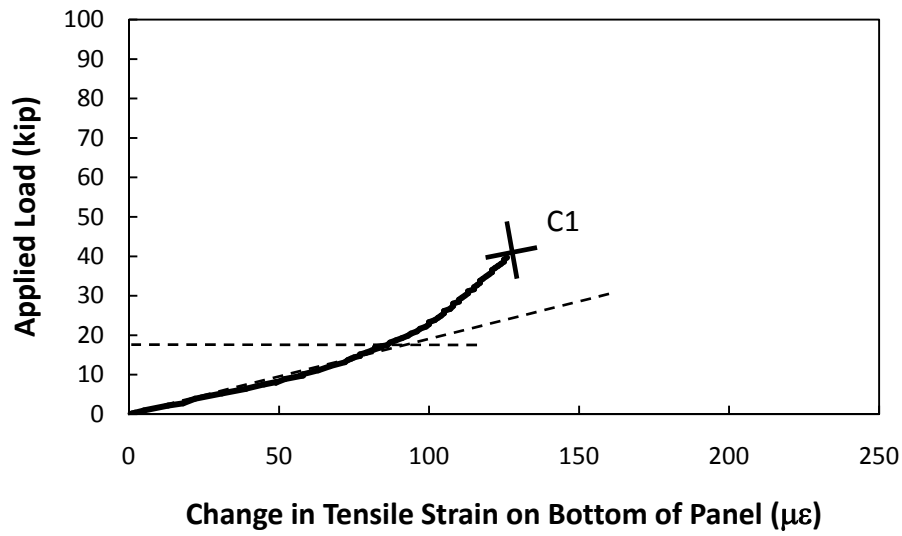


*Figure 5.45 – Change in Tensile Strain Data on Bottom of Precast Panel for Specimen P45P3 for Load Applied at Midspan of Skewed End after Fatigue Test*

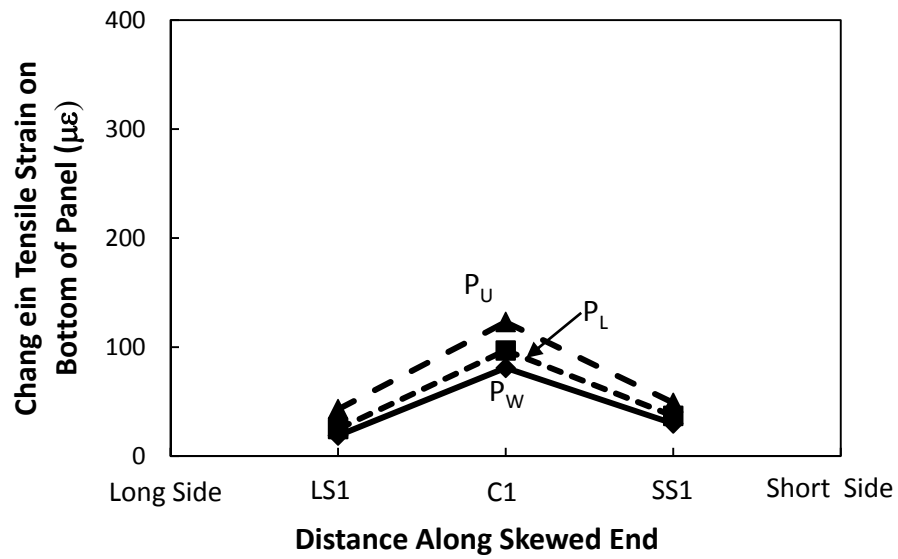


*Figure 5.46 – Distribution of Change in Concrete Strain on the Bottom of the Panel along Skewed End of Specimen P45P3 after Fatigue Test*

Compressive strain data at midspan of the SEJ are presented in Figure 5.47. The system changes stiffness at a load of approximately 48 kip, but this is not the cracking load because the specimen was already cracked during the fatigue test. Variation of strain along the SEJ is seen in Figure 5.48. Again, higher strains were observed at the quarter-span location near the short side than near the long side.

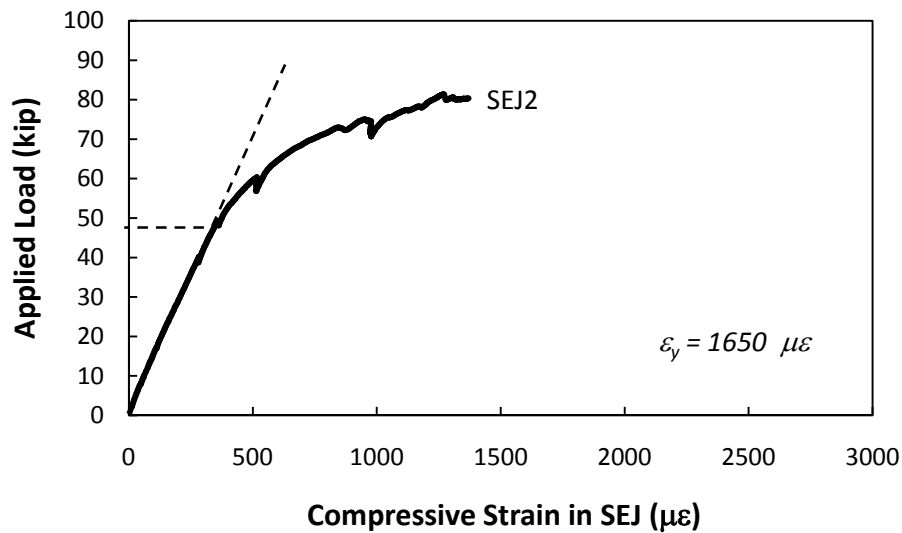


*Figure 5.47 – Measured Compressive Strain at Midspan of SEJ for Specimen P45P3 after Fatigue Test*

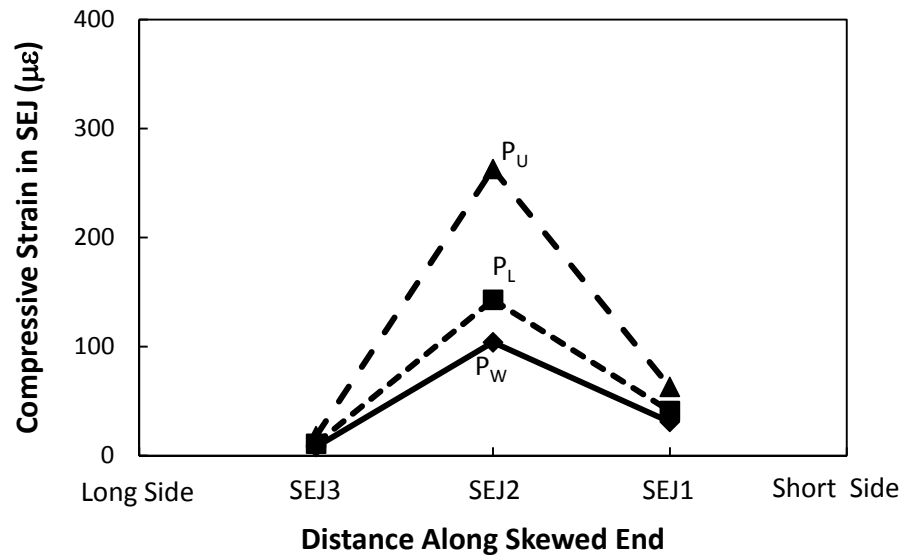


***Figure 5.48 - Variation of Strain on SEJ along Skewed End of Specimen P45P3 after Fatigue Test***

Live load induced tensile strains in prestressing strands S12 and S11 are plotted in Figure 5.49. No observation of cracking load can be made from the strand strain data because the specimen was already cracked before the start of the static load to failure. Variation of the change in the prestressing strand strain from the interior of the panel to the loaded end is presented in Figure 5.50. Strain changes are largest under the load point and drop off quickly as distance away from the loaded end increases. Strain gage S4 was damaged, and so it is not included in Figure 5.50.

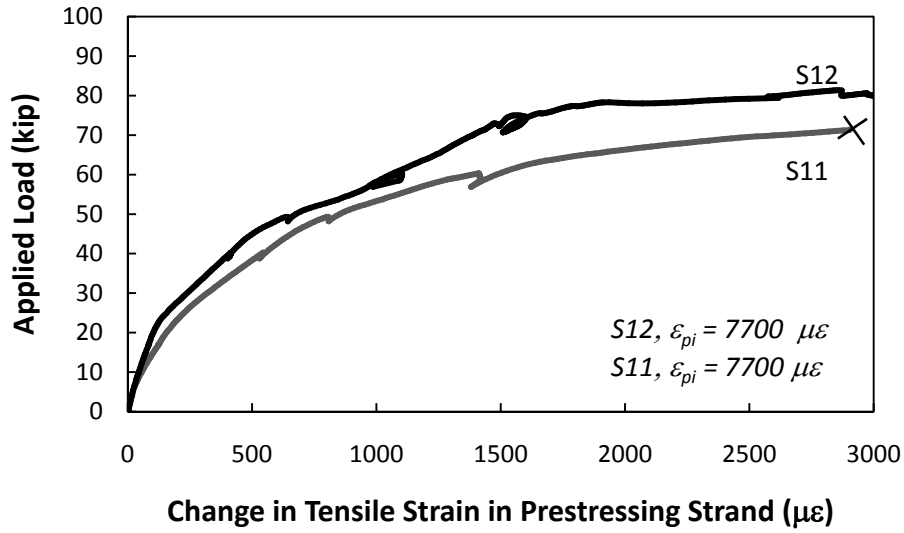


*Figure 5.49 – Measured Change in Tensile Strain in Prestressing Strand in Specimen P45P3 for Load Applied at Midspan of Skewed End after Fatigue Test*

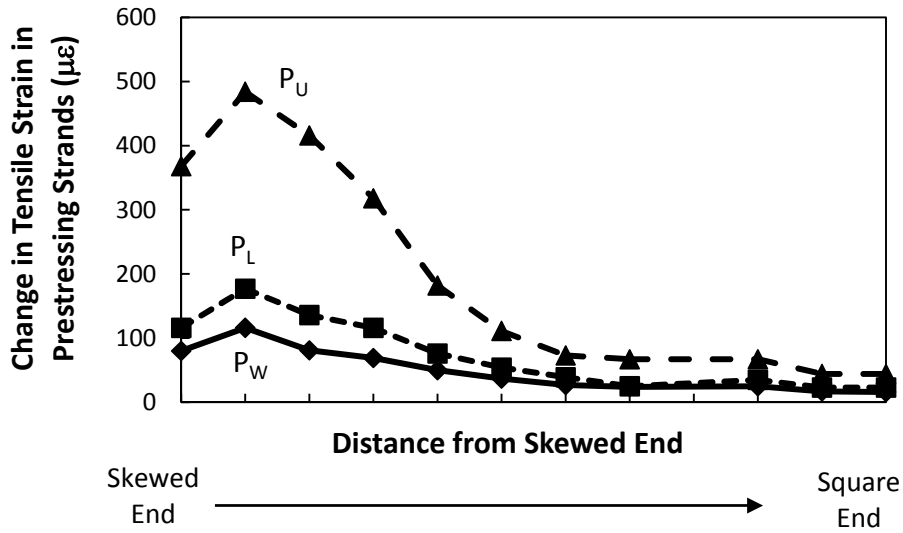
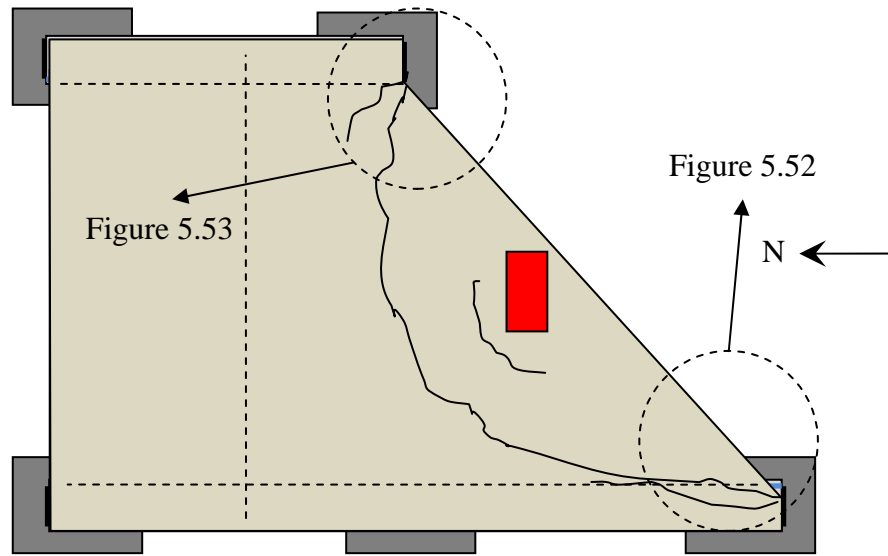


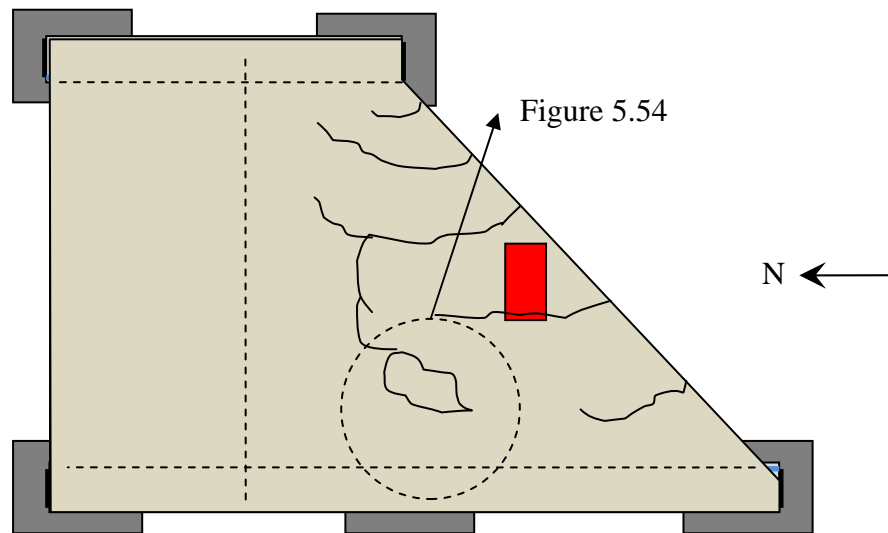
*Figure 5.50 – Variation of Maximum Strain in Prestressing Strands for Load Applied at Midspan of Skewed End for Specimen P45P3 after Fatigue Test*

Observed cracks in the specimen at the conclusion of the static test to failure are shown in Figure 5.51. The failure mechanism was a shear failure at the short side support,

and no delamination between the panel and topping slab was observed at the maximum applied load. Spalling on the bottom of the panel was observed at the maximum applied load, but no panel reinforcement was exposed. Photographs of the specimen at the conclusion of the test are provided in Figure 5.52, Figure 5.53, and Figure 5.54.



Predominant Cracks on Top Surface of Specimen



Predominant Cracks on Bottom Surface of Specimen

***Figure 5.51 – Observed Crack Pattern for Specimen P45P3 for Static Test to Failure***

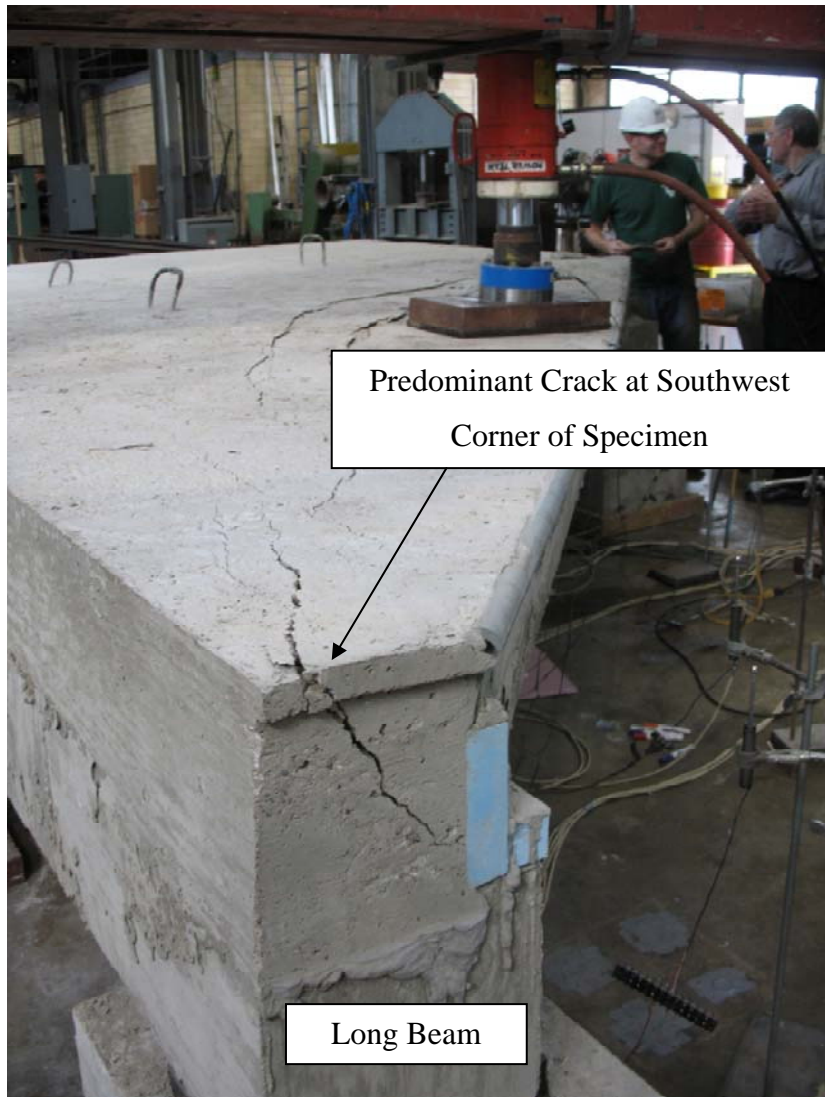
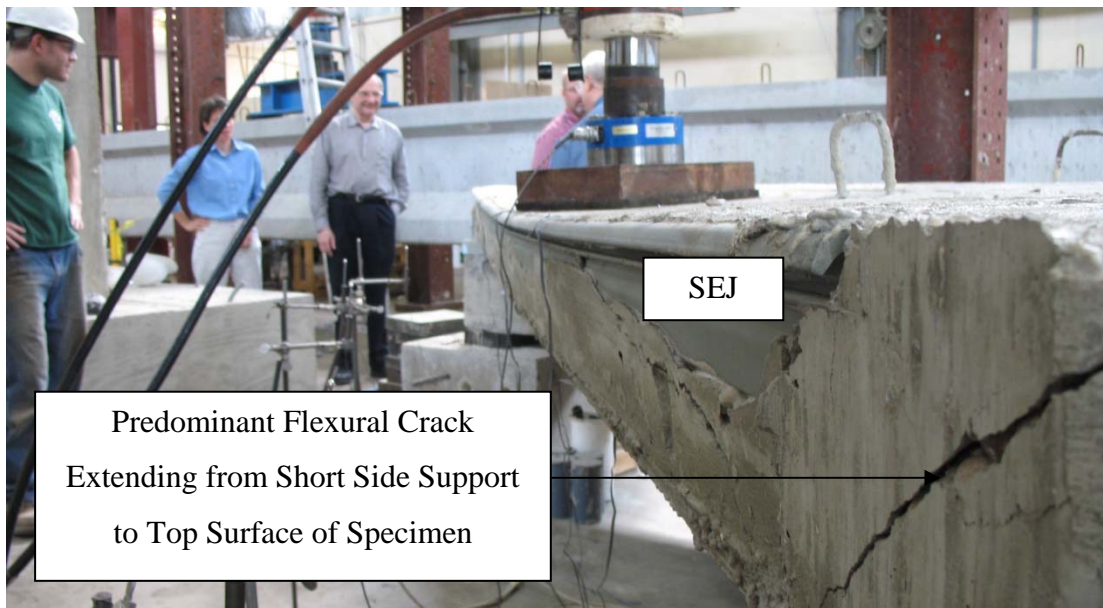


*Figure 5.52 – Predominant Cracks at Southwest Corner of Specimen at Conclusion of Static Test to Failure of Specimen P45P3*





(a) Southeast Corner of Specimen P45P3 Viewed from Side



(b) Southeast Corner of Specimen P45P3 Looking along Skewed End

***Figure 5.53 – Predominant Cracks at Southeast Corner of Specimen P45P3 at Conclusion of Static Test to Failure***

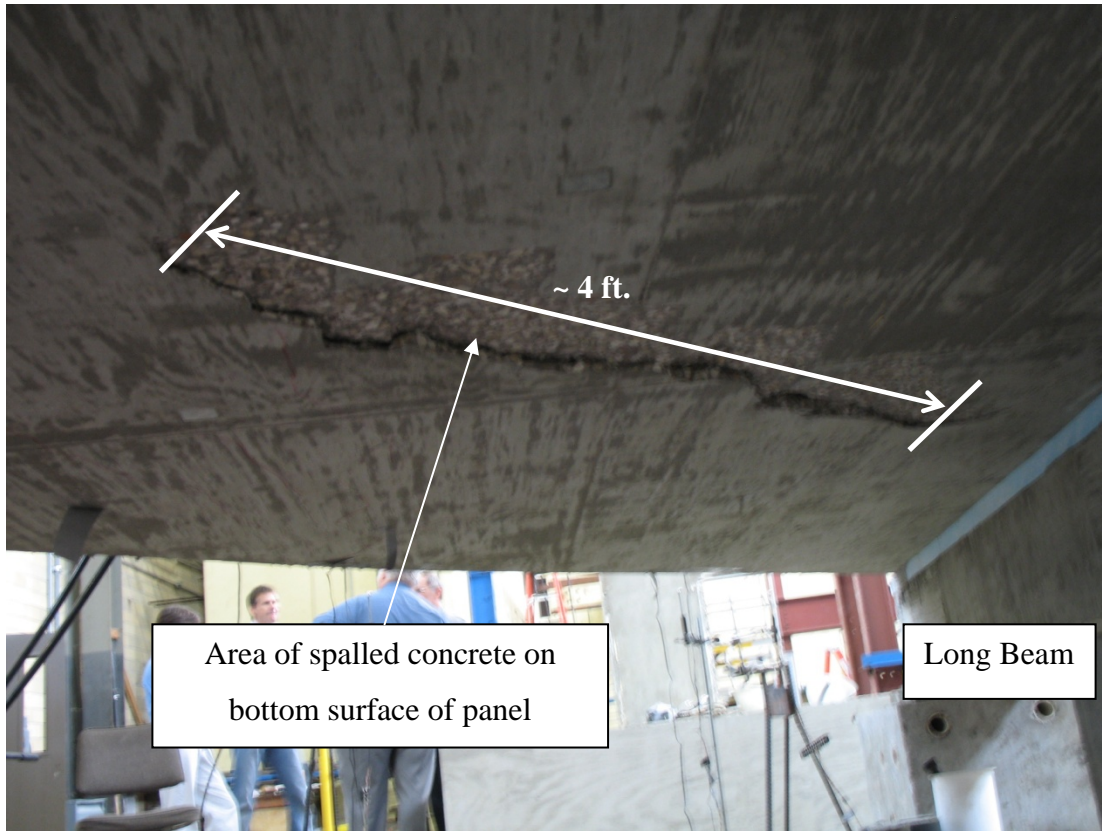


*Figure 5.54 – Spalling on Bottom Surface of Specimen P45P3 at Conclusion of Static Test to Failure*

## **5.4 MEASURED RESPONSE OF THE 30-DEGREE SPECIMENS**

Measured data from the two specimens with 30-degree skews are summarized in this section.

### **5.4.1 Specimen P30P1**

Specimen P30P1 was tested monotonically to failure two times. During the first test, the load was applied near midspan of the SEJ along the skewed end of the trapezoidal panel. During the second test, load was applied near midspan of the square end of the trapezoidal panel. Key data for this specimen include relative displacements of the loaded end, strain on the bottom of the panel, and strain on the top surface of the SEJ.

#### ***5.4.1.1 Load Applied at Midspan of Skewed End***

The load was applied monotonically to failure. The apparent cracking load of Specimen P30P1 for load applied at midspan of the skewed edge was 32 kip. The measured displacement response at midspan of the skewed end is shown in Figure 5.55. The displacement response shows a cracking load of approximately 32 kip, but the stiffness quickly decreased for larger loads. As the applied load approached 50 kip, delamination between the panel and topping slab was heard, but few cracks were visible on the surface of the specimen. After delamination, the specimen was unable to carry a maximum applied load higher than 50 kip. The distribution of displacements along the loaded end is shown in Figure 5.56.

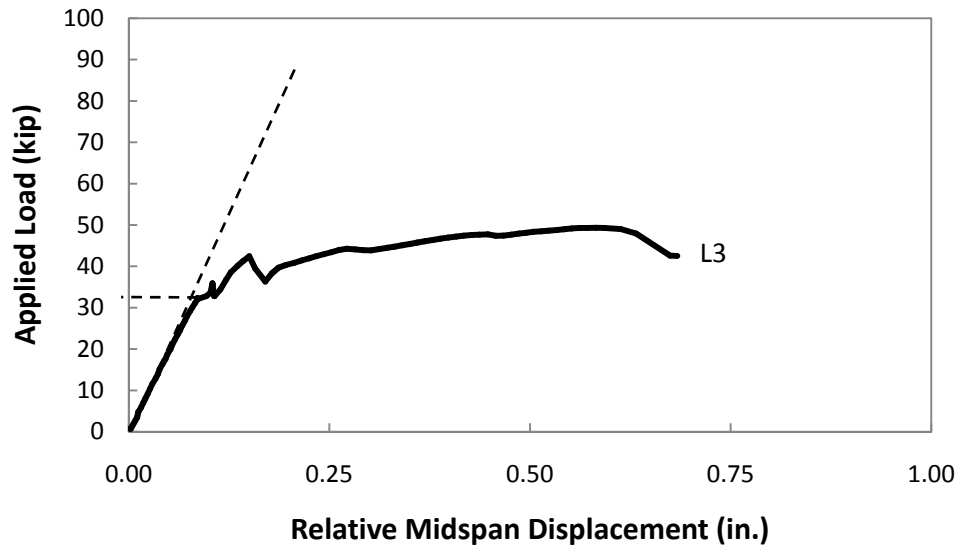


*Figure 5.55 – Measured Displacement Response of Specimen P30P1 for Load Applied at Midspan of Skewed End*

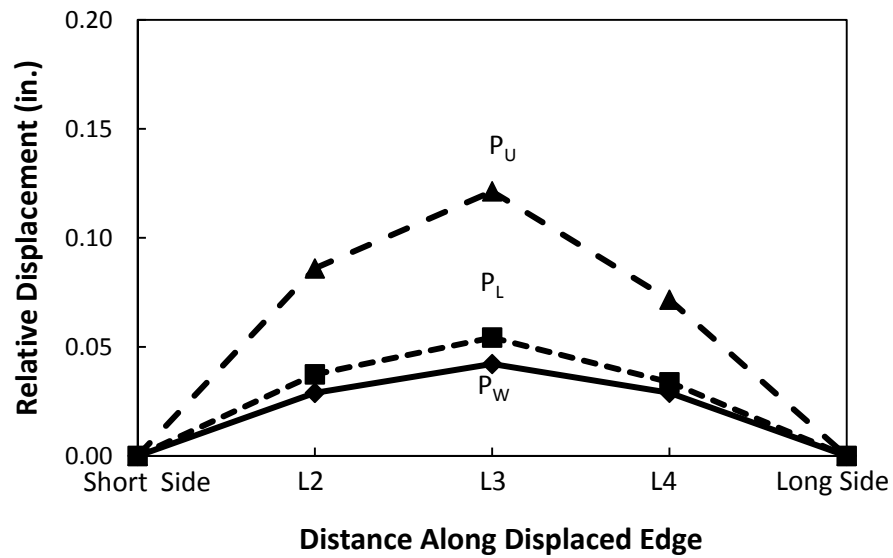


*Figure 5.56 - Variation of Displacement along Skewed End of Specimen P30P1*

The change in tensile strain data from the bottom of the panel at midspan of the skewed end are plotted in Figure 5.57. The data also indicate that the strain gage was damaged at a load of approximately 32 kip. Because no change in stiffness is apparent from the concrete strain data, a cracking load could not be inferred from this data set. Variation of strain on the bottom of the panel along the loaded end is provided in Figure 5.58. Live load induced strains were highest at midspan and lowest at quarter-span location near the long side.

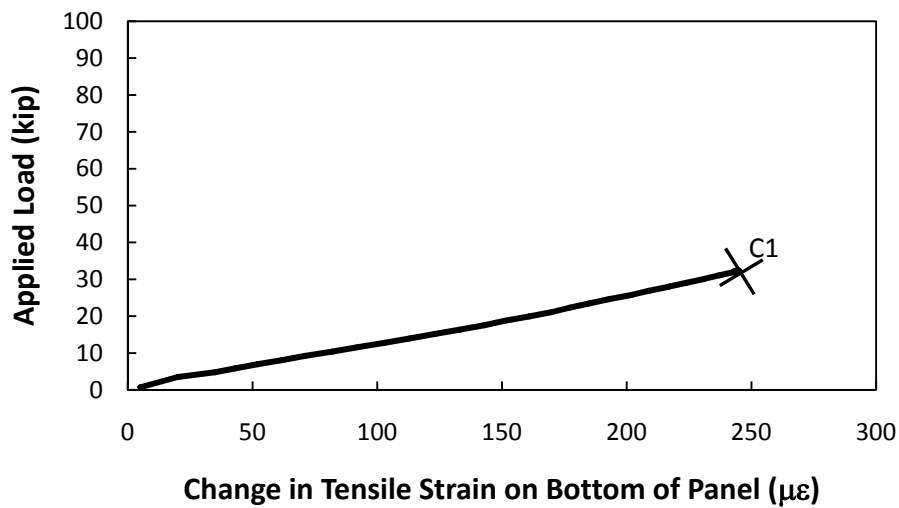


*Figure 5.57 – Change in Tensile Strain on Bottom of Panel at Midspan of Skewed End of Specimen P30P1*

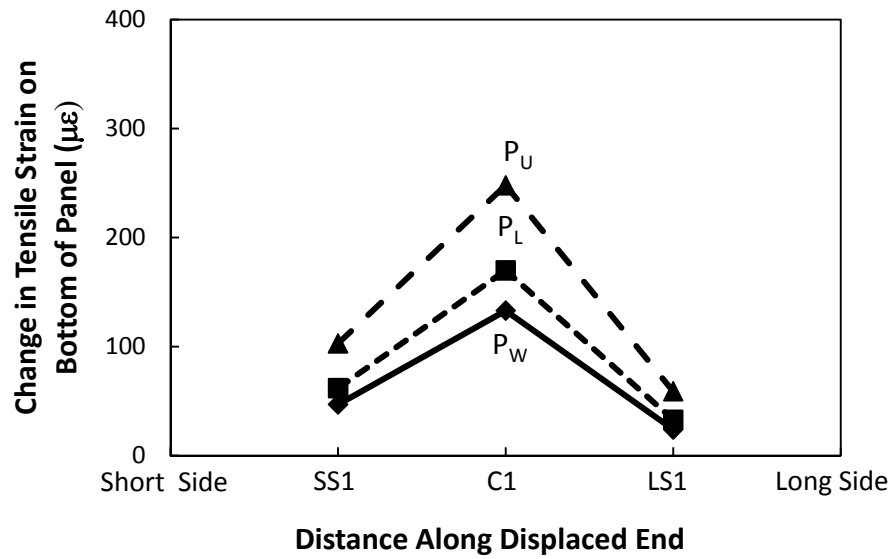


**Figure 5.58 – Distribution of Change in Concrete Strain on Bottom of Panel along Skewed End of Specimen P30P1**

Compressive strain data at midspan of the expansion joint are plotted in Figure 5.59; the SEJ data also indicate a cracking load for the specimen of approximately 33 kip. Variation of strain along the SEJ is shown in Figure 5.60. Strains were highest at midspan, and the strains at SEJ1 were higher than the strains at SEJ3.

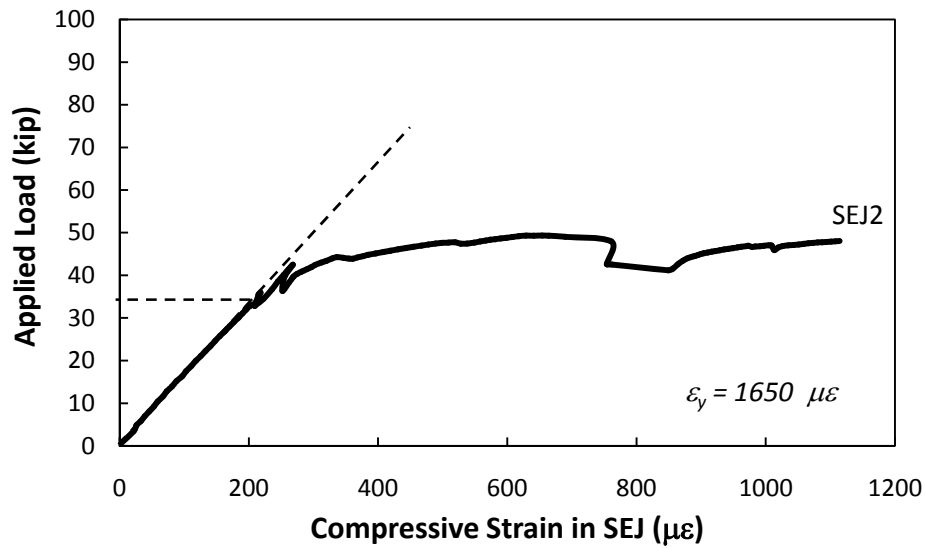


Figure 5.59 – Compressive Strain at Midspan of SEJ in Specimen P30P1

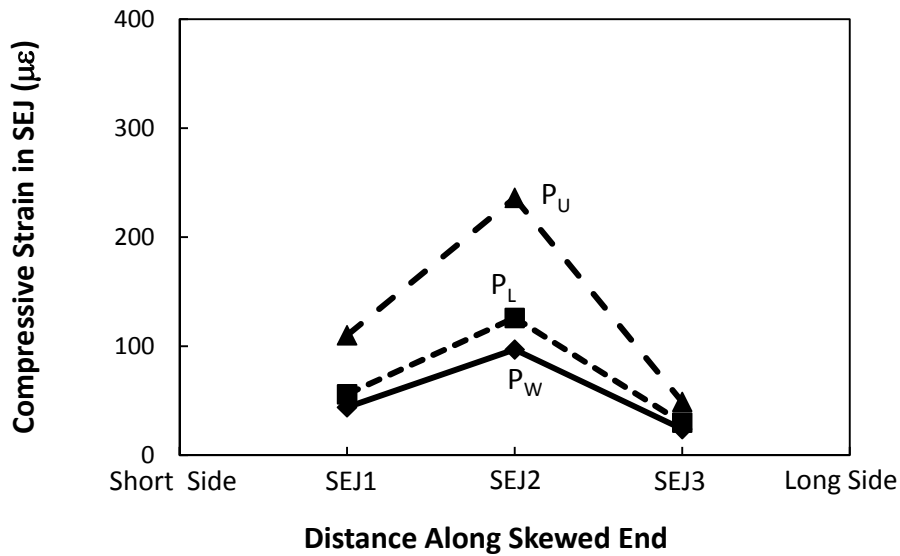


Figure 5.60 - Variation of Strain along SEJ of Specimen P30P1

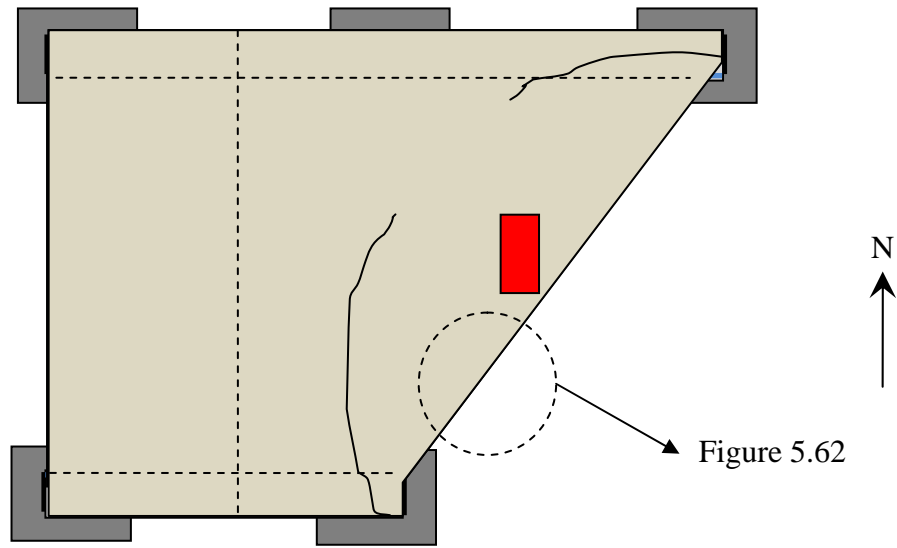
The inferred cracking loads from the instrumentation and the apparent cracking load for Specimen P30P1 are provided in Table 5.7.

**Table 5.7 – Initial Stiffness and Estimated Cracking Loads for Specimen P30P1 for Load Applied at Midspan of Skewed End**

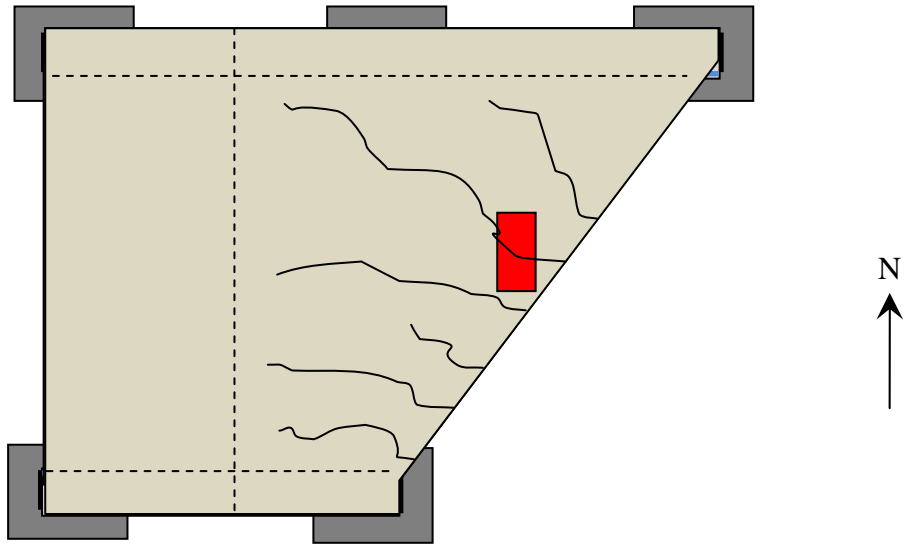
	Initial Stiffness (k/in, k/ $\mu\epsilon$ )	Inferred Cracking Load (kip)
Displacement	336.4	33
Concrete Strain on Bottom of Panel	0.143	-
SEJ Strain	0.162	32
Apparent Cracking	-	32

Observed cracks in the specimen at the conclusion of the test are shown in Figure 5.61. The failure mechanism for specimen P30P1 was delamination between the panel and topping slab for load applied at the skewed end of the specimen. Therefore, visible crack widths on the surface of the specimen at the conclusion of the skewed end loading were small. A photograph of the gap between the panel the topping slab due to the delamination is provided in Figure 5.62.





Predominant Cracks on Top Surface of Specimen



Predominant Cracks on Bottom Surface of Specimen

***Figure 5.61 – Observed Cracks at Conclusion of Static Test of Specimen P30P1 for Load Applied at Midspan of Skewed End***

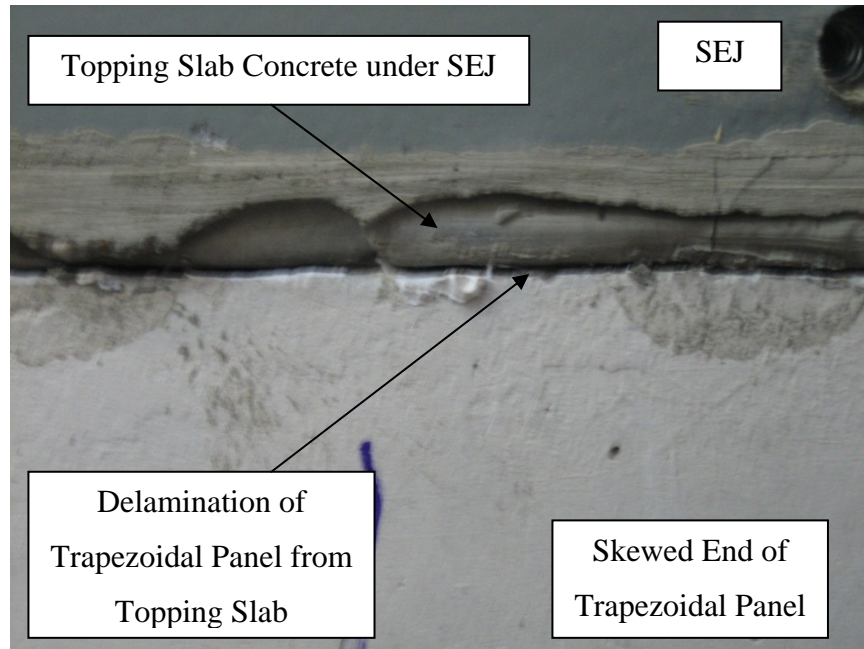


***Figure 5.62 – Photograph of Specimen P30P1 at Conclusion of Static Test for Load Applied at Midspan of Skewed End***

#### ***5.4.1.2 Load Applied at the Square End***

Specimen P30P1 was loaded at midspan of the square end after the test along the skewed end. Cracks from the skewed end loading damaged many of the strain gages on the bottom of the panel, so only displacement data for load applied at midspan of the square end were reliable. Also, because cracks formed during the test at midspan of the skewed end, it was not possible to identify the load at which new cracks appeared for load applied at midspan of the square edge.

Measured relative displacements at midspan of the square end are plotted in Figure 5.63. The data show a cracking load for the square end at 27 kip. Displacements of the square end remained small as the applied load approached 60 kip. Due to the previous delamination of the specimen, the linear potentiometers were removed at 60 kip to prevent damage to equipment in the case of complete separation of the panel from the test specimen. But the specimen demonstrated considerable ductility, and though

displacement data is not available at failure, the specimen failed due to punching shear in the topping slab at a load of 87 kip.

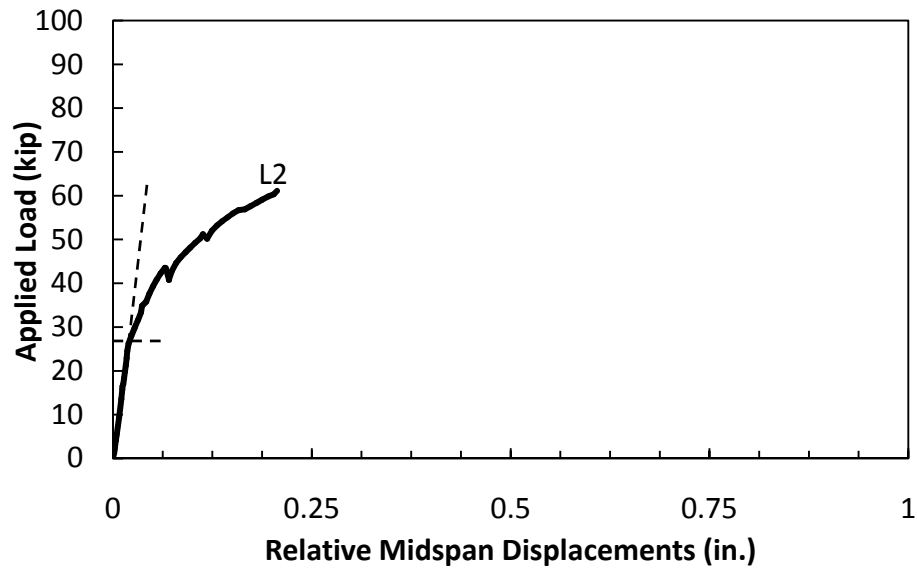
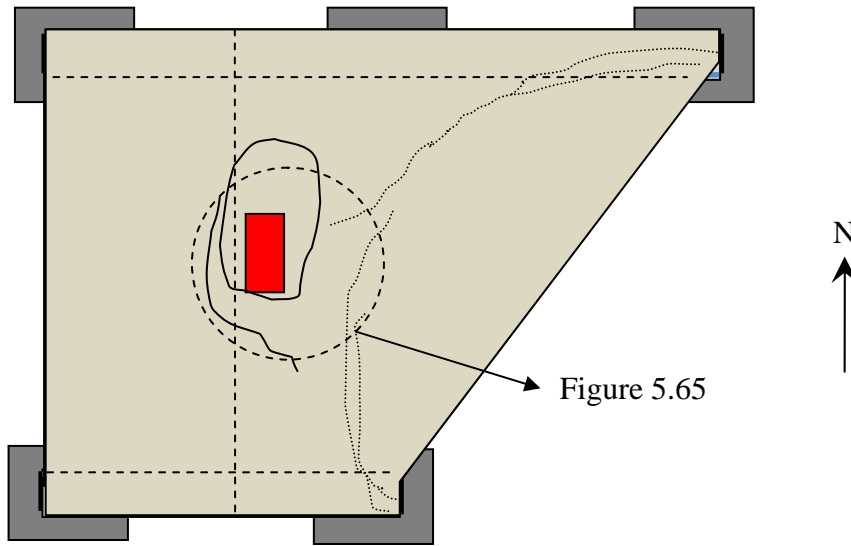
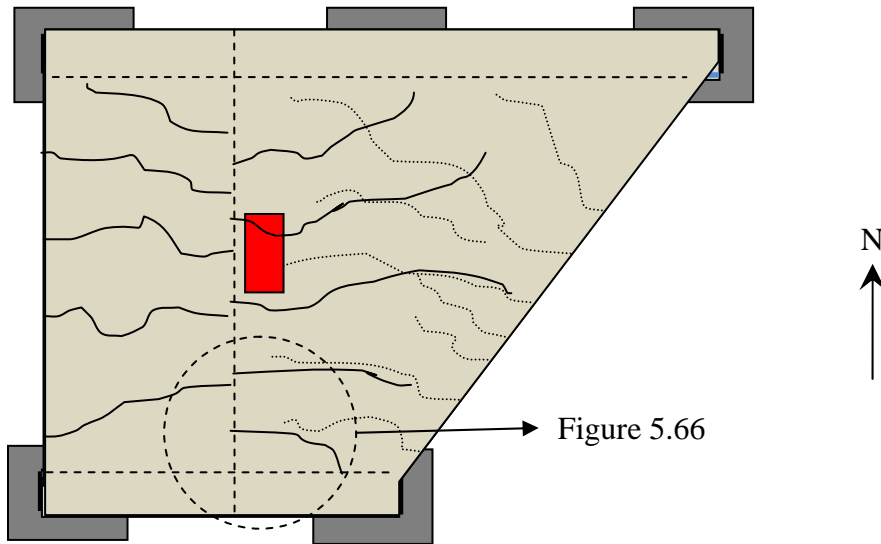


***Figure 5.63 – Measured Displacement Response at Midspan of Square End of Specimen P30P1***

Observed cracks at the conclusion of the test on the square end are shown in Figure 5.64. As mentioned, the specimen failed in punching shear in the topping slab. Photographs of the specimen at the conclusion of the test are in Figure 5.65 and Figure 5.66; Figure 5.65 shows the punching shear cracks on the top surface of the specimen, and Figure 5.66 shows the displacement of the delaminated panel under the punching shear cone.



Predominant Cracks on Top Surface of Specimen



Predominant Cracks on Bottom Surface of Specimen

***Figure 5.64 – Observed Crack Pattern at Conclusion of Static Test for Specimen P30P1 for Load Applied at Midspan of Square End***

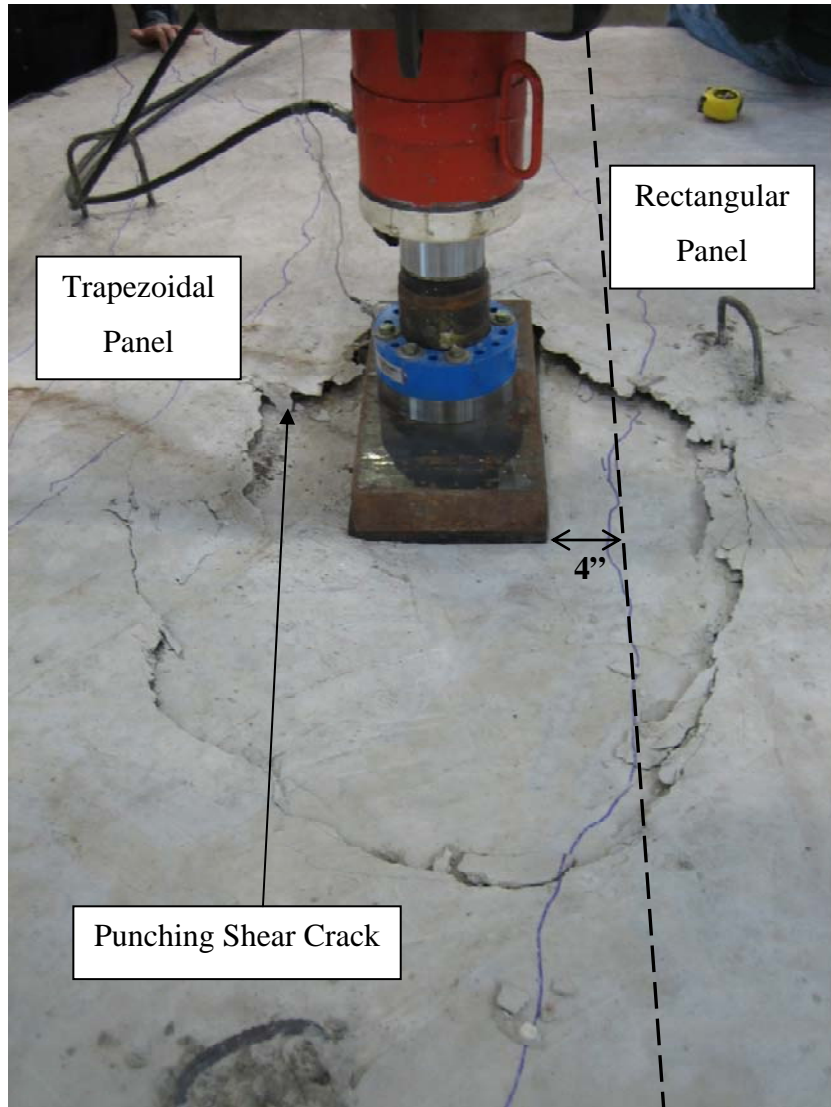


*Figure 5.65 – Photograph of Punching Shear Failure for Specimen P30P1 for Load Applied at Midspan of Square End*

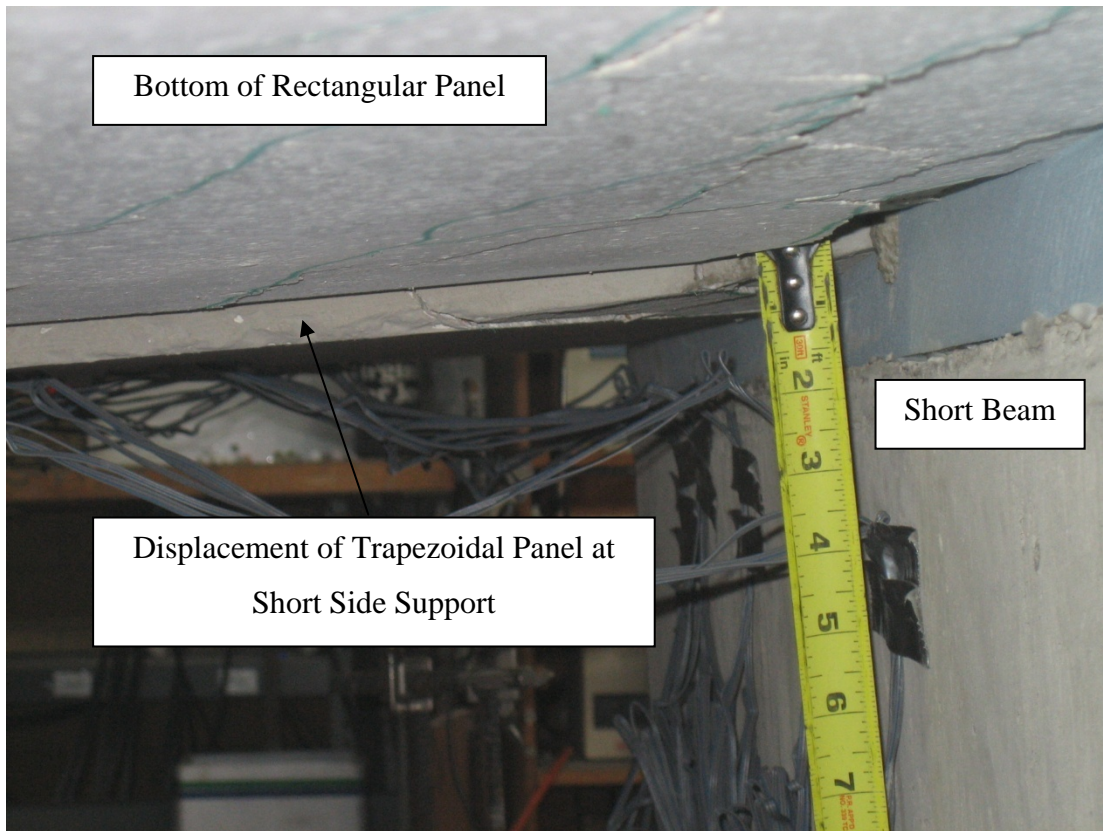


**Figure 5.66 – Photograph of Trapezoidal Panel Displacement at Conclusion of Test of Specimen P30P1 for Load Applied at Midspan of Square End**

#### **5.4.2 Specimen P30P2**

Specimen P30P2 was tested monotonically to failure two times. During the first test, the load was applied near midspan of the SEJ along the skewed end of the trapezoidal panel. During the second test, load was applied near midspan of the square end of the trapezoidal panel.

##### **5.4.2.1 Load Applied at Skewed End**

The measured displacement response at midspan of the skewed end is shown in Figure 5.67. The displacement response indicates a cracking load of approximately 22 kip. Cracks appeared on the surface of the specimen at a load of 25 kip. As the applied load approached 50 kip, delamination between the panel and topping slab was again

heard. After delamination the specimen was unable to carry a maximum applied load much higher than 50 kip. The distribution of displacements along the skewed end is shown in Figure 5.68. The linear potentiometers at locations L3 and L4 were positioned incorrectly and did not record displacement data for load increments up to approximately 13 kip. In order to compare the data along the skewed end of the panel, the procedure outlined in Appendix B was used to extrapolate the displacement data at locations L3 and L4 for low levels of applied load.

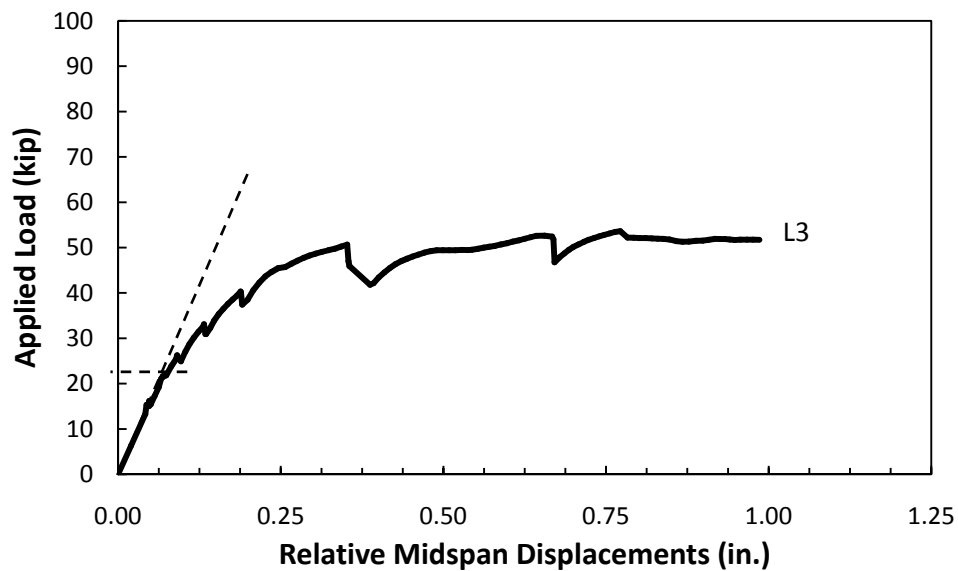


*Figure 5.67 - Measured Displacement Response at Midspan of Skewed End of Specimen P30P2*

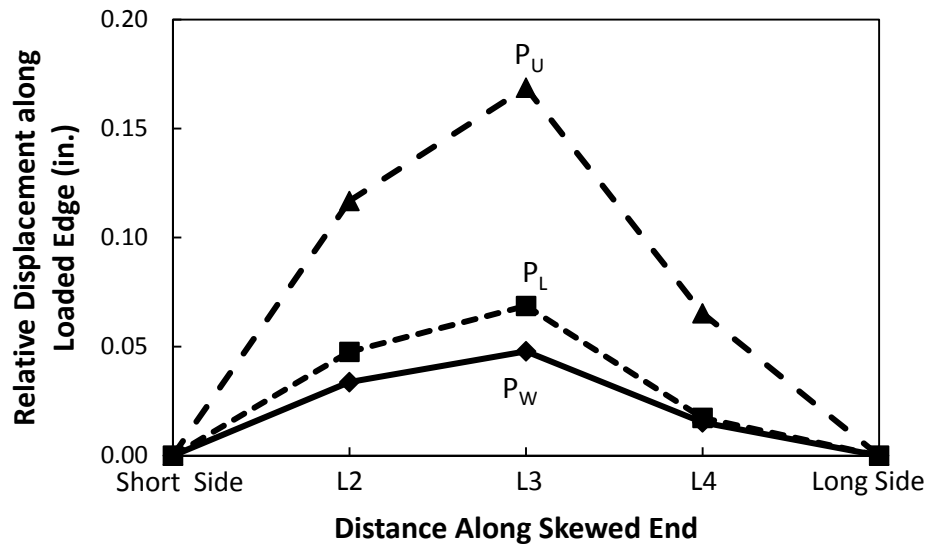


*Figure 5.68 - Variation of Displacements along Loaded End of Specimen P30P2 for Load Applied at Midspan of Skewed End*

The change in tensile strain on the bottom of the panel at midspan of the skewed end is plotted in Figure 5.69. The data indicate that the gage was damaged at a load of approximately 30 kip; therefore, the change in stiffness corresponding to the cracking load can not be approximated from this data. Variation of live load induced strain on the bottom of the panel along the loaded end is provided in Figure 5.70. All strain gages were damaged by the formation of flexural cracks, so only strain variation for  $P_W$  and  $P_L$  are plotted. Strains were highest at midspan and lowest at quarter-span location near the long side.



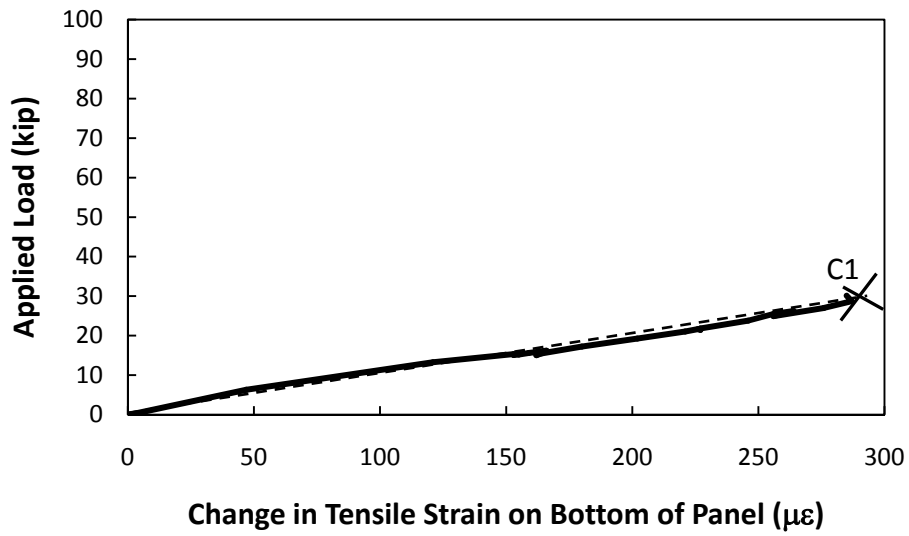


*Figure 5.69 – Change in Tensile Strain on Bottom of Precast Panel at Midspan of Skewed End of Specimen P30P2*

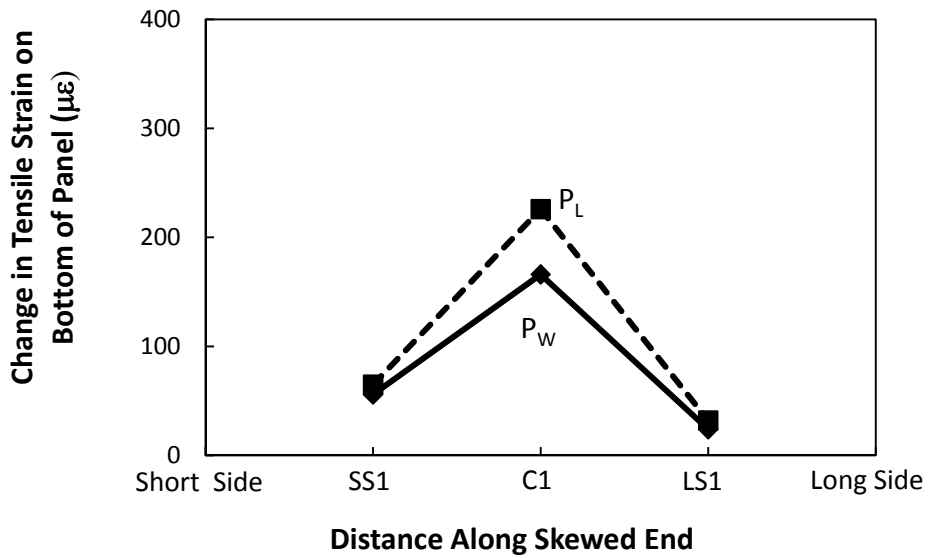


*Figure 5.70 - Variation of Change in Strain on Bottom of Panel along Skewed End of Specimen P30P2*

Compressive strain data at midspan of the expansion joint are plotted in Figure 5.71; the SEJ data indicate a cracking load for the specimen of approximately 31 kip. Variation of strain along the SEJ is shown in Figure 5.72. Strains were highest at midspan, and the strains at SEJ1 were higher than the strains at SEJ3.

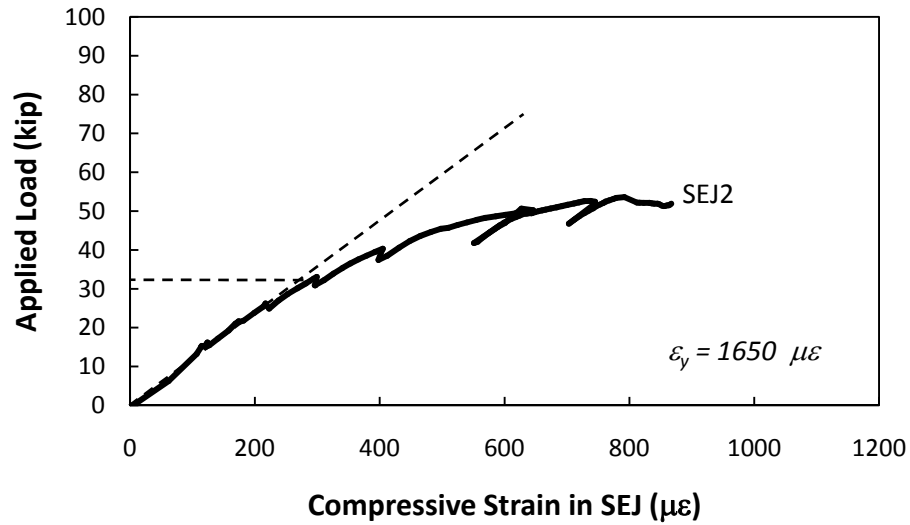


*Figure 5.71 – Compressive Strain at Midspan of SEJ in Specimen P30P2*

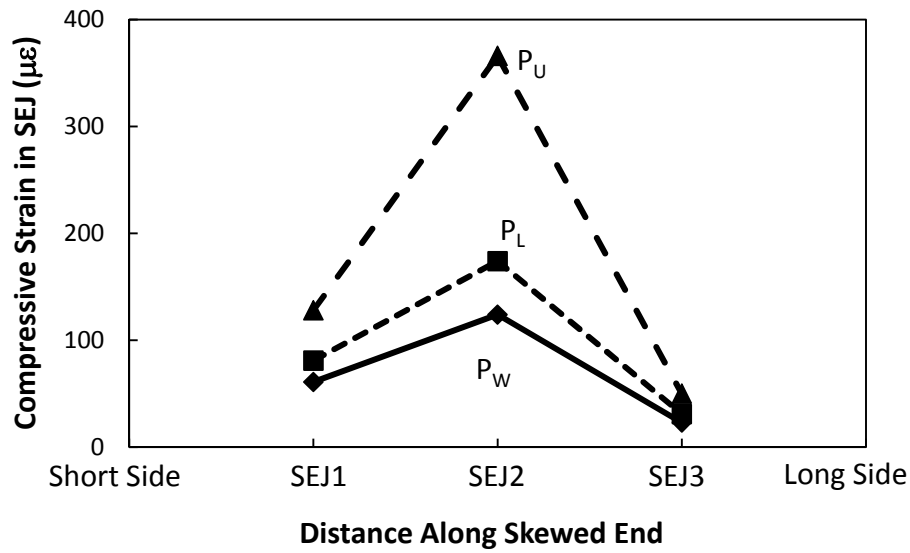


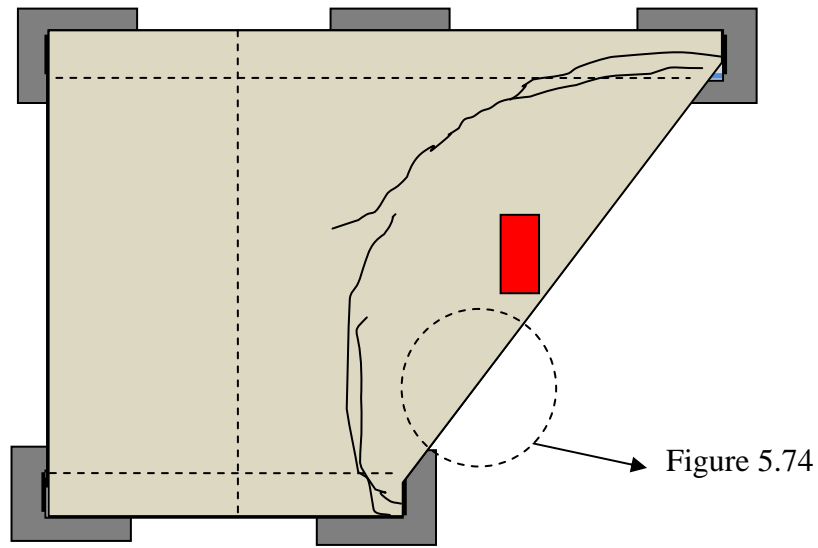
**Figure 5.72 - Variation of Strain in SEJ along Loaded End of Specimen P30P2 for Load Applied at Midspan of Skewed End**

The approximated cracking load from the instrumentation and the apparent cracking load for Specimen P30P2 are provided in Table 5.8.

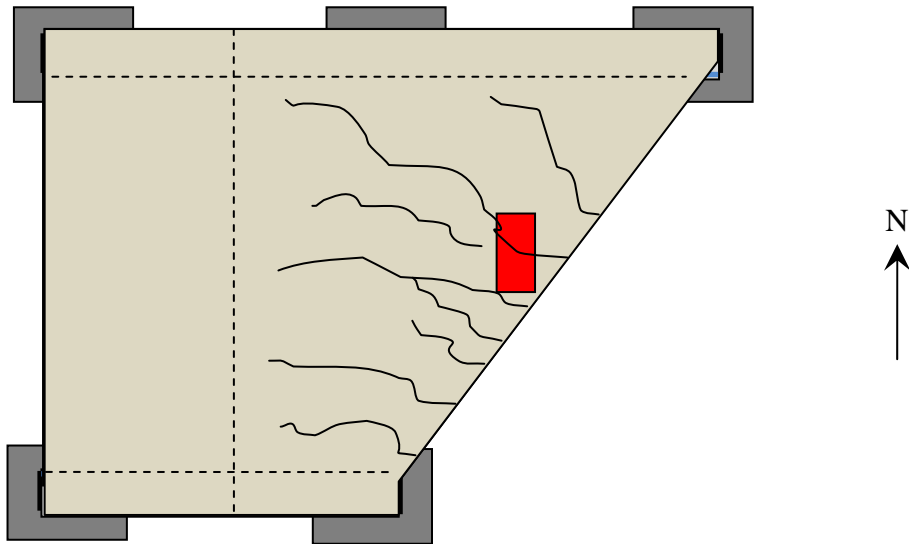
**Table 5.8 – Initial Stiffness and Inferred Cracking Loads for Specimen P30P2 for Load Applied at Midspan of Skewed End**

	Initial Stiffness (k/in, k/μϵ)	Inferred Cracking Load (kip)
Displacement	290	22
Concrete Strain on Bottom of Panel	0.106	-
SEJ Strain	0.111	31
Apparent Cracking	-	25

Observed cracks in the specimen at the conclusion of the test are shown in Figure 5.73. The failure mechanism for specimen P30P2 was delamination between the panel and topping slab for load applied at the skewed end of the specimen. The crack widths were quite small for the visible cracks on the surface of the specimen at the conclusion of the skewed end loading. A photograph of the gap between the panel the topping slab due to the delamination is provided in Figure 5.74.



Predominant Cracks on Top Surface of Specimen



Predominant Cracks on Bottom Surface of Specimen

*Figure 5.73 – Observed Crack Pattern for Specimen P30P2 for Load Applied at Midspan of Skewed End*

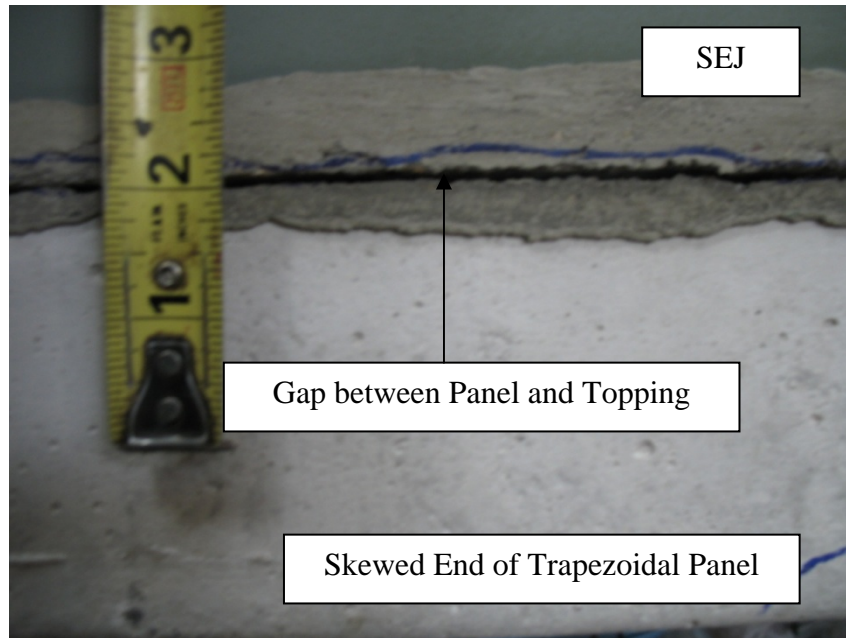


***Figure 5.74 – Photograph of Delamination of Trapezoidal Panel from Topping Slab for Specimen P30P2 for Load Applied at Midspan of Skewed End***

#### ***5.4.2.2 Load Applied at Midspan of Square End***

Specimen P30P2 was loaded at midspan of the square end after the test on the skewed end. Cracks from the skewed end loading damaged many of the strain gages on the bottom of the panel, so only displacement data for load applied at midspan of the square end were reliable.

Measured relative displacements at midspan of the square end are plotted in Figure 5.75. The linear potentiometer at location L3 was positioned incorrectly and did not record displacement data for load increments up to approximately 20 kip. In order to compare the data along the square end of the panel, the procedure outlined in Appendix B was used to extrapolate the displacement data at location L3 for low levels of applied load. The data show a cracking load for the square end at 45 kip. Despite delamination from the skewed end loading, the specimen demonstrated considerable strength and ductility for load applied at midspan of the square end. The maximum applied load of 84

kip resulted in a relative midspan displacement of more than 1.5 in., which is approximately  $L/80$  for a centerline beam spacing of 10 ft.

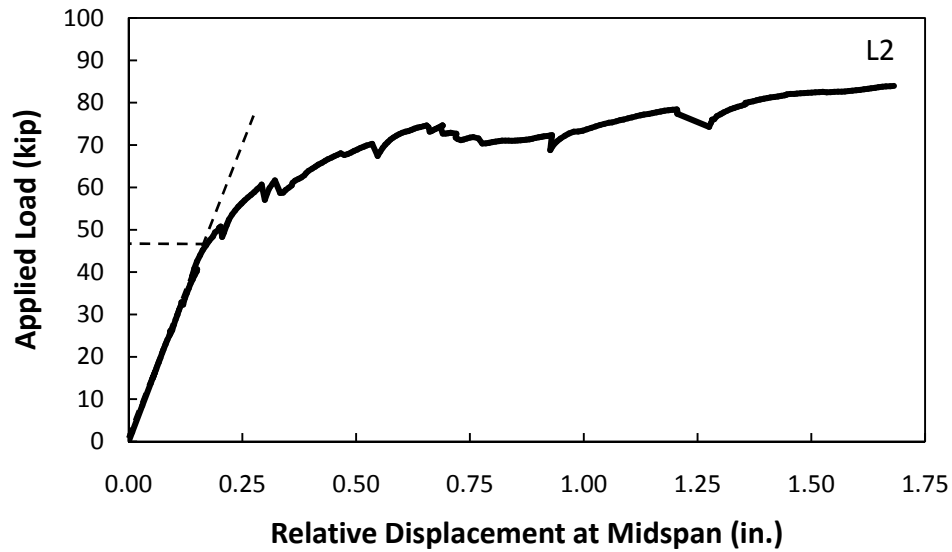
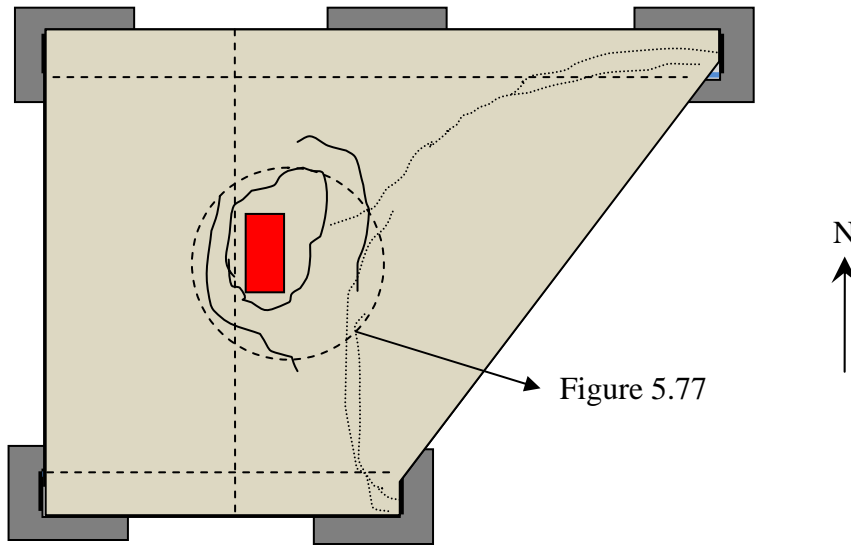
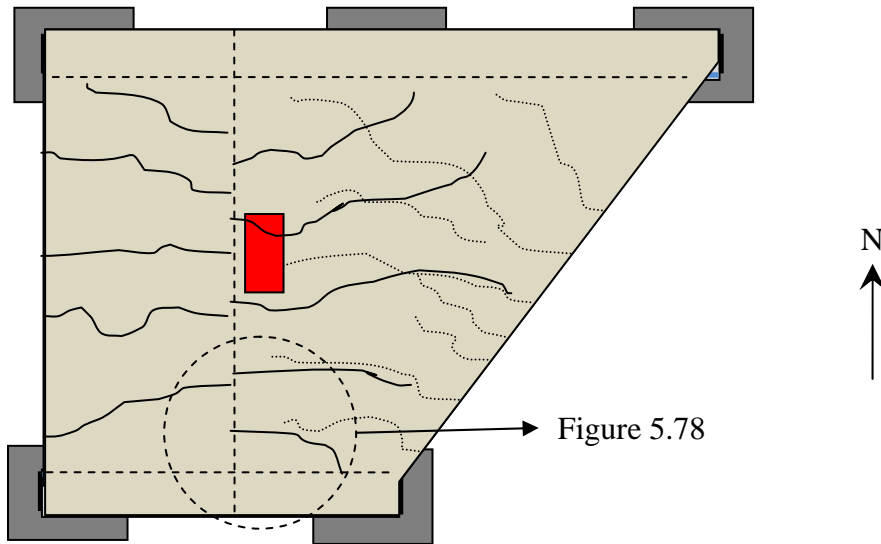


*Figure 5.75 – Measured Displacement Response at Midspan of Square End of Specimen P30P2*

Observed cracks at the conclusion of the test on the square end are shown in Figure 5.76. The specimen failed in punching shear in the topping slab, and then a large shear crack opened in the trapezoidal panel near the short side support. Photographs of the specimen at the conclusion of the test are in Figure 5.77 and Figure 5.78; Figure 5.77 shows the punching shear cracks on the top surface of the specimen, and Figure 5.78 shows the shear crack in the trapezoidal panel.



Predominant Cracks on Top Surface of Specimen



Predominant Cracks on Bottom Surface of Specimen

***Figure 5.76 – Observed Crack Pattern at Conclusion of Static Test for Specimen P30P2 for Load Applied at Midspan of Square End***



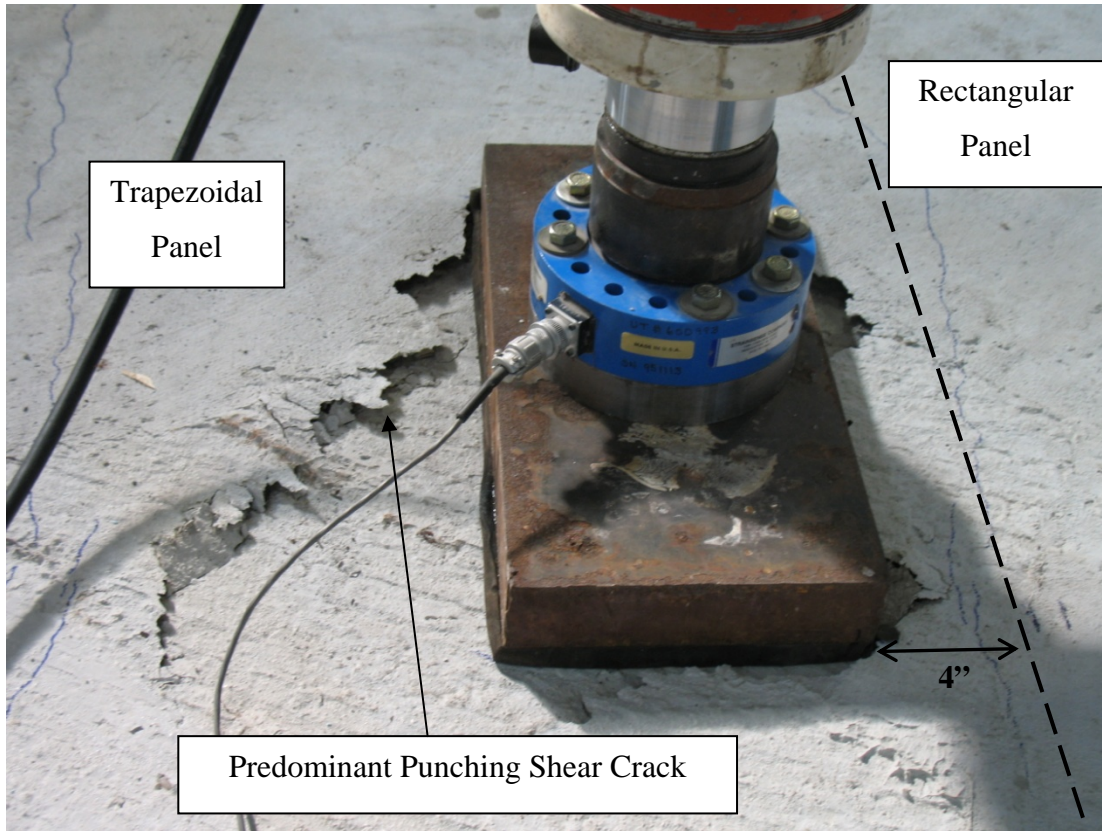


***Figure 5.77 – Photograph of Punching Shear Failure for Specimen P30P2 for Load Applied at Midspan of Square End***

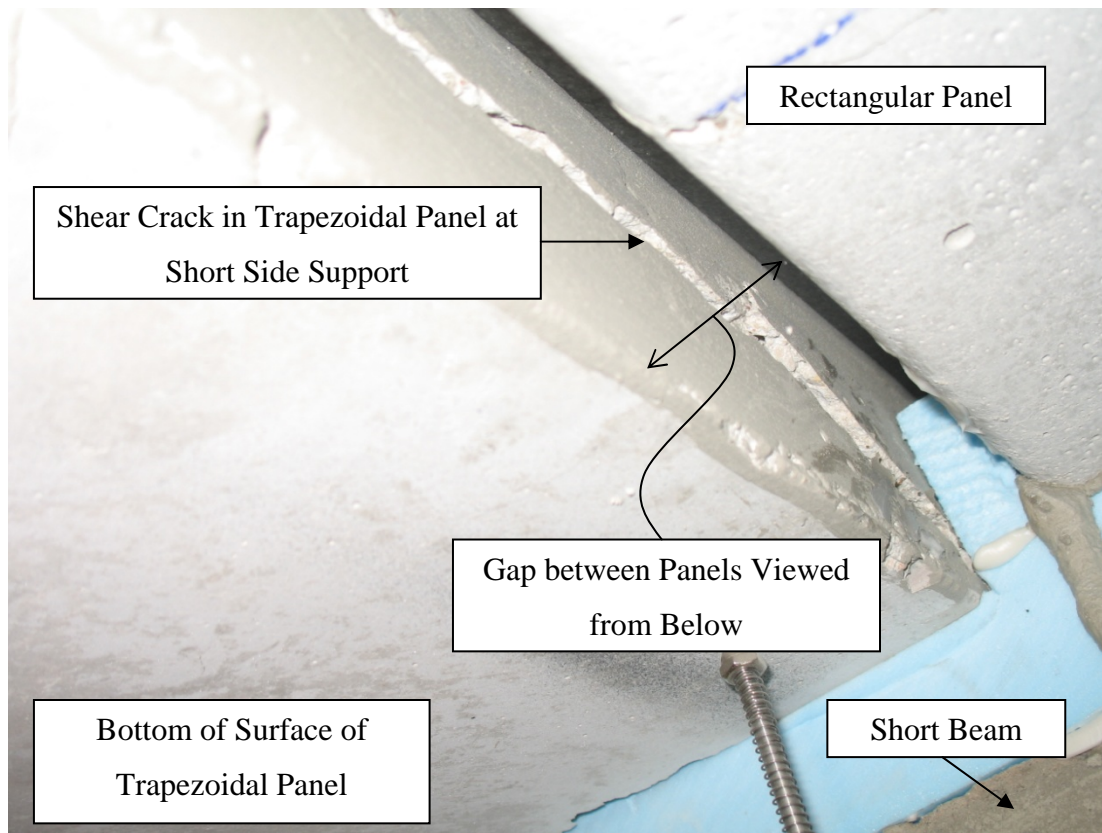


***Figure 5.78 – Photograph of Shear Crack in Trapezoidal Panel at Short Side Support in Specimen P30P2 for Load Applied at Midspan of Square End***

## **5.5 SUMMARY**

*A summary of the response of the test specimens to loads applied at midspan of the skewed and square ends is presented in*

Table 5.9.

For loads applied at midspan of the skewed end, cracking loads for all specimens were approximately 1.5 times the Design Wheel Load. However, the maximum applied loads for the 45-degree specimens were approximately 4 times the Design Wheel Load, whereas the 30-degree specimens were only able to carry maximum applied loads of 2.5 times the Design Wheel Load due to the delamination of the panels from the topping slab.

Data from the load tests on the square end show that the cracking load of the specimens on the square end was approximately 1.5 to 2 times the Design Wheel Load. Also the maximum applied load at the square end was approximately 4 to 5.5 times the Design Wheel Load.

Three failure modes were identified in the response of the test specimens: shear failure at the short side support, punching shear, and delamination of the panel from the topping slab. All three 45-degree specimens failed in shear at the short side support for load applied at midspan of the skewed end. The 30-degree specimens failed by delamination of the panel from the topping slab for load applied at midspan of the skewed end, and all specimens loaded at midspan of the square end failed in punching shear.

**Table 5.9 - Summary of Response of Test Specimens**

		Specimen				
		P45P1	P45P2	P45P3	P30P1	P30P2
Skewed End	Cracking Load, $P_{cr}$ (kip)	33	32	32	32	26
	$P_{cr}/P_W$	2.1	2.0	2.0	2.0	1.6
	$P_{cr}/P_L$	1.5	1.5	1.5	1.5	1.2
	$P_{cr}/P_U$	0.9	0.9	0.9	0.9	0.7
	Maximum Applied Load, $P_{max}$ (kip)	83	89	81	49	54
	$P_{max}/P_W$	5.2	5.6	5.1	3.1	3.4
	$P_{max}/P_L$	3.9	4.2	3.8	2.3	2.5
	$P_{max}/P_U$	2.2	2.4	2.2	1.3	1.4
Square End	Cracking Load, $P_{cr}$ (kip)	-	40	-	27	45
	$P_{cr}/P_W$	-	2.5	-	1.7	2.8
	$P_{cr}/P_L$	-	1.9	-	1.3	2.1
	$P_{cr}/P_U$	-	1.1	-	0.7	1.2
	Maximum Applied Load, $P_{max}$ (kip)	-	120	-	87	84
	$P_{max}/P_W$	-	7.5	-	5.4	5.3
	$P_{max}/P_L$	-	5.6	-	4.1	3.9
	$P_{max}/P_U$	-	3.2	-	2.3	2.3

## **Chapter 6: Discussion of Results**

### **6.1 INTRODUCTION**

The experimental results presented in Chapter 5 are summarized and discussed in this chapter. First, results from tests with the load applied at midspan of the skewed end are discussed, followed by a discussion of the results from tests with the load applied at midspan of the square end. Finally recommendations for the use of skewed panels in bridge deck construction are presented.

### **6.2 SUMMARY**

Over the past eight years, the Texas Department of Transportation has funded two investigations regarding the use of precast concrete panels as stay-in-place formwork adjacent to expansion joints in bridge deck construction. In TxDOT Project 0-4418, researchers constructed three full-scale bridge decks. One of the specimens used precast panels at a 0° skew (Coselli, 2004), and the results indicated that the precast panel system provided adequate strength and reduced construction costs compared with the traditional cast-in-place details at the expansion joint. In the first phase of the investigation in TxDOT Project 0-5367 (Agnew, 2007), the fatigue response of precast panels was evaluated at the expansion joint in 0° skew bridges, and it was determined that the precast panel system was more than adequate for service-level fatigue loads.

In this second phase of TxDOT Project 0-5367 (this investigation), the response of skewed precast panels at expansion joints was tested under static and fatigue loads. Two skew angles were tested: 30° and 45°. Five specimens were constructed and subjected to a total of nine tests. Test loads were applied at midspan of the skewed end of each specimen, and some specimens were also tested at midspan of the square end of the trapezoidal panels. The response of the specimens is summarized in Section 6.2.1 and Section 6.2.2.

### 6.2.1 Load Applied Along Skewed End

The three 45° specimens exhibited similar response to loads applied at midspan of the skewed end. The load-displacement plots for the 45° specimens are shown in Figure 6.1. Significant observations from the tests of the 45° specimens are listed below:

- Deflections at midspan of skewed end under the Design Wheel Load ( $P_L$ ) were approximately 1/16 in., which corresponds to approximately  $L/2400$  for a 9-ft clear span between girder flanges.
- Maximum applied loads were approximately 4 times the Design Wheel Load,  $P_L$ .
- The arrangement of the prestressing strands within the precast panel did not influence the strength or initial stiffness of the test specimens. The test specimens with fanned strands (P45P1) behaved essentially the same as the two specimens with prestressing strands parallel to the skewed end of the panel (P45P2 and P45P3).
- Fatigue loading of Specimen P45P3 did not significantly influence the stiffness of the specimen for load applied at midspan of the skewed end.

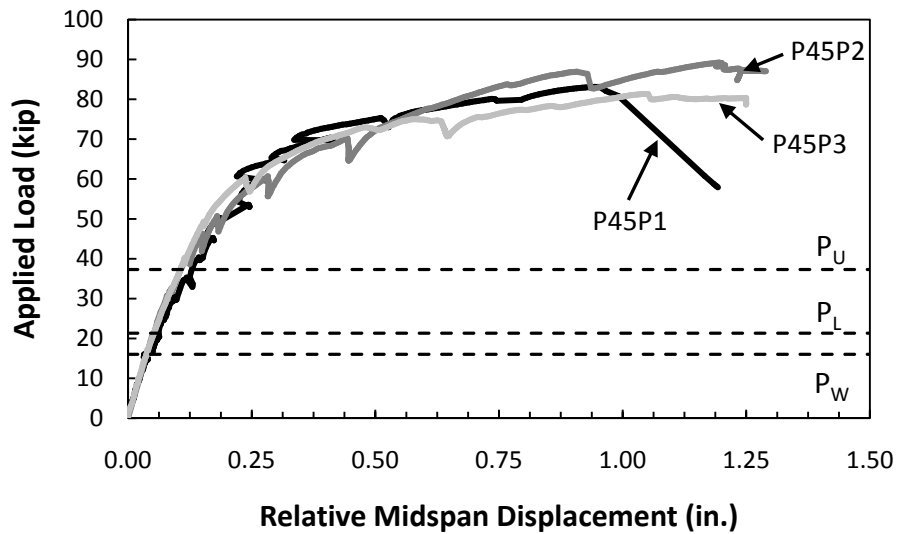


***Figure 6.1 – Measured Displacement Response of 45° Specimens for Load Applied at Midspan of Skewed End***

The response of the 45° specimens is compared with the 0° specimens subjected to positive moment (Agnew, 2007) in Figure 6.2. The 0° specimens achieved slightly higher loads and slightly larger displacements at failure; however, the overall response was essentially the same. The compressive strain response of the SEJ for the 45° specimens is compared with the 0° specimens in Figure 6.3. Initially, the compressive strains were lower in the 45° specimens for a given level of applied load; however, for loads above 60 kip, the response was essentially the same.

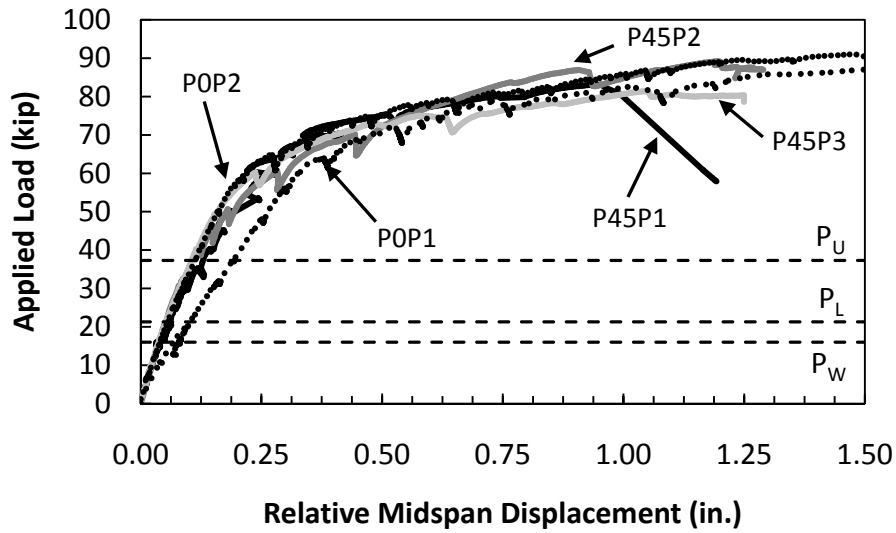


*Figure 6.2 – Comparison of Measured Displacement Response of 0° and 45° Specimens*

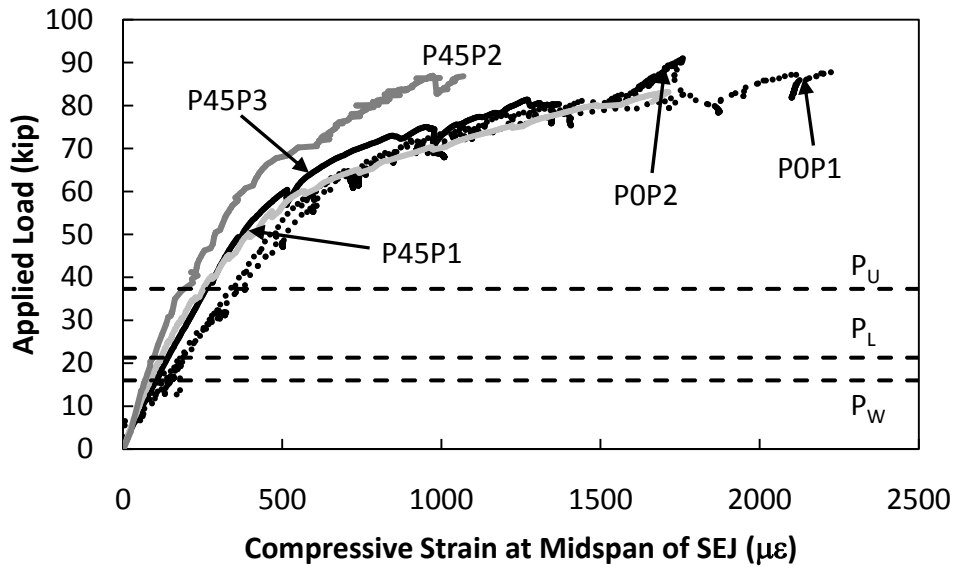


*Figure 6.3 – Measured Compressive Strain at Midspan of SEJ for 0° and 45° Specimens*

The response of the 45° panels was also compared to the 45°, full-scale bridge deck tested by Griffith (2003). Griffith investigated the I-beam thickened slab (IBTS) detail as well as an 8” cast-in-place slab (UTSE detail) at the two ends of a bridge deck



with a 45° skew. Comparisons between the positive moment tests by Griffith and tests of the 45° specimens in this investigation are provided in Table 6.1 and Figure 6.5. Griffith used a tandem wheel load to test the IBTS and UTSE detail; therefore, one half of the total load was applied at the end of the test specimen (Figure 6.4) and one half was applied 4 ft from the end. The total applied loads for Griffith's specimen exceeded those from this investigation because the load was distributed over a larger area of the bridge deck. Important comparisons between the response of different end details are listed below:

- Both the IBTS and UTSE details failed by punching shear. All three 45° precast panel specimens failed by shear at the short support.
- The cracking load per load point was more than two times larger for the precast panel specimens than the cast-in-place details. The primary reason for this difference is the precompression in the precast panels.
- The maximum applied loads per load point were also considerably larger for the precast panel specimens. This observation is consistent with Agnew's (2007) conclusion for 0° skew specimens. The presence of the SEJ also contributed to the observed differences.
- The maximum difference between displacements at failure for the two investigations is approximately 0.5 in. These results validate the use of simpler test specimens in the current investigation.

**Table 6.1 – Comparison of Precast Panel Detail to IBTS and UTSE Detail**

Detail/ Specimen	Loading Pattern	Cracking Load Per Load Point (kip)	Total Cracking Load (kip)	Maximum Applied Load Per Load Point (kip)	Total Maximum Load (kip)
IBTS, 45° skew	Tandem	15.0	30.0	48	90
UTSE, 45° skew	Tandem	12.5	25.0	56	112
Panel, P45P1	Wheel	33.0	33.0	83	83
Panel, P45P2	Wheel	32.0	32.0	89	89
Panel, P45P3	Wheel	32.0	32.0	81	81

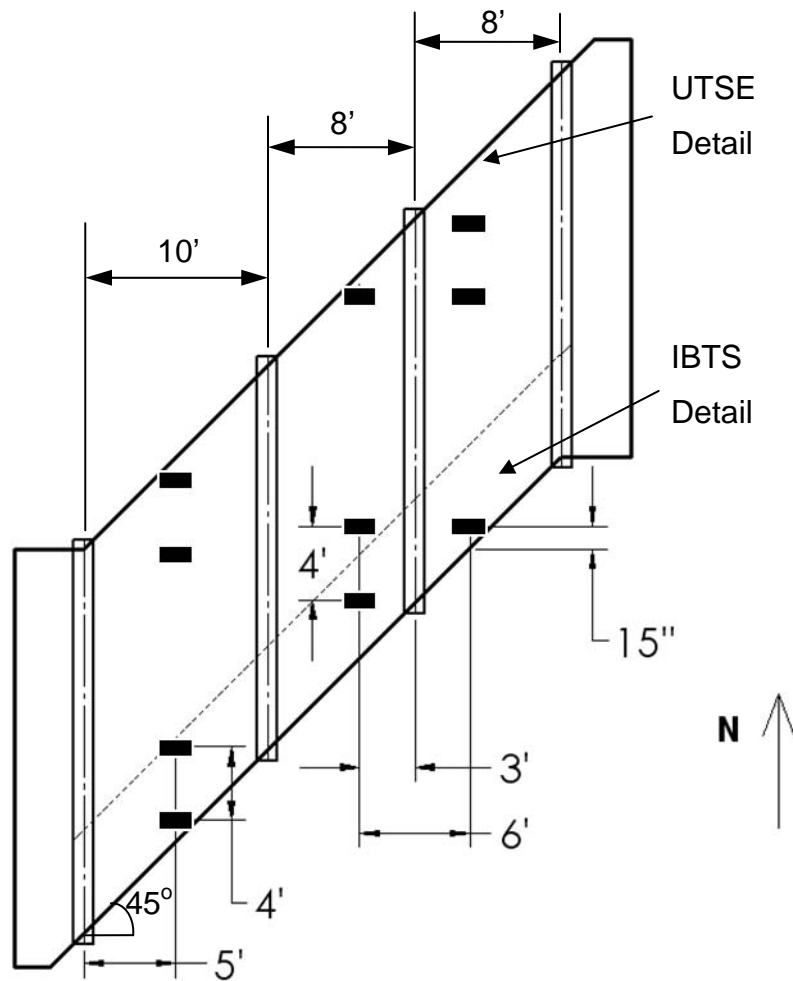


**Figure 6.4 – Points of Load Application for Full-scale Test of IBTS and UTSE Details**

*(Griffith, 2003)*

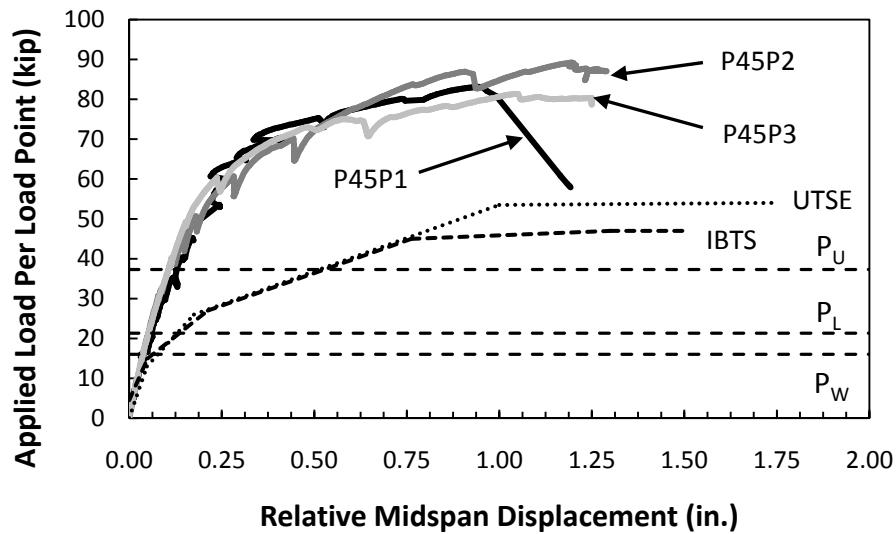


**Figure 6.5 – Comparison of Displacement Response of Precast Panel Detail, UTSE Detail, and IBTS Detail**

The two 30° specimens also exhibited similar behavior for loads applied at midspan of the skewed end. The load-displacement response for both 30° specimens is provided in Figure 6.6. Significant points from the skewed end behavior of the 30° specimens are listed below:

- The capacity of the 30° specimens was limited by the delamination of the panels from the cast-in-place topping slabs. Maximum applied loads were approximately 2.5 times the Design Wheel Load,  $P_L$ .
- Deflections at midspan of skewed end under the Design Wheel Load ( $P_L$ ) were approximately 1/16 in, which corresponds to  $L/2000$  for a 9-ft. clear span between girder flanges.

The response of the 30° specimens is compared with the 45° specimens in Figure 6.7. The initial stiffness of all the specimens is comparable; however, the strength of the 30° specimens was considerably less than the strength of the 45° specimens. This difference is attributed to delamination of the 30° panels from the cast-in-place topping.

The response of the 30° specimens is compared with the 0° specimens in Figure 6.8. Again, the differences in the strength are significant. The compressive strain response of the SEJ for the 30° specimens is compared with 0° specimens in Figure 6.9. The initial response of specimen P30P2 was essentially the same as the 0° specimens, whereas the strains in the SEJ in specimen P30P1 were less for a given level of axial load. As expected, the response of the two types of specimens was dramatically different after delamination occurred.

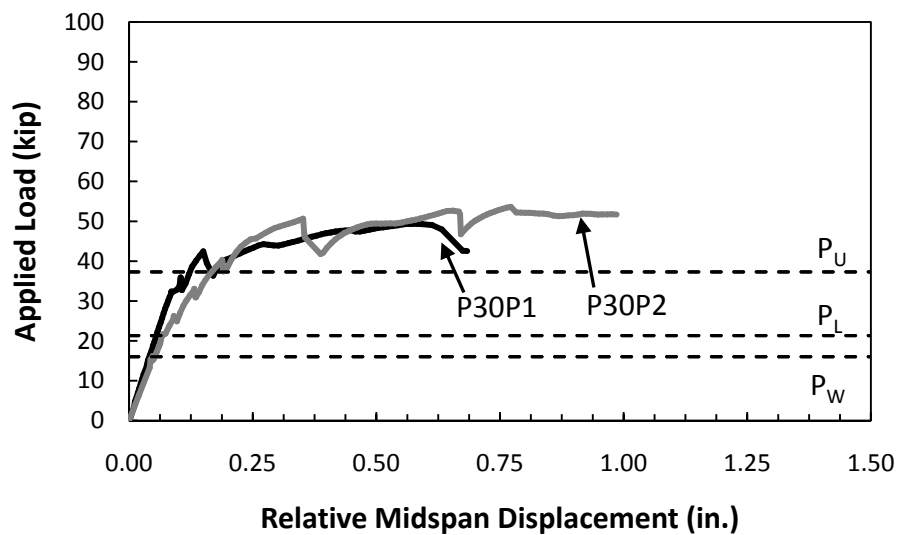


*Figure 6.6 – Measured Displacement Response for 30° Specimens for Load Applied at Midspan of Skewed End*

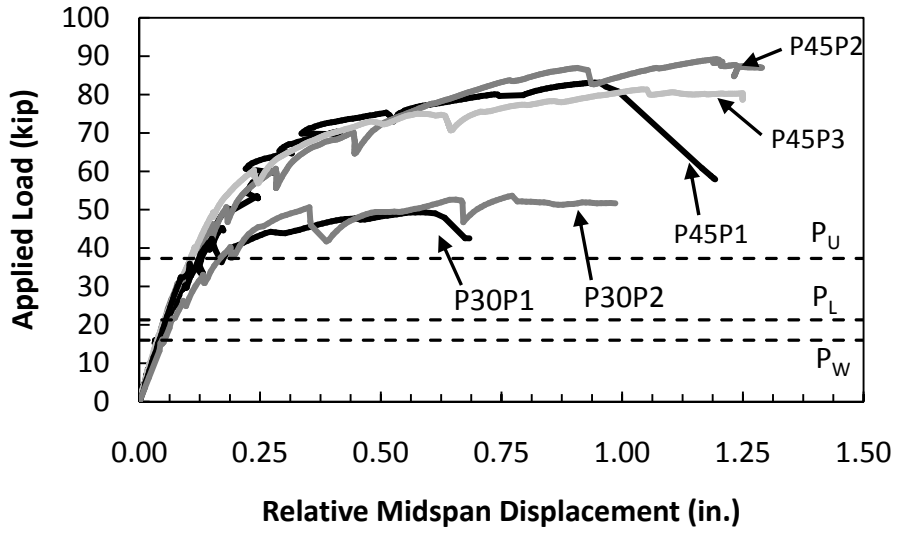


*Figure 6.7 – Comparison of Measured Displacement Response of 30° and 45° Specimens*

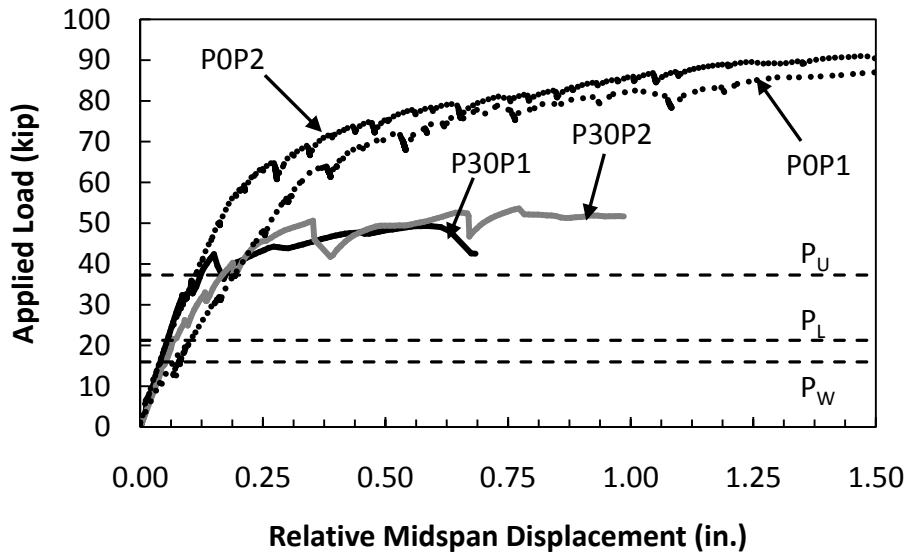


*Figure 6.8 – Comparison of Measured Displacement Response of 30° and 0° Specimens*

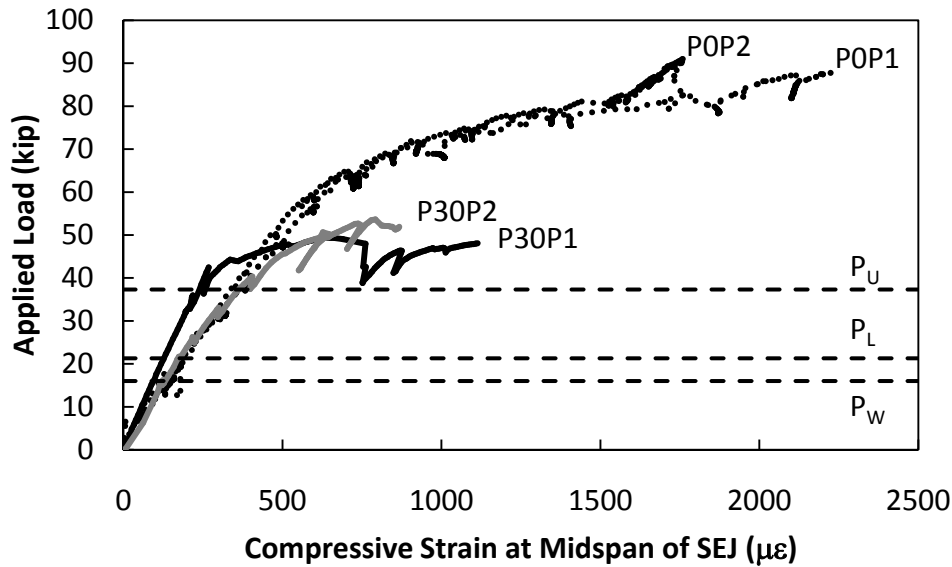


*Figure 6.9 – Measured Compressive Strain at Midspan of SEJ for 0° and 30° Specimens*

### 6.2.2 Loads Applied Along Square End

Three of the five skewed specimens were loaded at midspan of the square end of the trapezoidal panel after they had been loaded to failure at midspan of the skewed end. The displacement response of the three specimens is plotted in Figure 6.10. Important observations from these tests are summarized below:

- The test results were much less consistent when the load applied along the square end of the trapezoidal panel than the skewed end. This difference is likely due to the level of damage induced during the tests along skewed end. Delamination of the 30° panels caused extensive damage that could not be characterized by the crack patterns alone.
- In spite of the damage induced in the earlier tests, the maximum applied load at midspan of the square end always exceeded the maximum applied load at midspan of the skewed end.
- The maximum applied load along the square end was always limited by a punching shear failure.

- The non-prestressed corner of the skewed panels (with strands running parallel to the skewed end) did not limit of the punching shear strength of the specimens.

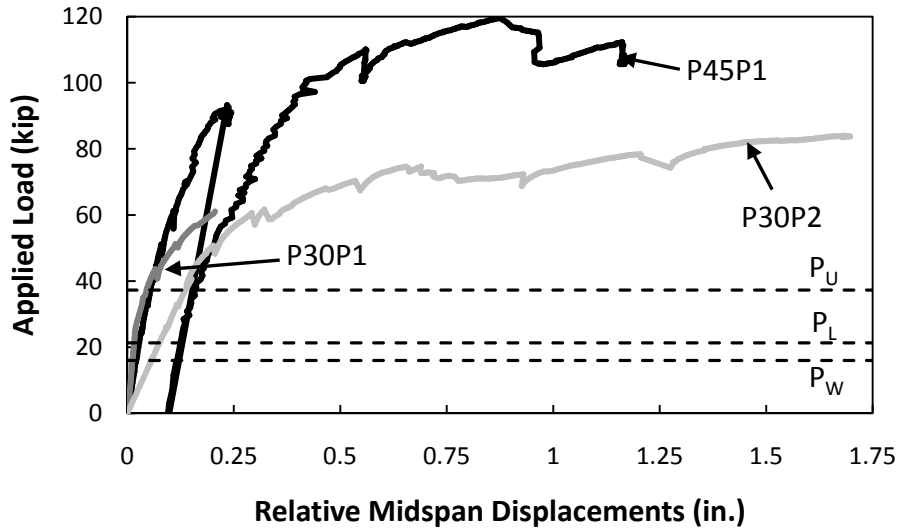


*Figure 6.10 – Measured Displacement Response of Specimens P45P2, P30P1, and P30P2 for Load Applied at Midspan of Square End*

### 6.3 RECOMMENDATIONS

The results of this research suggest that skewed precast panels provide adequate strength and stiffness for use adjacent to expansion joints in bridge decks. The response of the skewed panels to load applied at midspan of the expansion joint is similar to the response of non-skewed specimens. Trapezoidal panels with strands running parallel to the skewed end are easier to fabricate and do not sacrifice strength or stiffness. Current fabrication practices limit the skew angle to 30° because of fabrication limitations, but panels with skews as large as 45° have been tested and may be used with confidence.

The maximum load carrying capacity of these precast panel systems may be limited if the panels delaminate from the cast-in-place topping slab. Plans are currently

underway to test more skewed panels in the summer of 2008 to investigate further the role of panel surface roughness on the specimen response.



## **Chapter 7: Conclusions and Recommendations**

The research findings were presented and discussed in Chapter 5 and Chapter 6. This chapter draws conclusions about the use of trapezoidal precast panels as stay-in-place formwork in bridge decks adjacent to the expansion joint.

### **7.1 SUMMARY**

Traditionally, the Texas Department of Transportation used a detail known as the “IBTS” detail to thicken the bridge deck at slab ends around the expansion joint to act as a slab end diaphragm. In the past eight years, TxDOT has developed a detail using precast concrete panels as stay-in-place formwork immediately adjacent to the expansion joint for prestressed concrete bridges. The purpose of this investigation was to study the response of skewed precast panels under static and fatigue loads immediately adjacent to the expansion joint.

Five test specimens were subjected to point loads to simulate the loads from a single wheel of the rear axle from the HL-93 Design Truck. The applied loads generated positive moments in the bridge deck. The load was applied at midspan of the skewed end of all the specimens; additionally, three specimens (P45P2, P30P1, and P30P2) were tested at midspan of the square end of the trapezoidal precast panel. Specimen P45P3 was loaded in fatigue before being tested monotonically to failure.

### **7.2 CONCLUSIONS**

The research data show that trapezoidal precast panels used as stay-in-place formwork adjacent to expansion joints in bridge decks provide sufficient strength and stiffness for current design loads. Important observations from this investigation are summarized below:

- Skewed Panel Observations
  - Trapezoidal panels with strands oriented parallel to the skewed end are easier to fabricate than trapezoidal panels with fanned strand patterns.

The orientation of the strands in the precast panel did not influence the strength or stiffness of the test specimens.

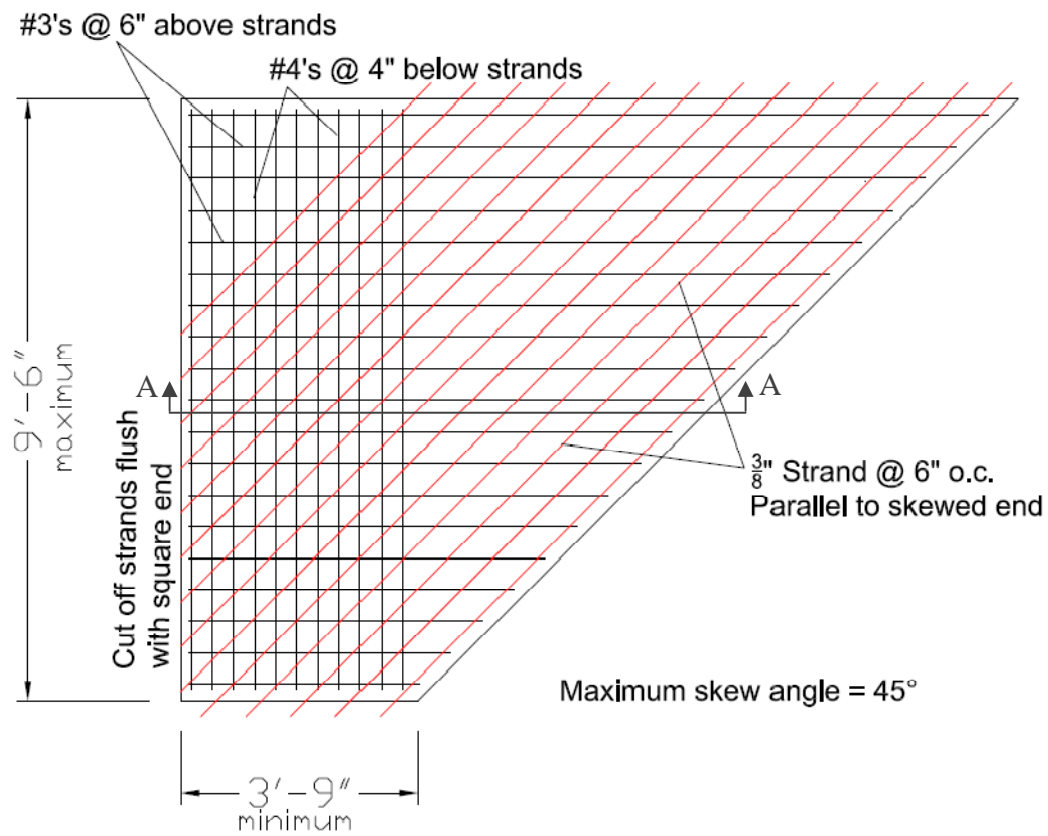
- Skewed panels exhibited similar strength and stiffness to rectangular panels, provided that the surface roughness was sufficient to prevent delamination of the panel from the topping slab. This result was not expected because the length of the free end of the slab is greater for the skewed specimens.
- Response of Specimens for Load Applied at Midspan of Skewed End
  - Test specimens with a  $45^\circ$  skew angle loaded at midspan of the skewed end exhibited maximum load carrying capacities 4 times greater than the 21.3-kip Design Wheel Load for the HL-93 Design Truck, and they failed in diagonal shear at the short side support.
  - The overall system response remained linear throughout the duration of the fatigue loading at service level loads, and no delamination or reduction of stiffness was observed with increasing fatigue loading.
  - Fatigue loading did not significantly affect overall system stiffness or the maximum load carrying capacity for the specimens for load applied at midspan of the skewed end compared to specimens with no previous load history.
  - Delamination of the  $30^\circ$  panels from the topping slab occurred when the specimens were loaded at midspan of the skewed end. Because of the delamination, the  $30^\circ$  specimens exhibited maximum load carrying capacities only 2.5 times greater than the Design Wheel Load. Panel surface roughness is likely the cause of panel delamination.
- Response of Specimens for Load Applied at Midspan of Square End
  - The test specimens loaded at midspan of the square end of the trapezoidal panel exhibited higher load carrying capacities than when

loaded on the skewed end, and the maximum load carrying capacity of the square end was limited by punching shear failure.

- The non-prestressed corner of the skewed panels (with strands running parallel to the skewed end) did not reduce the punching shear strength limit of the specimens for load applied at midspan of the square end of the trapezoidal panel.

The recommended trapezoidal, precast panel for use adjacent to the expansion joint in bridge decks, provided in Figure 7.1, is outlined below:

- Panel Reinforcement
  - Use 3/8" strands at 6" on center, parallel to the skewed end at mid-depth of the panel. Do not include strands less than 5 ft because the development length is insufficient to develop the prestress force.
  - Place #4 bars at 4" on center parallel to the square end of the panel, below strands. Continue the #4 bars for the entire length of the short side.
  - Place #3 bars at 6" on center parallel to the sides of the panel, above the prestressing strands.
- Dimensions
  - The maximum skew angle is 45°.
  - The short side of the trapezoidal panel should be no shorter than 3'-9". The length of the long side will vary depending on the skew angle.
- Other
  - It is recommended that 60-psi bedding strips be used to support the short side of the panel to avoid excessive compression of the bedding strip.



Section A-A

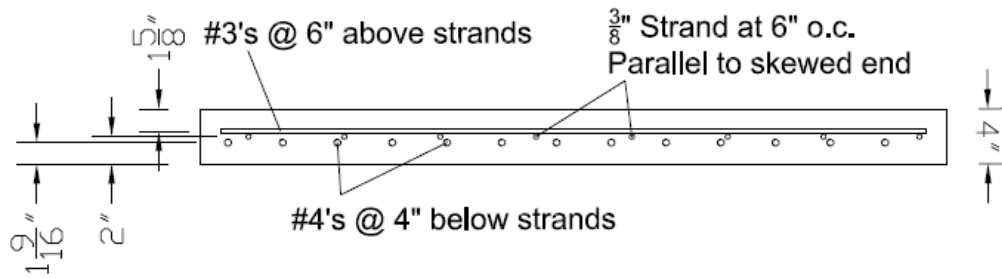


**Figure 7.1 – Recommended Trapezoidal Panel for Use at Expansion Joints in Skewed Bridge Decks**

### **7.3 RECOMMENDATIONS FOR FUTURE RESEARCH**

The results of this research suggest that delamination of the panels from the cast-in-place topping may significantly limit the maximum load carrying capacity of the system. Further tests are planned for the summer of 2008 to investigate further the role of panel surface roughness on specimen response.

The trapezoidal shape of the skewed panels may also cause complications with compression of the bedding strip at the short side of the trapezoidal panel. More research may be needed to address the issue of bedding strip compression under the short side of the trapezoidal panels.

## Appendix A: Nondestructive Testing on Specimen P45P2

### A.1 INTRODUCTION

As discussed in Chapter 3, regions of poorly consolidated concrete were visible under the SEJ in specimen P45P2 when the formwork was removed. Because the extent of the poor consolidation was unknown, nondestructive testing techniques, including Impact-Echo testing and Ultrasonic testing, were used to determine the extent of the zone of poorly consolidated concrete. A grid was marked on the top surface of the specimen along the SEJ (Figure A.1). Tests were performed in each are of the grid. This appendix summarizes the results of the nondestructive tests. Detailed explanations of the nondestructive testing techniques used are not included, though some general information is provided. All of the tests were performed by Dr. Jinying Zhu, an assistant professor in the Department of Civil, Architectural, and Environmental Engineering at the University of Texas at Austin.

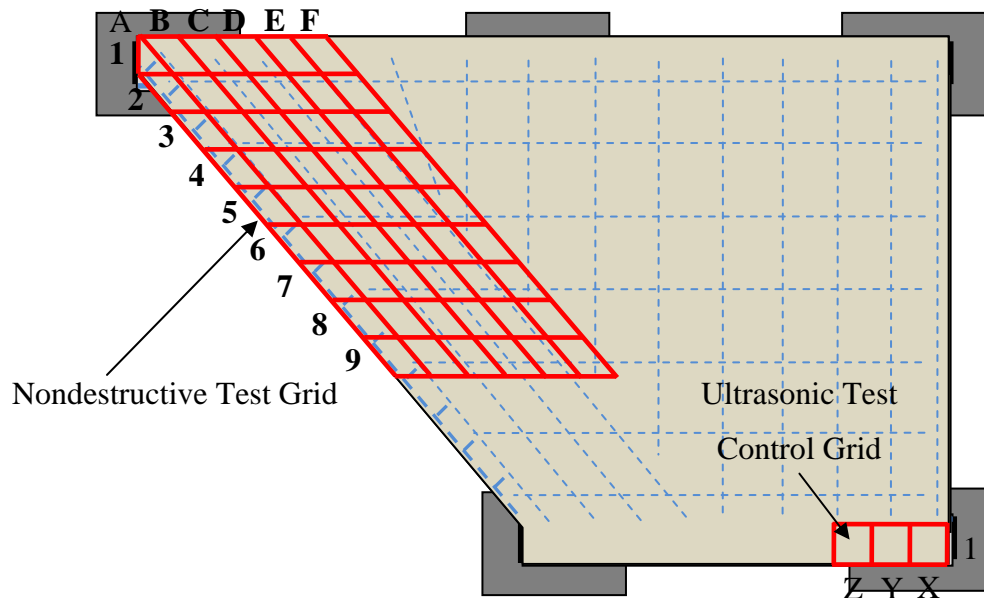


*Figure A.1 – Grid Locations for Nondestructive Testing on Specimen P45P2*

## A.2 IMPACT-ECHO TEST

The Impact-Echo technique is a simple method for detecting voids in concrete. A small hammer is used to impact the test area, and the return signal indicates the thickness of the solid concrete. If the poor consolidation extended into the panel, then the results would indicate that a void was present 4 in. below the top of the slab surface and that area of the grid would be labeled “bad”. If poor consolidation was not present, then the test would return the full 8 in. thickness, and the area was labeled “good”. This test did not include the area immediately adjacent to the SEJ because the studs caused too much interference with the signal to obtain a clear result. The results are presented in Table A.1. Grid location C9 was not tested because there was a lifting eye present directly in the center of the grid square.

*Table A.1 – Impact-Echo Test Results for Specimen P45P2*

Grid Location	1	2	3	4	5	6	7	8	9
A	Good	Good	Good	Good	Good	Good	Good	Good	Good
B	Good	Good	Good	Good	Good	Good	Good	Good	Good
C	Good	Good	Good	Good	Good	Good	Good	Good	No test
D	Good	Good	Good	Good	Good	Good	Good	Good	Good
E	Good	Good	Good	Good	Good	Good	Good	Good	Good
F	Good	Good	Good	Good	Good	Good	Good	Good	Good

The results of the Impact-Echo test show that in every grid location the full depth of the slab was detected. This means that there were no voids present in the interior of the slab, and the poorly-consolidated concrete was limited to the area immediately adjacent to the expansion joint.

## A.3 ULTRASONIC TEST

The Ultrasonic test was used to measure the density of the concrete, and it was primarily used to confirm the results of the Impact-Echo Test. Lower reported travel times corresponded to dense concrete and less likelihood of poor consolidation. Higher travel times translated to poorly consolidated concrete and the presence of voids. Control

times were obtained by measuring the travel times of the waves in the concrete in a different portion of the specimen where it was sure that good consolidation had been achieved. These times then provided a reference for the travel times in the grid locations. Not every grid location was tested with the Ultrasonic test, but enough were tested to satisfactorily confirm the results of the Impact-Echo data. The control times are provided in Table A.2. The test results in the area of concern are provided in Table A.3.

**Table A.2 – Control Times for Ultrasonic Tests for Specimen P45P2 ( $\mu\text{s}$ )**

Grid Location	1
X	48.1
Y	49.0
Z	51.9

**Table A.3 – Ultrasonic Travel Times for Specimen P45P2 ( $\mu\text{s}$ )**

Grid Location	1	2	3	4	5	6	7	8	9
A	47.6	50.3	50.2	50.4	51.4	51.5	50.2	49.1	48.6
B	50.3			51.7	50.7	50.7	50.5		
C		51.0	50.9						
D	50.6	50.5					49.9		
E									
F									

The results of the Ultrasonic test confirm that results of the Impact-Echo tests are correct. The concrete close to the SEJ shows slightly higher travel times indicating less consolidation of the concrete. But none of the tested areas show travel times outside of the control bounds. Therefore, no voids were expected in the interior of the slab.



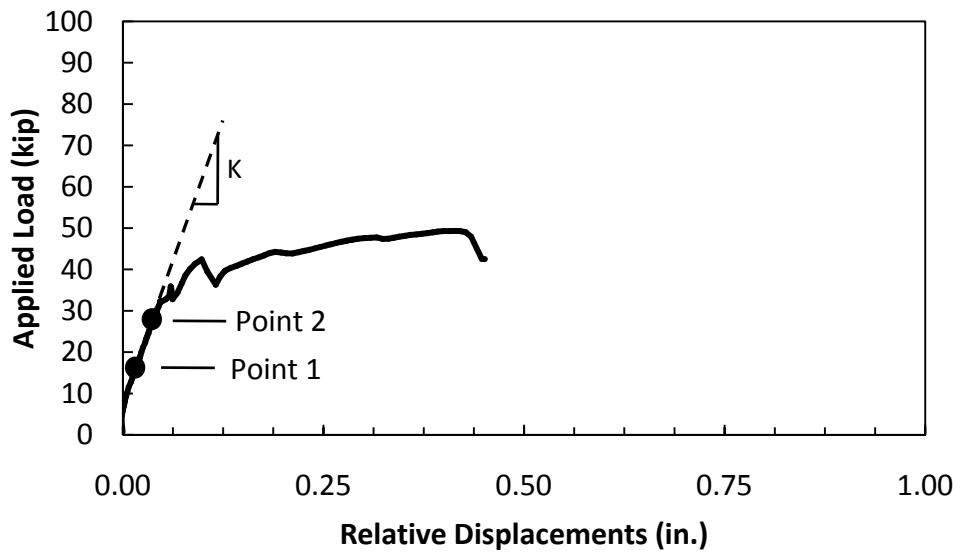
## Appendix B: Complete Set of Test Data

The measured response of the test specimens is summarized in Chapter 5. All the measured data are plotted in this appendix. The data are organized by specimen.

In some cases, the linear potentiometers did not record the displacement response for low levels of applied load. A procedure was developed to recover the lost data so that comparisons could be made with other measured responses. This was done following the procedure outlined in the example below, and a summary of the displacement data sets where this adjustment was made is provided in Table B.1.

### Example B.1:

Original Data Set



1. Two points,  $(P_2, \delta_2)$  and  $(P_1, \delta_1)$ , in the elastic portion of the curve were chosen, and the slope,  $K$ , of the elastic portion of the curve was calculated.
2. The slope calculated in Step 1 was used to estimate the absent data using Equation C.1.

$$\delta_a = \delta_1 - \frac{(P_1 - P_a)}{K} \quad (\text{Equation B.1})$$

where,

$\delta_a$  = absent displacement data point corresponding to  $y_a$

$\delta_1$  = known displacement data point in linear portion of curve

$P_1$  = load corresponding to  $\delta_1$

$P_a$  = known load at which  $\delta_a$  is to be determined

$K$  = slope of linear portion of curve

3. Finally the plot was shifted to the right an amount equal to the offset determined in Step 2 so that the plot passed through the origin.

#### Adjusted Data Set

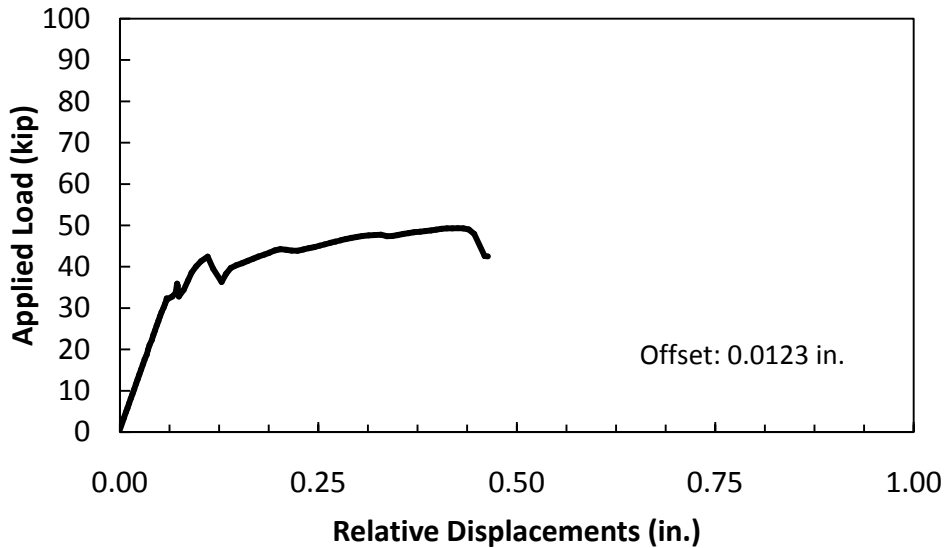


**Table B.1 – Adjusted Linear Potentiometer Data**

	Specimen				
	P45P1	P45P2	P45P3	P30P1	P30P2
Skewed End	-	-	L2, L4*	L2	L3, L5
Square End	NA	-	NA	L2	L1, L2, L3

\* Adjustments were only required for some of the periodic static tests

### B.1 SPECIMEN P45P1

The data for Specimen P45P1 presented in this section includes displacement data, strain data on the bottom of the panel, and strain data on the top surface of the SEJ.

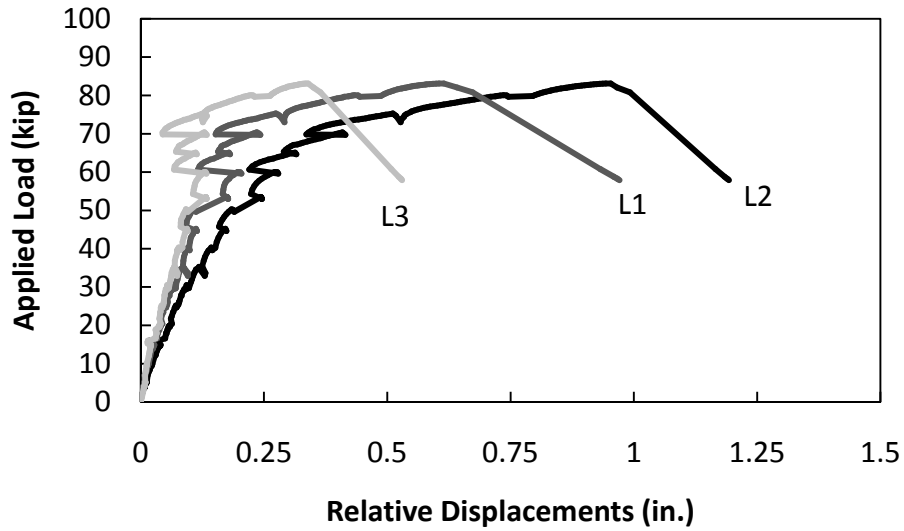


*Figure B.1 – Measured Relative Displacements along Skewed End of Specimen P45P1*

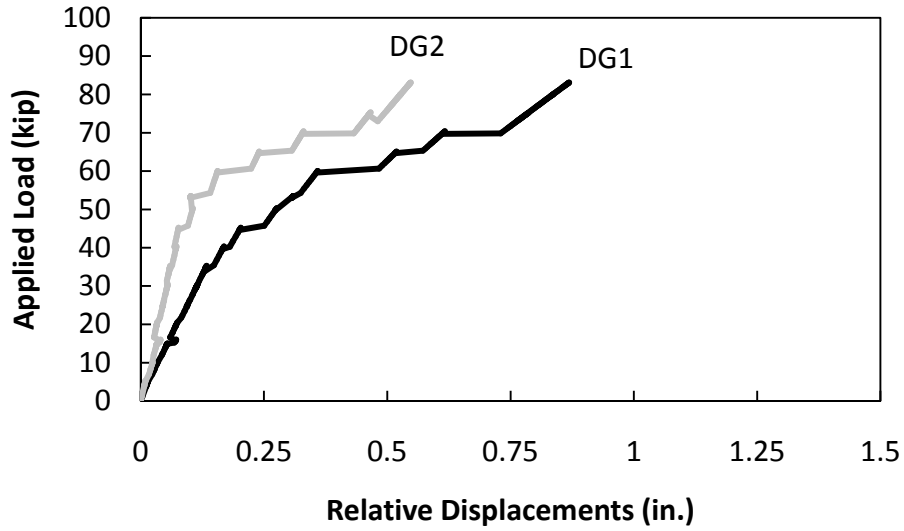


*Figure B.2 – Measured Support Displacements for Specimen P45P1 Loaded at Midspan of Skewed End*

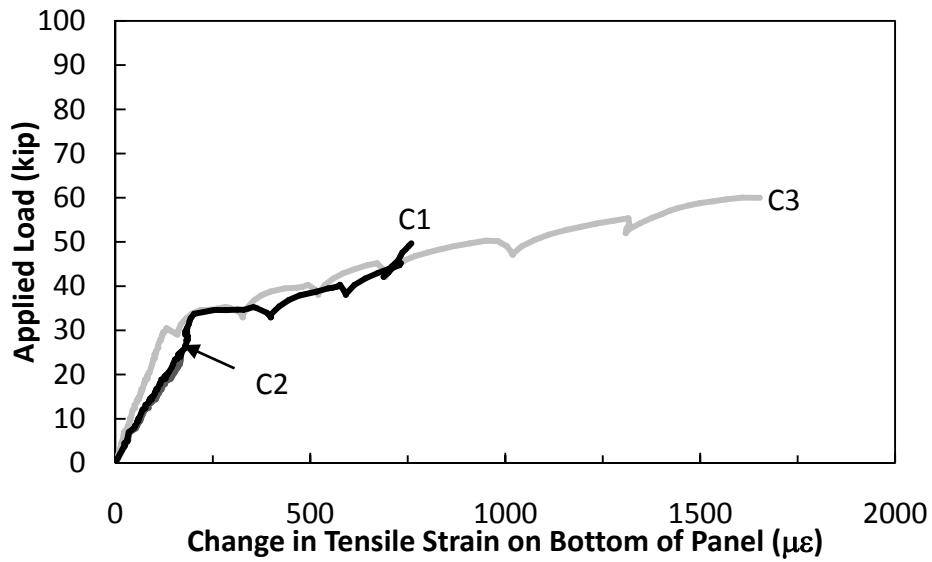


*Figure B.3 – Measured Change in Tensile Strain on Bottom of Panel for Specimen P45P1 for Load Applied at Midspan of Skewed End*

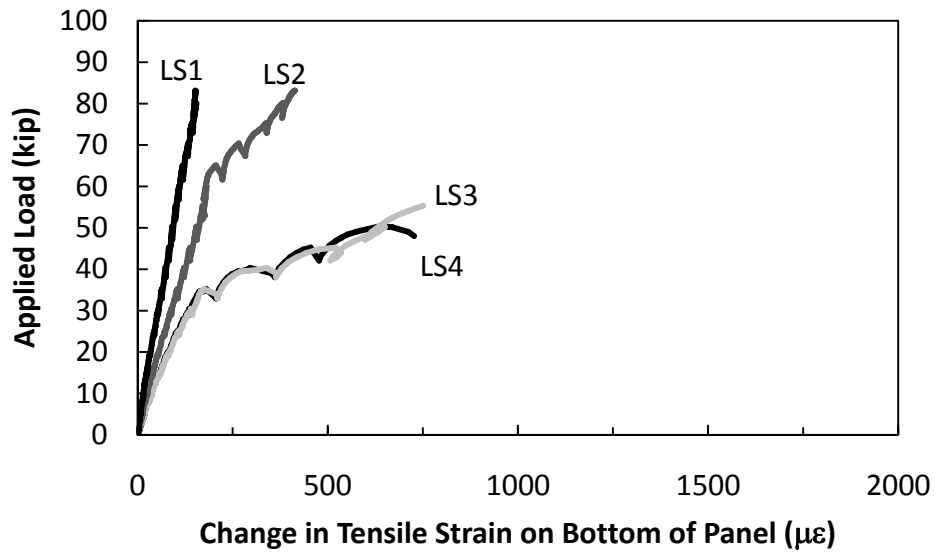


*Figure B.4 – Measured Change in Tensile Strain on Bottom of Panel for Specimen P45P1 for Load Applied at Midspan of Skewed End*

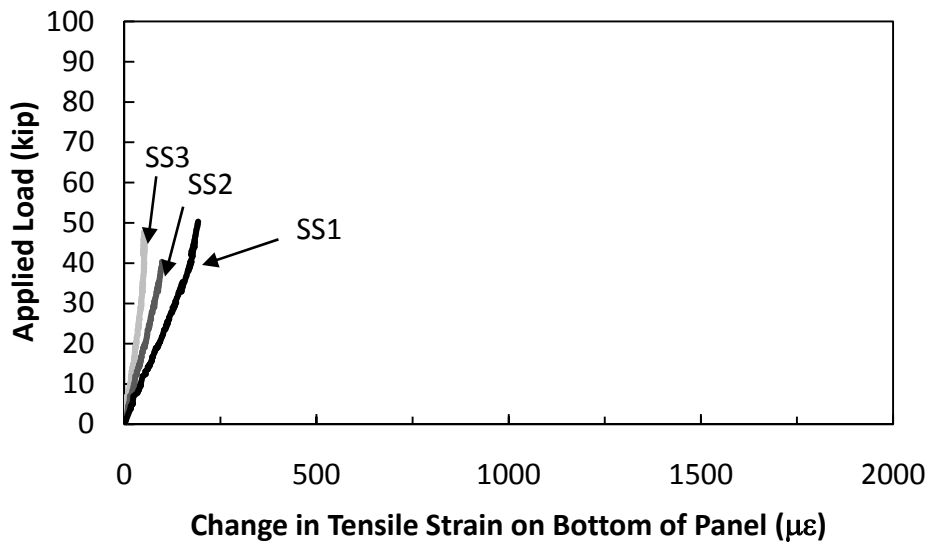


*Figure B.5 – Measured Change in Tensile Strain on Bottom of Panel for Specimen P45P1 for Load Applied at Midspan of Skewed End*

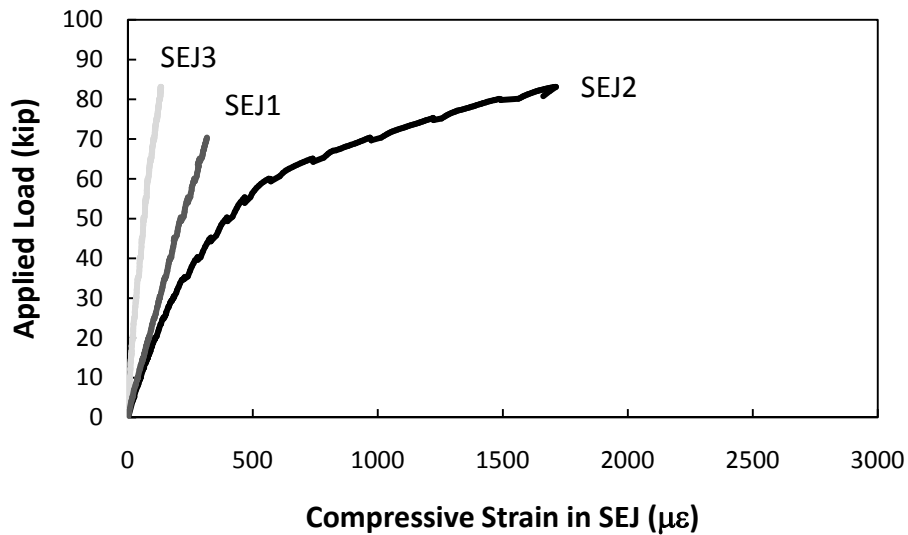


*Figure B.6 – Measured Compressive Strain in SEJ for Specimen P45P1 for Load Applied at Midspan of Skewed End*

**B.2 SPECIMEN P45P2**

The data for Specimen P45P2 are presented in this section. The data include displacements, strain on the bottom of the panel, strain in the SEJ, strain in the prestressing strands, and strain in the rebar in the trapezoidal panel.

**B.2.1 Load Applied at Midspan of Skewed End**

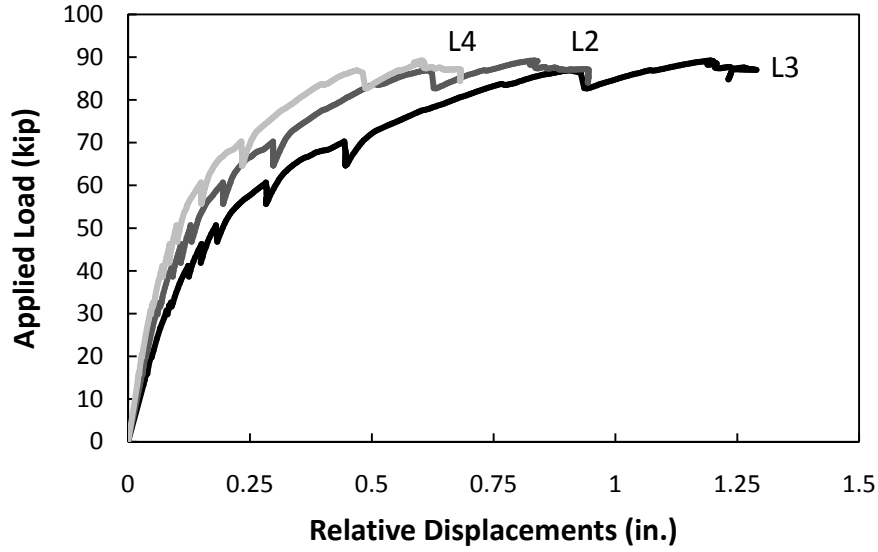


*Figure B.7 – Measured Relative Displacements for Specimen P45P2 for Load Applied at Midspan of Skewed End*

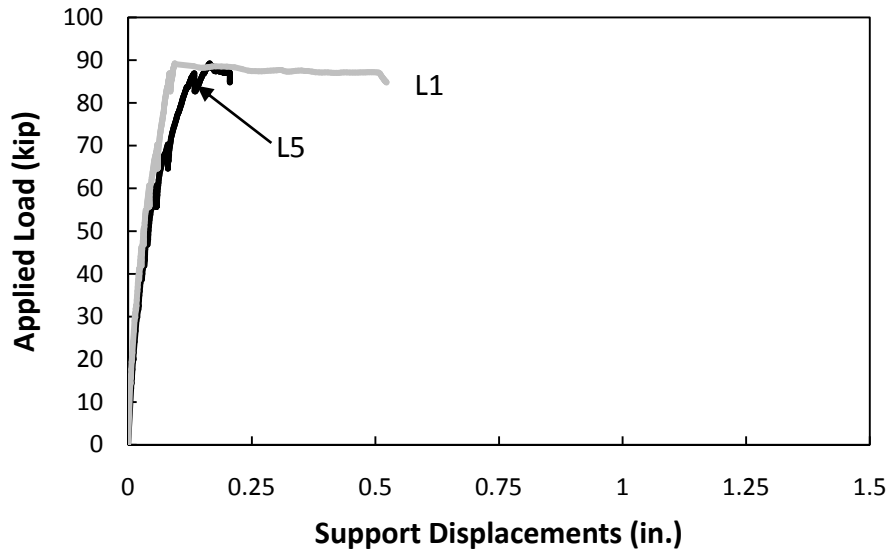


*Figure B.8 – Measured Support Displacements for Specimen P45P2 for Load Applied at Midspan of Skewed End*

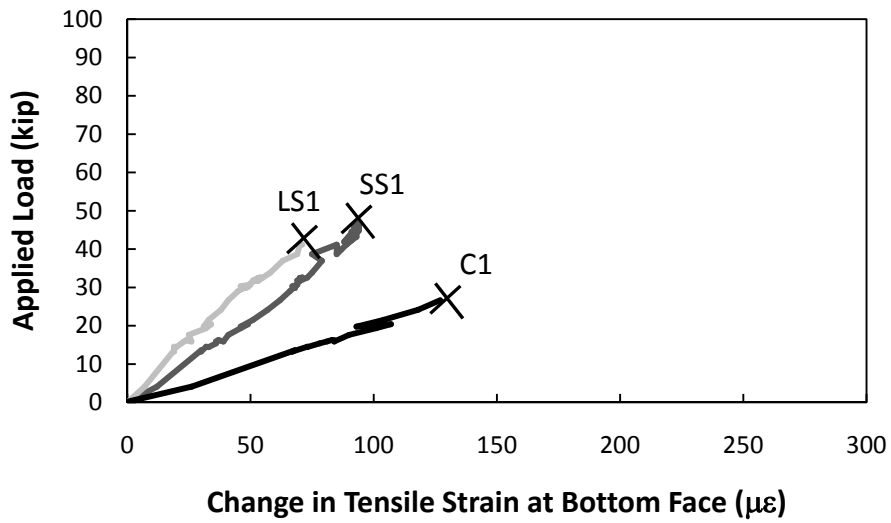


*Figure B.9 – Measured Change in Tensile Strains on Bottom of Panel for Specimen P45P2 for Load Applied at Midspan of Skewed End*

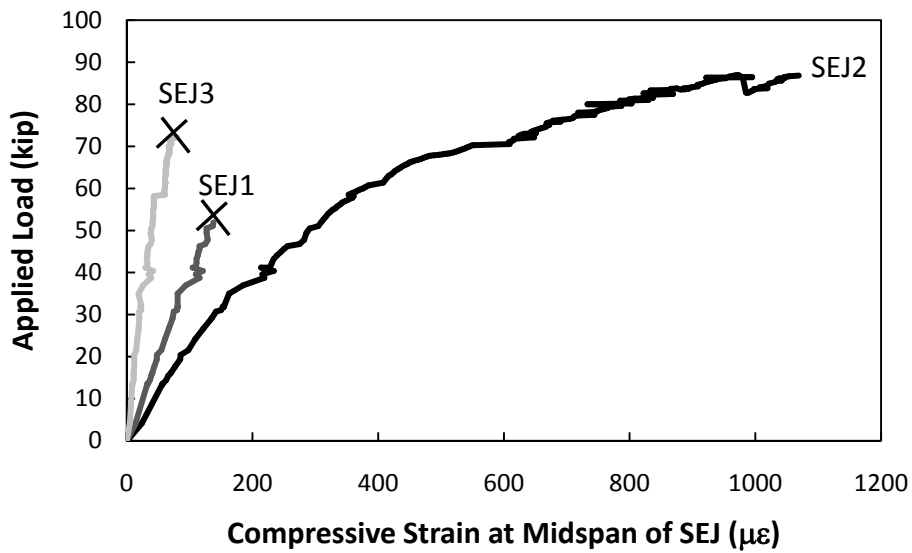


*Figure B.10 – Measured Compressive Strain in SEJ for Specimen P45P2 for Load Applied at Midspan of Skewed End*



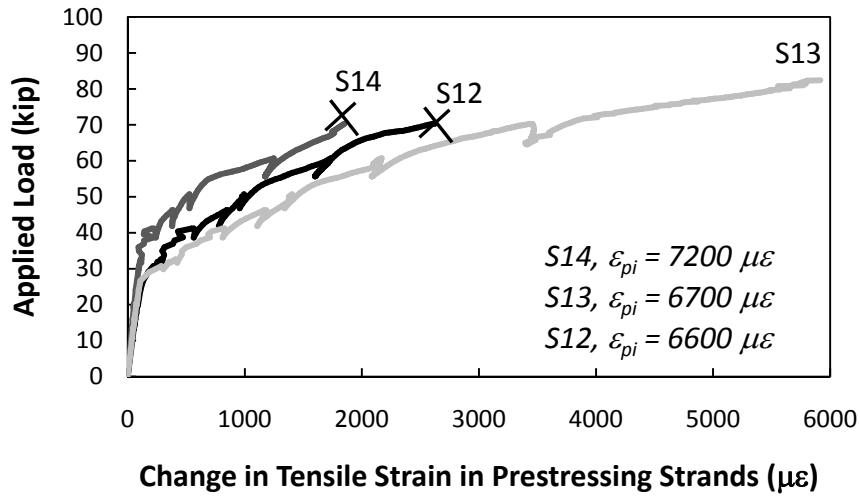


*Figure B.11 – Measured Change in Tensile Strain in Prestressing Strands S12, S13, and S14 for Specimen P45P2 for Load Applied at Midspan of Skewed End*

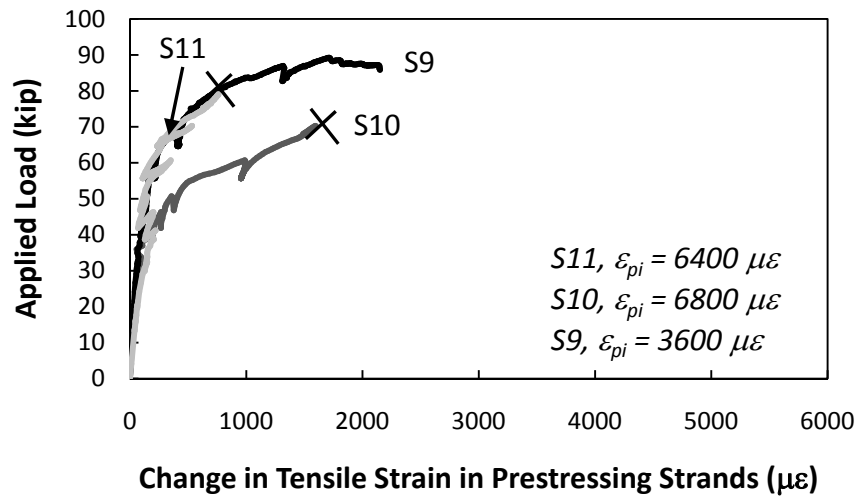


*Figure B.12 – Measured Change in Tensile Strains in Prestressing Strands S9, S10, and S11 for Specimen P45P2 for Load Applied at Midspan of Skewed End*

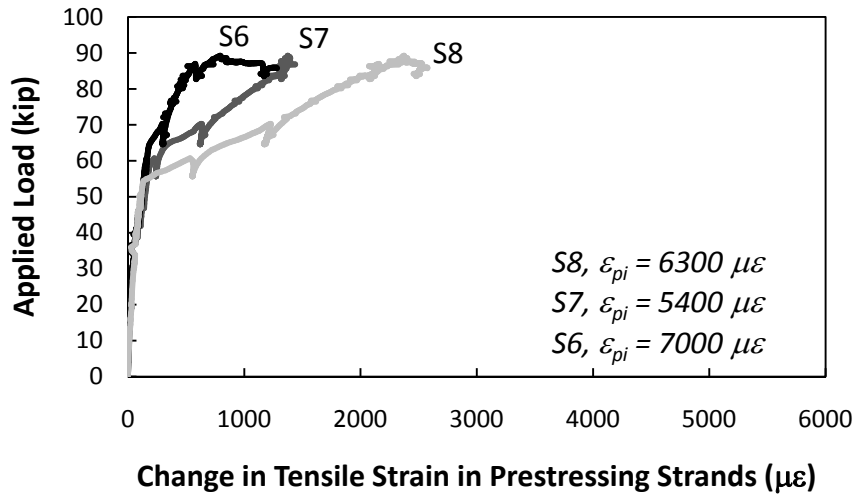


*Figure B.13 – Measured Change in Tensile Strain in Prestressing Strands S6, S7, and S8 for Specimen P45P2 for Load Applied at Midspan of Skewed End*

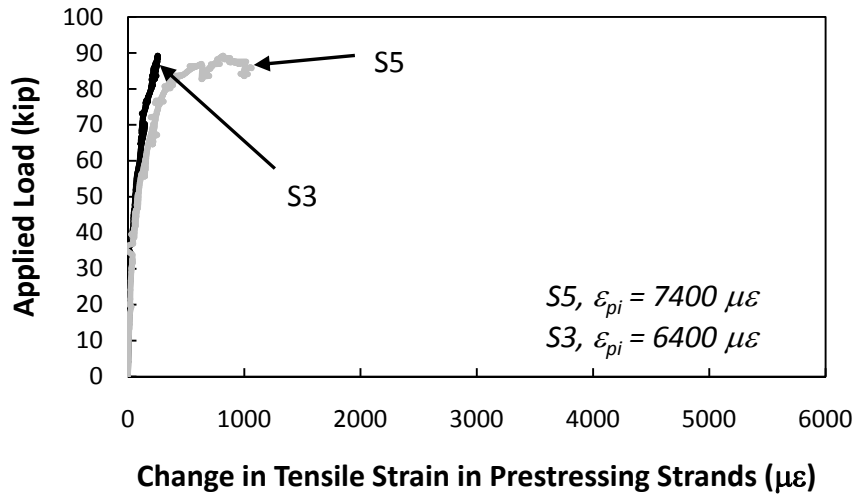


*Figure B.14 – Measured Change in Tensile Strain in Prestressing Strands S3 and S5 for Specimen P45P2 for Load Applied at Midspan of Skewed End*

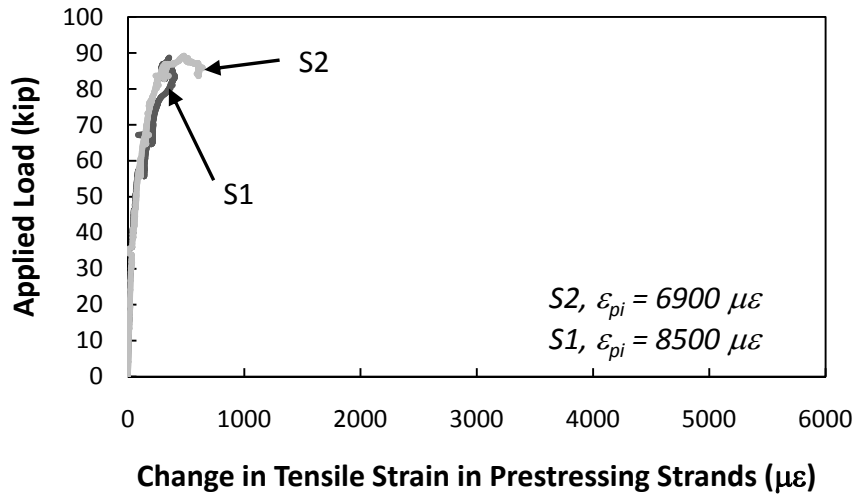


*Figure B.15 – Measured Change in Tensile Strain in Prestressing Strands S1 and S2 for Specimen P45P2 for Load Applied at Midspan of Skewed End*

**B.2.2 Loads Applied at Midspan of Square End**

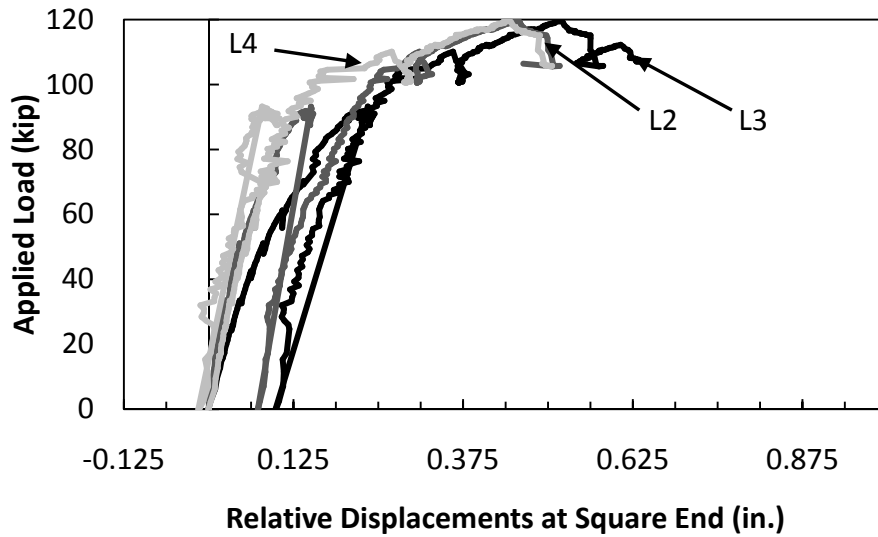


*Figure B.16 – Measured Relative Displacements for Specimen P45P2 for Load Applied at Midspan of Square End*

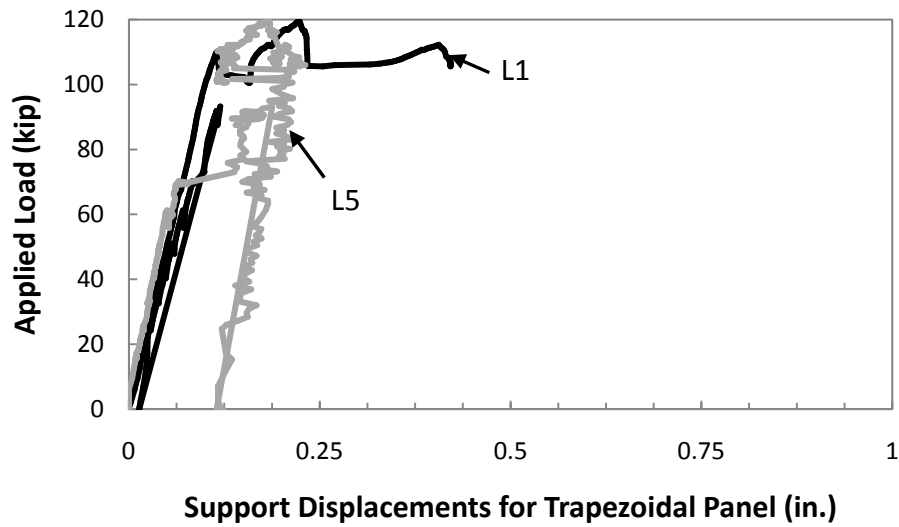


*Figure B.17 – Measured Support Displacements for Specimen P45P2 for Load Applied at Midspan of Square End*

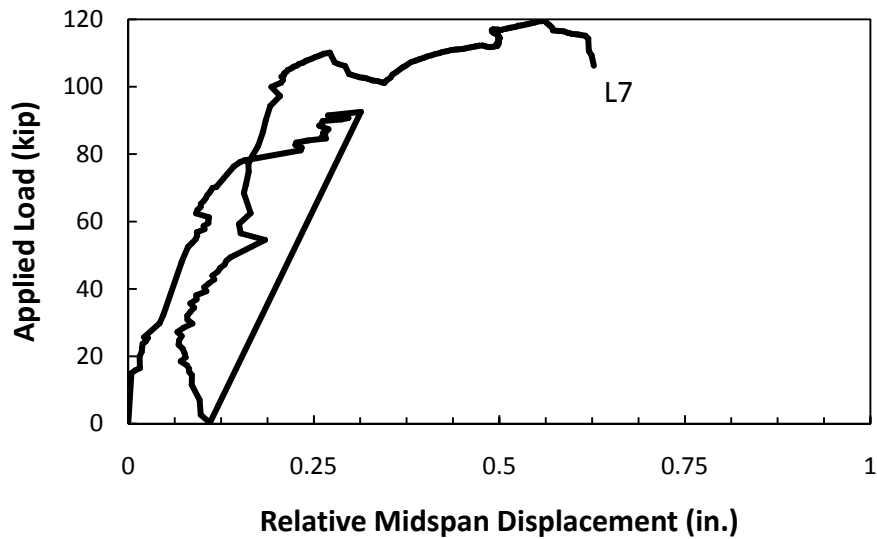


*Figure B.18 – Measured Relative Midspan Displacement for Rectangular Panel for Specimen P45P2 for Load Applied at Midspan of Square End*

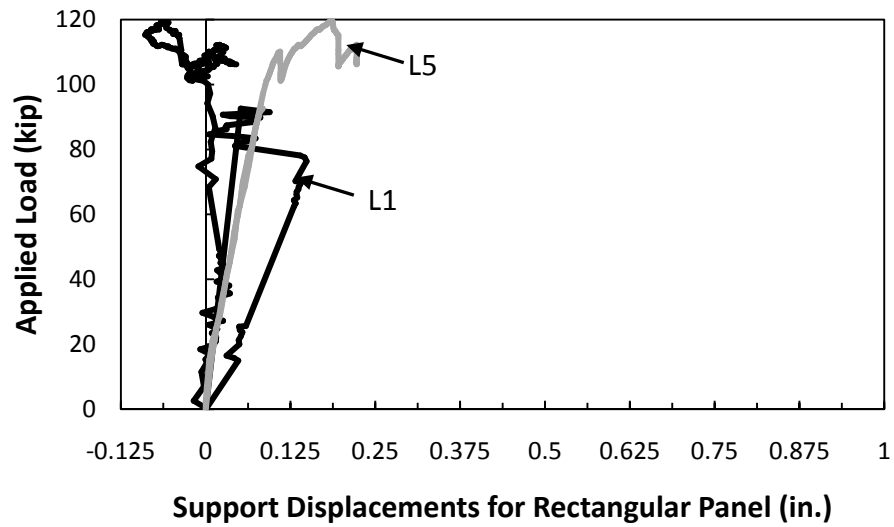


*Figure B.19 – Measured Support Displacements for Rectangular Panel for Specimen P45P2 for Load Applied at Midspan of Square End*

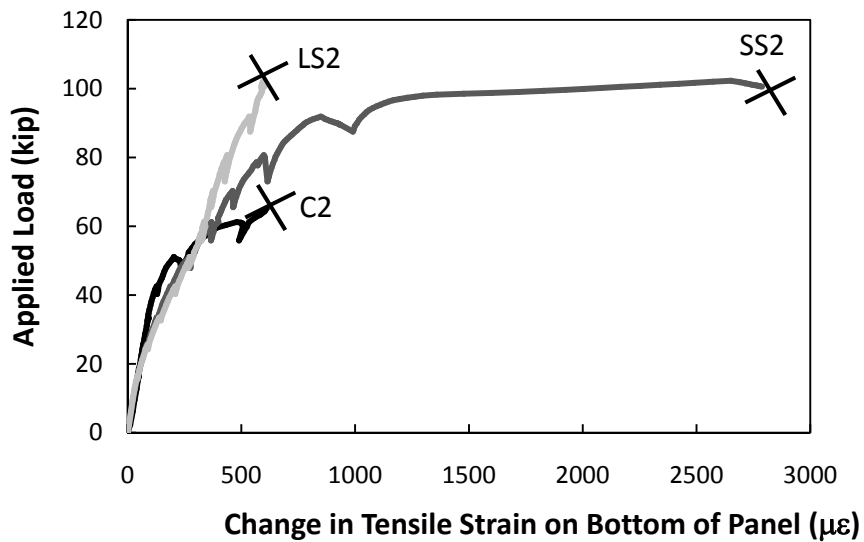


*Figure B.20 – Measured Change in Tensile Strain on Bottom of Panel for Specimen P45P2 for Load Applied at Midspan of Square End*

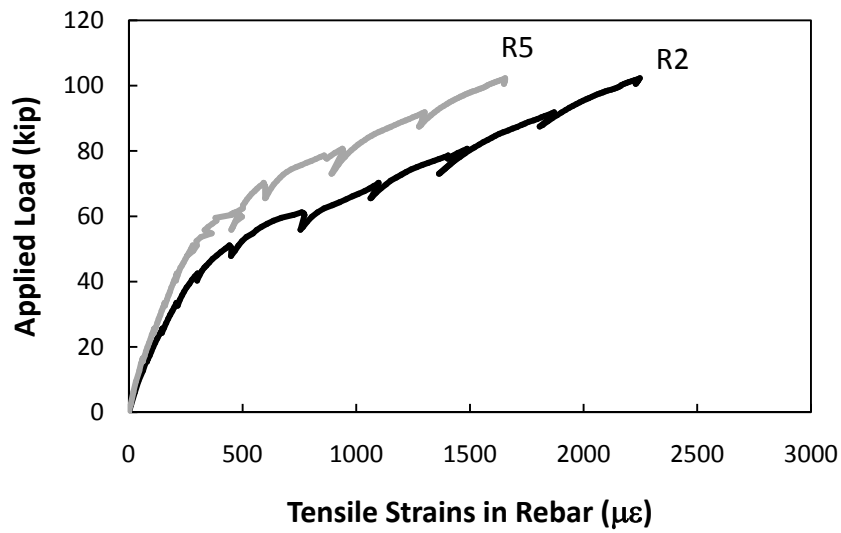


*Figure B.21 – Measured Tensile Strain in Rebar for Specimen P45P2 for Load Applied at Midspan of Square End*

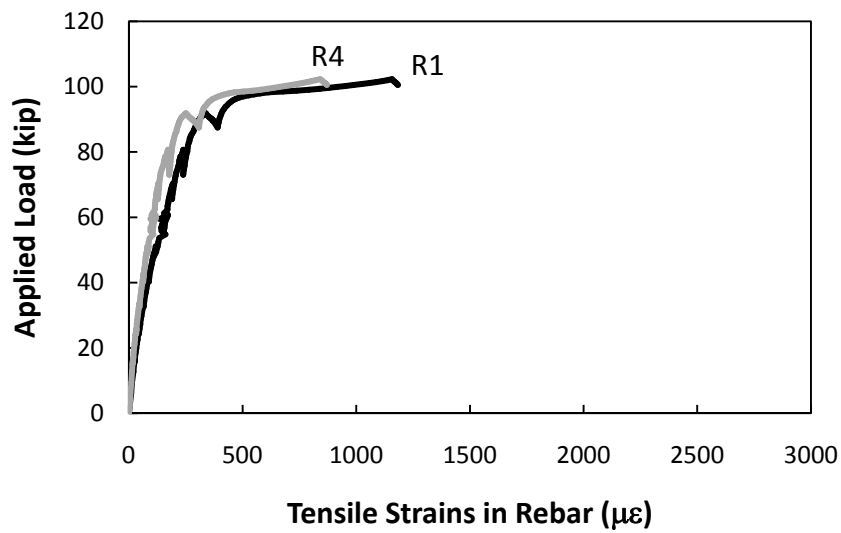


*Figure B.22 – Measured Tensile Strain in Rebar for Specimen P45P2 for Load Applied at Midspan of Square End*

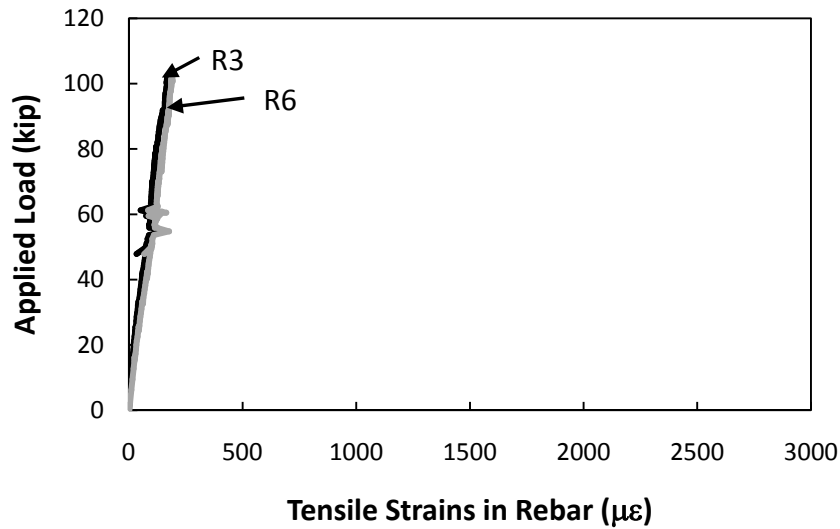


*Figure B.23 – Measured Tensile Strain in Rebar for Specimen P45P2 for Load Applied at Midspan of Square End*

### **B.3 SPECIMEN P45P3**

Specimen P45P3 was loaded first in fatigue and then statically to failure. Data for specimen P45P3 include displacement data, strain on the bottom of the panel, strain in the SEJ, and strain in the prestressing strands. Data from the periodic static tests during the fatigue loading are presented first, followed by data from the static test to failure.

#### **B.3.1 Periodic Static Tests during Fatigue Loading**

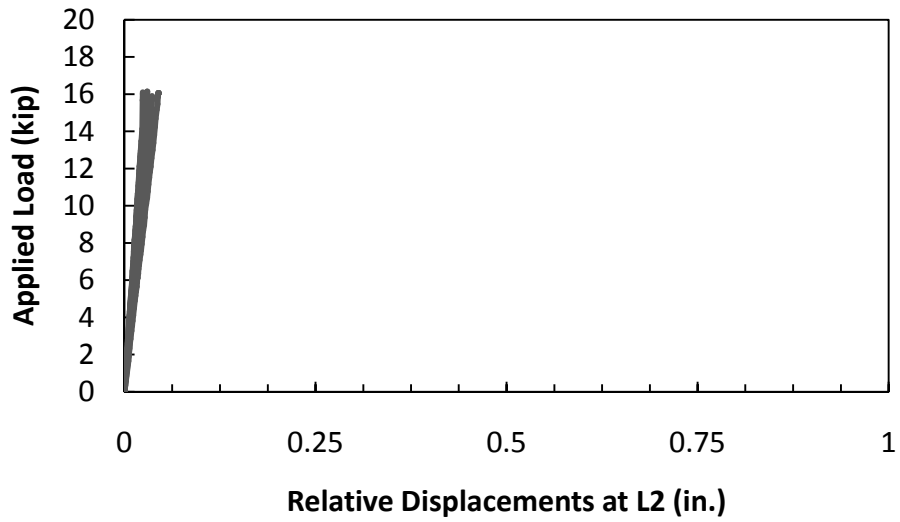


*Figure B.24 – Measured Relative Displacements at L2 for Periodic Static Tests during Fatigue Loading of Specimen P45P3 before Overload*

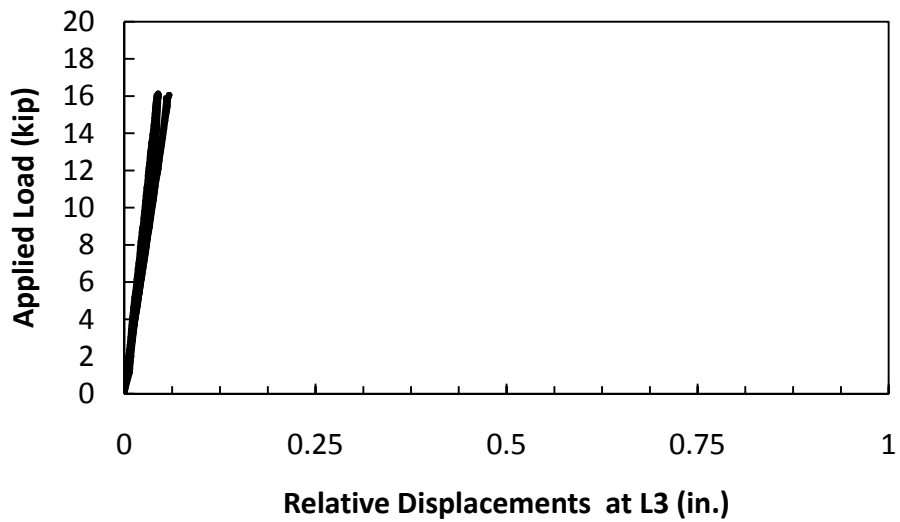


*Figure B.25 – Measured Relative Displacements at L3 for Periodic Static Tests during Fatigue Loading of Specimen P45P3 before Overload*



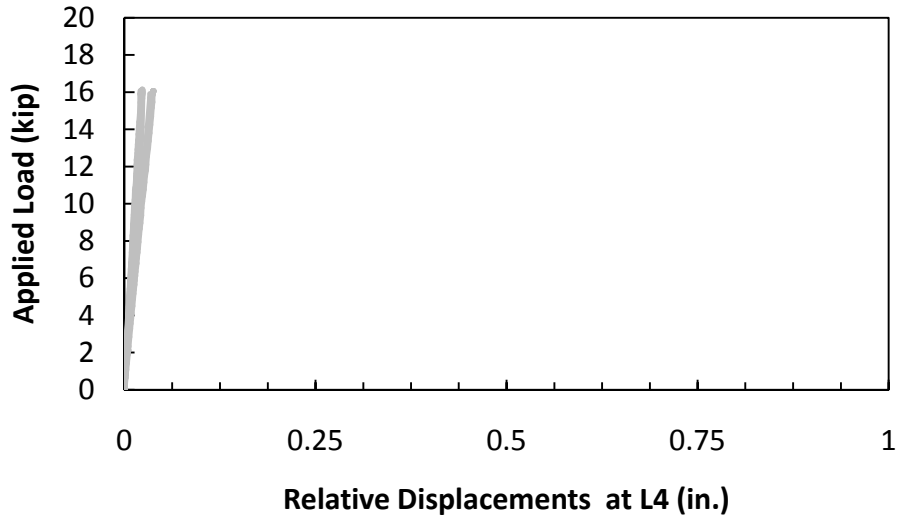


*Figure B.26 – Measured Relative Displacements at L4 for Periodic Static Tests during Fatigue Loading of Specimen P45P3 before Overload*

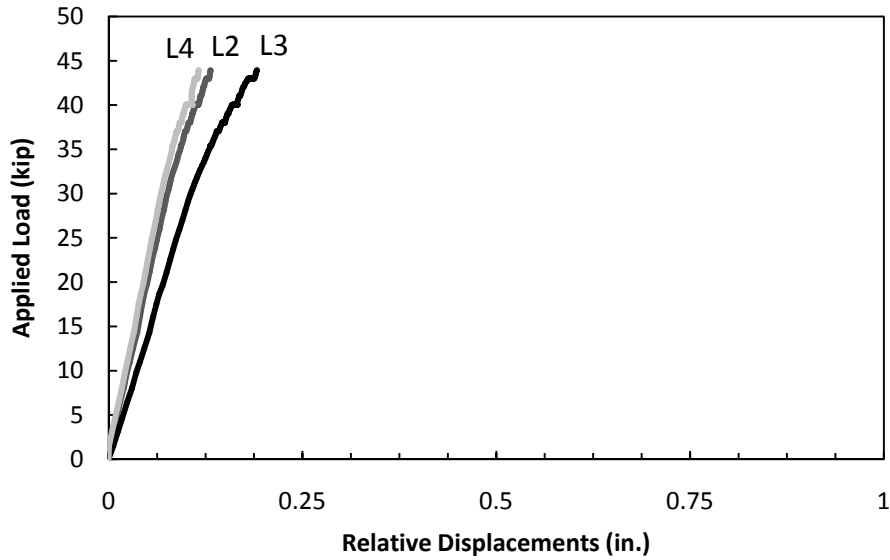


*Figure B.27 – Measured Relative Displacements for Static Overload of Specimen P45P3 during Fatigue Loading*

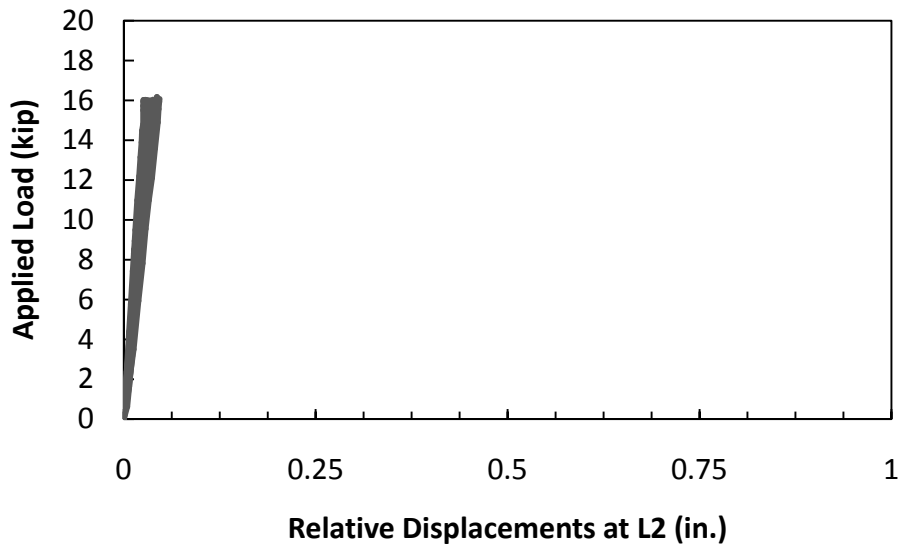


*Figure B.28 – Measured Relative Displacements at L2 for Periodic Static Tests during Fatigue Loading of Specimen P45P3 after Overload*

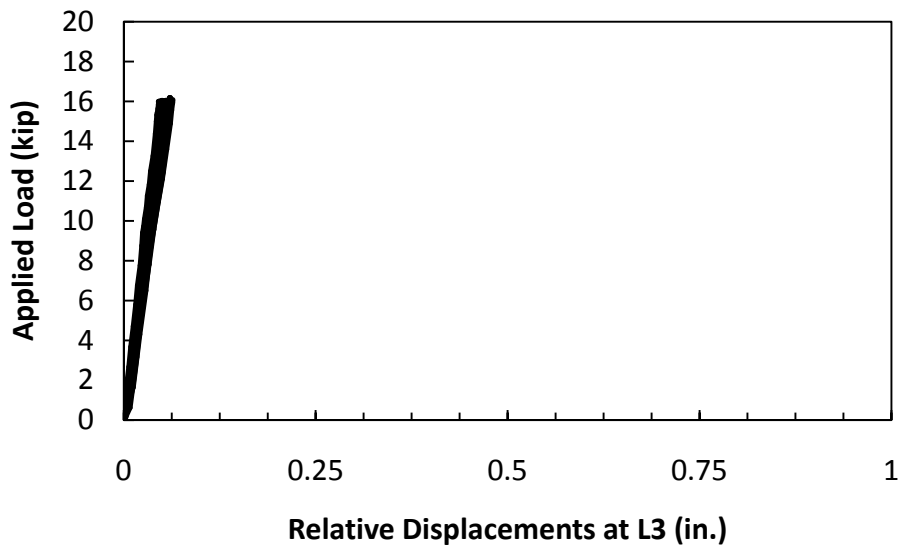


*Figure B.29 – Measured Relative Displacements at L3 for Periodic Static Tests during Fatigue Loading of Specimen P45P3 after Overload*

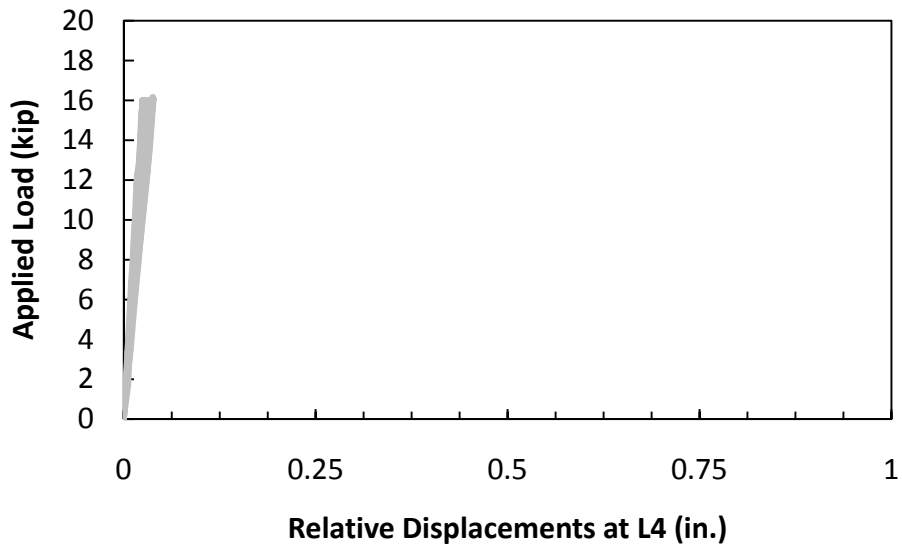


*Figure B.30 – Measured Relative Displacements at L4 for Periodic Static Tests during Fatigue Loading of Specimen P45P3 after Overload*

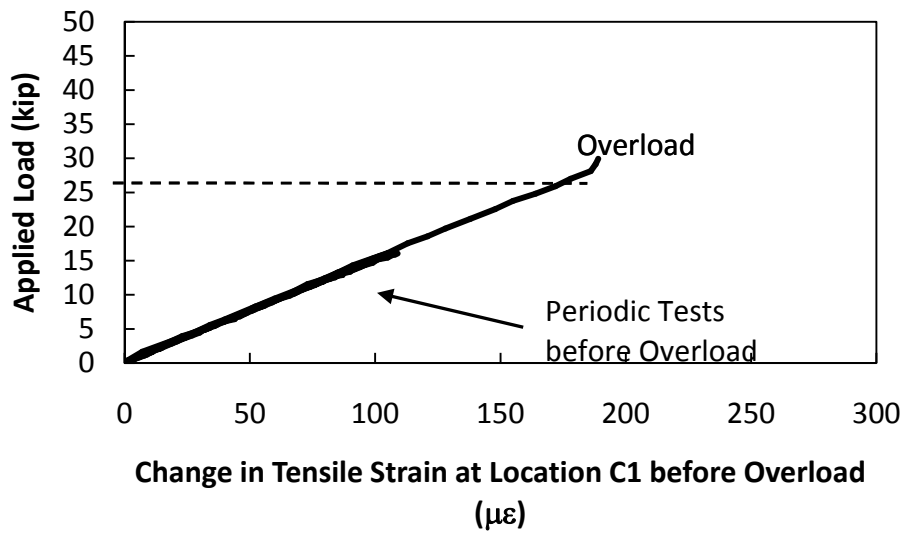


*Figure B.31 – Measured Change in Tensile Strain on Bottom of Panel at Location C1 during Fatigue Loading of Specimen P45P3 before Overload*

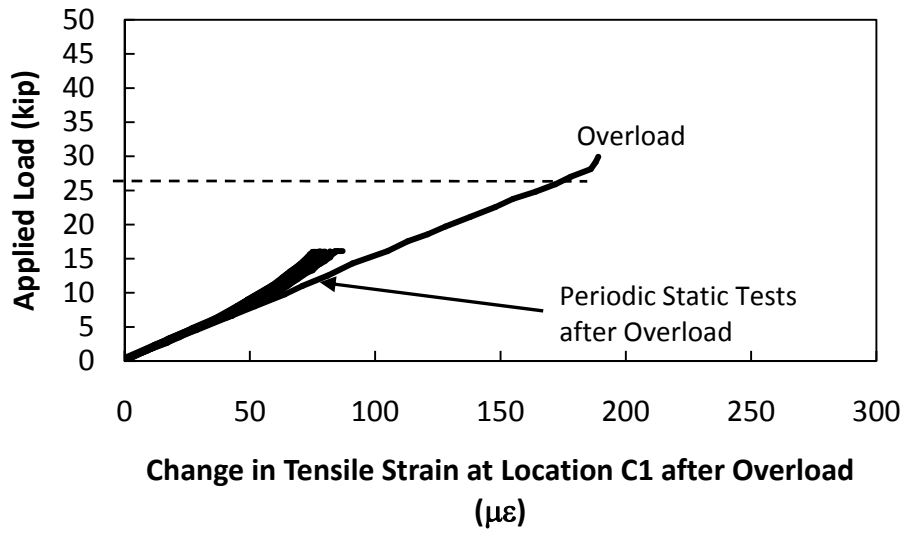


*Figure B.32 – Measured Change in Tensile Strain on Bottom of Panel at Location C1 during Fatigue Loading of Specimen P45P3 after Overload*

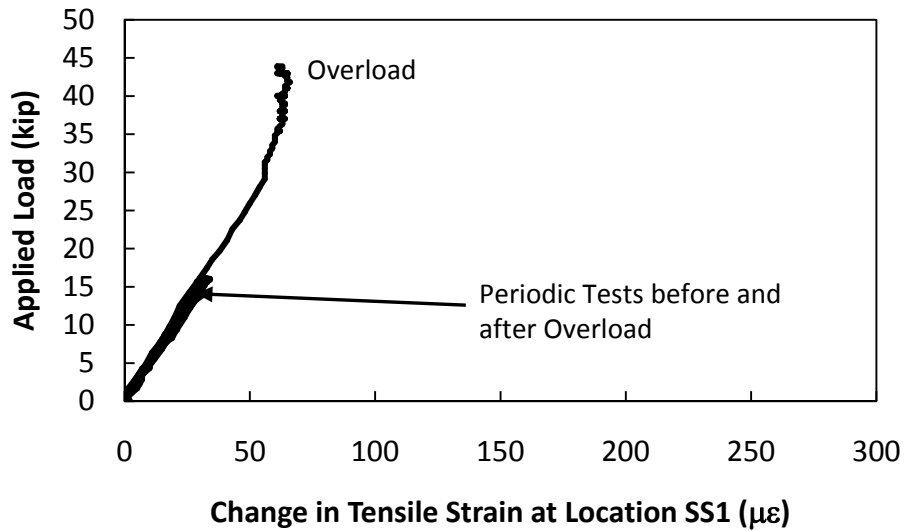


*Figure B.33 – Measured Change in Tensile Strain on Bottom of Panel at Location SS1 during Fatigue Loading Specimen P45P3 before and after Overload*

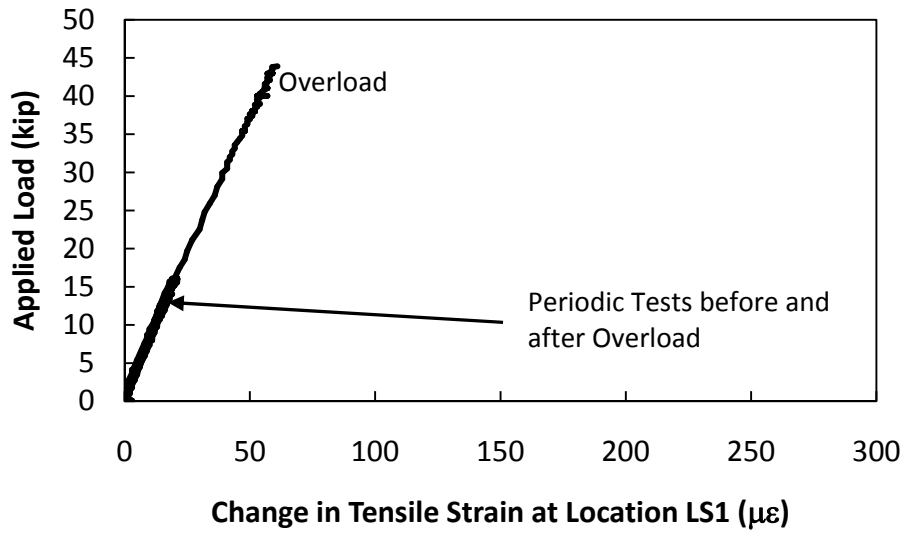


*Figure B.34 – Measured Change in Tensile Strain on Bottom of Panel for Periodic Static Tests during Fatigue Loading of Specimen P45P3 before and after Overload*

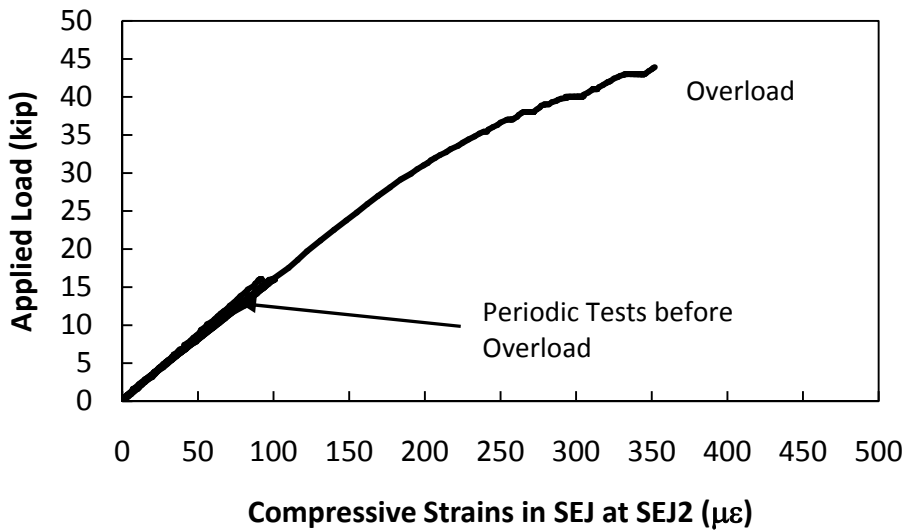


*Figure B.35 – Measured Compressive Strain on Top Surface of SEJ at SEJ2 for Periodic Static Tests during Fatigue Loading for Specimen P45P3 before Overload*

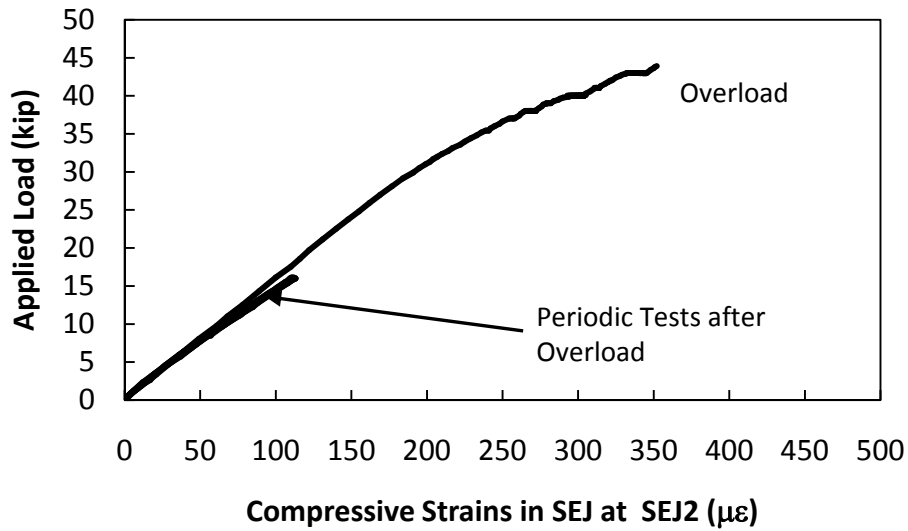


*Figure B.36 - Measured Compressive Strains on Top Surface of SEJ at SEJ2 for Periodic Tests during Fatigue Loading for Specimen P45P3 after Overload*

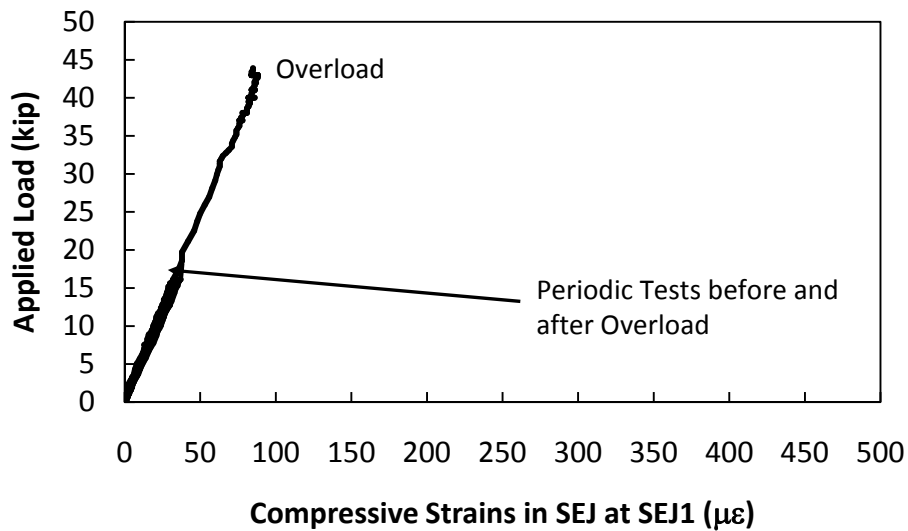


*Figure B.37 - Measured Compressive Strains on Top Surface of SEJ at SEJ1 for Periodic Static Tests during Fatigue Loading of Specimen P45P3 before and after Overload*

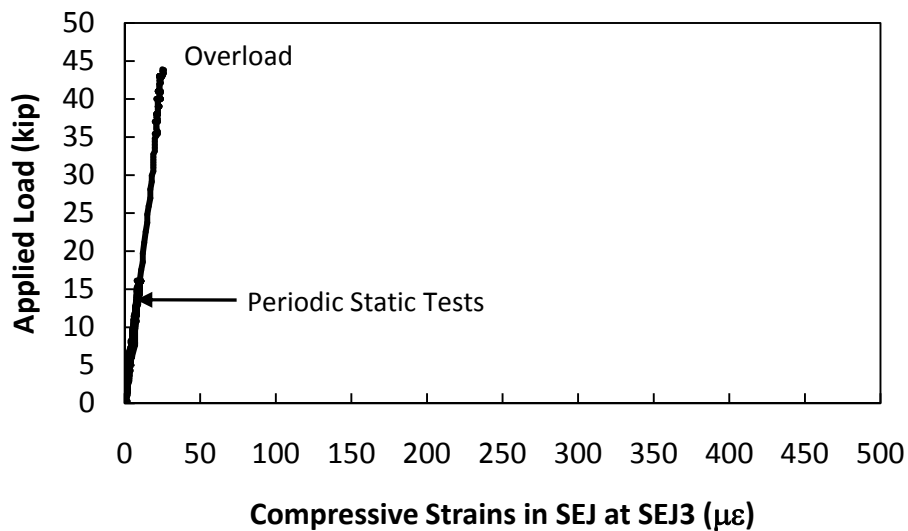


*Figure B.38 – Measured Compressive Strain on Top Surface of SEJ at SEJ3 for Periodic Static Tests during Fatigue Loading of Specimen P45P3 before and after Overload*

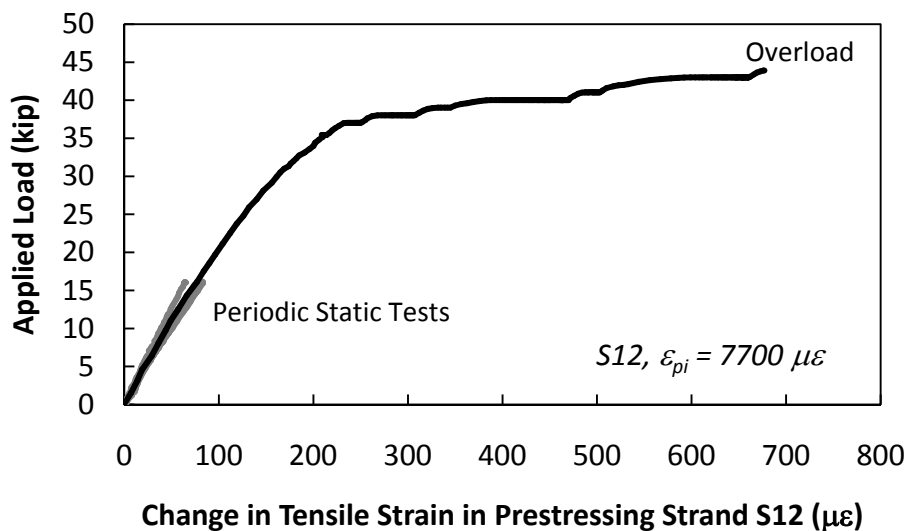


*Figure B.39 – Measured Change in Tensile Strain in Strand S12 for Periodic Static Tests during Fatigue Loading of Specimen P45P3 before Overload*

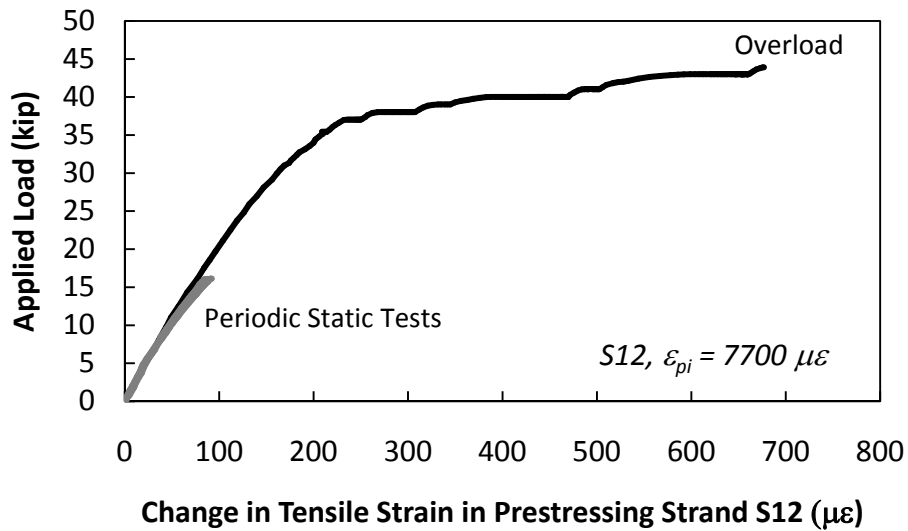


*Figure B.40 – Measured Change in Tensile Strain in Strand S12 for Periodic Static Tests during Fatigue Loading of Specimen P45P3 after Overload*

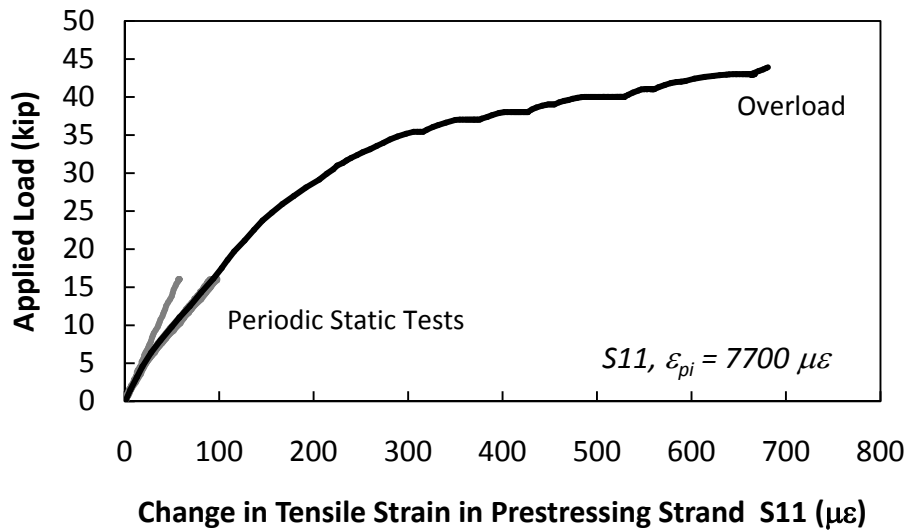


*Figure B.41 – Measured Change in Tensile Strain in Strand S11 for Periodic Static Tests during Fatigue Loading of Specimen P45P3 before Overload*



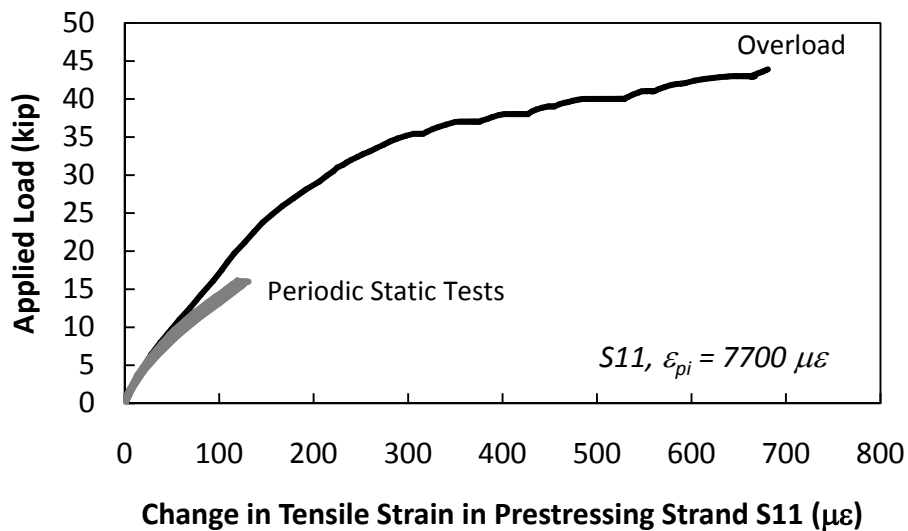


*Figure B.42 – Measured Change in Tensile Strain in Strand S11 for Periodic Static Tests during Fatigue Loading of Specimen P45P3 after Overload*

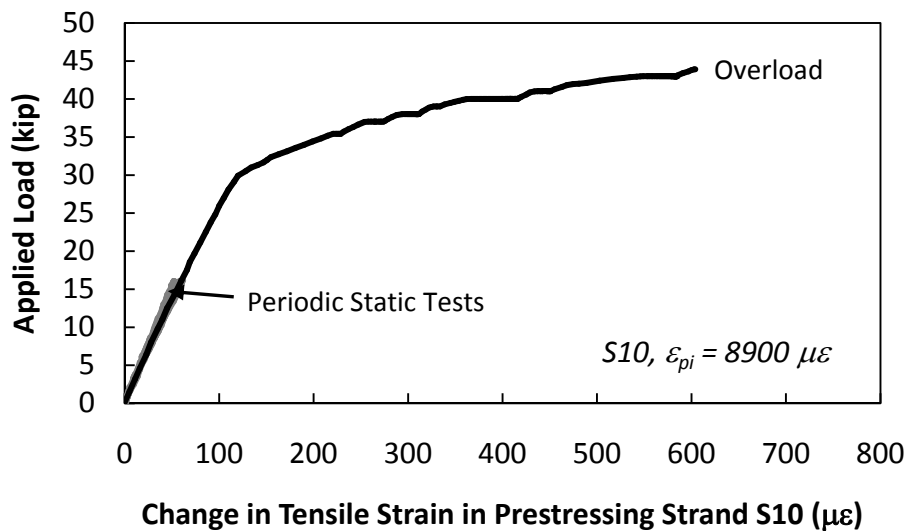


*Figure B.43 – Measured Change in Tensile Strain in Strand S10 for Periodic Static Tests during Fatigue Loading of Specimen P45P3 before Overload*

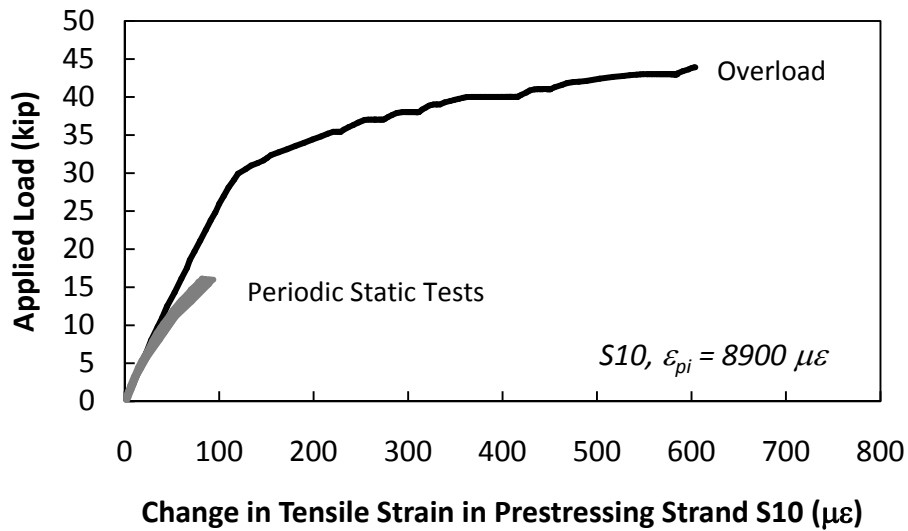


*Figure B.44 – Measured Change in Tensile Strain in Strand S10 for Periodic Static Tests during Fatigue Loading of Specimen P45P3 after Overload*

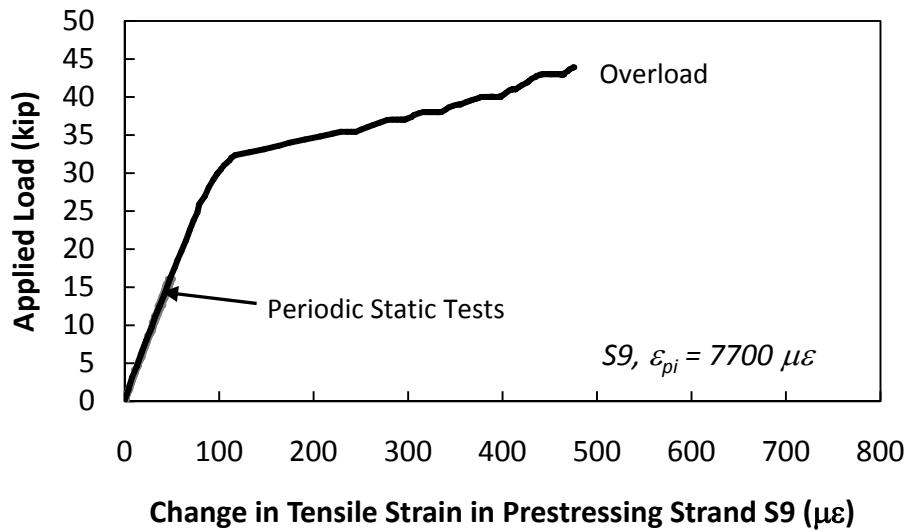


*Figure B.45 – Measured Change in Tensile Strains in Strand S9 for Periodic Static Tests during Fatigue Loading of Specimen P45P3 before Overload*

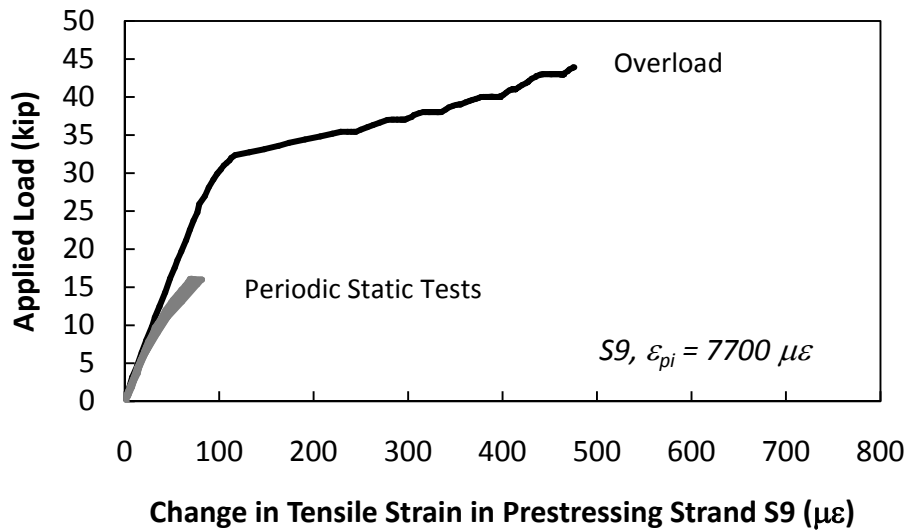


*Figure B.46 – Measured Change in Tensile Strain in Strand S9 for Periodic Static Tests during Fatigue Loading of Specimen P45P3 after Overload*

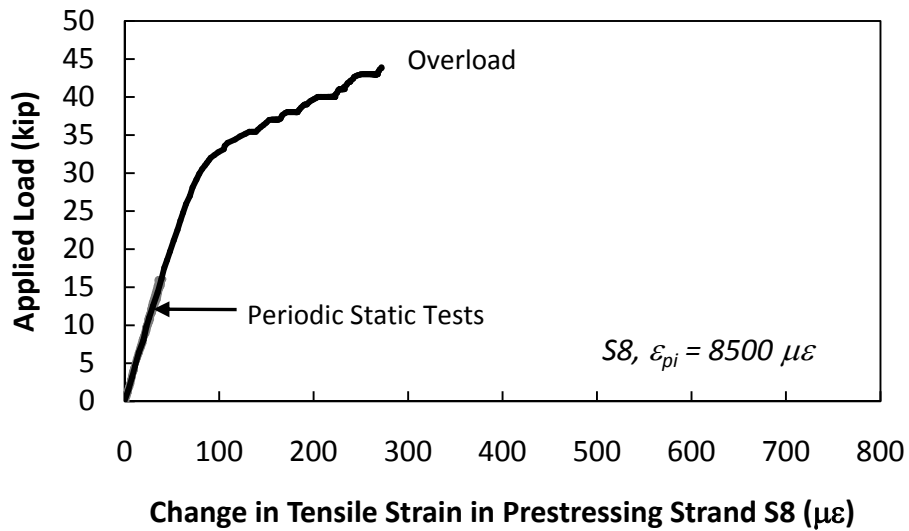


*Figure B.47 – Measured Change in Tensile Strain in Strand S8 for Periodic Static Tests during Fatigue Loading of Specimen P45P3 before Overload*

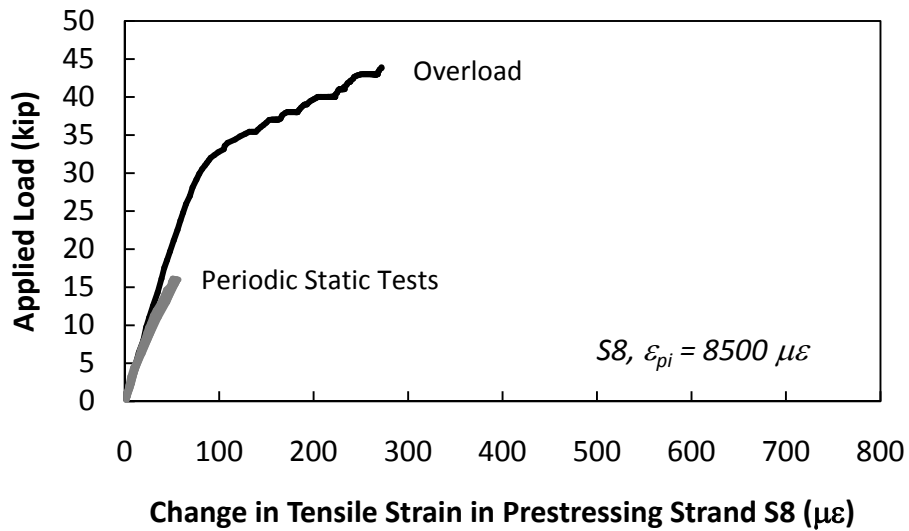


*Figure B.48 – Measured Change in Tensile Strain in Strand S8 for Periodic Static Tests during Fatigue Loading of Specimen P45P3 after Overload*

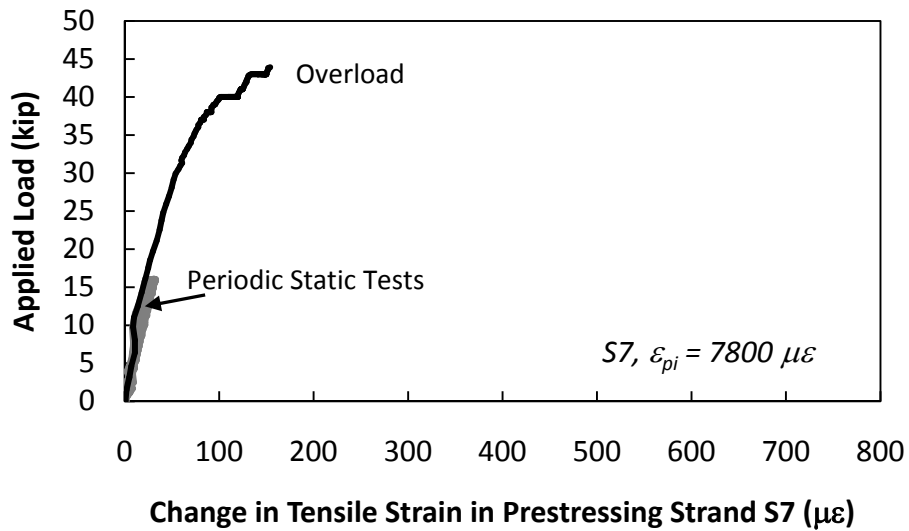


*Figure B.49 – Measured Change in Tensile Strain in Strand S7 for Periodic Static Test during Fatigue Loading of Specimen P45P3 before and after Overload*

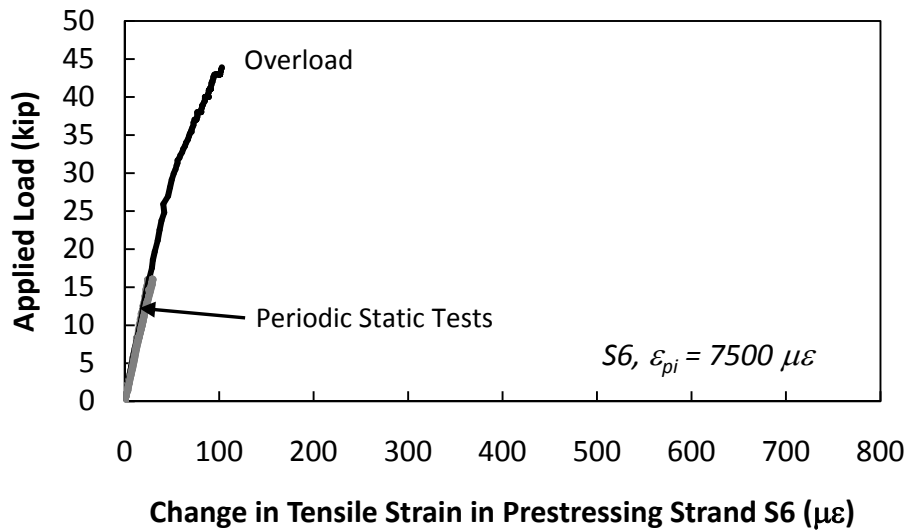


*Figure B.50 – Measured Change in Tensile Strain in Strand S6 for Periodic Static Tests during Fatigue Loading of Specimen P45P3 before and after Overload*

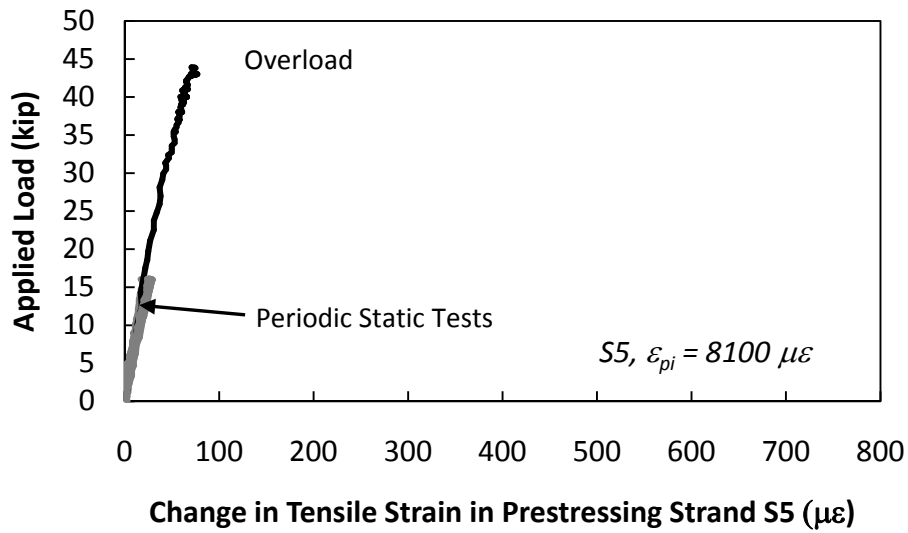


*Figure B.51 – Measured Change in Tensile Strain in Strand S5 for Periodic Static Tests during Fatigue Loading of Specimen P45P3 before and after Overload*

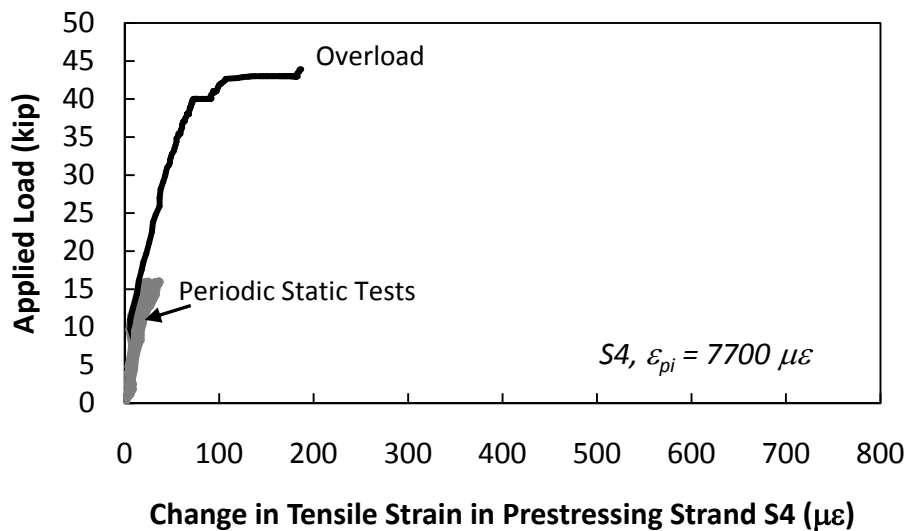


*Figure B.52 – Measured Change in Tensile Strain in Strand S4 for Periodic Static Tests during Fatigue Loading of Specimen P45P3 before and after Overload*

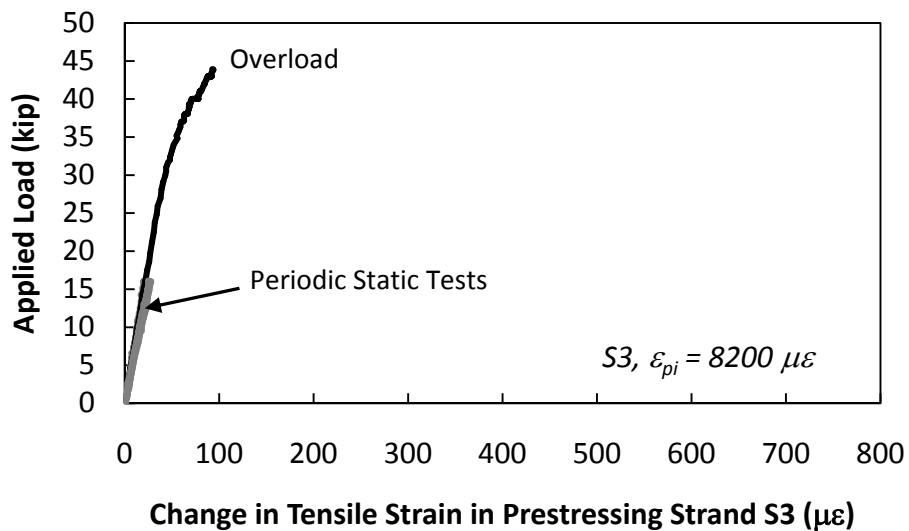


*Figure B.53 – Measured Change in Tensile Strain in Strand S3 for Periodic Static Tests during Fatigue Loading of Specimen P45P3 before and after Overload*

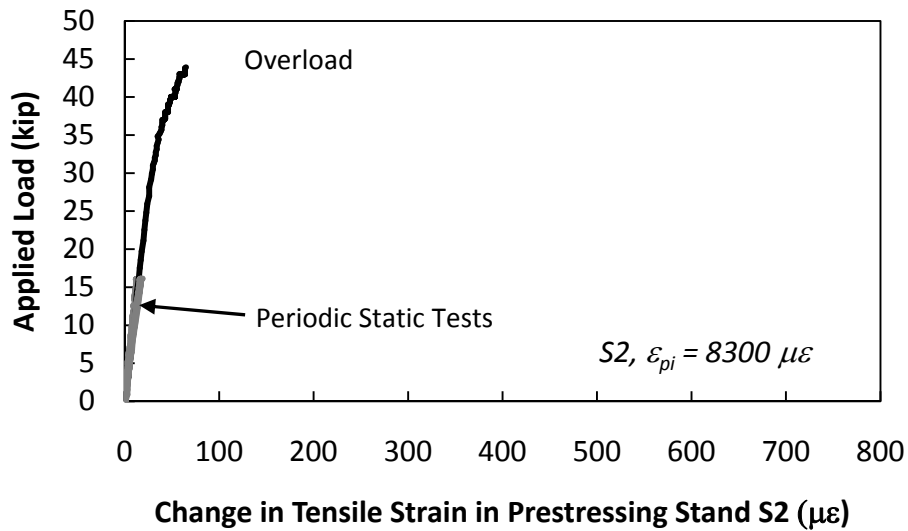


*Figure B.54 – Measured Change in Tensile Strain in Strand S2 for Periodic Static Tests during Fatigue Loading of Specimen P45P3 before and after Overload*

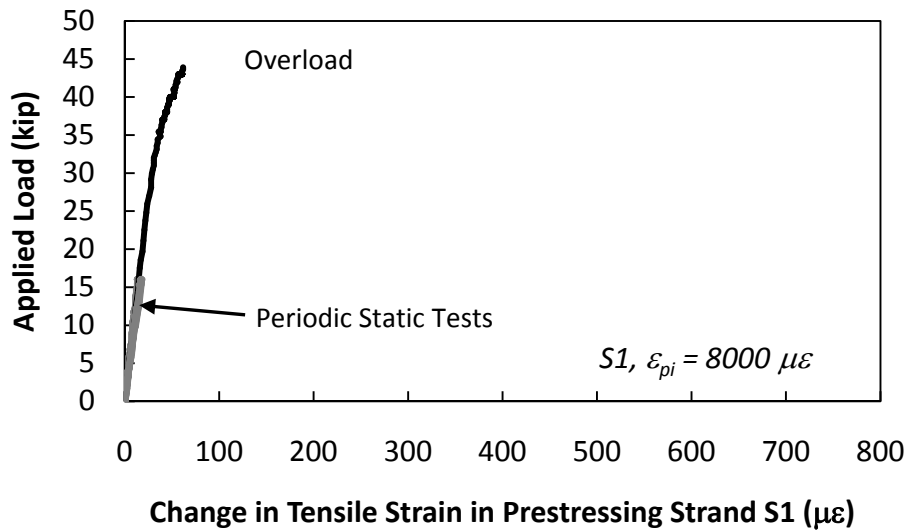


*Figure B.55 – Measured Change in Tensile Strain in Strand S1 for Periodic Static Tests during Fatigue Loading of Specimen P45P3 before and after Overload*

### B.3.2 Static Load to Failure

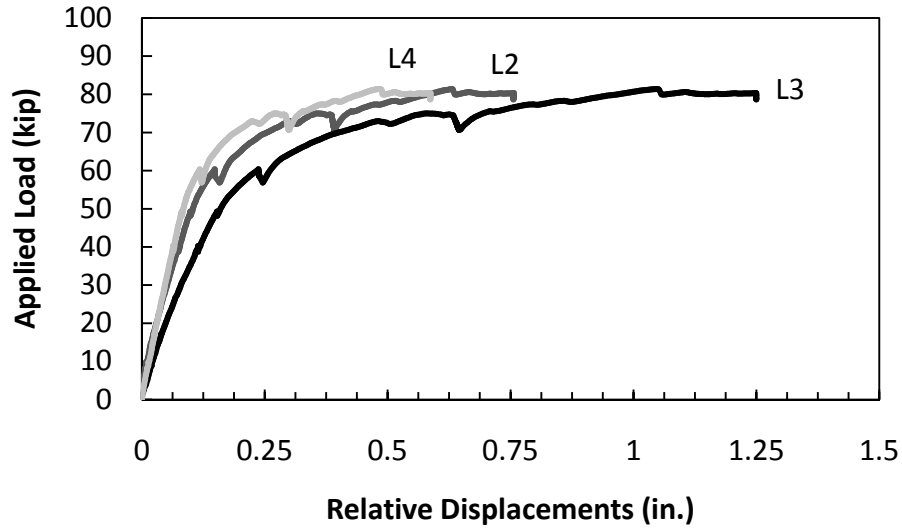


*Figure B.56 – Measured Displacements for Specimen P45P3 for Static Test to Failure for Load Applied at Midspan of Skewed End*

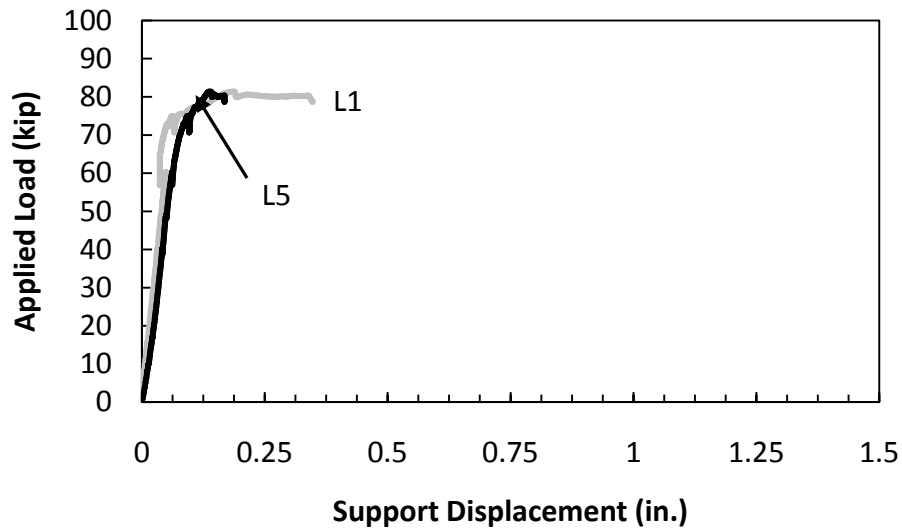


*Figure B.57 – Measured Support Displacements for Specimen P45P3 for Static Test to Failure for Load Applied at Midspan of Skewed End*



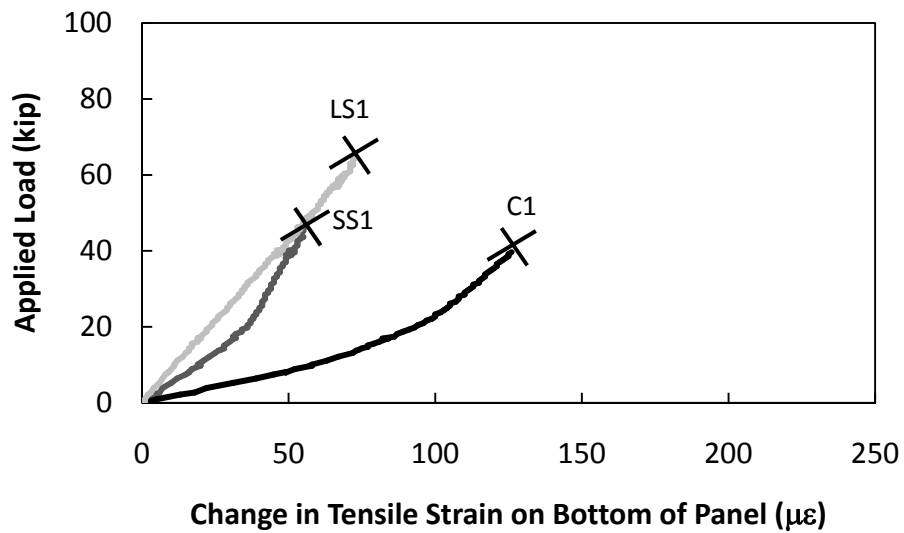


*Figure B.58 – Measured Change in Tensile Strain on Bottom of Panel for Specimen P45P3 for Static Overload for Load Applied at Midspan of Skewed End*

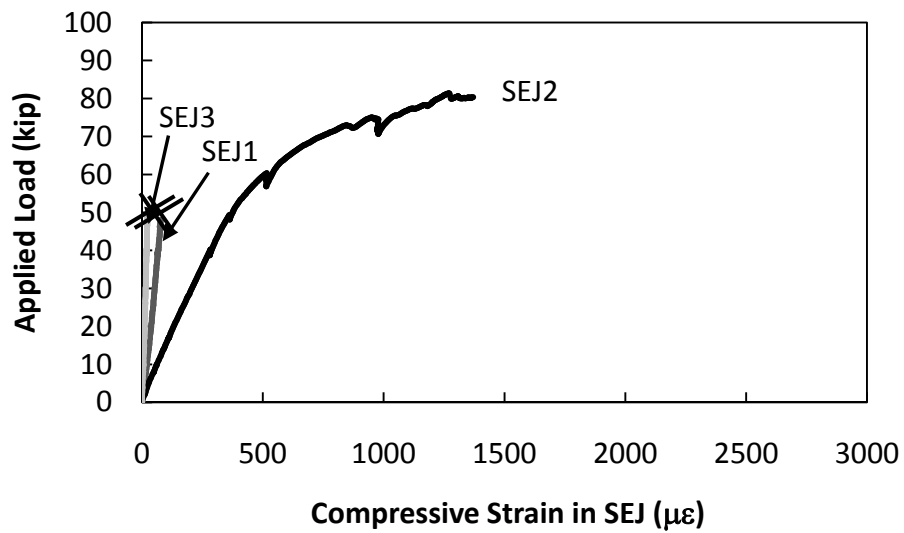


*Figure B.59 – Measured Compressive Strain in SEJ for Specimen P45P3 for Static Overload for Load Applied at Midspan of Skewed End*

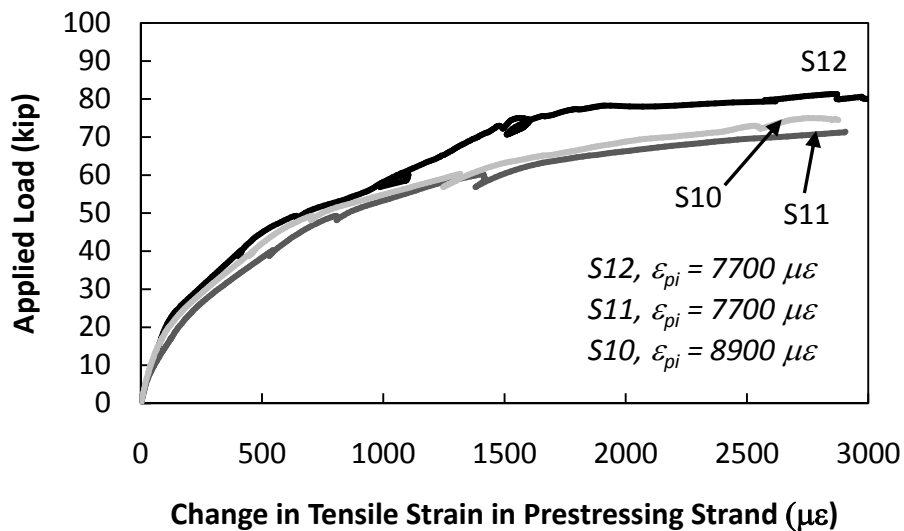


*Figure B.60 – Measured Change in Tensile Strain in Strands S10, S11, and S12 in Specimen P45P3 for Static Overload Test for Load Applied at Midspan of Skewed End*

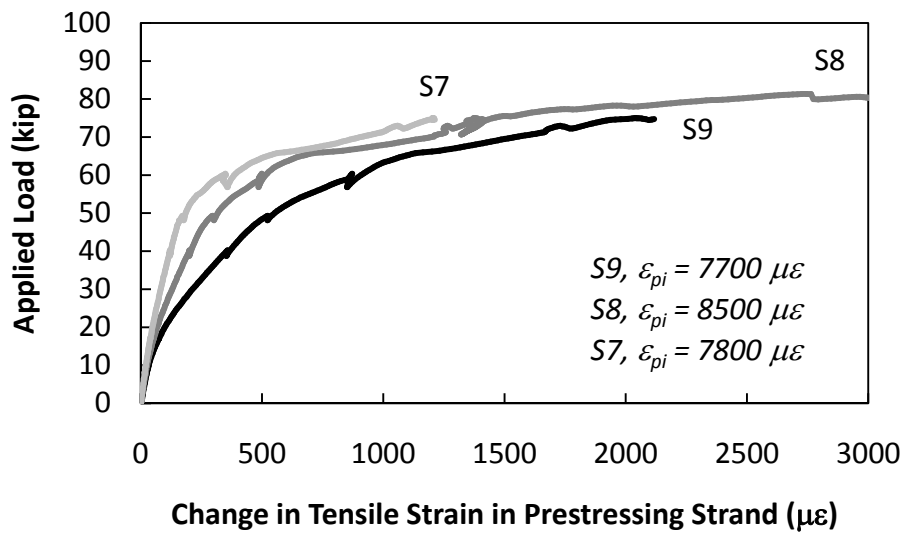


*Figure B.61 – Measured Change in Tensile Strain in Strands S7, S8, and S9 in Specimen P45P3 for Static Overload Test for Load Applied at Midspan of Skewed End*

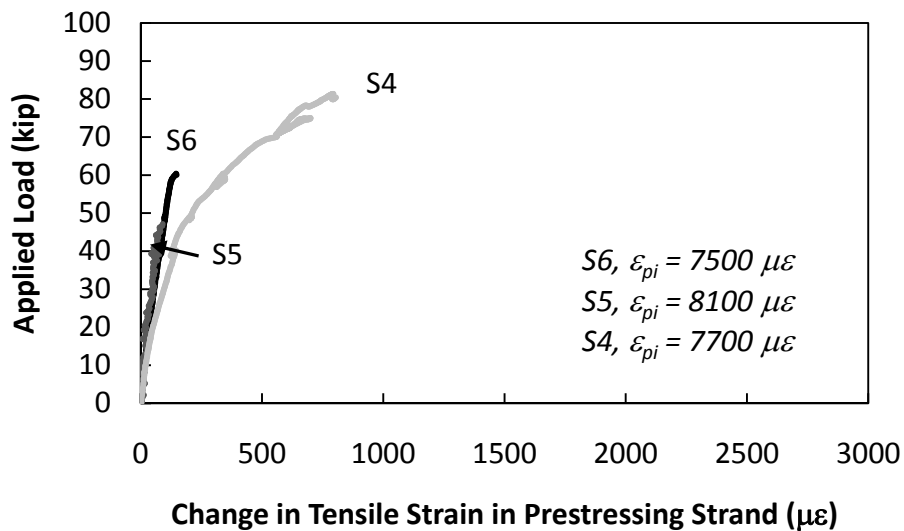


*Figure B.62 – Measured Change in Tensile Strain in Strands S4, S5, and S6 for Specimen P45P3 for Static Overload Test for Load Applied at Midspan of Skewed End*

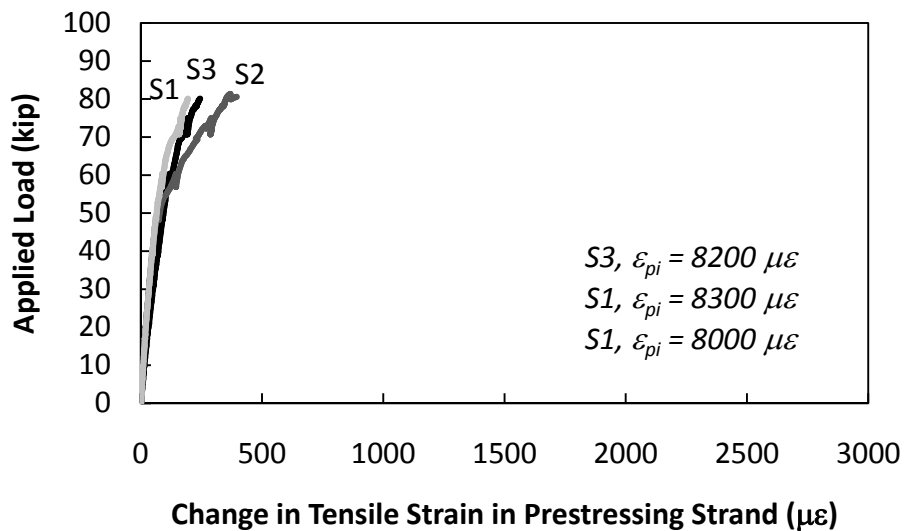


*Figure B.63 – Measured Change in Tensile Strain in Strands S1, S2, and S3 for Specimen P45P3 for Static Overload Test for Load Applied at Midspan of Skewed End*

## B.4 SPECIMEN P30P1

Specimen P30P1 was loaded first in the skewed end and then on the square end. Data for Specimen P30P1 include displacement data, strain on the bottom of the panel, and strain in the SEJ. Data for load applied to the skewed end are provided first followed by the data for load applied on the square end. Strain gages on the square end were damaged during the loading on the skewed end, so only strain on the bottom of the panel for load applied at the skewed end was available.

### B.4.1 Load Applied at Midspan of Skewed End

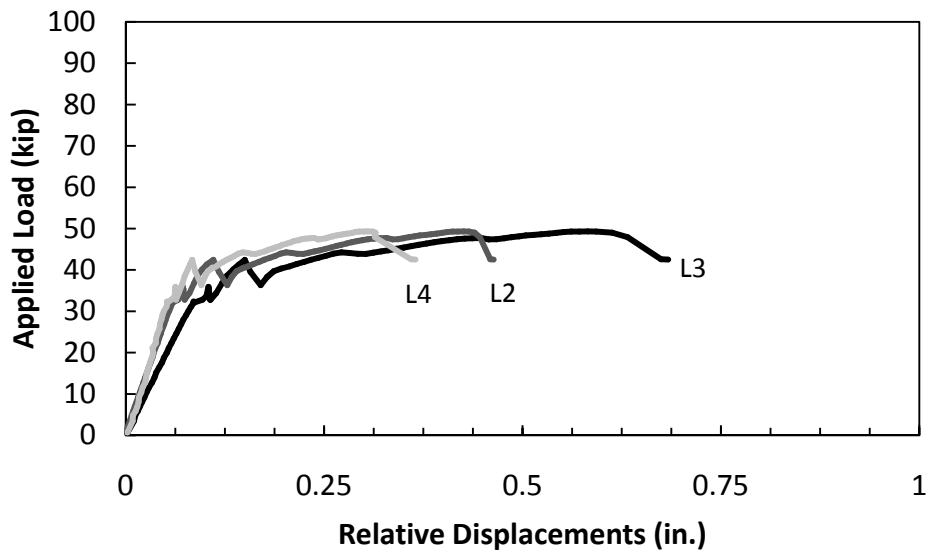


*Figure B.64 – Measured Relative Displacements for Specimen P30P1 for Load Applied at Midspan of Skewed End*

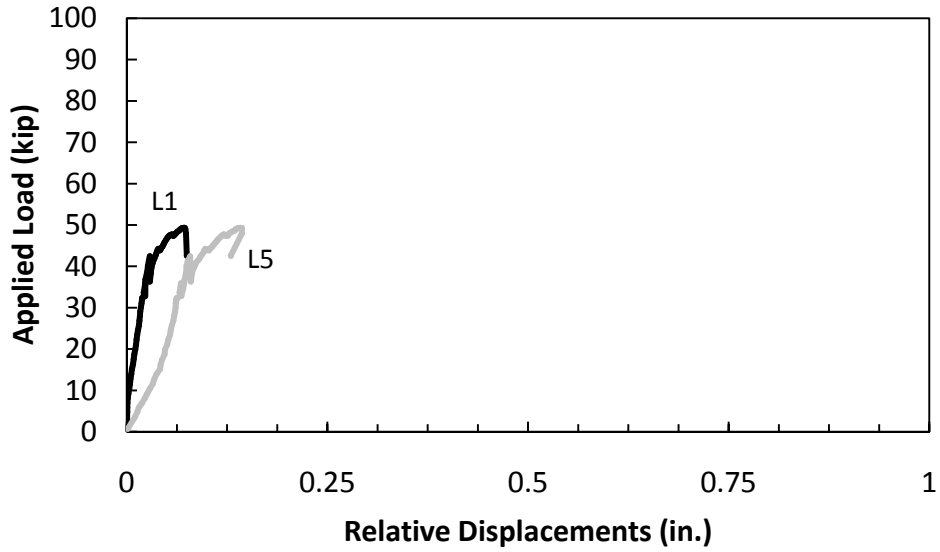


*Figure B.65 – Measured Support Displacements for Specimen P30P1 for Load Applied at Midspan of Skewed End*

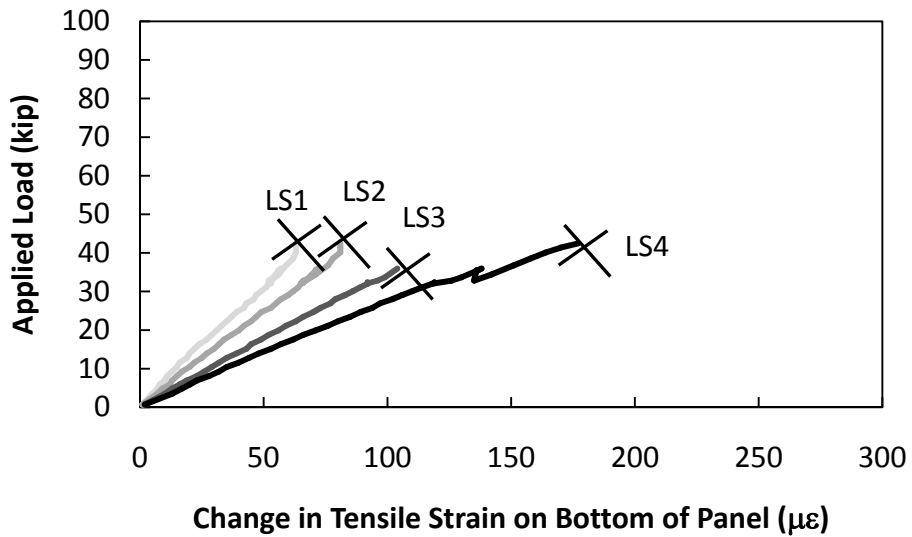


*Figure B.66 – Measured Change in Tensile Strain on Bottom of Panel for Specimen P30P1 for Load Applied at Midspan of Skewed End*

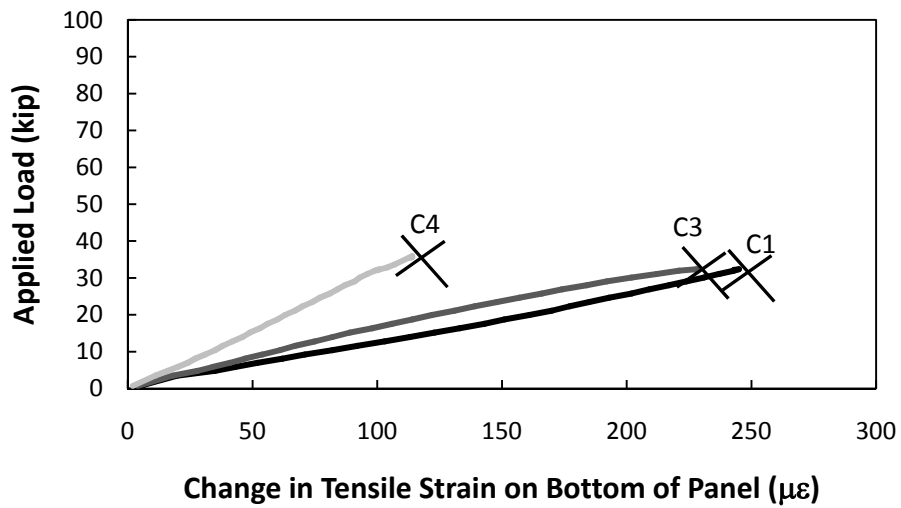


*Figure B.67 – Measured Change in Tensile Strain on Bottom of Panel for Specimen P30P1 for Load Applied at Midspan of Skewed End*

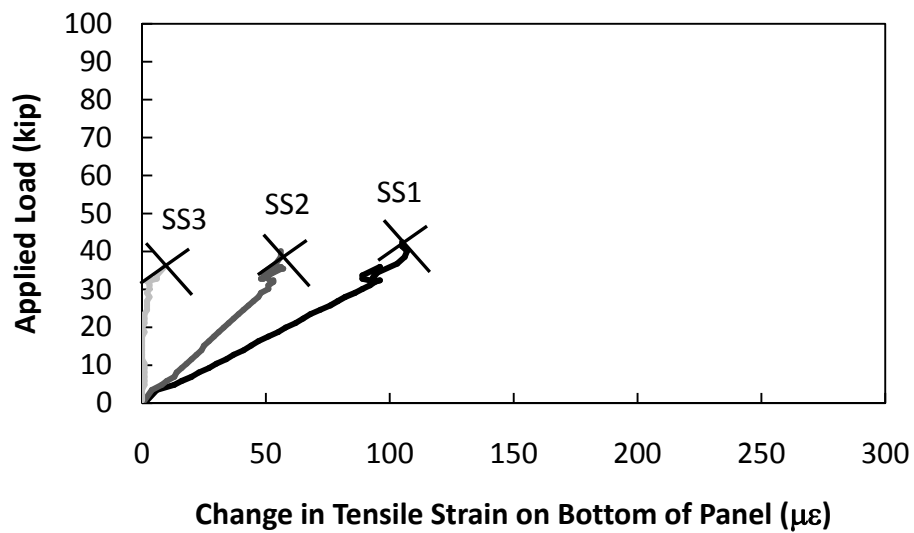


*Figure B.68 – Measured Change in Tensile Strain on Bottom of Panel for Specimen P30P1 for Load Applied at Midspan of Skewed End*

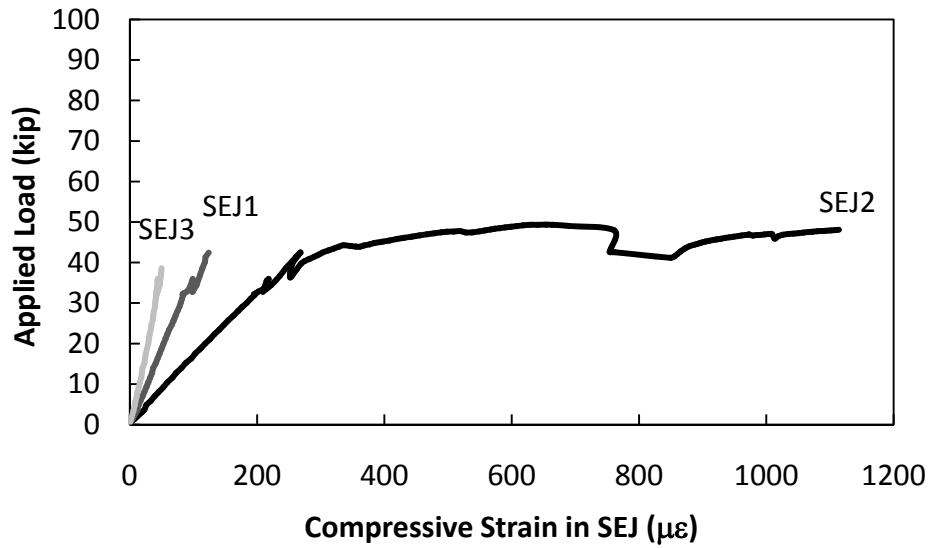


*Figure B.69 – Measured Compressive Strain in SEJ for Specimen P30P1 for Load Applied at Midspan of Skewed End*

**B.4.2 Load Applied at Midspan of Square End**

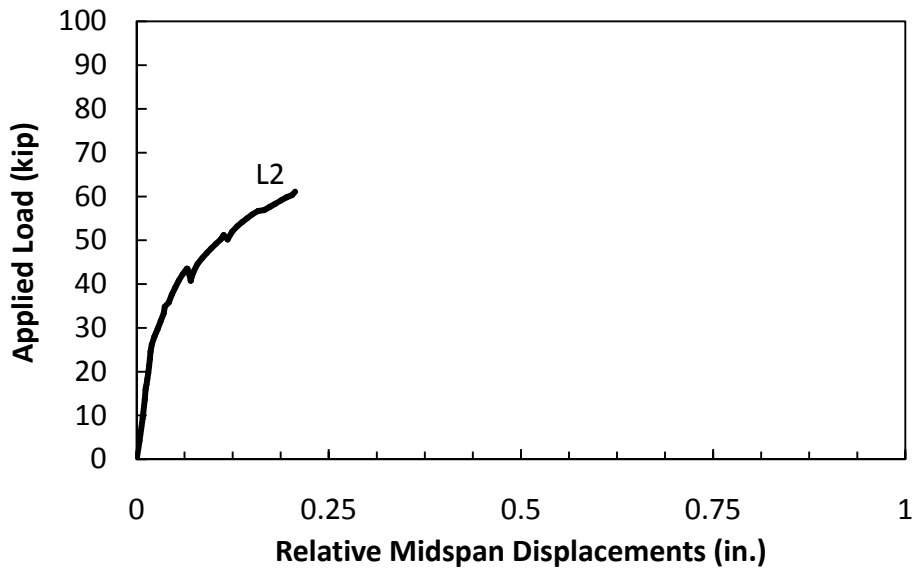


*Figure B.70 – Measured Relative Displacement at Midspan of Square End of Specimen P30P1 for Load Applied at Midspan of Square End*

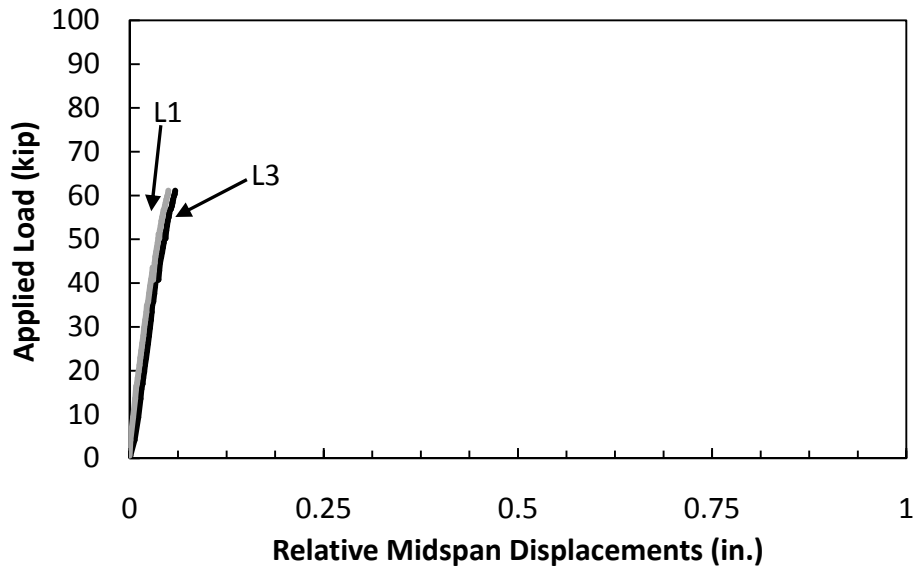


*Figure B.71 – Measured Support Displacements for Specimen P30P1 for Load Applied at Midspan of Square End*

### **B.5 SPECIMEN P30P2**

Specimen P30P2 was also loaded on the skewed end followed by the square end. Data for this specimen include displacement data, strain on the bottom of the panel, and strain in the SEJ. The load applied at midspan of the skewed end damaged many of the concrete gages on the square end, so no strain data was available for load applied at midspan of the square end. Data for load applied at midspan of the skewed end are presented first, followed by data from load applied at midspan of the square end.



### B.5.1 Load Applied at Midspan of Skewed End

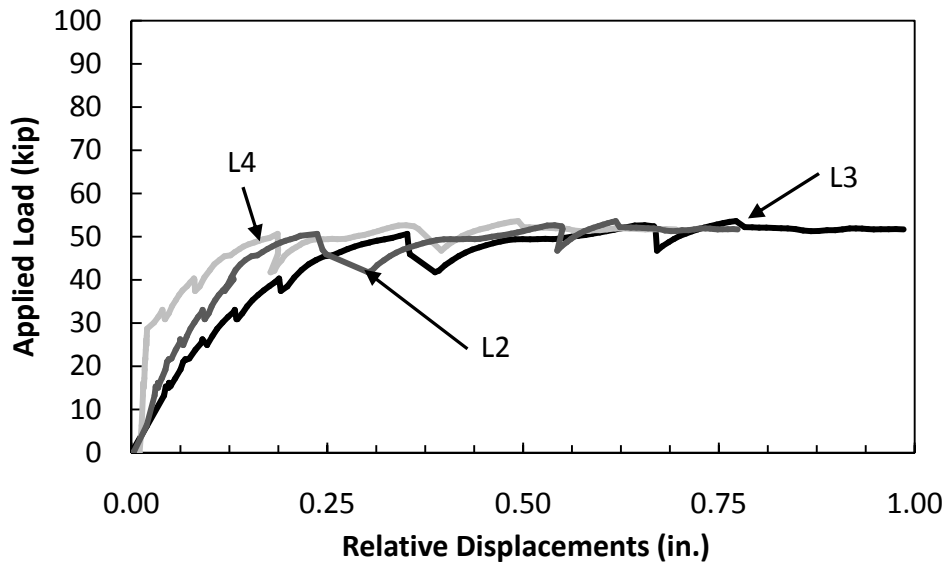


*Figure B.72 – Measured Relative Displacements for Specimen P30P2 for Load Applied at Midspan of Skewed End*

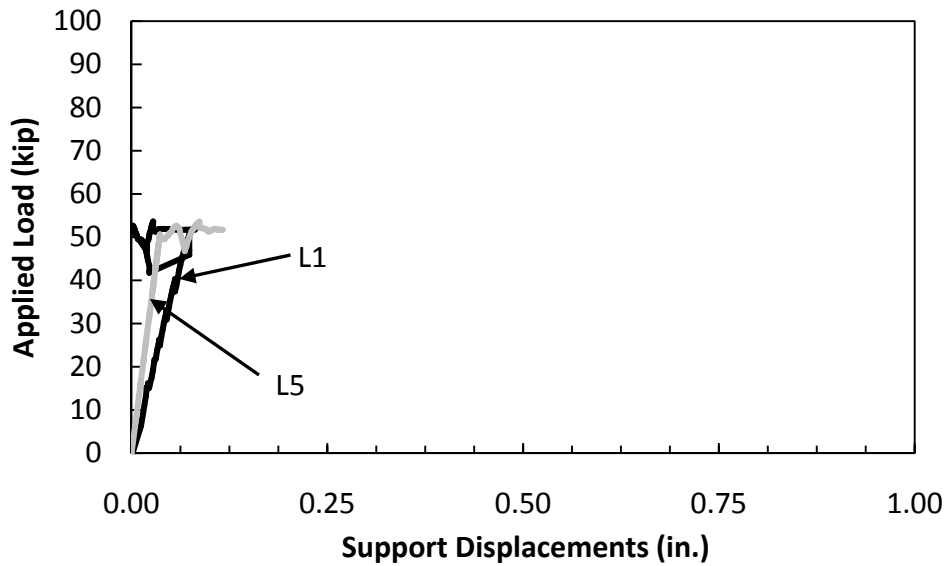


*Figure B.73 – Measured Support Displacements for Specimen P30P2 for Load Applied at Midspan of Skewed End*

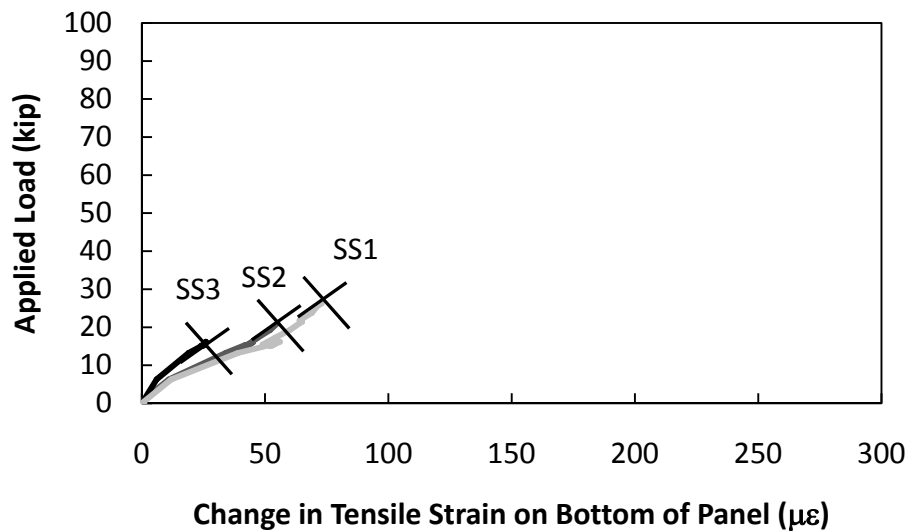


*Figure B.74 – Measured Change in Tensile Strain on Bottom of Panel for Specimen P30P2 for Load Applied at Midspan of Skewed End*

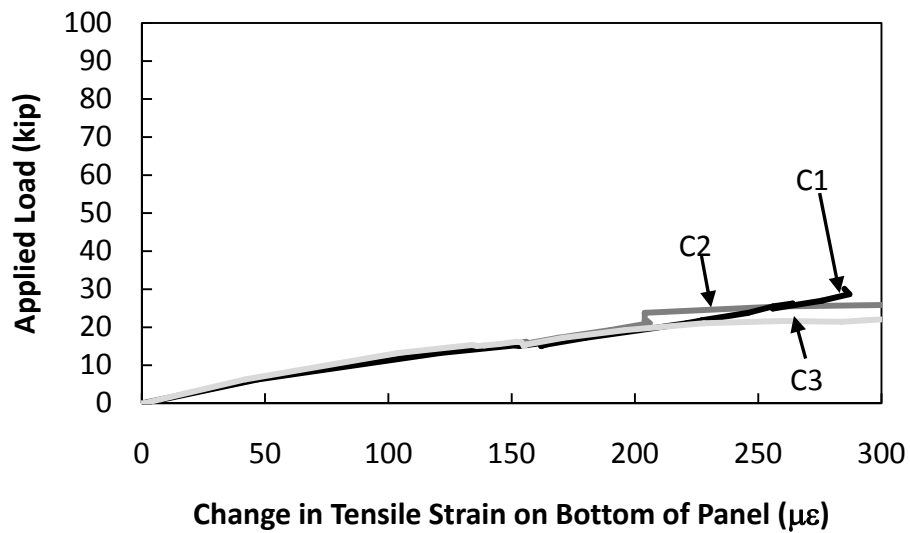


*Figure B.75 – Measured Change in Tensile Strain on Bottom of Panel for Specimen P30P2 for Load Applied at Midspan of Skewed End*

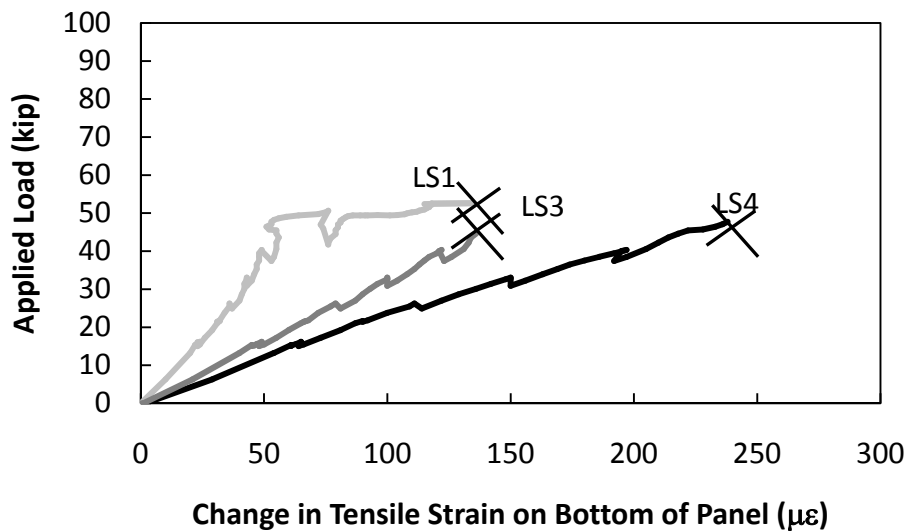


*Figure B.76 – Measured Change in Tensile Strain on Bottom of Panel for Specimen P30P2 for Load Applied at Midspan of Skewed End*

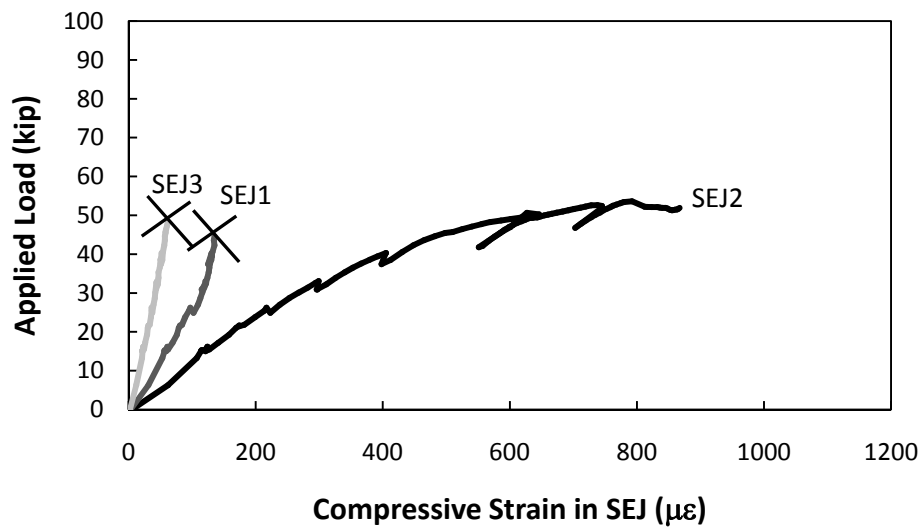


*Figure B.77 – Measured Compressive Strain on Top Surface of SEJ for Specimen P30P2 for Load Applied at Midspan of Skewed End*

### B.5.2 Load Applied at Midspan of Square End

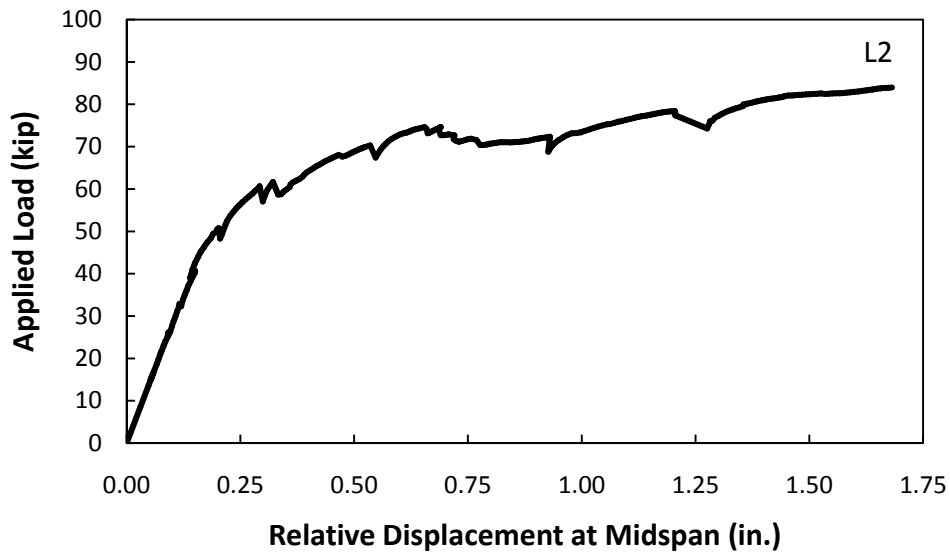


*Figure B.78 – Measured Relative Displacement at Midspan of Square End for Load Applied at Midspan of Square End*

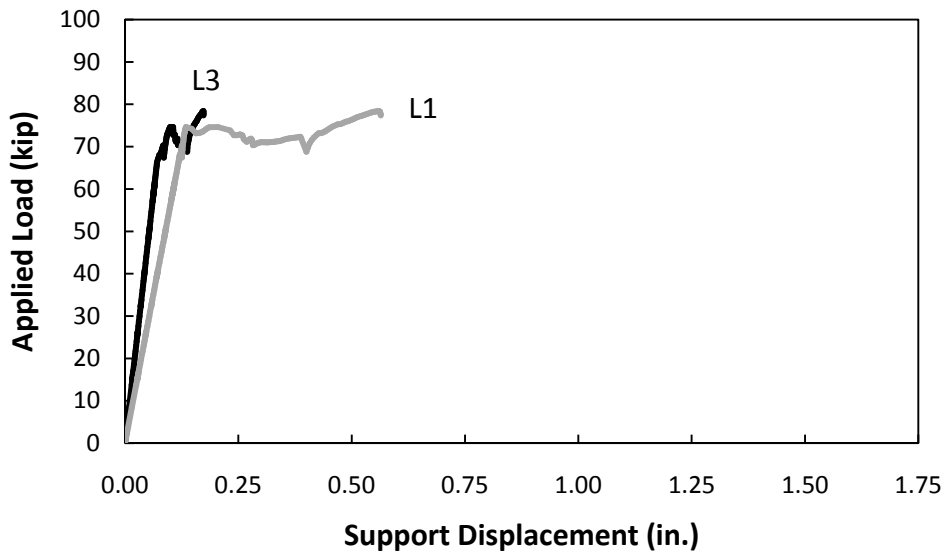


*Figure B.79 – Measured Support Displacements for Specimen P30P2 for Load Applied at Midspan of Square End*

## References

Abendroth, R. E. (1994). Deformations in Composite Prestressed Concrete Bridge Deck Panels. *Journal of Structural Engineering* , Vol. 120, No. 11.

Agnew, L. S. (2007). *Evaluation of the Fatigue Behavior of Bridge Decks with Precast Panels at Expansion Joints*. Austin, TX: The University of Texas at Austin.

Barker, J. M. (1975). Research, Application, and Experience with Precast Prestressed Bridge Deck Panels. *PCI Journal* , Vol. 20, No. 6.

Coselli, C. J. (2004). *Behavior of Bridge Decks with Precast Panels at Expansion Joints*. Austin, TX: The University of Texas at Austin.

Dowell, R. K., & Smith, J. W. (2006). Structural Tests of Precast, Prestressed Concrete Deck Panels for California Freeway Bridges. *PCI Journal* , March-April, 2-13.

Griffith, E. M. (2003). *Behavior of Bridge Slab Ends at Expansion Joints*. Austin, TX: The University of Texas at Austin.

Kreisa, A. R. (2008). *Constructability of Prestressed Concrete Panels for Use at Skewed Expansion Joints*. Austin, TX: The University of Texas at Austin.

Merrill, B. D. (2002). *Texas' Use of Precast Concrete Stay-in-Place Forms for Bridge Decks*. Austin, TX: Texas Department of Transportation.

TxDOT. (2008, May). "Prestressed Concrete Panels". *Detail of Standard Drawings* . Retrieved from:  
<ftp://ftp.dot.state.tx.us/pub/txdot-info/cmd/cserve/standard/bridge/pcpstde1.pdf>.

Van Landuyt, D. (2006, September). "Survey of Skew Angles of TxDOT Bridges". Austin, TX: Results presented at research project meeting.

## **Vita**

Clifton Adam Boswell, the son of C. Eric and Gloria J. Boswell, was born in Provo, Utah on February 20, 1982. He is the oldest of six children and was raised in Montgomery, Alabama. After graduating from Booker T. Washington Magnet High School in 2000, he enrolled in Auburn University in Auburn, Alabama. In the summer of 2001, he left school for two years to serve as a full-time missionary for the Church of Jesus Christ of Latter-day Saints in Belo Horizonte, Brazil. He returned to Auburn University in the fall of 2003 and received the degree of Bachelor of Civil Engineering. In the fall of 2006, he enrolled in the Graduate School of the University of Texas at Austin.

Permanent Address: 3013 Merrimac Court

Montgomery, Alabama 36111

This thesis was typed by the author.